Sheffield Hallam University
School of Science and Mathematics
Division of Applied Physics

Theoretical Investigation of Sound Reduction by Finite Barriers

A Thesis submitted for the Degree of Master of Philosophy

Gerald Arthur Tinkham

March 1997

Sheffield Hallam University

Abstract

School of Science and Mathematics
Division of Applied Physics

Master of Philosophy

Theoretical Investigation of Sound Reduction by Finite Barriers

by

Gerald Arthur Tinkham

Noise pollution in factories has become a major problem which has been highlighted in recent years. This thesis attempts to construct a model which will predict sound attenuation by finite barriers within enclosures, thus simulating factory conditions.

The research uses the classical Kirchhoff-Fresnel diffraction theory outlined in Born and Wolf[1] to develop a model by which the barriers' surface is divided into elements. Using Babinet's Principle, sound attenuation was predicted for a finite barrier in free space. The sound source was assumed to be a point source of monotonic frequency.

The free space environment served as a basic theoretical model where computer programs compared the zero and first-order models. This comparison showed that the first-order model was the more productive and identified the optimum element size to give an accuracy within the precision grade of measurement.

After validating the theory, the model was adapted to predict insertion loss, using a finite barrier in contact with the ground. There is much contemporary literature for this model but little research has been undertaken in predicting sound losses due to finite barriers within enclosures.

A further extension to the research was to place the barrier in a flat room, where reflections of the sound waves from the roof as well as the floor were included. This model also allowed the effect on insertion loss to be examined by increasing the aspect ratio of width/height of the barrier.

Finally, side walls were introduced into the model to see if they have any significant effect on insertion loss as compared to the flat room model.

MEMORANDUM

This thesis is an account of original research performed by the author in the School of Science, Division of Applied Physics, Sheffield Hallam University.

ACKNOWLEDGEMENTS

Throughout the years of my research many people have given me advice and encouragement, and it is with great pleasure that I thank them for their help.

I will always be indebted to the late Dr David Allen-Booth, who was my Director of Studies. He persuaded me to undertake this project and when times were difficult he was the one who gave me encouragement. David was a kind, understanding and gentle man, who as well as being my Supervisor, became a very good friend. His kindness, intelligence and humour will have a lasting impression on my life.

I should also like to thank David's wife, Alison, who always welcomed me to their home, even when times were very difficult.

My thanks also go to Dr Glinn Rodgers, who took over as my Director of Studies when Dr David Allen-Booth became too ill to continue. His hard work and advice will always be appreciated.

I shall always be indebted to Professor J McNulty for his technical advice, helpful suggestions and general encouragement.

Many thanks to Dr John Young and his colleagues in the Applied Physics Department, to Dave Jefferies for his help in computing and to Val Slinn for her excellent typing.

Finally my very special thanks go to my wife, Sylvia, and my children, Kevin and Jill.Their love, encouragement and help have been so important to me. Thank you.

CONTENTS

CONTENTS

List of Figures and Tables

1 INTRODUCTION

Hearing loss, due to excessive noise in industry, is a serious problem that has been highlighted in recent years. This report attempts to construct theoretical models which use barriers to reduce noise in enclosures and hence simulate factory conditions. Although there has been a great deal of research into straight-edged semi-infinite barriers, the work presented in this thesis predicts noise reduction produced by barriers in finite enclosures. To the author's knowledge little work has been done on this aspect of the subject.

Initially, the report uses the classical Kirchhoff-Fresnel diffraction theory outlined in Born and Wolf[1] to develop a model by which the barriers' surface was divided into elements. By incorporating Babinets' Principle into the model, sound attenuation was predicted for a barrier in free space.

The Kirchhoff-Fresnel theory is described in Section 1.1.

1.1 The Integral Theorem of Kirchhoff

The basic idea of the Huygens-Fresnel theory is that the disturbance at a point P arises from the superposition of secondary waves that proceed from a surface situated between this point and the source. This idea was put on a sounder mathematical basis by Kirchhoff, who showed that the Huygens-Fresnel principle may be regarded as an approximate form of a certain integral theorem which expresses the solution of the homogeneous wave equation, at an arbitrary point in the field, in terms of the values of the solution and its first derivatives at all points on an arbitrary closed surface surrounding P.

We consider first a strictly monochromatic scalar wave:

$$V(x,y,z,t) = \cup(x,y,z)e^{-i\omega t} \qquad (1.1.1)$$

In vacuum the space-dependent part then satisfies the time-independent wave equation:

$$\left(\nabla^2 + k^2\right)\cup = 0 \qquad (1.1.2)$$

where $k = \omega/c$ or $k = \frac{2\pi}{\lambda}$, λ being the wavelength of the medium. Equation (1.1.2) is known as the Helmholtz equation and was first deduced for monochromatic accoustic waves. It implies that there is no dissipation or absorption. This is not strictly true in air - especially over long disances.

Let v be a volume bounded by a closed surface s, and let P be any point within it; we assume that $\cup$ possesses continuous first- and second-order partial derivatives within and on this surface. If $\cup^1$ is any other function which satisfies the same continuity requirements as $\cup$, we have by Green's theorem:

$$\iiint_v \left(\cup\nabla^2 \cup^1 - \cup^1 \nabla^2 \cup\right)dv = \iint_s \left(\cup\frac{\partial \cup^1}{\partial n} - \cup^1 \frac{\partial \cup}{\partial n}\right)dS, \qquad (1.1.3)$$

where $\partial/\partial n$ denotes differentiation along the inward normal to S (Green's theorem is usually expressed in terms of the outward normal, but the inward normal is more convenient in the present application). In particular, if $\cup^1$ also satisfies the time-independent wave equation, ie if

$$\left(\nabla^2 + k^2\right)\cup^1 = 0 \qquad (1.1.4)$$

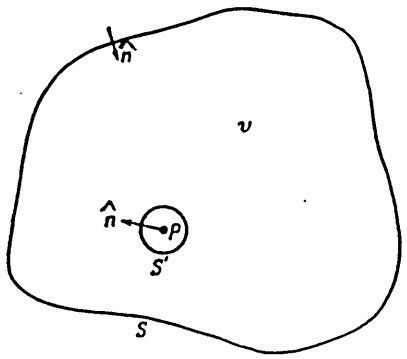

Figure 1:

Derivation of the Helmholtz-Kirchhoff integral theorem: region of integration

then it follows at once from (1.1.2) and (1.1.4) that the intergrand on the left of (1.1.3) vanishes at every point of v, and consequently:

$$\iint_S \left(\cup \frac{\partial \cup^1}{\partial n} - \cup^1 \frac{\partial \cup}{\partial n} \right) dS = 0 \qquad (1.1.5)$$

Suppose we take $\cup^1(x,y,z) = e^{iks}/s$, where s denotes the distance from P to the point (x,y,z). This function has a singularity for $s = 0$, and since $\cup^1$ was assumed to be continuous and differentiable, P must be excluded from the domain of integration. We shall therefore surround P by a small sphere of radius ϵ and extend the integration throughout the volume between S and the surface S^1 of this sphere (Figure 1). In place of (1.1.5), we then have:

$$\iint_S + \iint_{S^1} \left\{ \cup \frac{\partial}{\partial n}\left(\frac{e^{iks}}{s}\right) - \frac{e^{iks}}{s}\frac{\partial \cup}{\partial n} \right\} dS = 0$$

whence
$$\iint_S + \iint_{S^1} \left\{ \cup \frac{\partial}{\partial n}\left(\frac{e^{iks}}{s}\right) - \frac{e^{iks}}{s}\frac{\partial \cup}{\partial n} \right\} dS = -\iint_{S^1} \left\{ \cup \frac{e^{iks}}{s}\left(ik - \frac{1}{s}\right) - \frac{e^{iks}}{s}\frac{\partial \cup}{\partial n} \right\} dS^1$$

$$= \iint_\Omega \left\{ \cup \frac{e^{ik\epsilon}}{\epsilon}\left(ik - \frac{1}{\epsilon}\right) - \frac{e^{ik\epsilon}}{\epsilon}\frac{\partial \cup}{\partial s} \right\} \epsilon^2 \, d\Omega,$$

(1.1.6)

where $d\Omega$ denotes an element of the solid angle. Since the integral over s is independent of $\epsilon \to 0$; the first and third terms in this integral give no contribution in the limit, and the total contribution of the second term is $4\pi \cup (P)$. Hence

$$\cup(P) = \frac{1}{4\pi} \iint_S \left\{ \cup \frac{\partial}{\partial n}\left(\frac{e^{iks}}{s}\right) - \frac{e^{iks}}{s}\frac{\partial \cup}{\partial n} \right\} dS \qquad (1.1.7)$$

This is one form of the 'integral theorem of Helmholtz and Kirchhoff'.

We note, that as $k \to 0$, the time independent wave equation (1.1.2), reduces to Laplace's equation $\nabla^2 \cup = 0$, and (1.1.7) then goes over into the well known formula of potential theory.

$$\cup(P) = \frac{1}{4\pi} \iint_S \left\{ \cup \frac{\partial}{\partial n}\left(\frac{1}{s}\right) - \frac{1}{s}\frac{\partial \cup}{\partial n} \right\} dS \qquad (1.1.8)$$

If P lies outside the surface S, but $\cup$ is still assumed to be continuous and differentiable up to the second order within S, and if as before we take $\cup^1 = e^{iks}/s$, equation (1.1.3) remains valid through out the whole volume within S. According to (1.1.5) the surface integral then has the value zero.

There is a complementary form of the Helmholtz-Kirchhoff theory for the case when $\cup$ is continuous and differentiable up to the second order outside and on a closed surface S (sources inside). In this case, however, as in other problems of propagation in an infinite medium, the boundary values on S are no longer sufficient to specify the solution uniquely and additional assumptions must be made about the behaviour of the solution as $S \to \infty$.

1.2 **Kirchhoff's Diffraction Theory**

Whilst the integral theorem of Kirchhoff embodies the basic idea of the Huygens-Fresnel principle, the laws governing the contributions from different elements of the surface are more complicated than Fresnel assumed. Kirchhoff showed, however, that in many cases the theorem may be reduced to an approximate but much simpler form, which is essentially equivalent to the formulation of Fresnel, but which in addition gives an explicit formula for the inclination factor that remained undetermined in Fresnel's theory.

So far we have considered strictly monochromatic waves. We now derive a general form of Kirchhoff's theorem which applies to waves that are not necessarily monochromatic.

Let $V(x,y,z,t)$ be a solution of the wave equation

$$\nabla^2 V = \frac{1}{C^2}\frac{\partial^2 V}{\partial t^2} \tag{1.1.9}$$

and assume that V can be represented in the form of a Fourier integral

$$V(x,y,z,t) = \frac{1}{\sqrt{2\pi}} \int_{-\infty}^{\infty} \cup_{\omega}(x,y,z) e^{-i\omega t} d\omega \qquad (1.1.10)$$

Then, by the Fourier inversion formula

$$\cup_{\omega}(x,y,z) = \frac{1}{\sqrt{2\pi}} \int_{-\infty}^{\infty} V(x,y,z,t) e^{i\omega t} dt \qquad (1.1.11)$$

Since $V(x,y,z,t)$ is assumed to satisfy the wave equation (1.1.9), the time independent component $\cup_{\omega}(x,y,z)$ will satisfy the time independent equation (1.1.2).

Also, if V satisfies the appropriate regularity conditions within and on a closed surface S (concerning the first and second derivatives), we may apply the Kirchhoff formula separately to each Fourier component $\cup_{\omega}(x,y,z) = \cup_{\omega}(P)$.

Hence $$\cup_{\omega}(P) = \frac{1}{4\pi} \iint_S \left\{ \cup_{\omega} \frac{\partial}{\partial n}\left(\frac{e^{iks}}{s}\right) - \frac{e^{iks}}{s} \frac{\partial \cup_{\omega}}{\partial n} \right\} dS \qquad (1.1.12)$$

Combining equations (1.1.10) and (1.1.12), changing the order of integration and replacing k by $\frac{\omega}{c}$ gives:

$$V(P,t) = \frac{1}{4\pi} \iint_S dS \frac{1}{\sqrt{2\pi}} \int_{-\infty}^{\infty} \left\{ \cup_{\omega} \frac{\partial}{\partial n}\left(\frac{e^{-i\omega\left(t-\frac{s}{c}\right)}}{s} \right) - \frac{e^{-i\omega\left(t-\frac{s}{c}\right)}}{s} \frac{\partial \cup_{\omega}}{\partial n} \right\} d\omega$$

$$= \frac{1}{4\pi} \iint_S dS \frac{1}{\sqrt{2\pi}} \int_{-\infty}^{\infty} \left\{ \cup_{\omega} \left\{ \frac{\partial}{\partial n}\left(\frac{1}{s}\right) + \frac{i\omega}{sc} \frac{\partial S}{\partial n} \right\} e^{-i\omega\left(t-\frac{s}{c}\right)} - \frac{e^{-i\omega\left(t-\frac{s}{c}\right)}}{s} \frac{\partial \cup_{\omega}}{\partial n} \right\} d\omega$$

We note from equation 1.1.10 that

$$\frac{\partial\left(V(x,y,z,t)\right)}{\partial t} = \frac{1}{\sqrt{2\pi}} \int_{-\infty}^{\infty} \cup_{\omega}(x,y,z) - \left(i\omega e^{-i\omega t}\right) d\omega$$

and $$\frac{\partial V}{\partial n} = \frac{1}{\sqrt{2\pi}} \int_{-\infty}^{\infty} \frac{\partial \cup_{\omega}}{\partial n} e^{-i\omega t} d\omega$$

This enables us to write:

$$V(P,t) = \frac{1}{4\pi}\iint_S \left\{ [V]\frac{\partial}{\partial n}\left(\frac{1}{s}\right) - \frac{1}{cs}\frac{\partial s}{\partial n}\left[\frac{\partial V}{\partial t}\right] - \frac{1}{s}\left[\frac{\partial V}{\partial n}\right] \right\} dS \qquad (1.1.13)$$

where the square brackets denote 'retarded values' ie values of the function taken at the time $(t - \frac{s}{c})$. Equation 1.1.13 is the general form of Kirchhoff's Theorem.

Consider a monochromatic wave, from a point source *Po*, propagated through an opening in a plane opaque screen and let *P* (as before) be the point at which the light disturbance is to be determined.

We assume that the linear dismensions of the opening, although large compared with the wavelength, are small compared to the distances of both *Po* and *P* from the screen.

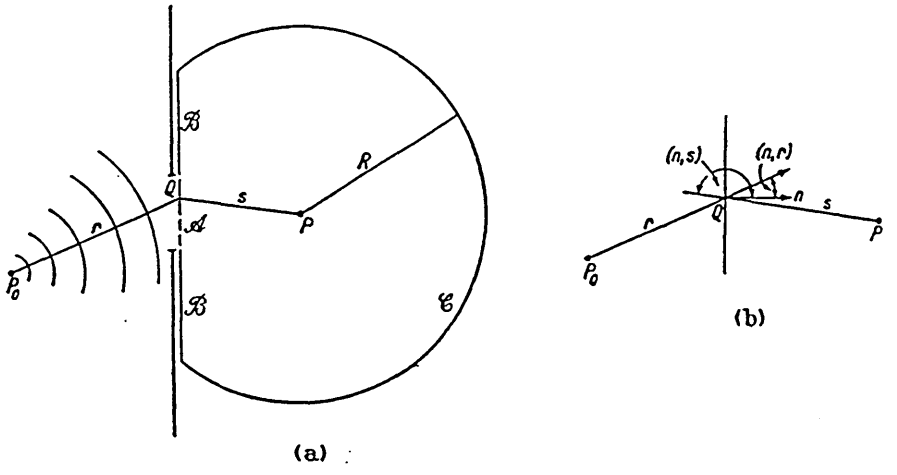

Figure 2 Opening in a plane opaque screen

To find the disturbances at *P* we take the Kirchhoff integral over a surface *S* formed by $\mathcal{A}$, the opening in the screen, $\mathcal{B}$, a portion of the non illuminated side of the screen and $\mathcal{C}$, a portion of a large sphere of radius *R*, centred at *P* which, together with $\mathcal{A}$ and $\mathcal{B}$, forms a closed surface.

Applying Kirkhhoff's Theorem (equation 1.1.7) to this surface gives:

$$\cup(P) = \frac{1}{4\pi}\left[\iint_{\mathcal{A}} + \iint_{\mathcal{B}} + \iint_{\mathcal{C}} + \right]\left\{ \cup\frac{\partial}{\partial n}\left(\frac{e^{iks}}{s}\right) - \left(\frac{e^{iks}}{s}\right)\frac{\partial \cup}{\partial n} \right\} dS \qquad (1.1.14)$$

where, as before, s is the distance of the element dS from P and $\frac{\partial}{\partial n}$ denotes differentiation along the inward normal to the surface of integration.

The difficulty is that the values of $\cup$ and $\frac{\partial \cup}{\partial n}$ on $\mathcal{A}$, $\mathcal{B}$ and $\mathcal{C}$ which should be substituted into (1.1.14) are not known exactly.

However, it is reasonable to suppose that everywhere on $\mathcal{A}$, except in the immediate neighbourhood of the rim of the opening, $\cup$ and $\frac{\partial \cup}{\partial n}$ will not differ appreciably from the values obtained in the absence of the screen, and that on $\mathcal{B}$ these quantities will be approximately zero. Kirchhoff accordingly set:

$$\left.\begin{aligned} &\text{on } \mathcal{A}: \ \cup = \cup^{(i)}, \frac{\partial \cup}{\partial n} = \frac{\partial \cup^{(i)}}{\partial n} \\ &\text{on } \mathcal{B}: \ \cup = 0 \quad , \frac{\partial \cup}{\partial n} = \quad 0 \end{aligned}\right\} \tag{1.1.15}$$

where

$$\cup^{(i)} = \frac{Ae^{ikr}}{r}, \frac{\partial \cup^{(i)}}{\partial n} = \frac{Ae^{ikr}}{r}\left[ik - \frac{1}{r}\right]\cos(n,r)$$

The derivative is obtained as follows:

$$\frac{\partial \cup^{(i)}}{\partial r} = A\left\{\frac{r\, ike^{ikr} - e^{ikr}}{r^2}\right\} = \frac{Ae^{ikr}}{r}\left[ik - \frac{1}{r}\right]$$

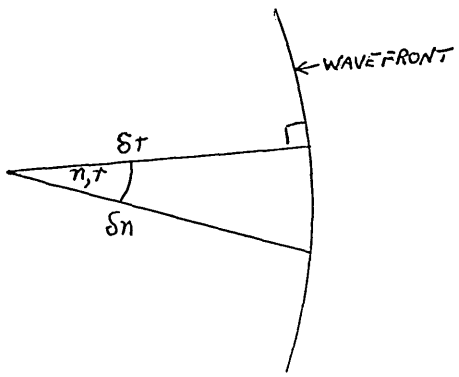

From the diagram shown, provided that we make δr, δn small, the wavefront can be regarded as essentially plane and so

$$\frac{\partial r}{\partial n} \approx \cos(n,v)$$

as $\delta r \to 0$ we have $\frac{\delta r}{\delta n} = \cos(n,r)$

now $$\frac{\partial \cup^{(i)}}{\partial n} = \frac{\partial \cup^{(i)}}{\partial r} \bullet \frac{\partial r}{\partial n} = \frac{Ae^{ikr}}{r}\left[ik - \frac{1}{1}\right]\cos(n,r) \qquad (1.1.16)$$

The approximation set in 1.1.15 are called Kirchhoff's Boundary Conditions and are the basis of Kirchhoff Diffraction Theory.

We must now consider the spherical portion $\mathcal{C}$. The assumption is made that the radius R of the sphere at $\mathcal{C}$ can be made sufficiently large so that the radiation does not reach $\mathcal{C}$ until time $t = t_0$. At any time before that time we can ignore the integral over $\mathcal{C}$. (This implies a departure from monochromacy since a perfectly monochromatic field must exist for all time t.)

It is now possible to substitute (1.1.15) and (1.1.16) into (1.1.14) to obtain a more explicit form of $\cup(P)$.

Consider the term $\cup\frac{\partial}{\partial n}\left(\frac{e^{iks}}{s}\right)$

By the same argument as was applied to the deduction that

$$\frac{\partial r}{\partial n} = \cos(n,r) \text{ we have } \frac{\partial s}{\partial n} = \cos(S,r)$$

Now $$\frac{\partial}{\partial s}\left(\frac{e^{iks}}{s}\right) = \frac{S.i.k.e^{iks} - e^{iks}}{s^2}$$

or $$\frac{\partial}{\partial s}\left(\frac{e^{iks}}{s}\right) = \frac{e^{iks}}{s}\left(ik - \frac{1}{s}\right)$$

Hence, from (1.1.16)

$$\cup\frac{\partial}{\partial n}\left(\frac{e^{iks}}{s}\right) = \frac{Ae^{ikr}}{r} \bullet \frac{e^{iks}}{s}\left(ik - \frac{1}{s}\right) \bullet \cos(n,s)$$

$$= \frac{Ae^{ik(r+s)}}{rs} \bullet \left(ik - \frac{1}{s}\right)\cos(n,s)$$

Also, from (1.1.16)

$$\frac{e^{iks}}{s}\bullet\frac{\partial \cup}{\partial n}=\frac{e^{iks}}{s}\bullet\frac{Ae^{ikr}}{r}\left[ik-\frac{1}{r}\right]\cos(n,r)$$

$$=\frac{Ae^{ik(r+s)}}{rs}\left(ik-\frac{1}{r}\right)\cos(n,r)$$

Therefore equation (1.1.14) can now be rewritten as:

$$\cup(P)=\frac{1}{4\pi}\iint_A\frac{Ae^{ik(r+s)}}{rs}\left[\left(ik-\frac{1}{s}\right)\cos(n,s)-\left(ik-\frac{1}{r}\right)\cos n,r\right]dS \qquad (1.1.17)$$

This is the exact form of the Fresnel-Kirchhoff diffraction formula. In the optical treatment, because of the short wavelength both $\frac{1}{s}$ and $\frac{1}{r}$ are neglected in comparison with k. Making this approximation and setting $k=\frac{2\pi}{\lambda}$ gives:

$$\cup(P)=-\frac{iA}{2\lambda}\iint_A\frac{e^{ik(r+s)}}{rs}\left[\cos(n,r)-\cos(n,s)\right]dS \qquad (1.1.18)$$

The way in which the theory is modelled allows attenuation to be calculated regardless of the shape and size of the barrier and of the proximity of source and receiver to the barrier. A method of predicting sound attenuation for a barrier in contact with the ground is then described. This model makes provision for sound being reflected from changing ground conditions as well as that taking the direct route.

The model was then extended to that of a flat room, where reflections from the roof, as well as the ground, contribute to sound loss due to the barrier. Finally, walls were introduced into the model, allowing the insertion loss to be predicted using a barrier within an enclosure.

2 REVIEW OF PREVIOUS RESEARCH

During the period up to 1980, much investigation, which develops and extends optical diffraction theory for the purpose of predicting sound levels behind barriers is summarised by T Isei, T F W Embleton and J E Piercy[2]. They classify both theoretical and experimental work in their area into four categories:

(i) To obtain generality for different geometries, the attenuation or insertion loss of a barrier has been derived as a function of non-dimensional variables which are determined by barrier geometry. Redfearn[3] showed the attenuation by a barrier to be a function of the non-dimensional ratio of the length of the perpendicular from the edge of the barrier to the line between source and receiver, divided by wavelength, using the diffraction angle as a parameter.

Maekawa[4,5], developed his well known chart, in which attenuation is shown as a function of Fresnel number, by extending Kirchhoffs diffraction theory and correcting the theoretical values empirically to allow for the presence of the ground. Kurze and Anderson[6] have given a similar chart for an incoherent line source, also in terms of Fresnel number. Kawai et al[7] have developed a simple, approximate expression for Bowman and Senior's formula[8], which is based on MacDonald's rigorous solution[9], again using the Fresnel number. Most of these prediction schemes are based on the idea of a semi-infinite screen, which does not allow for interference due to reflection from the ground.

(ii) Several studies have been made of the effectiveness of absorbent material on the barrier surface. Kawai et al[7] have discussed the effect of the image source in a perfectly reflecting barrier using the second term of the approximate expression[8] of MacDonald's solution. Fujiwara et al[10] showed the intensity of the diffracted field due to the image in the barrier by introducing the complex pressure reflection coefficient for incident plane waves into the second term of MacDonald's

equation[8]. Yuzawa[11] also evaluated the diffracted field due to the image source in the barrier, using the second term of an approximate solution by Pierce[12], but regarded the imaginary part of the admittance of the barrier surface as zero. This work on absorptive barriers also assumes semi-infinite barriers, and so does not allow for interference which arises in the presence of the ground.

(iii) Diffraction theory has been developed for different shaped obstacles, such as a wedge or a thick barrier. Pierce[12] developed the theory for diffraction by a wedge and extended it to double-edge diffraction, and, hence, to a thick barrier, using Keller's geometrical theory of diffraction[13]. Fujiwara et al[14] have discussed the effect of barrier thickness in terms of MacDonald's theory[9].

(iv) Some work has been presented which allows for the presence of the ground, and also interference due to waves reflected from the ground, Scholes et al[15] carried out full scale barrier measurements on grass-covered ground. They observed an interference pattern due to reflection at the ground on measurements both with and without the barrier. Isei et al[16] have also observed interference patterns using a motor-driven artificial line source on the ground. Jonasson[17] has proposed a method for calculating the noise reduction of a barrier on ground of finite impedance. To evaluate the diffracted field due to ground reflections, Jonasson introduced Ingard's theory[18] of sound propagation along a boundary, into the first term of MacDonald's solution, neglecting the second term, and assumed that the ground-reflected field could be set equal to the field due to the real source when source and receiver were both situated close to the reflecting surface. Thus he found a simple approximate solution for the diffracted and reflected fields due to barrier and ground which includes only one phase-dependent term. He concluded that the insertion loss of a barrier is often small, even negative, and this tendency appears when the excess attenuation due to the ground is large. Thomasson[19-22] developed a new ground impedance model[19,22] and introduced it into a diffraction theory based on numerical integration of the direct and complex reflected waves

over the surface of the barrier. Application of Babinet's principle yields the diffracted field at the receiver behind the barrier. In Thomasson's model, the admittance of the ground is described by four parameters that are adjusted for best fit to measurements of a sound field above the same type of ground. Thomasson also carried out full-scale barrier experiments[22] on several kinds of ground and found good agreement with his theory.

In their work on barriers, T Isei, T F W Embleton and J E Piercy[23.24] reported on one calculation scheme and have used it to quantitatively analyse the interference pattern measured in the diffracted field behind barriers. In this scheme the Weyl-van der Pol[25] equation is applied to the sound field on each side of the barrier: the diffraction of each direct, reflected, and ground wave thus appears explicitly.

Isei, T F W Embleton and J E Piercy[2] seek a better understanding of barrier performance in practical situations. Sound levels behind barriers on the ground, as predicted by five different theories, are first compared with each other and with measured results.

The five theories are:

1 Keller's geometrical theory of diffraction[13]

2 Kirchhoff-Fresnel diffraction theory[1.26]

3 Thomasson's theory based on Babinet's principle[21.22]

4 Edge-integral diffraction theory based on the Young-Rubinowicz formula[27]

5 A modification of MacDonald's diffraction theory[28].

Despite the vast amount of research described above, there is a dearth of published work on noise attenuation due to finite barriers.

Maekawa[4.5] postulated a method for the prediction of the attenuation due to a finite barrier on reflecting ground by applying the method of calculation of diffraction over the top edge of a semi-infinite screen also to the ends of the finite

screen. However, his theory limits the location of source and receiver and also the barrier is restricted to rectangular shapes. Kurze and Anderson[6] deal with finite barriers in a way which predicts the length of the barrier required in the presence of an infinite line source that gives approximately the same attenuation as an infinitely long barrier.

From the background work, described above, it can be seen that predicted solutions have been confined to straight-edged semi-infinite barriers. The work described in this report subdivides the barrier into elements to enable a rigorous solution of any barrier shape. H Medwin[31], in 1989, described a technique for calculating the acoustical shadowing due to finite barriers. More than 20 years previous to Medwin's paper Biot and Tolstoy's[32] paper on normal coordinates provided a closed form solution to the diffraction of a pulse by an infinite rigid wedge. Medwin made use of Biot and Tolstoy's pulse solution for an infinite wedge as a building block, which when used in conjunction with a computer, can produce both time- and frequency-domain solutions to real-world problems of shadowing by finite noise barriers.

The advantage of the pulse description when adapted to digital computer calculations is the same as in physical model experiments which use pulse techniques; a diffracted contribution from each barrier edge can be initiated at the least time when the pulse diffracts from the edge and it can be terminated at the instant when the diffracted pulse from the end of the edge has passed. Superposition gives the total impulse when there is more than one edge. The total temporal response can then be Fourier tranformed digitally to provide the desired frequency response of the finite barrier.

In 1982, Y Nicolas, T F W Embleton and J E Piercy[54] chose to concentrate on the effects of diffraction and to minimise the effects of ground reflection. They chose to compare three different methods of performing the diffraction part of the

calculation using the same method for calculating ground effects. For the latter, a method was chosen which had previously been successful for predicting the propagation of sound over various ground surfaces (without barriers). The Weyl-Van der Pol formulation familiar for the propagation of electromagnetic waves[33] is used as adapted for acoustics by Rudnick[34] and corrected by Chessell[35]. The ground is considered as a semi-infinite porous medium whose acoustic properties can be specified using a single parameter, the flow resistivity, by empirical equations of Delany and Bazley[36].

The three methods used for the diffraction part of the calculation are:

(1) *The first order approximate Macdonald solution*

The computer program 'SCREEN' of Isei et al[2] is used for prediction here, including the effect of the ground. The reflection coefficient of the barrier is assumed to be unity.

(2) *Line integral solution*

The classical theory of diffraction is the Kirchhoff-Fresnel theory which is much used in optics. Embleton[27] removed the approximations implicit in using a constant obliquity factor, unity or otherwise, by numerically evaluating a line integral formulation based on the Young-Rubinowicz solution. The program 'DIFRCT' described by Isei et al[2] is used for this calculation, and it too includes the effect of the ground.

(3) *Macdonald solution*

The more exact solution proposed originally by Macdonald[9] in 1915 for diffraction by a rigid wedge has been improved by a number of investigations. Ambaud and Bergassoli[37] computed the amplitudes of the diffracted wave, and confirmed them by measurements in an anechoic chamber. While useful, these results do not form a satisfactory basis for the design of noise barriers because

(a) there are extreme computational difficulties[38], (b) distances between the barrier and source or receiver are limited to a small number of wavelengths for both the computational method and the measurements, (c) the environmental field is perfectly anechoic, without the reflecting ground plane, and (d) tests are done for only one frequency, 10 kHz.

Fortunately, Hadden and Pierce[38] have adapted the theory to a form which can readily be integrated numerically with established Laguerre techniques.

Due to the increase in interest in protection against noise in industrial enclosures, E Katarbinska[39] presented a method of calculating the insertion loss of an acoustic barrier in a flat room. The calculation requires that both diffraction and reflection phenomena are taken into account.

A relatively simple case is a barrier in a flat room where the energy of the waves reflected from the boundary walls is negligibly small compared with the energy of a direct wave and waves reflected from the floor and the roof. Bolleter[40] describes a flat room as a room the height of which is at least five times lower than the other two dimensions.

Kurze[41] has presented the theoretical model of the shielding by a barrier in a flat room, filled with randomly distributed, small scatterers. The barriers insertion loss is due to the shielding of the direct and diffuse field and enhancement of the scattered field because of reflections from a barrier. This approach is based on the statistical concept of the scattered sound.

Katarbinska presented a different approach. To analyse both reflection and diffraction phenomena new assumptions to the image source method have been introduced. The analysis of barrier performance is made for a semi-infinite rigid screen, located in a flat empty room, when the sound source is an omnidirectional

point source. The energy of airborne sound and of sound energy going through the barrier is neglected.

Katarbinska concluded that the insertion loss of a barrier in a flat room is influenced by:

(a) the reduction or limitation of the direct waves and the waves reflected from the floor and the roof;

(b) the presence of the waves diffracted over the barriers edges and the reflected-diffracted waves.

The new assumptions of the expanded image source method allow for geometrical analysis of the reflected wave and the reflected-diffracted wave field, which lead to a simple algorithm of the barriers insertion loss.

The theoretical model of the barrier's performance in a flat room was initially verified by model scale measurements.

André L'Esperance[42] presented a paper in 1989, the purpose being to extend, to the case of finite barriers, the method suggested by Jonasson[17] for computing the insertion loss of infinite barriers on the ground. It combines diffraction theory with a model for sound propagation over the ground to estimate the diffracted field created by each diffracted path. The diffracted paths are identified by simple geometrical considerations. The method was compared with the models proposed by Thomasson[21] and Medwin[31] and with experimental measurements. However, the barriers studied by Thomasson were rather long compared to their height, which did not allow a significant diffraction contribution around the sides of the barrier. Also, the source-barrier and barrier-receiver distances that he considers are quite large in comparison to the height of the screen (a typical ratio is 10:1). In practical situations, barriers are often erected near the source or receiver, making his model inappropriate.

Medwin[31] studied the case of a barrier with a height-length ratio of approximately 0.5, with comparable source-barrier and receiver-barrier distances.

In 1991, D C Hothersall, S N Chandler-Wilde and M N Hajmirzae[43] used a numerical model to investigate the sound field in the region of outdoor noise barriers using the boundary element method. The model can be applied to barriers of different cross-sectional shapes and arbitrary distribution of surface cover. The model is two-dimensional but results show good agreement with those obtained for the three-dimensional problem of propagation from a point source over a noise barrier of infinite length. The model is used to compare the efficiency of a wide range of constructions of single noise barriers of different height, cross-sectional shape and surface cover. The effects of the ground are also considered.

The results of the numerical model do not predict the absolute values of the insertion loss of barriers for incoherent line sources such as road traffic. However, the model provides useful predictions of the relative performance of the barrier forms for this type of source.

The numerical model confirms that barrier height is of fundamental importance to the attenuation produced. Also, the type of ground cover has a large effect upon the calculated insertion loss of barriers. However, for the configurations considered it appears that this effect is largely independent of the form of the barrier.

For barriers with reflecting surfaces, those with vertical or nearly vertical sides perform significantly better than those with shallow sloping sides. There is general agreement that the insertion loss for the wedge is lower than for the screen, but no concensus as to the magnitude of this effect.

Kawai and Terai[44], in 1990, theoretically investigated diffracted fields by thin rigid or absorbant barriers by using integral equations derived from Helmholtz-

Kirchhoff's formula and from its normal derivative. The surface of the barrier is divided into elements to solve the integration equations numerically and the potential is assumed to be uniform on each element. For the numerical treatment of the integral equations in three dimensions, the integral including the strongly singular kernel is evaluated by the line integral along the edge of the element: this reduces the amount of computation and avoids the difficulty due to singularity. A numerical method which removes the problem of singularity is also presented to solve the integral equations in two dimensions. For a flat rigid barrier, farfield solutions in the high frequency range are evaluated asymptotically on the basis of Kirchhoff's boundary conditions and compared with exact solutions.

In 1992, Trevor J Cox and Y W Lam[45] concentrated on the application of various solutions of the Helmholtz-Kirchhoff integral equation to predict the scattering from simple finite sized rigid reflectors commonly found in auditoria. These were plane panels and cylindrically curved panels. For the more approximate prediction methods their limitations were defined in terms of the accuracy achieved and the range over which the methods were applicable. These methods were also used to investigate the use of a cut-off frequency to describe the limit above which specular type reflections dominate the scattering. It was found to be applicable only close to the geometric scattering angle. The scattering due to curvature was predicted by considering the variation in the direction of the local normal to the panel surface.

Also, in 1992, Y W Lam an S C Roberts[46] developed a simple model of diffraction that predicts accurately the insertion loss of finite length barriers. The model is based on the geometric theory of minimum diffracted paths. Assumptions were made on the phase and amplitude of each diffracted wave to obtain a new and rather simple formulation of the solution. It provides a clear picture of the sound attenuation performance of a barrier as a function of barrier length. Extensive model experiments are used to verify the model. The model's accuracy in

predicting the overall pattern of the narrow-band insertion loss is found to be comparable to that of an integral equation method, although the latter method produces better prediction in the fine details of the sound field. The model is much simpler than and as accurate as other methods that apply the usual geometric solutions to each diffracted path, and represents a major improvement on Maekawa's energy summation method for octave band finite barrier calculations.

In 1994, Y W Lam[47] describes a simple model for the calculation of finite length barrier insertion loss, based on the concept of minimum diffraction paths. It makes use of Maekawa's empirical curve to estimate the attenuation associated with each diffracted path. However, instead of summing the energy contributions of the diffracted waves as suggested by Maekawa, a new formulation of phase relationships between the waves is developed to allow pressure summation. The result is a model which is simple to use and yet has accuracy substantially better than Mackawa's energy summation method, in predicting both narrow and octave band insertion loss of finite length barriers. It is believed that the model is both simple and accurate enough to replace Maekawa's energy summation method in engineering practice.

Also, in 1994, Y W Lam[48] developed a simple model for the calculations of the attenuation of complex ground terrain profiles. The model is based on the simple ground reflection and minimum diffraction path developed by Y W Lam and S C Roberts[46]. The ground model is compared with existing environmental noise calculation models: the draft ISO[50] model, the CONCAWE[51,52] model and ENM[53]. It is found that the new ground model has the best overall performance and agrees well with measured data on a variety of ground terrain profiles and conditions. The measured data are taken from the existing literature and cover both short- and long-range propagation. Serious errors are also found in the draft ISO model and in ENM which cast doubts on their suitability as standard environmental noise calculation models.

Takagi, Hotta and Yamamoto[49], in 1994, presented a practical expression for the estimation of sound attenuation by a finite barrier. The attenuation is determined by taking account of sound contributions from rectangular sections of a plane barrier located between a point source and a receiver. The expression for the attenuation due to a finite length barrier is finally formulated by combining the attenuations due to semi-infinite plane barriers.

Scale model experiments were carried out to check the validity of the expression and the results showed good agreement between them. It is shown that the expression obtained is useful and applicable to the design of a finite length barrier when the sound source has a broad band spectrum and the overall sound pressure level is a matter of interest.

The aim of this work is to predict by calculation the noise reduction by finite barriers. The theoretical background is based on Kirchhoff-Fresnel diffraction theory, from which an easy to use computer package has been compiled.

The work described in this thesis, therefore, gives greater flexibility in predicting noise reduction by finite barriers in free space, in outside conditions and also in enclosures. Comparison is made with results obtained by other workers for similar barrier geometries.

3 DESCRIPTION OF WORK PRESENTED IN THIS REPORT

Although much work has been carried out on the predicuction of sound losses by semi-infinite barriers in outside conditions, little research has been undertaken in predicting sound losses due to finite barriers within enclosures. The main aim of this thesis, therefore, was to ultimately construct a model which will predict sound attenuation by finite barriers within enclosures, and thus simulate conditions which may prevail in factories. In recent years, hearing loss, due to excess noise in factories, has become a major issue and this thesis tries to predict ways of minimising this noise before the practical difficulties are encountered.

The research began by using the classical diffraction theory outlined by Born and Wolf[1] to develop a model by which the barriers' surface was divided into elements. By incorporating Babinets' Principle, this allowed the attenuation of sound to be predicted by a finite barrier in free space. It was assumed that the sound source was a point source of monotonic frequency. This assumption was made for two reasons, firstly because this type of source lends itself most favourably to a clear description of the diffraction technique and secondly because it acts as a basic model upon which the theory for more complex types of source may be developed at some later stage.

The barrier was assumed to be two-dimensional and the free space environment was initially assumed, again, because it served as a basic theoretical model which allowed other models to be developed to suit more complex environments later on.

Computer programs were written in Fortran, for both the zero and first order models. The models were compared to discover which was the more productive and used to identify the optimum element size to give an accuracy within the precision grade of measurement

Validation of the basic theory was accomplished by comparison with Fresnel and Fraunhofer diffraction theory. Further validation was accomplished by using the

elemental computer model, with no barrier present, to examine the effect of extending the source-receiver distance.

Having established a theory that gave flexibility in calculating attenuation by a finite barrier in free space, the model was extended to predict insertion loss, using a barrier in contact with the ground. There is much contemporary literature for this model and the author compares his findings with other workers for similar barrier geometries.

A further extension to the research was to place the barrier in a flat room, which includes reflections of the sound waves from the roof as well as the floor, but ignores the contribution of the walls. This model examines the effect on insertion loss of increasing the aspect ratio of width/height of the barrier. Although there is a dearth of research using barriers in enclosures, the author is able to compare the trends of his model with that of other recent work.

Finally, side walls were introduced into the model to see if there have any significant effect as compared to the flat room model.

4 NUMERICAL SOLUTION OF THE KIRCHHOFF-FRESNEL DIFFRACTION EQUATION

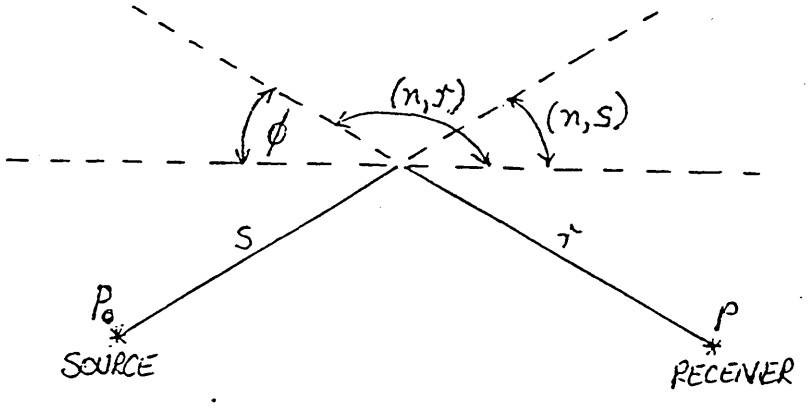

According to the Kirchhof-Fresnel diffraction theory, the amplitude at P, due to sound diffracted through the hole is given by:

$$\cup_{(P)} = \frac{A}{4\pi}\iint_S \frac{e^{ik(r+s)}}{rs}\left[\left(ik-\frac{1}{r}\right)\cos(n,r)-\left(ik-\frac{1}{s}\right)\cos(n,s)\right]dS \qquad (4.1)$$

where S = surface of the hole

A = amplitude at unit distance from the source

k = wave number = $\frac{2\pi}{\lambda}$

It is more convenient to introduce $\theta = (n, s)$ and $\varnothing = 180° - (n, r)$ so that

$$\cos\theta = \cos(n, s)$$

$$-\cos\varnothing = \cos(n, r)$$

[NOTE: The diagram above is actually in three dimensions so that generally the vectors r and s do not lie in the same plane.]

$$\cup_{(P)} = -\frac{A}{4\pi}\iint_S \frac{e^{ik(r+s)}}{rs}\left[\left(ik-\frac{1}{r}\right)\cos\varnothing+\left(ik-\frac{1}{s}\right)\cos\theta\right]dS \qquad (4.2)$$

Now we can re-write equation (4.2) as follow:

$$\cup_{(P)} = -\frac{A}{4\pi}\iint_S e^{ik(r+s)}F(r,s)dS \tag{4.3}$$

$$\text{where } F(r,s) = \frac{1}{rs}\left[\left(ik-\frac{1}{r}\right)\cos\varnothing + \left(ik-\frac{1}{s}\right)\cos\theta\right] \tag{4.3}$$

At high frequencies, the variations of $k(r + s)$ and hence $e^{ik(r+s)}$ will be considerably greater than the variation of $F(r, s)$ as we move across the area over which the integration is taking place. Therefore it should be possible to obtain a more rapid convergence of a finite element integration if $F(r, s)$ is treated as a constant over the area of integration whilst the term $e^{ik(r+s)}$ is integrated explicitly.

Hence by making s sufficiently small we may effect the following simplifications of equation (4.3).

$$\cup_{(P)} = -\frac{A\,F(r,s)}{4\pi}\iint_S e^{ik(r+s)}ds \tag{4.4}$$

Consider a small rectangular area in the generalised barrier plane shown below:

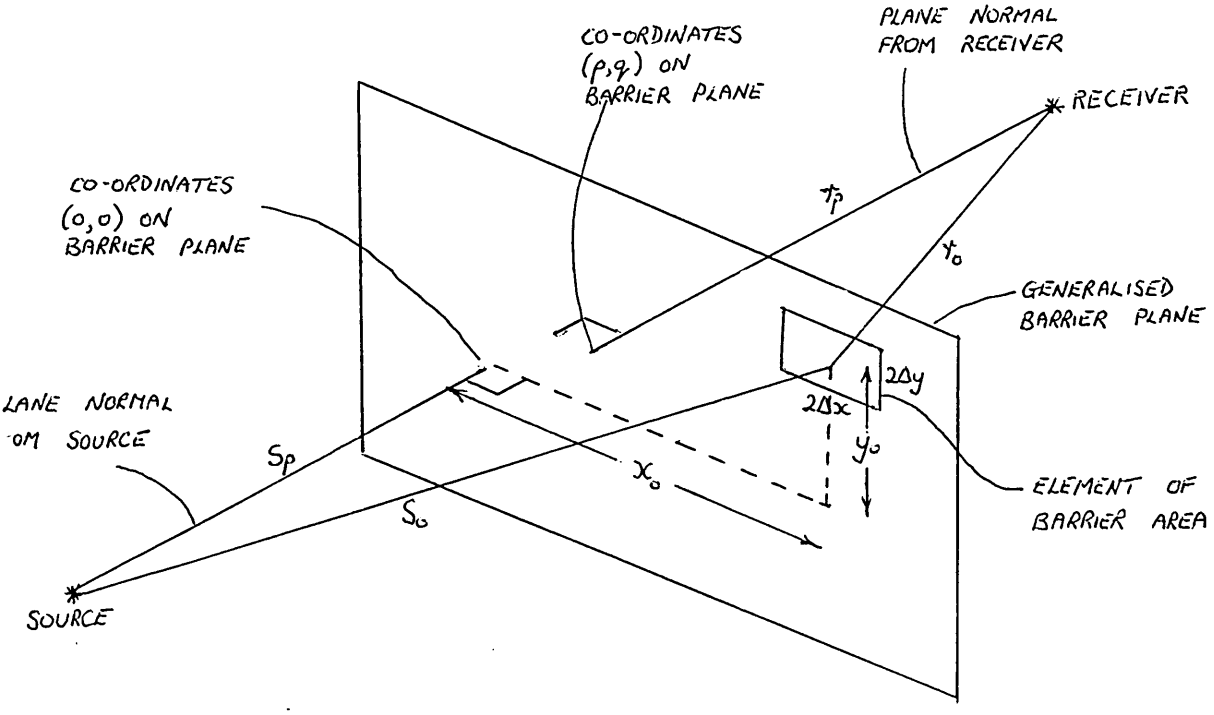

Figure 3 Small rectangular area in a generalised barrier plane

The intersection between the barrier plane normal to the source and the barrier plane has coordinates (o, o) along x and y where both x and y are specified as being in the barrier plane.

Let the centre of the element under consideration, from the source, be specified by coordinates $(x_o + x, y_o + y)$ where x, y may take values between $\pm\Delta x$, $\pm\Delta y$ respectively.

Then, for a general point:

$$s = \sqrt{s_p^{\,2} + (x_o + x)^2 + (y_o + y)^2}$$

ie $$s = \left(s_p^{\,2} + x_0^{\,2} + 2x_o x + y_o^{\,2} + 2y_o y + x^2 + y^2\right)^{\frac{1}{2}}$$

However, x^2 and y^2 are very small compared to the other terms and can be ignored.

But from the diagram:

$$s_o^{\,2} = s_p^{\,2} + x_o^{\,2} + y_o^{\,2}$$

so $$s \approx \sqrt{s_o^{\,2} + 2(x_o x + y_o y)} \text{ for small } x, y$$

ie $$s \approx s_o \sqrt{1 + \frac{2}{s_o^{\,2}}(x_o x + y_o y)}$$

or $$s \approx s_o + \frac{1}{s_o}(x_o x + y_o y)$$

Now in the case of r

$$r = \sqrt{r_p^{\,2} + (x_o - p + x)^2 + (y_0 - q + y)^2}$$

ie

$$r = \left(r_p^{\,2} + x_o^{\,2} - 2px_o + 2x_o x - 2px + p^2 + x^2 + y_o^{\,2} - 2qy_o + 2y_o y - 2qy - q^2 + y^2\right)^{\frac{1}{2}}$$

But $$r_o = \sqrt{r_p^{\,2} + x_o^{\,2} - 2px_o + p^2 + y_o^{\,2} - 2qy_o + q^2}$$

giving $$r = \sqrt{r_o^{\,2} + 2x_o x - 2px + 2y_o y - 2qy + x^2 + y^2}$$

Again x^2 and y^2 are very small compared to the other terms and can be ignored.

ie $$r \approx r_o + \frac{1}{r_o}\left[x(x_o - p) + y(y_o - q)\right]$$

and so $r + s$ may be written as:

$$r + s = r_o + s_o + x\left[\frac{x_o}{s_o} + \frac{(x_o - p)}{r_o}\right] + y\left[\frac{y_o}{s_o} + \frac{(y_o - q)}{r_o}\right]$$

or more conveniently:

$$r + s = r_o + s_o + ax + by$$

where $a = \left[\frac{x_o}{s_o} + \frac{(x_o - p)}{r_o}\right]$, $b = \left[\frac{y_o}{s_o} + \frac{(y_o - q)}{r_o}\right]$

and equation (4.4) then becomes:

$$\cup_{(p)} = -\frac{A.F(r_o, s_o)}{4\pi} . e^{ik(r_o + s_o)} \int_{-\Delta y}^{\Delta y} \int_{-\Delta x}^{\Delta x} e^{ikax} . e^{ikby} dxdy$$

Now, $\int_{-\Delta y}^{\Delta y} \int_{-\Delta x}^{\Delta x} e^{ikax} . e^{ikby} dxdy = \int_{-\Delta y}^{\Delta y} e^{ikby} dy \int_{-\Delta x}^{\Delta x} e^{ikax} dx$

$$= \left[\frac{e^{ikby}}{ikb}\right]_{-\Delta y}^{\Delta y} \left[\frac{e^{ikax}}{ika}\right]_{-\Delta x}^{\Delta x}$$

$$= \frac{1}{ikb}\left[e^{ikb\Delta y} - e^{-ikb\Delta y}\right] \frac{1}{ika}\left[e^{ika\Delta x} - e^{-ika\Delta x}\right]$$

But $\frac{1}{i}\left(e^{ix} - e^{-ix}\right) = 2\sin x$

so the integral becomes:

$$\frac{4}{k^2 ab} \sin(kb\Delta y) \sin(ka\Delta x)$$ and is therefore ALL REAL

As a result, two approximations now become possible.

(1) **"Crude" Zero Order Approximation**

As $\Delta x, \Delta y \rightarrow 0$

and hence $ka\Delta x, kb\Delta y \rightarrow 0$

$\sin(ka\Delta x), \sin(kb\Delta y) \rightarrow ka\Delta x, kb\Delta y$

$$\cup_{(p)} = \sum_{\substack{\text{all} \\ \text{elements}}} -\frac{AF(r,s)}{4\pi} e^{ik(r_o+s_o)} \frac{4}{k^2 ab} ka\Delta x, kb\Delta y$$

and for (r,s) in $F(r,s)$ we must choose $r = r_o$, $s = s_o$ as the best mean values, so

$$\cup_{(p)} = \sum_{\substack{\text{all} \\ \text{elements}}} -\frac{A}{\pi} F(r_o, s_o) e^{ik(r_o+s_o)} \Delta x, \Delta y$$

(2) **"More Refined" 1st Order Approximation**

$$\cup_{(p)} = \sum_{\substack{\text{all} \\ \text{elements}}} -\frac{A}{\pi} F(r_o, s_o) e^{ik(r_o+s_o)} \frac{\sin(ka\Delta x)\sin(kb\Delta y)}{k^2 ab}$$

4.1 **Computational Details**

The term $F(r_o, s_o) e^{ik(r_o+s_o)}$ needs to be separated into real and imaginary parts.

Now $F(r_o, s_o) = \frac{1}{r_o s_o}\left[\left(ik - \frac{1}{r_o}\right)\cos\varnothing + \left(ik - \frac{1}{s_o}\right)\cos\theta\right]$

$$= -\frac{1}{r_o^2 s_o^2}(r_o \cos\theta + s_o \cos\varnothing) + \frac{ik}{r_o s_o}(\cos\theta + \cos\varnothing)$$

Also, $e^{ik(r_o+s_o)} = \cos[k(r_o + s_o)] + i \sin[k(r_o + s_o)]$

Real terms are:

$$-\frac{1}{r_o^2 s_o^2}[\cos[k(r_o + s_o)](r_o \cos\theta + s_o \cos\varnothing)] - \frac{ik}{r_o s_o}[\sin[k(r_o + s_o)](\cos\theta + \cos\varnothing)]$$

Imaginary terms are:

$$-\frac{i}{r_o^{\,2}s_o^{\,2}}\left[\sin\left[k(r_o+s_o)\right](r_o\cos\theta+s_o\cos\varnothing)\right]+\frac{ik}{r_o s_o}\left[\cos\left[k(r_o+s_o)\right](\cos\theta+\cos\varnothing)\right]$$

In order to calculate these real and imaginary terms, $x_0$and y_0 must first be specified for the element.

Then s_o can be calculated from:

$$s_o=\left(s_p^{\,2}+x_o^{\,2}+y_o^{\,2}\right)^{1/2}$$

and r_o from:

$$r_o=\left(r_p^{\,2}+(x_o-p)^2+(y_0-q)^2\right)^{1/2}$$

This in turn enables cosθ to be calculated from:

$$\cos\theta=\frac{s_p}{s_o}$$

and cos∅ from:

$$\cos\varnothing=\frac{r_p}{r_o}$$

The "constants" a and b need to be evaluated as they have a particular value for each element.

$$a=\left[\frac{x_o}{s_o}+\frac{x_o-p}{r_o}\right]$$

$$b=\left[\frac{y_o}{s_o}+\frac{y_o-q}{r_o}\right]$$

We are now able to compute the intensity of sound which would pass through a hole which has the same geometry as the barrier. However, in order to calculate the effect of the barrier rather than the effect of the hole of the same geometry we use Babinet's principle:

$$\cup_{(B)} = \cup_{(D)} - \cup_{(H)}$$

where $\cup_{(B)}$ is the sound pressure at the receiver when the barrier is present

$\cup_{(D)}$ is the sound pressure at the receiver in the absence of any sort of barrier

$\cup_{(H)}$ is the sound pressure at the receiver due to a hole the same size and geometry as the barrier

Now $\cup_{(D)} = \dfrac{Ae^{ikd}}{d}$

but $e^{ikd} = \cos(kd) + i\sin(kd)$ and d is the distance between the source and receiver and is given by:

$$d = \left(\left(r_p + s_p\right)^2 + p^2 + q^2\right)^{\frac{1}{2}}$$

The attenuation due to the barrier will therefore be:

$$\text{Attenuation} = 10\log\left[\frac{\cup_{(B)} d^2}{A^2}\right](dB)$$

Sound attenuation can then be calculated by the programs in Appendices 1 and 2. The program in Appendix 1 uses the first order approximation and the program in Appendix 2 uses the zero order model.

The programs in Appendices 3 and 4 are respective derivations of the programs in Appendices 1 and 2, which enable us to investigate what effect reducing the size of the elements, and hence increasing the number of elements, might have on the accuracy of the results.

4.2 **Investigation on the effect of element size on convergence**

Figure 4 compares the zero and first order models at a frequency of 1kHz, using a 10 m square barrier. Figures 5 and 6 examine the number of elements required for a 5 m square and a 15 m square barrier to converge to its ultimate sound attenuation. Figure 7 uses a high frequency, 10 kHz, in order to find the optimum element size that will give accuracy within precision grade measurement.

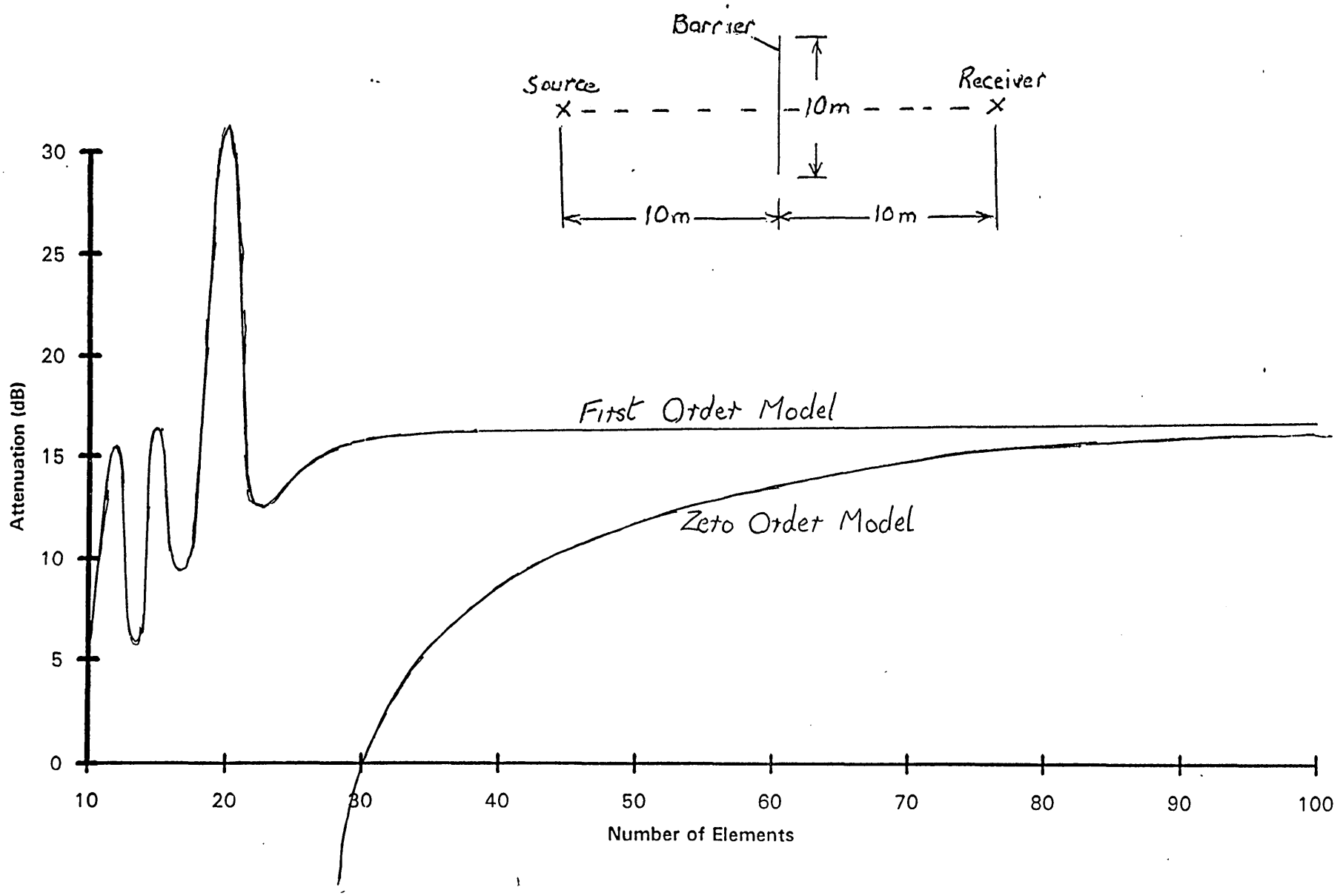

Figure 4 Comparison of 'zero' and first order models at a frequency of 1kHz, using a 10 m square barrier in free space

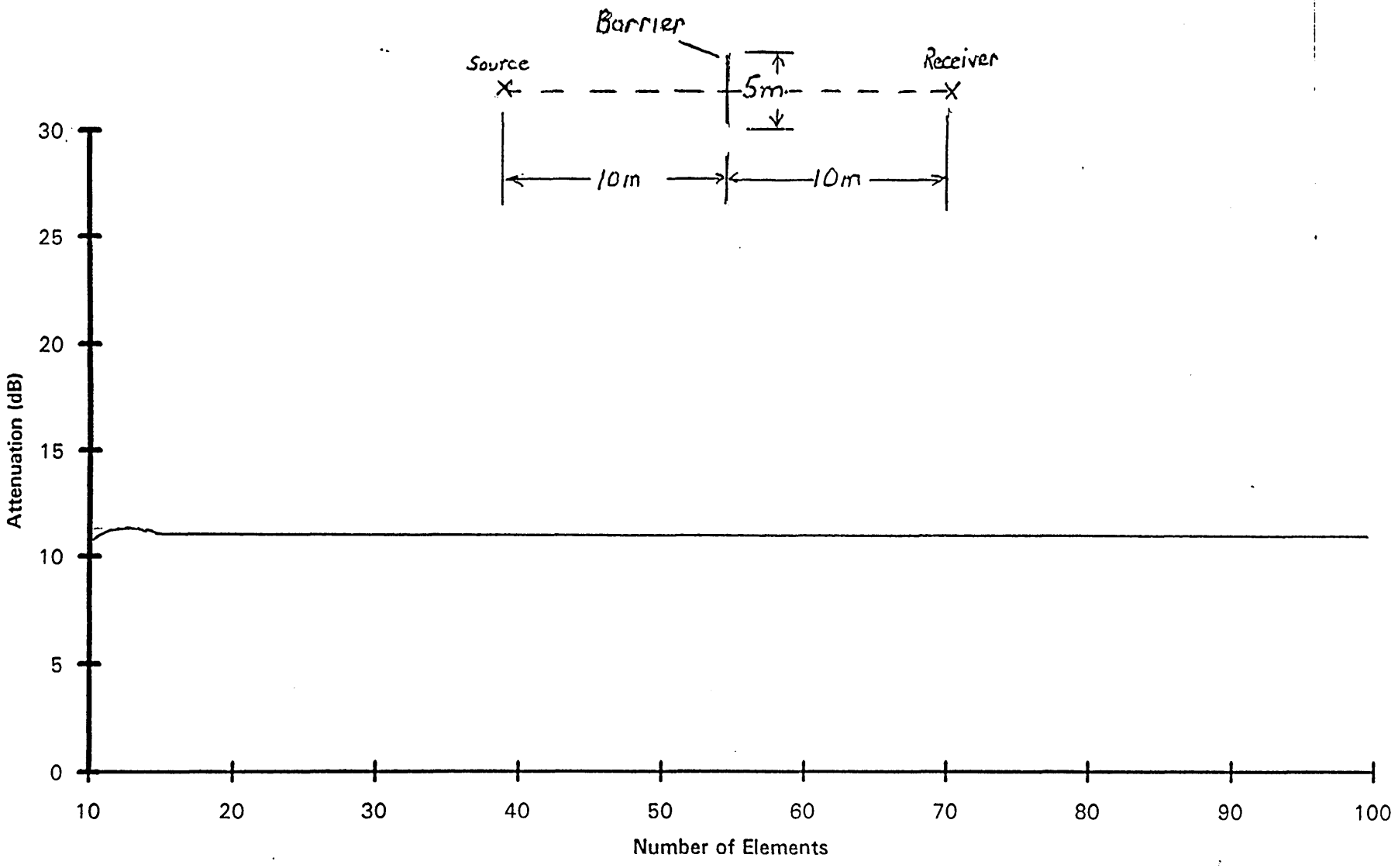

Figure 5 Investigation on the effect of element size on convergence using the first order model for a 5 m square barrier in free space at a frequency of 1kHz.

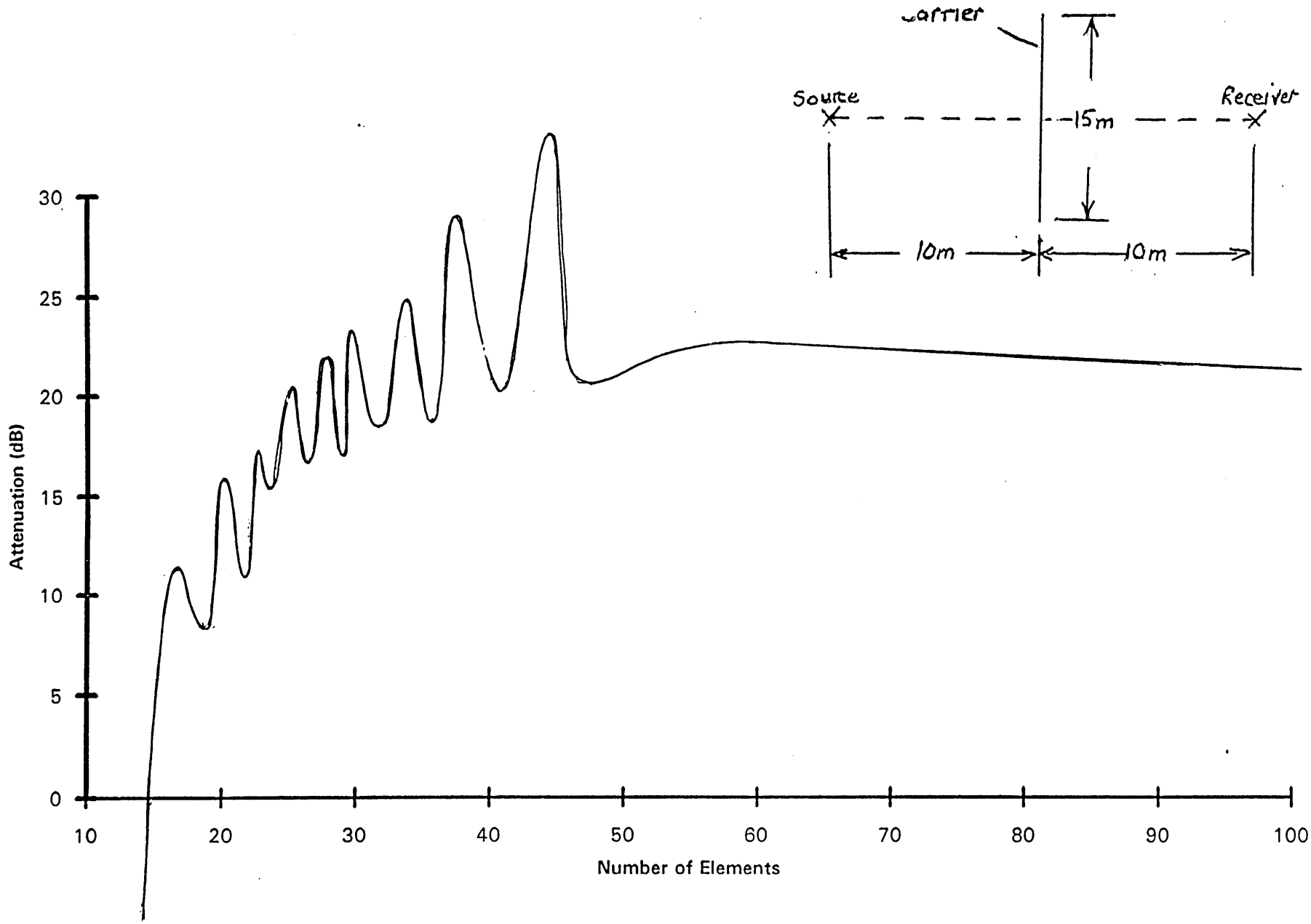

Figure 6 Investigation on the effect of element size on convergence using the first order model for a 15 m square barrier in free space at a frequency of 1kHz

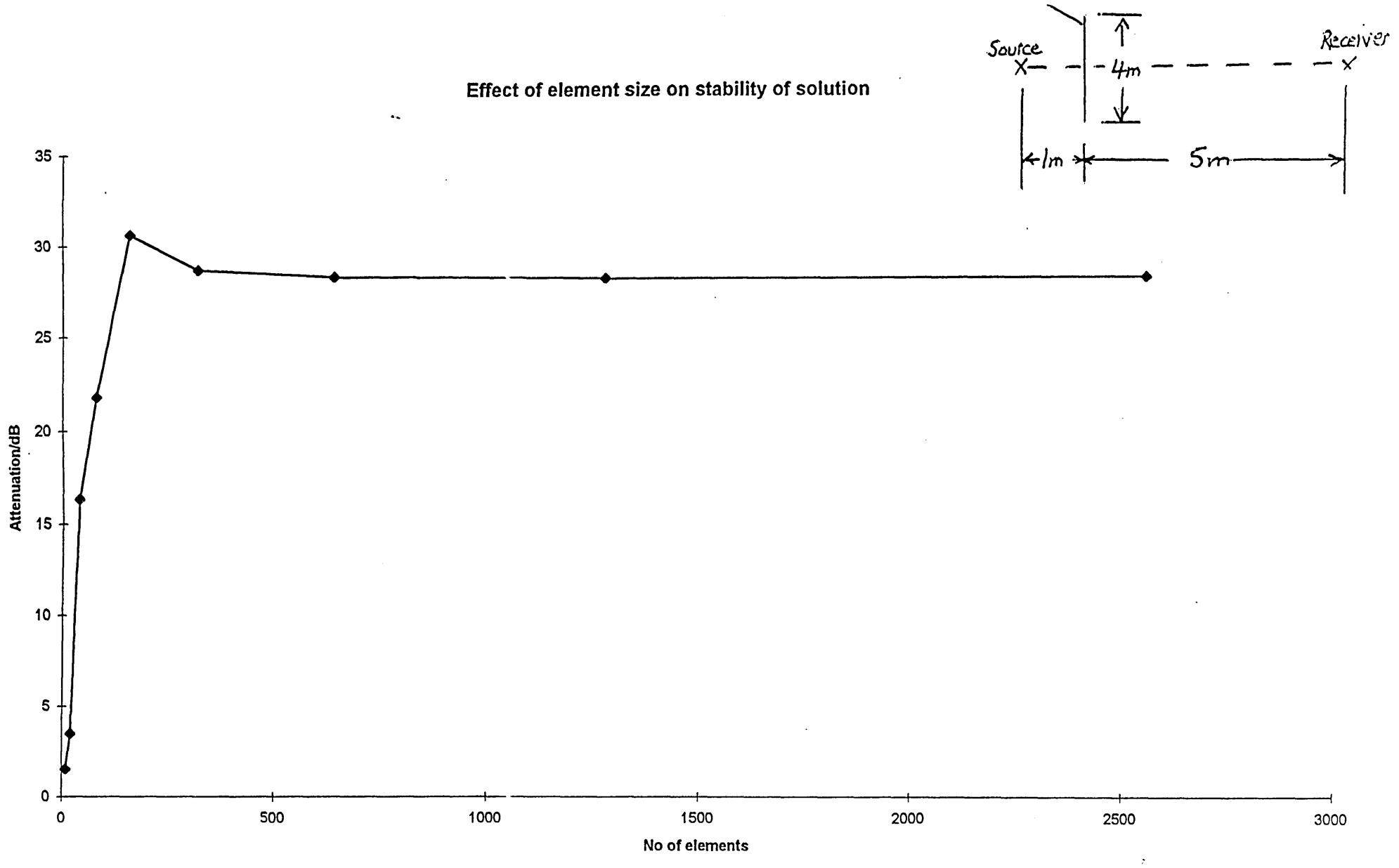

Figure 7 Investigation on the effect of element size on convergence using the first order model for a 4 m square barrier in free space at a frequency of 10kHz

4.3 Discussion on the effect of element size on convergence

Figure 4 shows the attenuation, using a barrier in free space, and highlights the contrast in the results using a first order model, based on the Kirchhoff-Fresnel integral, to that of a zero order model. Using a 10 m square barrier at a frequency of 1 kHz, the first order model converged to within 1% of its ultimate value using just 1600 elements, ie 40 elements per side. The zero order model only reached 55% of this value when the same number of elements were used. It is therefore more productive to use the first order model with fewer elements.

Figures 5 and 6 use the first order model to predict the attentuation for a 5 m square and a 15 m square barrier respectively. The 5 m square barrier converges using 400 elements, ie 20 elements per side, and the 15 m square barrier converges using 6400 elements, ie 80 elements per side.

At a high frequency of 10 kHz, figure 7 demonstrates that more elements are required for the sound attenuation to converge to it's ultimate value. For a 4 m square barrier, 102400 elements, ie 320 elements per side, were required to predict a sound attenuation within 2% of the ultimate value. This 2% accuracy represents a change of 0.57 dB, and in context of measurement standards 0.57 dB can be compared to the degree of uncertainty using a precision grade sound level meter, where at mid-frequency the tolerance is ± 1dB. Thus, it is justified in this work to consider an optimum element size for accuracy within the precision grade of measurement, which is approximately 0.0125 m.

5 VALIDATION OF RESULTS

Ideally we should now set up a barrier in free space and practically verify the results that have been obtained from the computer model. This, however, is not a possibility, so the results from the computer model have to be validated by other means.

Diffraction phenomena are divided into two classes:

(i) those where the source or receiver, or both, are at finite distance from the aperture, called Fresnel diffraction, and

(ii) those where the source and receiver are effectively at infinite distance from the aperture, called Fraunhofer diffraction.

Showing that the results from the computer model accurately reflect Fresnel diffraction, and in certain circumstances give a reasonable approximation to Fraunhofer diffraction will support the validity of the computer model.

5.1 Simulation of Fresnel Diffraction using Kirchhoff-Fresnel Diffraction Computer Model

Figure 8 in Jenkins and White[29] shows the effect of adding the amplitudes of successive half-period zones, which are alternately positive and negative.

To simulate the Fresnel diffraction theory from Jenkins and White[29], we sub-divide the half-period zones into smaller zones, and convert the zero order computer model. This program adds the amplitudes due to the areas of these successive circular zones, increasing the radius of each area by a small amount, Δx, each time, see Figure 9.

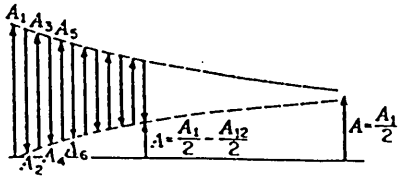

FIGURE 8:
Addition of the amplitudes from half-period zones.

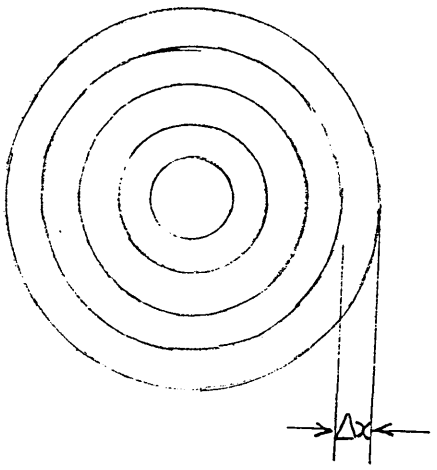

Figure 9 Addition of the amplitudes due to the areas of successive circular zones

Now

$$\left.\begin{array}{r}\text{Area of zone 1} = \pi(\Delta x)^2 \\ \text{Area of zones 1 and 2} = \pi(2\Delta x)^2 = 4\pi(\Delta x)^2\end{array}\right\} \therefore \text{Area of zone 2} = 4\pi(\Delta x)^2 - \pi(\Delta x)^2 = 3\pi(\Delta x)^2$$

$$\left.\begin{array}{r}\text{Area of zones 1 2 and 3} = \pi(3\Delta x)^2 = 9\pi(\Delta x)^2\end{array}\right\} \therefore \text{Area of zone 3} = 9\pi(\Delta x)^2 - 4\pi(\Delta x)^2 = 5\pi(\Delta x)^2$$

$$\left.\begin{array}{r}\text{Area of zones 1 2 3 and 4} = \pi(4\Delta x)^2 = 16\pi(\Delta x)^2\end{array}\right\} \therefore \text{Area of zone 4} = 16\pi(\Delta x)^2 - 9\pi(\Delta x)^2 = 7\pi(\Delta x)^2 \quad \text{etc...}$$

The area of each successive zone can be found by the relationship $(2n-1)\pi(\Delta x)^2$. The program in Appendix 5 converts the zero order model to simulate Fresnel diffraction.

Fresnel diffraction theory predicts that the distance from the outer edge of each half-period zone is half a wavelength further away from the receiver than the previous one. This is shown in Figure 10.

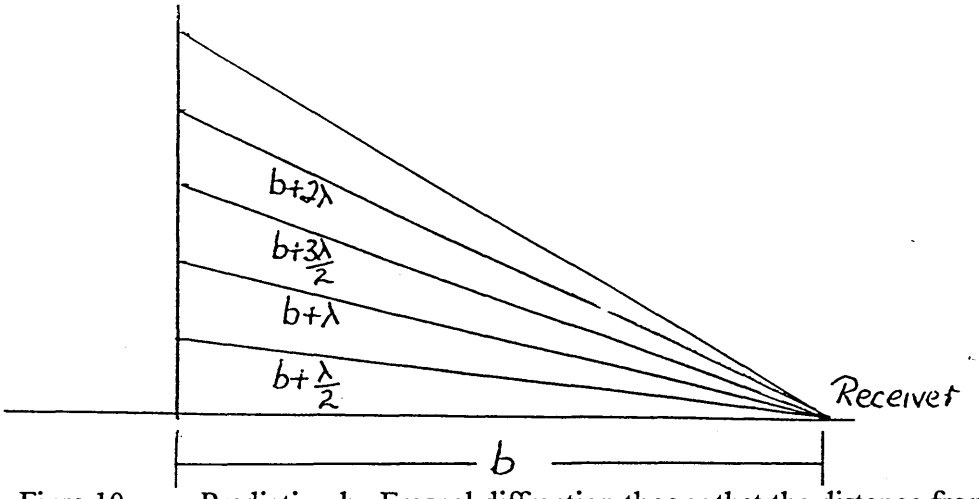

Fiure 10 Prediction by Fresnel diffraction theory that the distance from the outer edge of each half-period zone is half a wavelength further away from the receiver than the previous one

However, since we have a point source, the half-period zones are formed by each outer edge being a quarter of a wavelength further from both source and receiver, than the previous one, Figure 11.

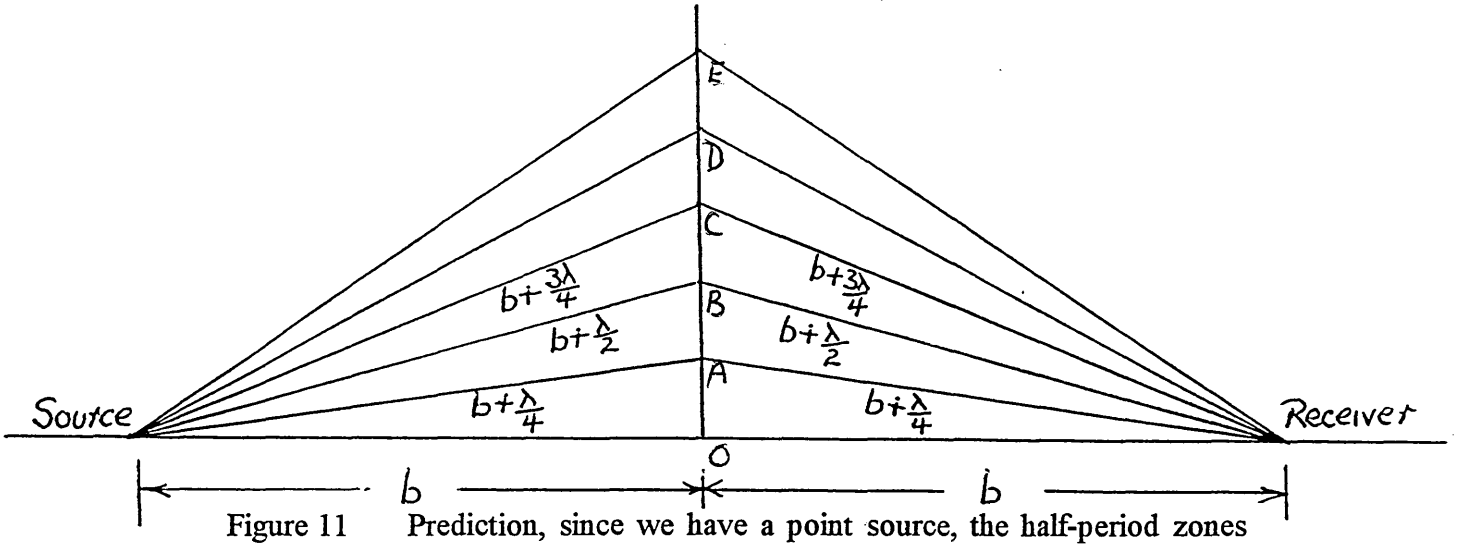

Figure 11 Prediction, since we have a point source, the half-period zones are formed by each outer edge being a quarter of a wavelength further from both source and receiver, than the previous one

Taking a round hole, where the distance of the source and receiver from the hole are 10 m the wavelength is 0.34 m and the element size is 0.025 m, we are able to predict the position of each half-period from zone using Pythagoras' Theorem:

$$OA = \surd (10.085^2 - 10^2) = 1.307 \quad \equiv \quad \frac{1.307}{0.025} = 52 \text{ elements}$$

$$OB = \surd (10.17^2 - 10^2) = 1.852 \quad \equiv \quad \frac{1.852}{0.025} = 74 \text{ elements}$$

$$OC = \surd (10.255^2 - 10^2) = 2.273 \quad \equiv \quad \frac{2.273}{0.025} = 91 \text{ elements}$$

$$OD = \surd (10.34^2 - 10^2) = 2.630 \quad \equiv \quad \frac{2.630}{0.025} = 105 \text{ elements}$$

$$\vdots \qquad = 118 \text{ elements}$$

$$\vdots \qquad = 129 \text{ elements}$$

$$\vdots \qquad = 140 \text{ elements}$$

$$\vdots \qquad = 150 \text{ elements}$$

$$\vdots \qquad = 159 \text{ elements}$$

etc

The amplitude at the receiver should, therefore, be a maximum after 52 elements, a minimum after 74 elements, a maximum after 91 elements, a minimum after 105 elements, and should continue to alternate in this way. We should also observe that the maximum values should steadily decrease while the minimum values should steadily increase.

The program in Appendix 5, which simulates Fresnel diffraction, produced results which used the same parameters as were used in the prediction from the theory. The graph, in Figure 12, of relative amplitude against half-period zone, from these results, clearly shows that the relative amplitude alternates to give steadily decreasing maxima and steadily increasing minima. The results also show that these maxima and minima occur at exactly the positions which were predicted from the theory.

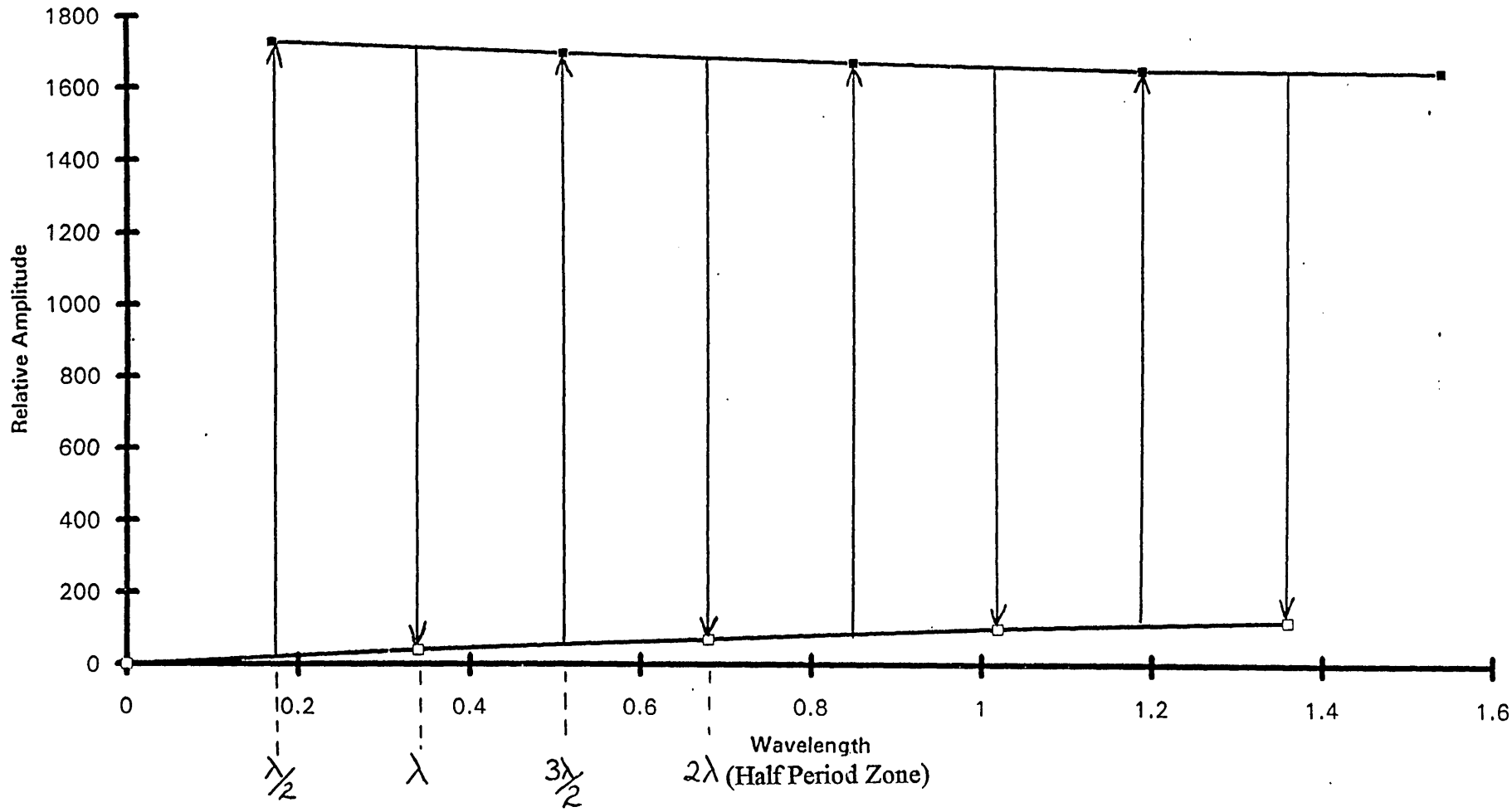

Figure 12 Simulation of Fresnel Diffraction using an increased circular aperture at a frequency of 1kHz where the source and receiver distances are 10 m

5.2 Simulation of Fraunhofer Diffraction using Kirchhoff-Fresnel Diffraction Computer Model

Jenkins and White[30] illustrate that Fraunhofer diffraction at a single slit gives a minimum value of intensity when $\beta = \pm\pi$, $\pm 2\pi$, $\pm 3\pi$, etc, and a maximum value of intensity when $\beta = \pm 1.433\pi$, $\pm 2.46\pi$, $\pm 3.47\pi$, $\pm 4.4774\pi$, etc. β is a convenient variable, which signifies one-half the phase difference between the contributions coming from opposite edges of the slit, see fig. 13.

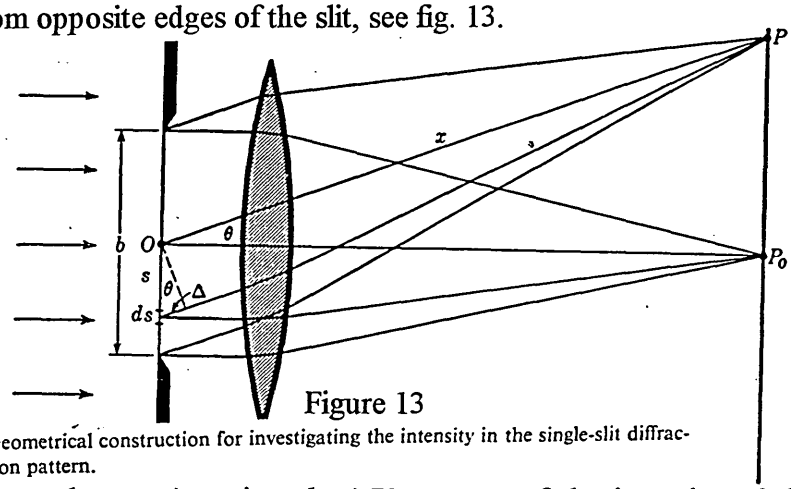

Figure 13

Geometrical construction for investigating the intensity in the single-slit diffraction pattern.

The first secondary maximum is only 4.72 percent of the intensity of the central maximum, while the second and third secondary maxima are only 1.65 and 0.83 percent respectively.

For a minimum, we have

$$\beta = m\pi = \frac{\pi b(\sin i + \sin\theta)}{\lambda}$$

where b is the slit width, i is the angle that incident light makes with the normal and θ is the angle where each secondary wave reaches point P.

but $\sin i = 0$

Therefore, $m\pi = \dfrac{\pi b \sin\theta}{\lambda}$

ie. $\sin\theta = \dfrac{m\lambda}{b}$

For a maximum, we have

at 1st secondary, $.43\pi = \frac{\pi b \sin\theta}{\lambda}$

therefore, $\sin\theta = \frac{1.43\lambda}{b}$

at 2nd secondary, $\sin\theta = \frac{2.46\lambda}{b}$

at 3rd secondary, $\sin\theta = \frac{3.47\lambda}{b}$, etc

If we use the above theory, with a 2 m wide slit, wavelength of 0.34 m and the source and receiver placed centrally 50 m either side of the slit, we can calculate the positions of the maxima and minima when the receiver position is moved away from its central position.

The following table illustrates these calculations:

Maxima		**Minima**	
θ(degree)	**Offset from centre of slit (m)**	**θ(degree)**	**Offset from centre of slit (m)**
0	0	9.79	8.62
14.04	12.53	19.88	18.08
24.72	23.02	30.66	29.65
36.15	36.53	42.84	46.37

The program in Appendix 6 converts our original computer model to simulate the above calculations by the first order approximation.

The results from the program in appendix 6 give maximum and minimum values of intensity at almost the predicted positions. The results give first, second and third secondary maxima of 4.6%, 1.3% and 0.47% of the central maxima for intensity. This compares with respective values of 4.72%, 1.65% and 0.83% from the Fraunhofer diffraction theory.

The results from the computer model are shown graphically, Figure 14, where relative intensity is plotted against receiver offset.

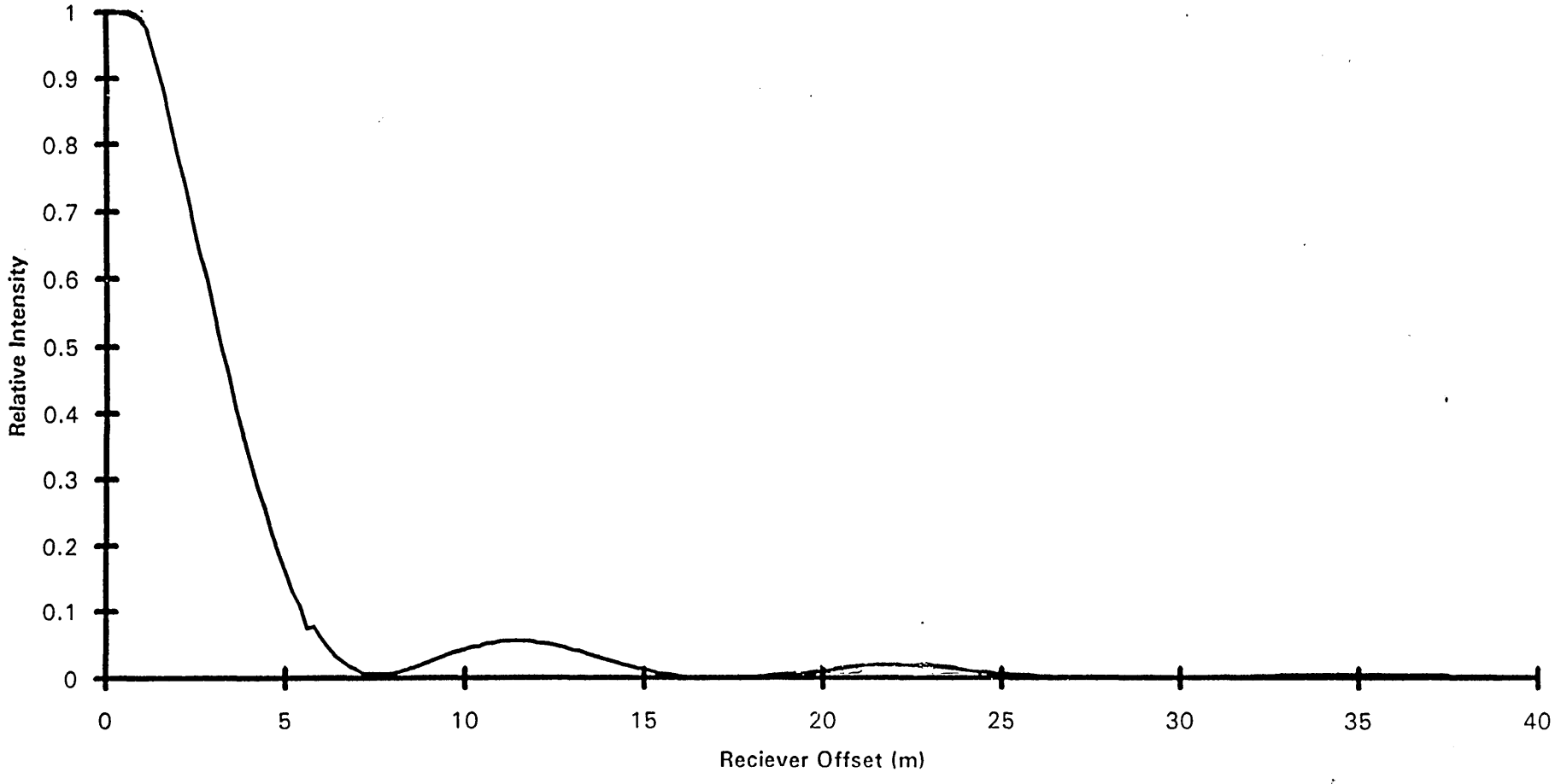

Figure 14 Simulation of Fraunhofer Diffraction using a 2 m wide slit, wavelength 0.34 m, and source and receiver distances of 50 m

5.3 Using the elemental model to effect the sound level by increasing the source-receiver distance, with no barrier present

In using Babinet's Principle, the sound pressure at the receiver in the absence of any sort of barrier, $\cup_D$, is given by:

$$\cup_D = \frac{Ae^{ikd}}{d}$$

The same values for this sound pressure can be attained by the elemental theory of the basic model if this theory is correct. Using a 50 m square area to represent free space, with element sizes of 0.025 m, the source-receiver distance was progressively doubled, using a frequency of 1 kHz. Figure 15 shows a 6 dB reduction in sound level for each doubling of source-receiver distance, and so confirms the well known theoretical result.

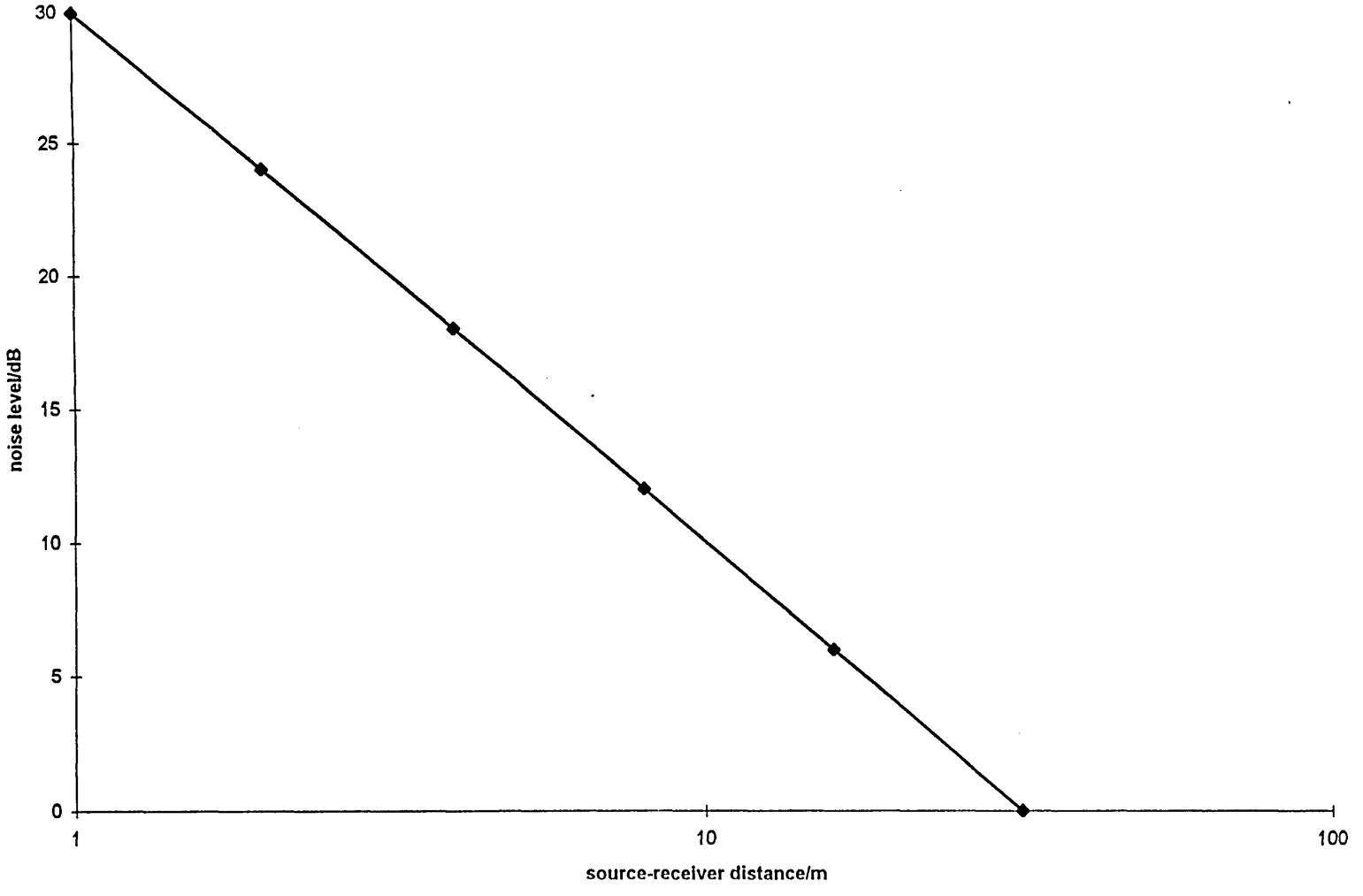

Figure 15 6dB reduction in sound level for each doubling of source-receiver distance

5.4 **Results for a barrier in free space**

Having verified the behaviour of the model it is now possible to generate results for a rectangular barrier in free space.

Using a 2 m x 4 m barrier, Figure 16 shows the variation of attenuation with increasing frequency when the receiver-barrier distance is successively doubled. Figure 17 shows what effect moving the receiver away from the central position has on the level of sound attenuation.

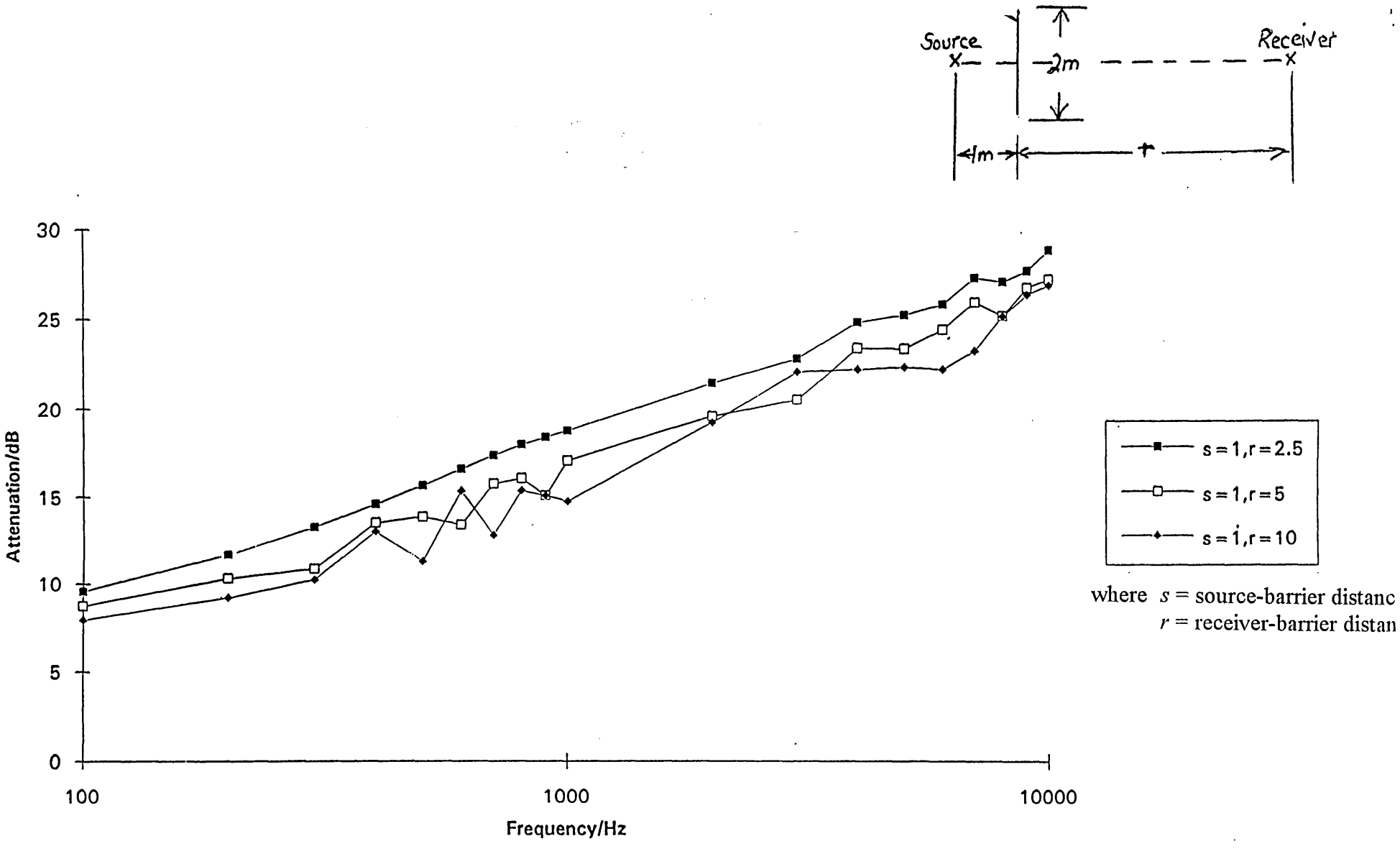

Figure 16 Variation of attenuation with frequency for a barrier in free-space

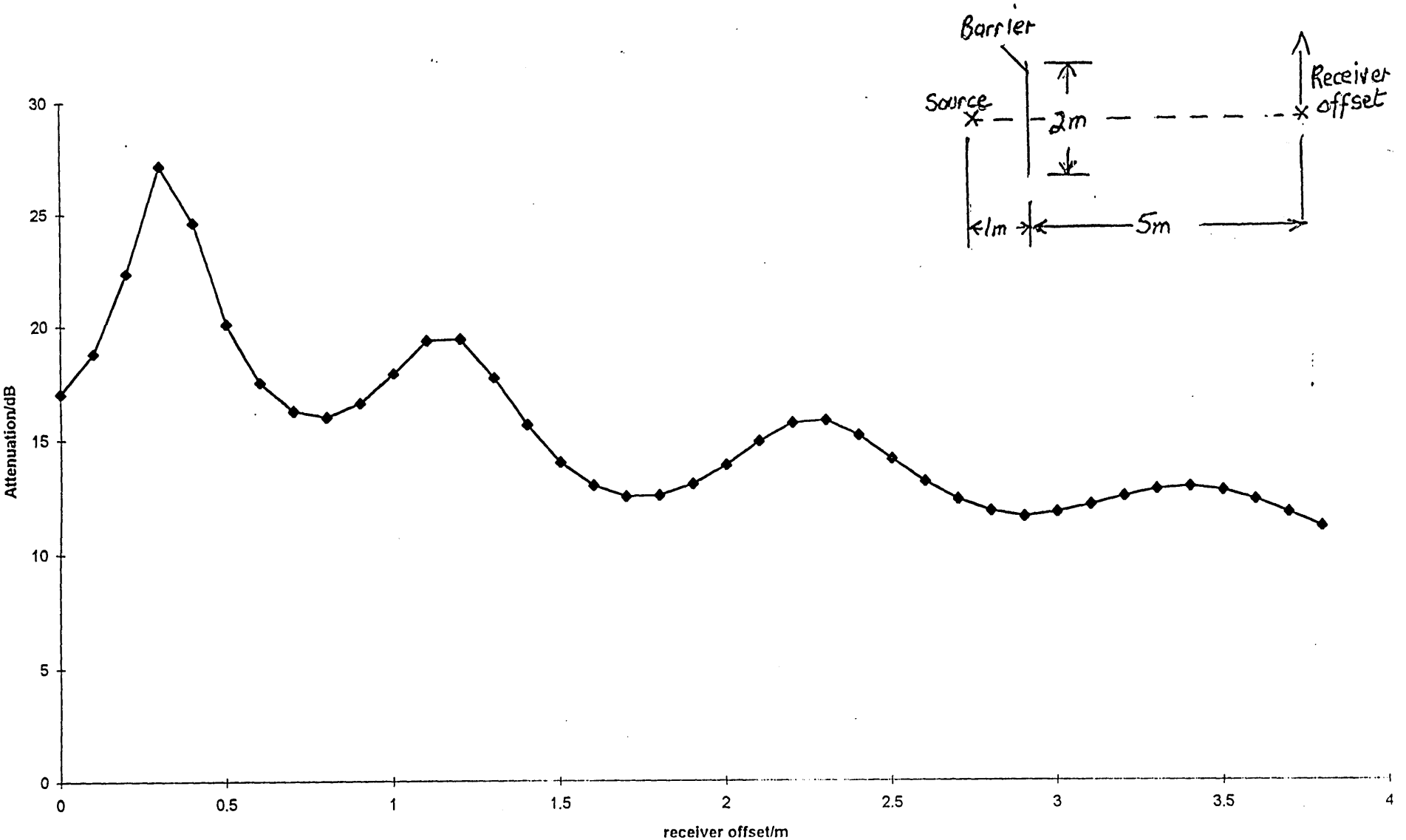

Figure 17 Effect of changing receiver position for a barrier in free-space

5.5 Discussion of results for a barrier in free space

Much of the research in this thesis uses a barrier size of 4 m x 2 m, and in free space conditions Figure 16 shows three curves where the receiver-barrier distances are successively doubled from 2.5 m, 5 m and 10 m. Each curve shows a trend of attenuation steadily increases with respective increases in frequency. Also, increasing the receiver distance lowers the sound attenuation for respective frequencies, but introduces more rapid deviations from the line of general trend.

These recalcitrant deviations from the general trend are caused by the sensitivity of the trigonometric terms, $\cos[k(r_o + s_o)]$ and $\sin[k(r_o + s_o)]$. Instability will occur at high frequencies where the wave number $k = 2\pi/\lambda$ will change rapidly due to the low values of the wavelength λ. These same trigonometric terms will also oscillate more rapidly, and so become more sensitive, as the source-element, s_o, and/or receiver-element, r_o, distances are increased.

Figure 17 shows variations in attenuation as the receiver is moved away from its central position. We see that the sound attenuation decreases with increasing receiver offset, but the curve oscillates about the general reducing trend. The sound pressure at the receiver when the barrier is present, $\cup_B$, is calculated using Babinet's Principle, $\cup_B = \cup_D - \cup_H$, where $\cup_D$ is the sound pressure at the receiver in the absence of the barrier, and $\cup_H$ is the sound pressure at the receiver due to a hole the same size as the barrier. Now $\cup_D$ and $\cup_H$ are constantly changing phase so the sound pressure, $\cup_B$, will vary according to the difference in the amplitudes due to these phase changes. The sound pressures are greatest near the central position and so the phase changes produce greater deviations from the general trend in central positions.

Changing the position of the receiver has the same effect as leaving the receiver in a stationary position and changing the angle of the barrier, therefore increased attenuation may be possible sloping the barrier away from the normal.

6 BARRIER IN CONTACT WITH THE GROUND

The principles employed for calculating the sound attenuation by a barrier in free space, are again used for a barrier in contact with the ground. The calculation becomes more complex, however, because we now have to consider reflected contributions from the ground as well as the direct sound pressure, as discussed in chapter 4.

In order to find the attenuation of a barrier in contact with the ground we apply Babinet's Principle rigidly. The sound diffracted round the barrier is simply the difference between what reaches the receiver directly and what passes through a hole of the same geometry as the barrier. We then need no longer worry about subtle aspects of the barrier geometry.

In order to perform the calculation correctly, the direct amplitude $\cup_D$ must include the reflected component. This is a simple reflection problem, but the complex reflection coefficient, Cr, can be incorporated for the specular angle of reflection. Figure 18 shows the angle of incidence, *i*, and the angle of reflection, *r*, for the reflected sound path.

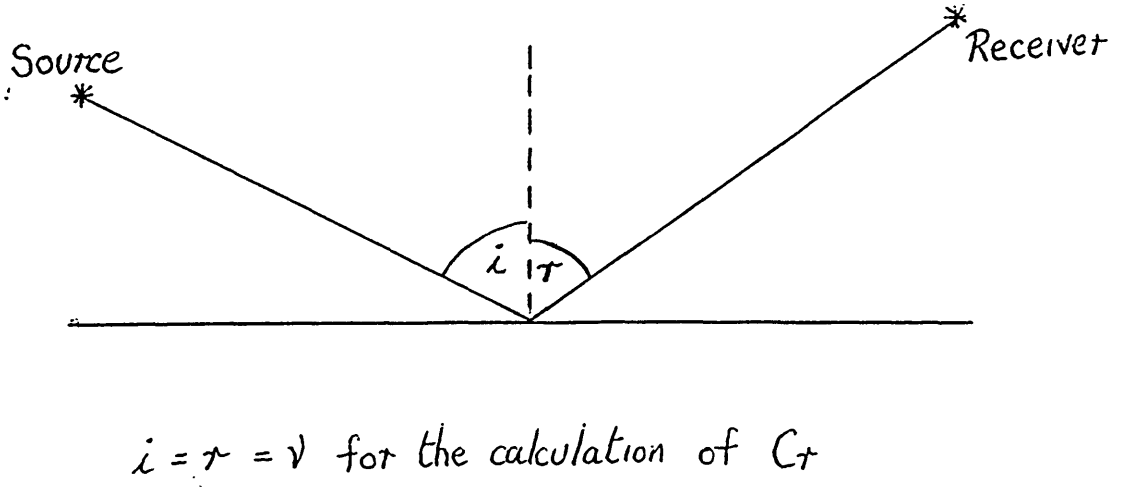

Figure 18 Reflected sound path, showing angle of incidence and reflection

Referring to Theoretical Acoustics by Philip M Morse and K Uno Ingard pages 259-264, for frequency - dependent surface impedance, the reflection coefficient, Cr, is given by:

$$Cr + \frac{(\omega^2 - \omega_o^2) + i\omega[R/m) - ((\rho c / m\cos v)]}{(\omega^2 - \omega_o^2) + i\omega[(R/m) + (\rho c / m\cos v)]}$$

Where

ω is the frequency of the applied medium

ω_o is the resonant frequency of the ground material

R is the mechanical resistance factor

m is the effective mass per unit area

ρc is the characteristic impedance of the medium

For very low frequencies ($\omega << \omega_0$), the reflection coefficient, Cr, becomes unity, independent of v: the incident pressure wave is reflected with no change in amplitude or phase: thus no energy is absorbed by the reflecting material. This is also true for very high frequencies ($\omega >> \omega_0$). At resonance ($\omega \approx \omega_0$), however, Cr is smaller than unity and dependent on the angle of incidence v. The reflected intensity at resonance is smallest when the angle of incidence is arccos ($\rho c/R$), if $R > \rho c$, or for normal incidence, if $R < \rho c$.

To remove complex numbers from the denominator of the expression for Cr, we multiply both numerator and denominator by the complex conjugate of the denominator.

Therefore

$$Cr = \frac{(\omega^2 - \omega_o^2) + i\omega[(R/m) - ((\rho c / m\cos\nu)]}{(\omega^2 - \omega_o^2) + i\omega[(R/m) + (\rho c / m\cos\nu)]} \cdot \frac{(\omega^2 - \omega_o^2) - i\omega[R/m) + (\rho c / m\cos\nu)]}{(\omega^2 - \omega_o^2) - i\omega[R/m) + (\rho c / m\cos\nu)]}$$

$$Cr = (\omega^2 - \omega_o^2)^2 + \omega^2[(R/m) - (\rho c / m\cos\nu)].[(R/m) + (\rho c / m\cos\nu)]$$

$$\frac{+i\omega(\omega^2 - \omega_o^2)[(R/m) - \rho c / m\cos\nu)] - i\omega(\omega^2 - \omega_o^2)[(R/m) + (\rho c / m\cos\nu)]}{(\omega^2 - \omega_o^2)^2 + \omega^2[(R/m) + (\rho c / m\cos\nu)]^2}$$

$$Cr = \frac{(\omega^2 - \omega_o^2)^2 + \omega^2[(R/m)^2 - (pc / m\cos\nu)^2] - 2i\omega(\omega^2 - \omega_o^2)(pc / m\cos\nu)}{(\omega^2 - \omega_o^2) + \omega^2[(R/m) + (pc / m\cos\nu)]^2}$$

or Cr = CORL -iCOIM

where $CORL = \dfrac{\left(\omega^2 - \omega_o^{\,2}\right)^2 + \left[(R/m)^2 - (\rho c / m\cos\nu)^2\right]}{\left(\omega^2 - \omega_o^{\,2}\right)^2 + \left[(R/m) + (\rho c / m\cos\nu)\right]^2}$

and $COIM = \dfrac{2\omega\left(\omega^2 - \omega_o^{\,2}\right)(\rho c / m\cos\nu)}{\left(\omega^2 - \omega_o^{\,2}\right)^2 + \left[(R/m)^2 - (\rho c / m\cos\nu)^2\right]}$

6.1 **Computational Details**

Calculation of the sound passing through the a hole, the same geometry as the barrier.

The following cases need to be considered:

1 Direct diffracted sound, source-receiver

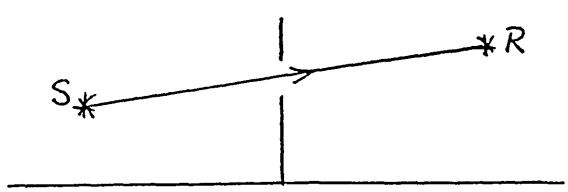

2 Sound initially reflected and then diffracted

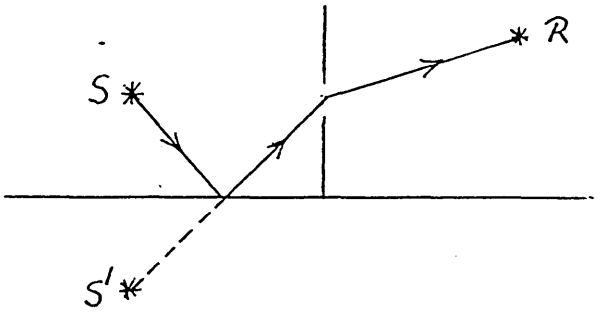

3 Sound initially diffracted and then reflected

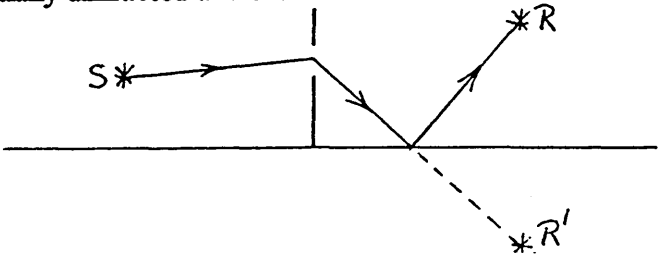

4 Sound initially reflected, then diffracted and then reflected again

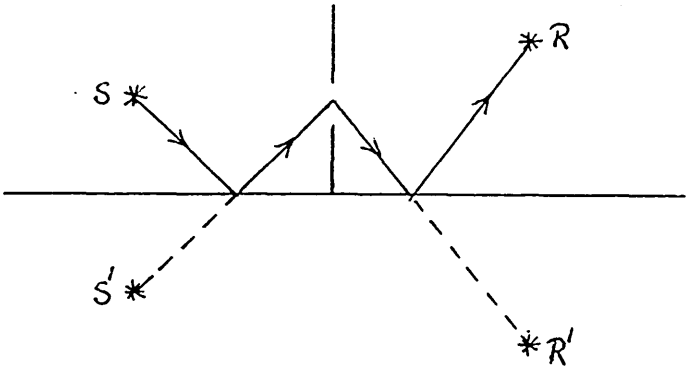

All four sound pressures need to be combined to produce a total complex sound pressure for that passing through the hole, ie $\cup_H$.

Then, the pressure of the sound around the barrier, $\cup_B = \cup_D - \cup_H$.

Computation of the above four stages

(1) The direct diffracted sound is computed in exactly the same way as that in free space.

(2) Sound initially reflected and then diffracted

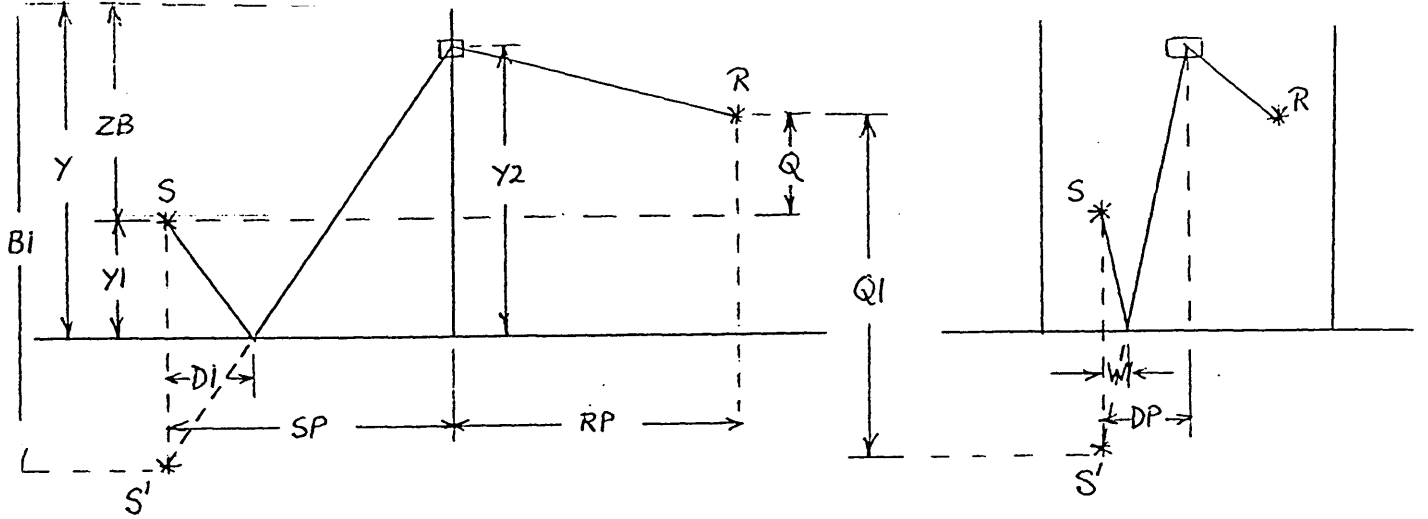

where y = barrier height and I and J are the respective horizontal and vertical locations of the element

$$ZB1 = ZB + 2.Y1$$

$$Q1 = Q + 2.Y1$$

For each element we compute the real and imaginary parts of the reflection coefficient ie *CORL* and *COIM*, and to do this we require the 3-dimensional angle ν, between the sound path and the normal.

On the side elevation

$$Y2 = Y - J.DY + DY/2$$

where *DY* is the size of the vertical element

and using similar triangles

$$\frac{Y1}{D1} = \frac{Y2}{(SP - D1)}$$

$$\therefore D1 = \frac{(Y1.SP)}{(Y1 + Y2)}$$

and for the end elevation

$$DP = \left((ZL - I.DX + DX/2)^2\right)^{1/2}$$

where DX is the size of the horizontal element

and again using similar triangles

$$\frac{Y1}{W1} = \frac{Y2}{(DP - W1)}$$

$$\therefore W1 = \frac{(Y1.DP)}{(Y1 + Y2)}$$

So

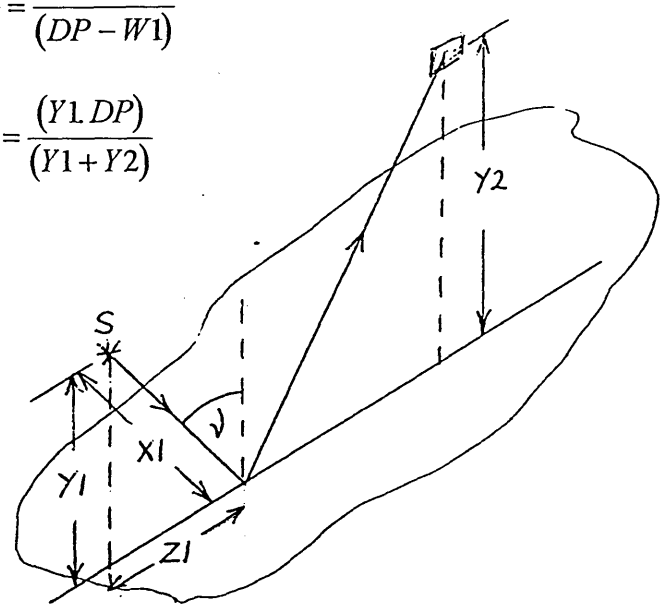

$$Z1 = \left(D1^2 + W1^2\right)^{1/2}$$

$$X1 = \left(Y1^2 + D1^2 + W1^2\right)^{1/2}$$

$$v = \arcsin\left(Z1/X1\right)$$

The sound pressure, which is initially reflected and then diffracted, can then be computed where

$$SOUNDPRESSURE = (RL.CORL + UNRL.COIM) + i(UNRL.CORL - RL.COIM)$$

where RL = real part of the sound pressure
UNRL = imaginary part of the sound prssure

(3) Sound initially diffracted and then reflected

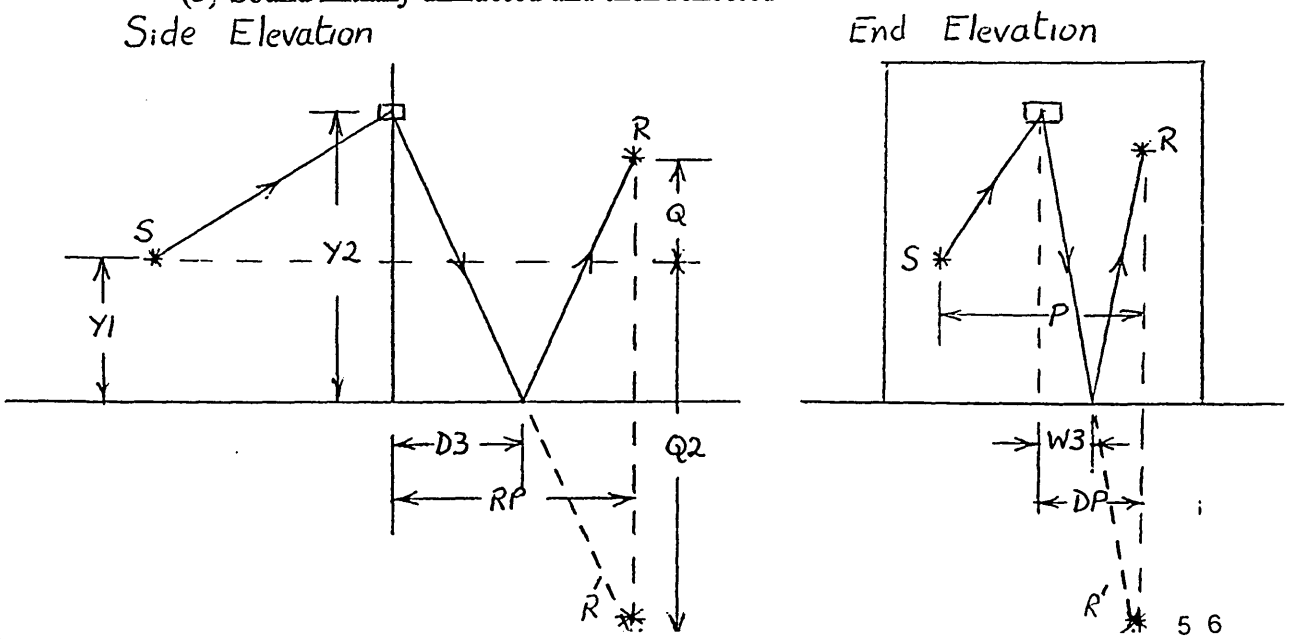

$$Q2 = -(Q + (2.Y1))$$

For each element we compute the real and imaginary parts of the reflection coefficient ie *CORL* and *COIM*, and to do this we require the 3-dimensional angle ν, between the sound path and the normal.

On the side elevation

$$Y2 = Y - J.DY + DY/2$$

and using similar triangles

$$\frac{Y2}{D3} = \frac{Q + Y1}{RP - D3}$$

$$\therefore D3 = \frac{(Y2.RP)}{(Y1 + Y2 + Q)}$$

and for the end elevation

$$DP = \left((XL - I.DX + DX/2 + P)^2\right)^{1/2}$$

and again using imilar triangles

$$\frac{Y2}{W3} = \frac{Y2.DP}{DP - W3}$$

$$\therefore W3 = \frac{(Y2.DP)}{(Y1 + Y2 + Q)}$$

So

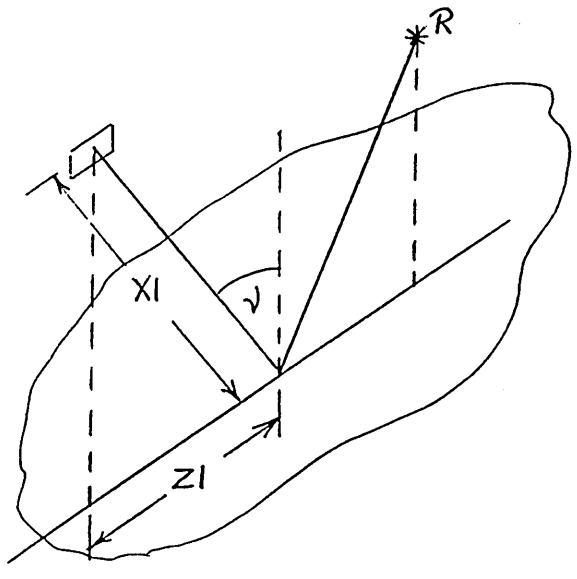

$$Z1 = \left(D3^2 + W3^2\right)^{1/2}$$

$$X1 = \left(Y2^2 + D3^2 + W3^2\right)^{1/2}$$

$$v = \arcsin\left(Z1/X1\right)$$

The sound pressure, which is initially diffracted and then reflected, can then be computed where

$$SOUND\ PRESSURE = \left(RL.CORL + UNRL.COIM\right) + i\left(UNRL.CORL - RL.COIM\right)$$

(4) Sound initially reflected, then diffracted and finally reflected again.

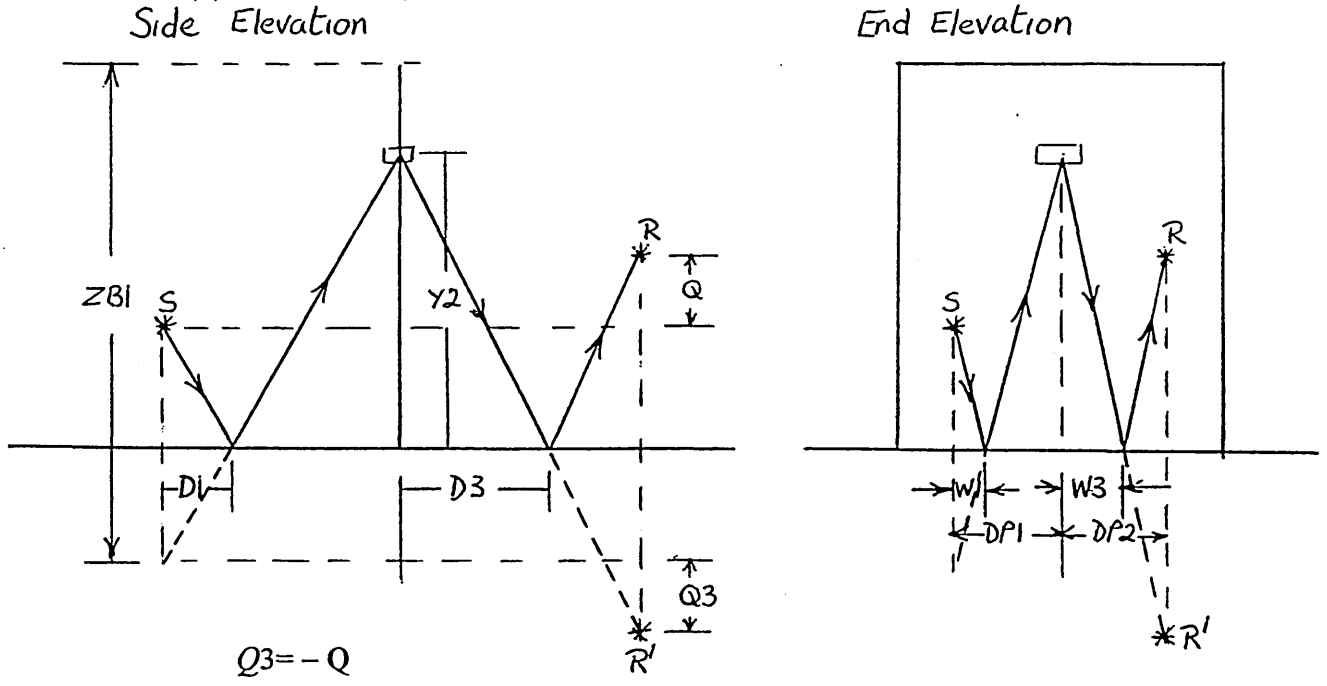

For each element we compute the real and imaginary parts of the reflection coefficient before diffraction takes place, ie CORL1 and COIM1, and also the real and imaginary parts of the reflection coefficient after diffraction, ie CORL2 and COIM2. In order to do this we require the respective 3-dimensional angles v_1 and v_2, which lie between the sound path and the normals at the respective points of reflection.

On the side elevation

$$Y2 = Y - J.DY + DY/2$$

and using similar triangles

$$D1 = \frac{(Y1.SP)}{(Y1+Y2)}$$

$$D3 = \frac{(Y2.RP)}{(Y1+Y2+Q)}$$

and for the end elevation

$$DP1 = \left((ZL - I.DX + DX/2)^2\right)^{1/2}$$

$$DP2 = \left((XL - I.DX + DX/2 + P)^2\right)^{1/2}$$

and again using similar triangles

$$W1 = \frac{(DP1.Y1)}{(Y1+Y2)}$$

$$W3 = \frac{(DP2.Y2)}{(Y1+Y2+Q)}$$

$$Z1 = \left(D1^2 + W1^2\right)^{1/2}$$

$$X1 = \left(Y1^2 + D1^2 + W1^2\right)^{1/2}$$

$$Z2 = \left(D3^2 + W3^2\right)^{1/2}$$

$$X2 = \left(Y2^2 + D3^2 + W3^2\right)^{1/2}$$

$$v_1 = \arcsin\left(Z1/X1\right)$$

$$v_2 = \arcsin\left(Z2/X2\right)$$

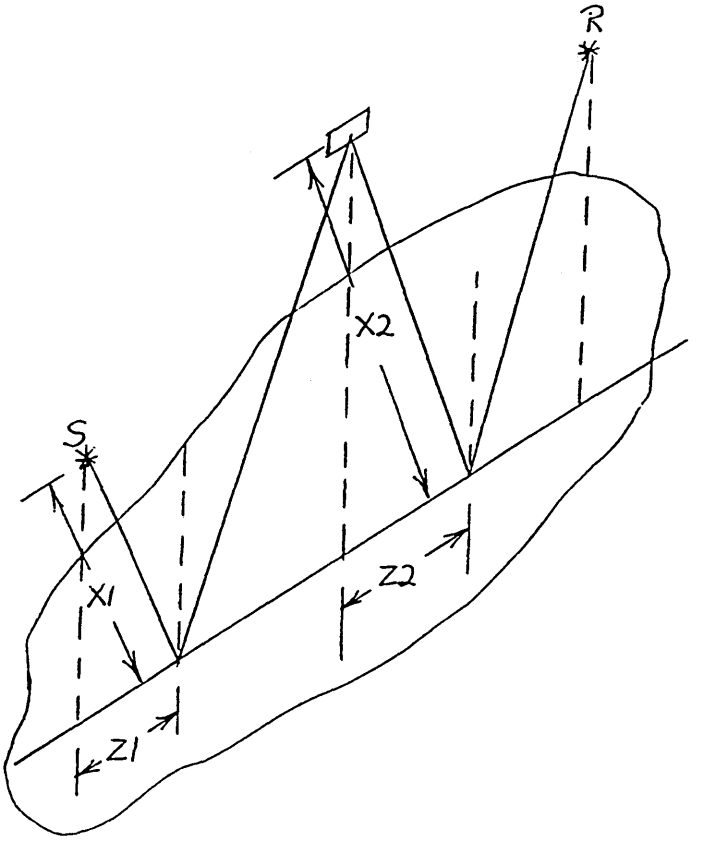

The sound pressure, which is initially reflected, then diffracted and then reflected again, can then be computed where

$$SOUND\ PRESSURE = (RL + iUNRL)(CORL1 - iCOIM1)(CORL2 - iCOIM2)$$

$$= (RL.CORL1.CORL2 + UNRL.COIM1.CORL2 + UNRL.CORL1.COIM2 - RL.COIM1.COIM2)$$

$$+i(UNRL.CORL1.CORL2 - RL.COIM1.CORL2 - RL.CORL1.COIM2 - UNRL.COIM1.COIM2)$$

The free space conditions were relatively easy to model because the sound pressure at the receiver in the absence of a barrier, $\cup_D$, was

$$\cup_D = \frac{Ae^{ikd}}{d}$$

The sound pressure in the absence of a barrier, where ground conditions exist, becomes a more complicated problem.

The problem is solved by treating the sound pressure, in the absence of a barrier, in exactly the same way as calculating the sound pressure at the receiver due to a hole, the same size and geometry as an 'infinite' barrier. We, therefore, need to know what size 'hole' represents the term, $\frac{Ae^{ikd}}{d}$, to a given accuracy. By using the free-space model, this was achieved by increasing the size of the barrier until the sound attenuation converged to a maximum value. The procedure for calculating the sound pressure at the receiver, in the absence of a barrier, then becomes the same as that for sound passing through the 'hole'

The sound attenuation that results from a barrier in contact with the ground can then be computed by the program in Appendix 8. This program allows the position of the receiver to be systematically changed in a vertical direction.

6.2 Results for a barrier in contact with the ground

Having generated results for a barrier in free space, the model is modified and able to produce results for similar barriers in contact with a concrete surface. Figures 19-24 represent the change in insertion loss for increasing frequency of the sound wave from 100 Hz to 10,000 Hz, for various barrier geometries. Some results represent the author's chosen model geometries while other geometries are chosen to compare the author's results with those of other workers. Figure 25 shows the variation in insertion loss as the receiver is moved away from its central position, in a vertical direction.

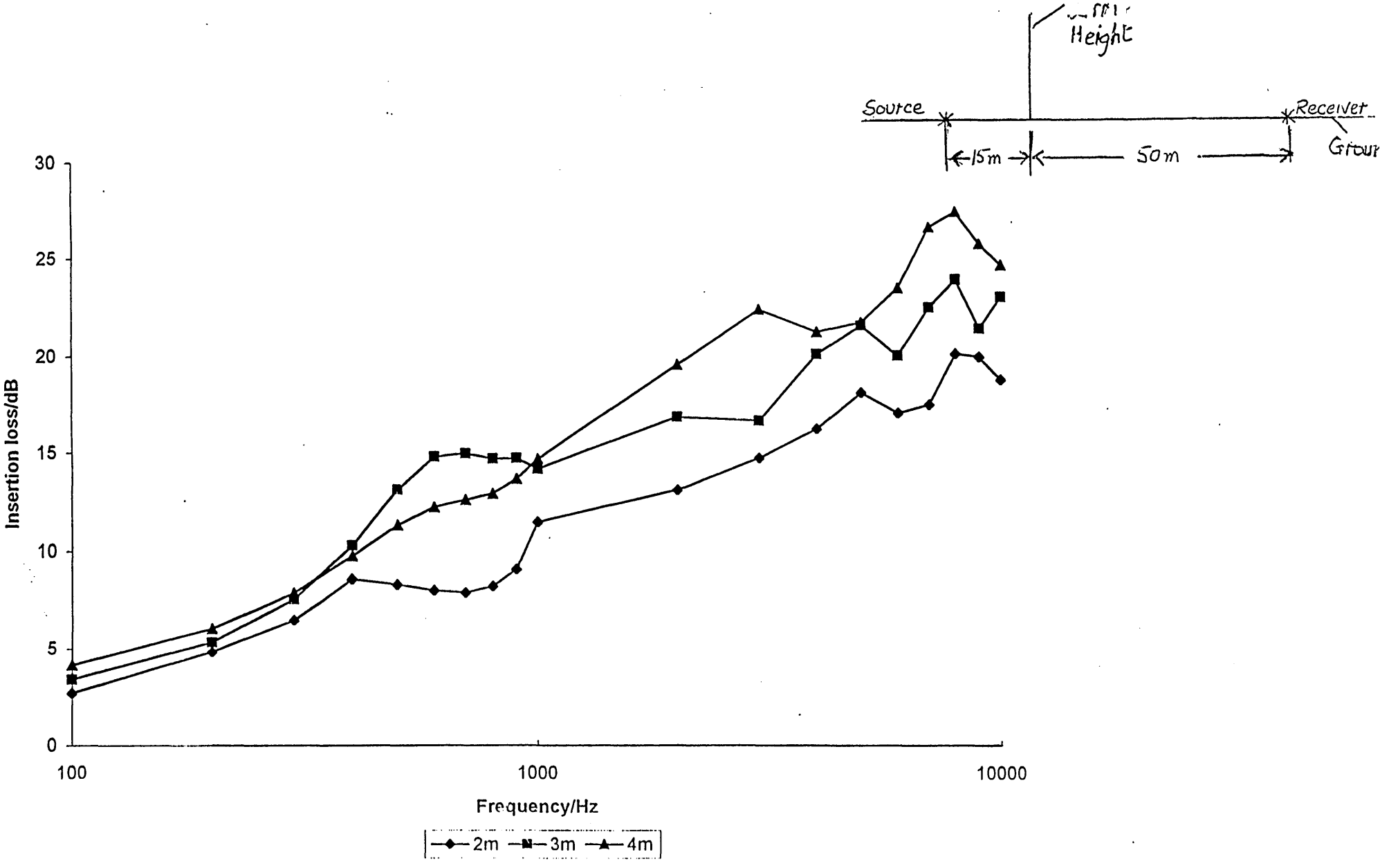

Figure 19 Insertion loss of a 10 m wide barrier on a concrete surface

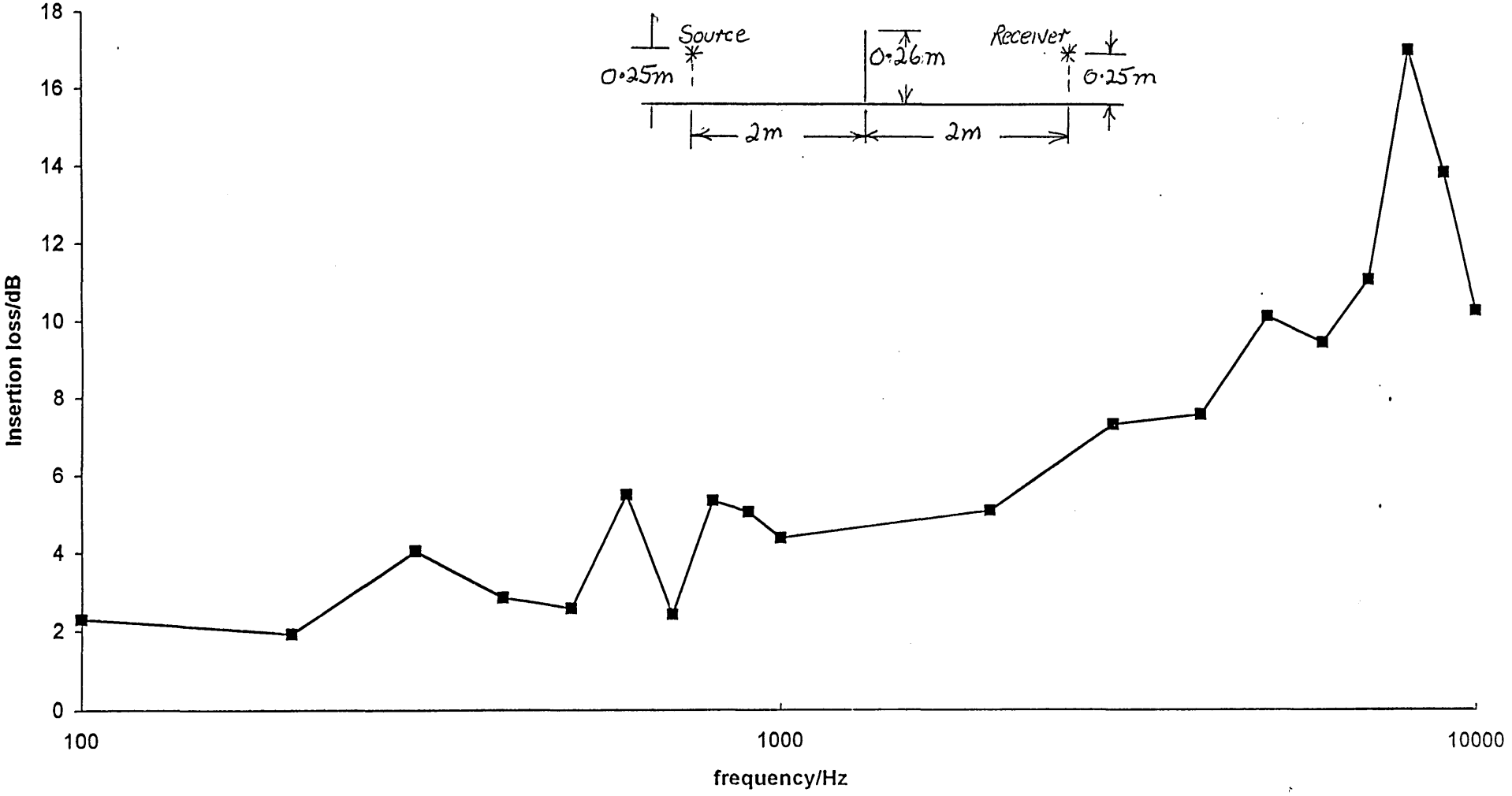

Figure 20 Insertion loss of a 4 m wide barrier of hight 0.26 m, on a concrete surface

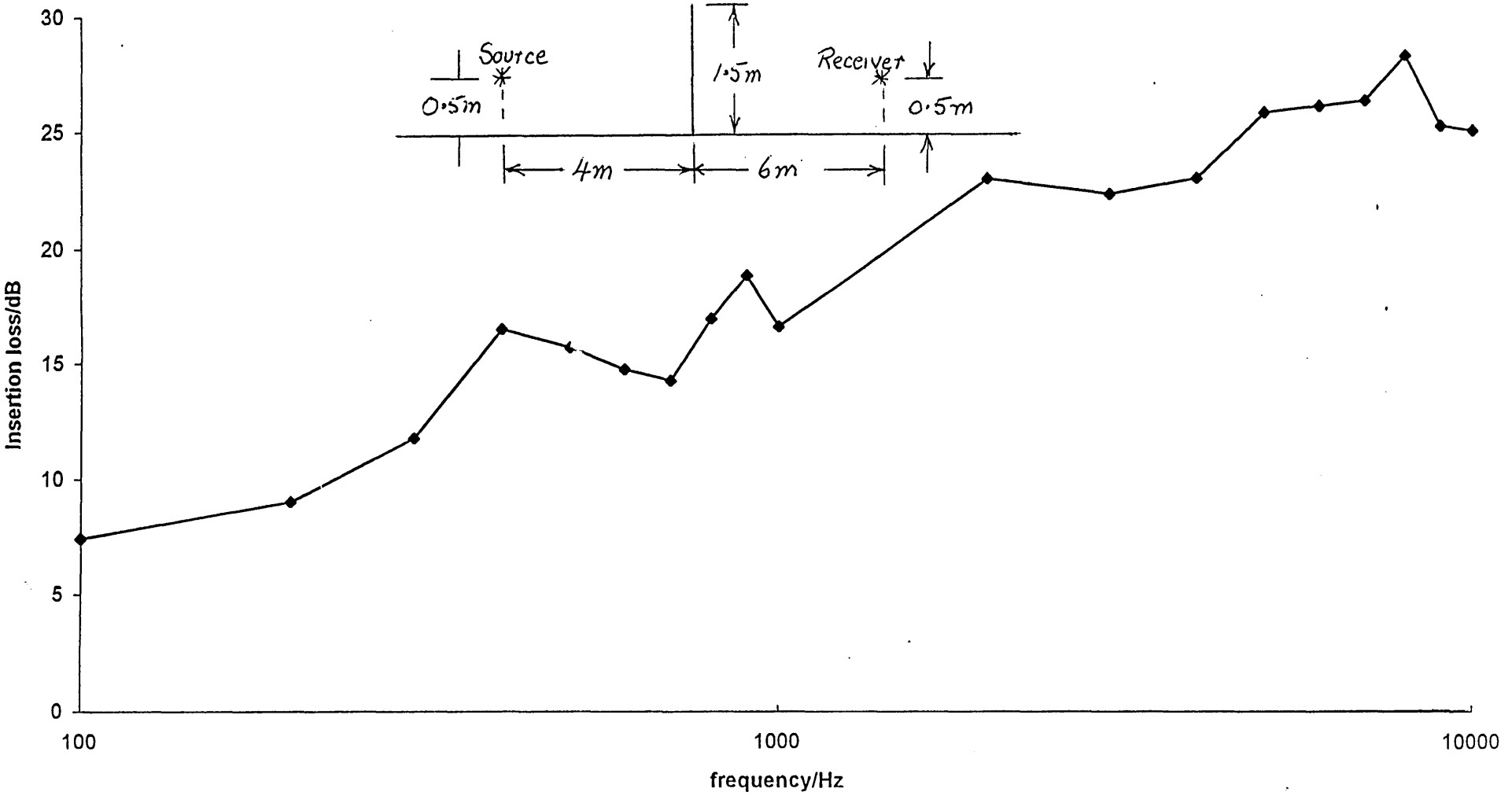

Figure 21 Insertion loss of a 4 m wide barrier, of height 1.5 m, on a concrete surface

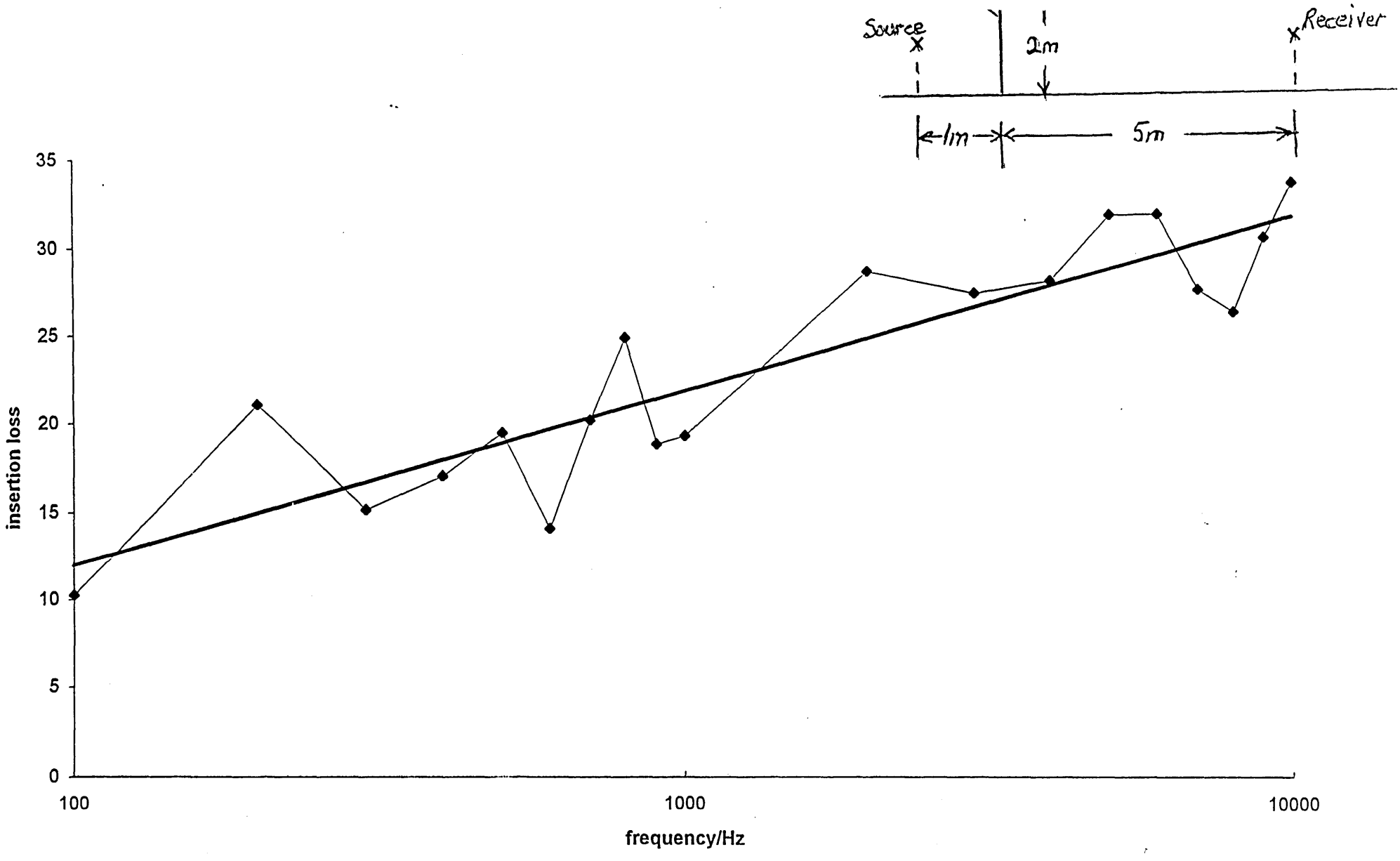

Figure 22 Insertion loss of a 4 m wide barrier, of height 2 m, on a concrete surface, showing the line of best fit

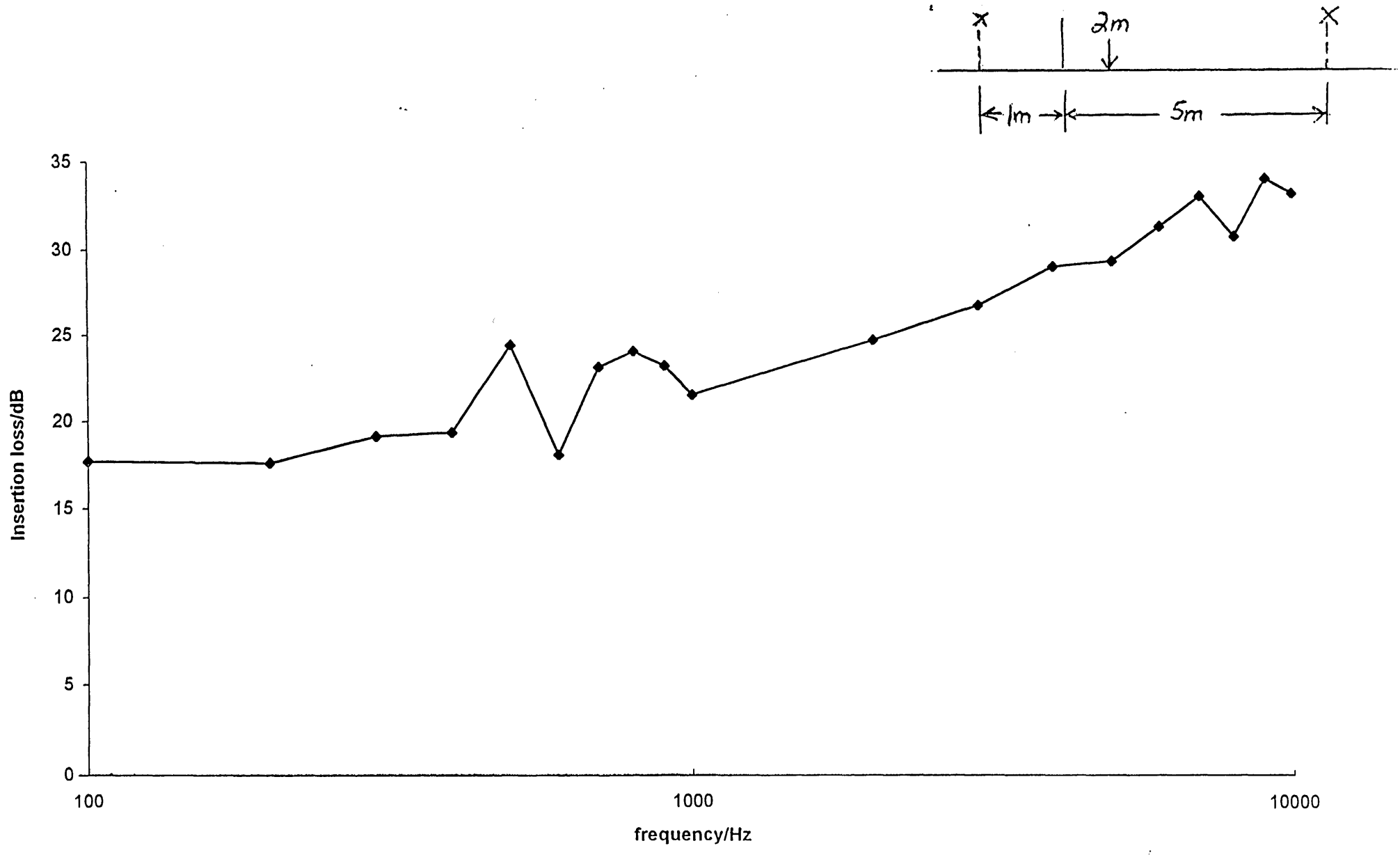

Figure 23 Insertion loss of a 10 m wide barrier, of height 2 m, on a concrete surface

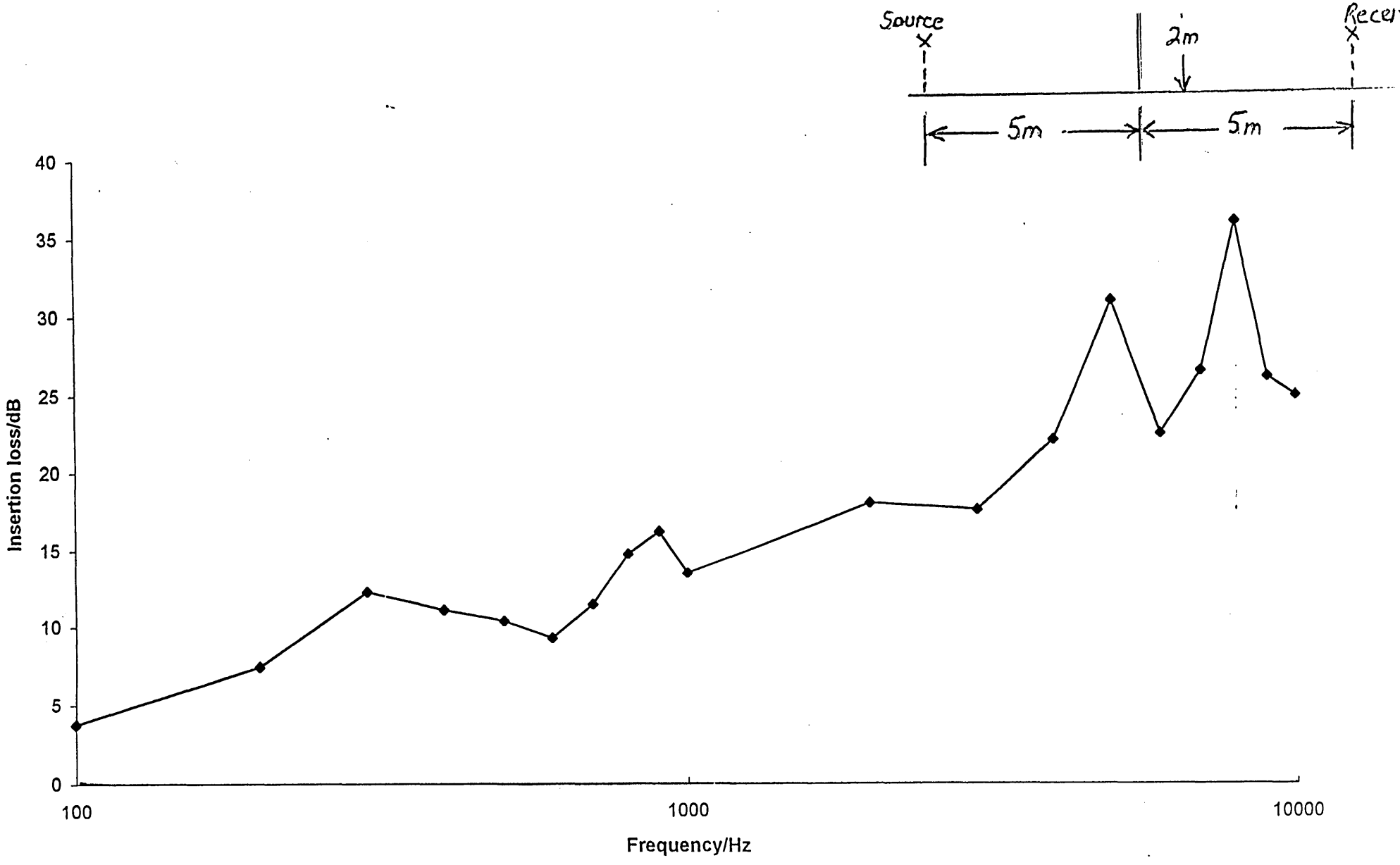

Figure 24 Insertion loss of a 4 m wide barrier on a concrete surface with an increased source-barrier distance

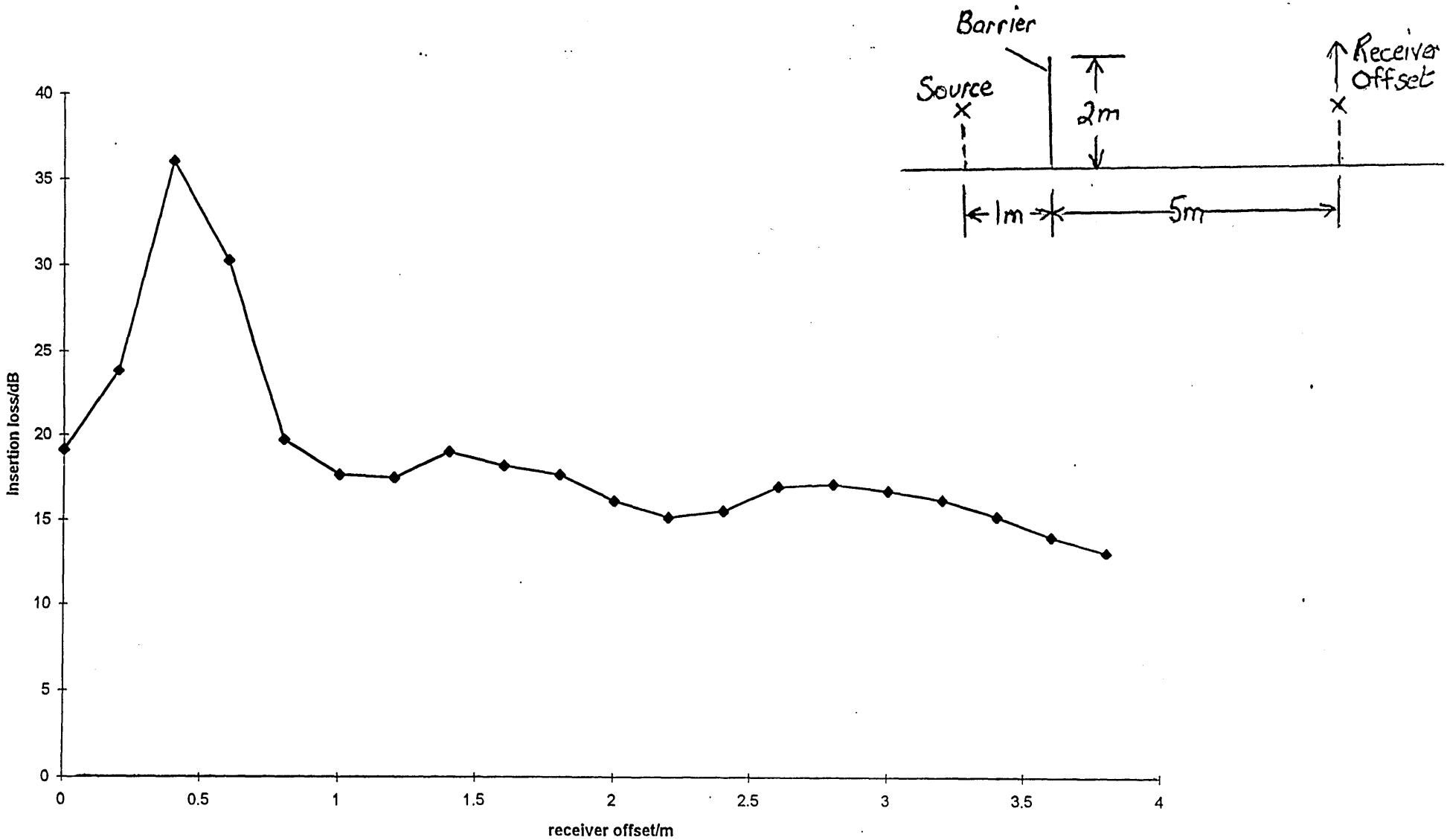

Figure 25 4 m wide barrier on a concrete surface - effect on insertion loss by changing the receiver position, using a frequency of 1 kHz

6.3 Discussion of results for a barrier in contact with the ground.

This model uses direct contributions and reflected contributions from the ground, so introducing interference effects similar to those incurred in Lloyd's Mirror experiment in optics. There is a wealth of contemporary literature on this subject, some of which is validated by experimental detail. The author, therefore, compares his results with those of other workers, using the same barrier geometries where possible.

D C Hothersall, S N Chandler-Wilde and M N Hajmirzae (1991) introduced a numerical model for a barrier in contact with the ground, using the boundary element method. They found that if the source is above the surface, the monofrequency sound field varies in a complicated way due to the interference between the two waves originating from the source and from the image of the source in the ground surface. This interference produces complicated variations in the received sound behind the barrier, which have been found to be related to the configuration of the interference pattern in the region above the barrier. The received levels thus depend strongly on the source height and barrier height. In order to simplify the results, they eliminated interference effects caused by reflected waves, by placing the source at ground level. Typical results from their model, Figure 26, show similar trends to that of the author's model, Figure 19 , where insertion loss increases with respective increases in frequency at the rate of ≈3 dB/octave.

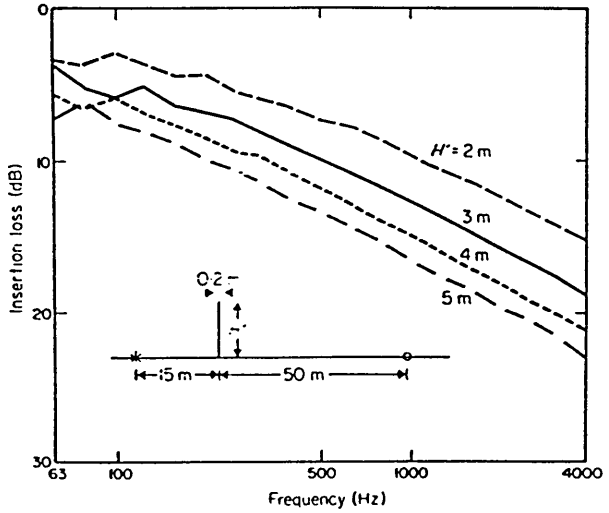

Figure 26 Insertion loss spectra for vertical screens. The source, barrier and receiver geometry is indicated. All surfaces have zero admittance.

In 1994, Y W Lam developed a simple model for calculating the attenuation of complex ground terrains. He compares his ground model with existing environmental noise calculation models: the draft ISO model, the CONCAWE model, and ENM. It is found that the new ground model has the best overall performance and agrees well with measured data on a variety of ground terrain profiles and conditions. For the respective data, Figures 20 and 21 show that the author's model behaves in a simlar way to that of Lam, Figures 27 and 28, although the author's model is closer to the ISO model at low frequncies. The conditions do differ, however, in that the author uses a 10 m wide barrier and hard ground conditions, whereas Lam uses an infinite barrier with softer ground conditions.

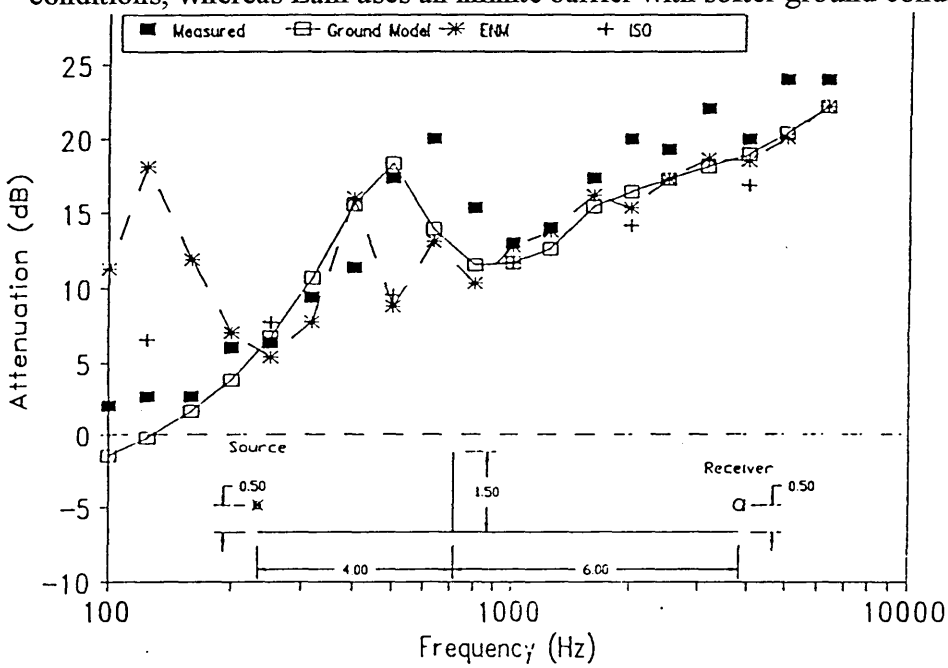

Fig. 27 Attenuation of a thin barrier on a ground with a flow resistivity of 300 kN sm $^{-4}$. The measured data are taken from Leang *et al.*[55]

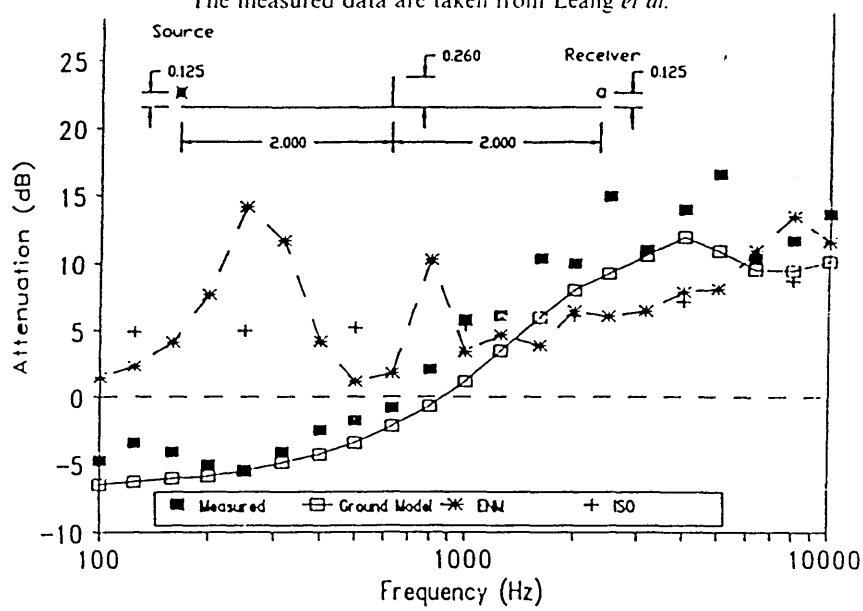

Fig. 28 Attenuation of a thin barrier on a ground with flow resistivity of 20 000 kN sm $^{-4}$ on the source side and 300 kNsm $^{-4}$ on the receiver side. The measured data are taken from Isei *et al.*[2]

Using a 2 m x 4 m finite barrier, Figure 2 2 shows a steady increase in insertion loss as the frequency rises. A line of best fit is superimposed on the data and deviations from this line can be observed. This model still encounters instabilities where the trigonometric terms $\cos[k(r_\circ + s_\circ)]$ and $\sin[k(r_\circ + s_\circ)]$ are sensitive to change in frequency at low values of wavelength, but interference effects from the direct and reflected sound waves also contribute to the deviations from the general trend, shown by the line of best fit. The ground model is time consuming, due to the high number of elements used in computing the sound pressure with no barrier present when Babinet's Principle is applied. The deviations away from the general trend would therefore be reduced if time allowed more elements to be used in the calculation. The results were obtained using an element length of 0.05 m, whereas it was shown earlier that an element length of 0.0125 m was required to give accuracy within precision grade measurement.

Figure 23 shows that a smoother curve is obtained by increasing the width of the barrier from 4 m to 10 m. Many of the curve's instabilities are removed because diffraction and interference effects around the sides of the barrier become less significant in wider positions. Figure 24 demonstrates that increasing the source-barrier distance from 1 m to 5 m amplifies the sensitivity of the trigonometric terms, which results in large deviations from the general trend at the high end of the frequency spectrum.

Figure 25 shows a steady reduction in insertion loss as the receiver is moved vertically from it's central position, but the curve oscillates around the general trend, with a large initial peak. Comparing this curve to that in Figure 17, for free space conditions, the initial peak value for insertion loss is seen to be larger. The difference in sound pressures due to phase changes between $\cup_D$ and $\cup_H$ must therefore be larger for this receiver position than that respective position in free space. This large peak value in insertion loss may be reproduced by sloping the

barrier, which seems equivalent to moving the position of the receiver, an argument that was discussed earlier for a barrier in free space.

7 BARRIER IN A FLAT ROOM

Because the object of this work is to calculate insertion loss, due to finite barriers in enclosures, the next logical step is to introduce a roof to the existing ground model, discussed in Chapter 6. This model is referred to as the 'flat-room' model because at this stage there are no walls present.

In calculating the insertion loss due to a barrier in contact with the ground we applied Babinet's Principle. Also, in this model we included the reflected contribution from the ground in addition to the direct component. The same principles apply to the flat room model, but this time further complications are introduced by adding the reflected contribution from the roof. The complex reflection coefficient, Cr, is incorporated once again for the specular angle of reflection for both the ground and the roof. Two sets of results are incorporated in this model: one using single reflections and one using multi-reflections between the ground and the roof.

7.1 Computational Details

Calculation of the sound passing through the barrier shaped hole are the same for that of the model using ground conditions, plus the following cases:

1 Sound initially reflected and then diffracted

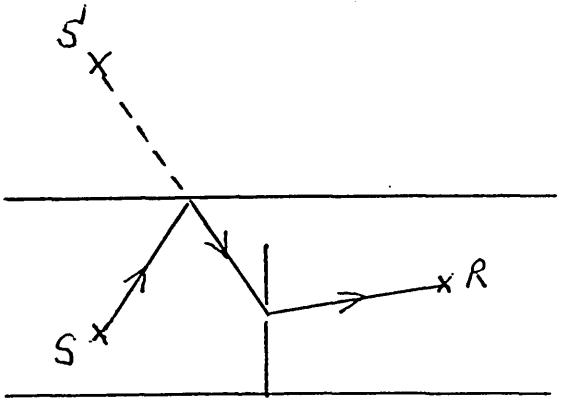

2 Sound initially diffracted and then reflected

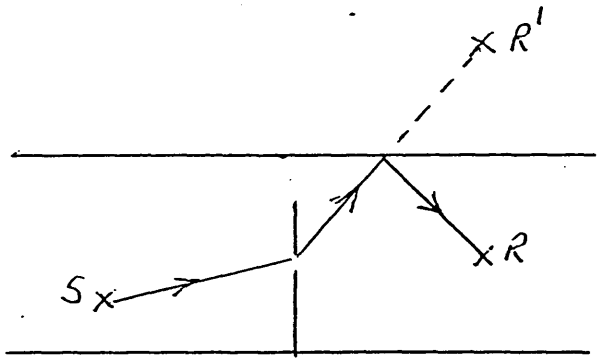

3 Sound initially reflected, then diffracted and then reflected again

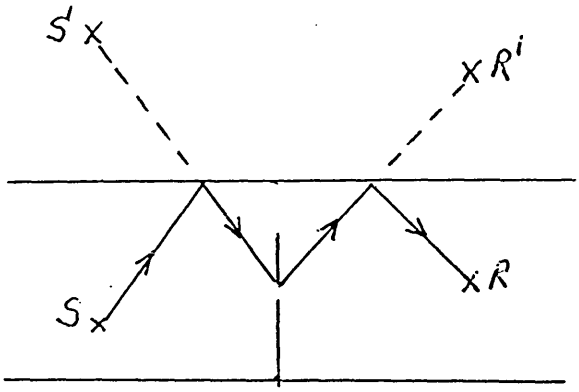

4 Sound initially reflected twice, and then diffracted

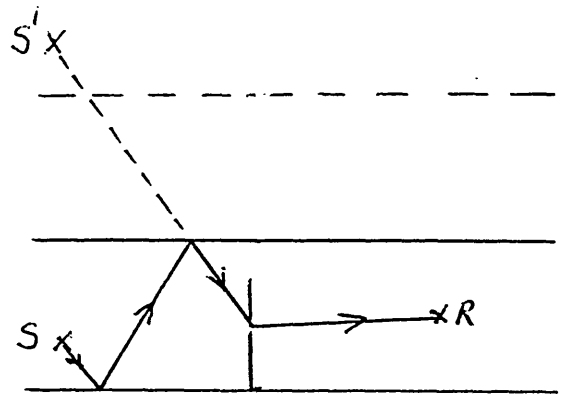

5 Sound initially diffracted and then reflected twice

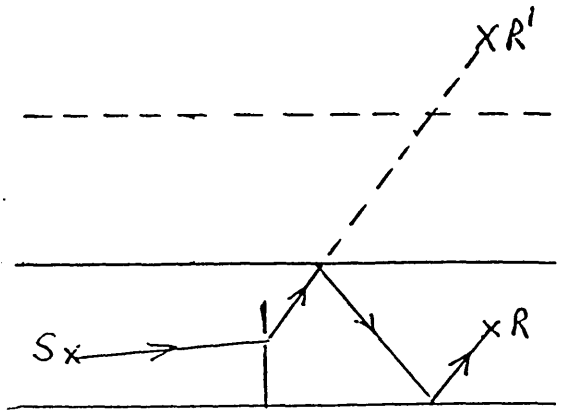

6 Sound initially reflected twice, then diffracted and then reflected twice again

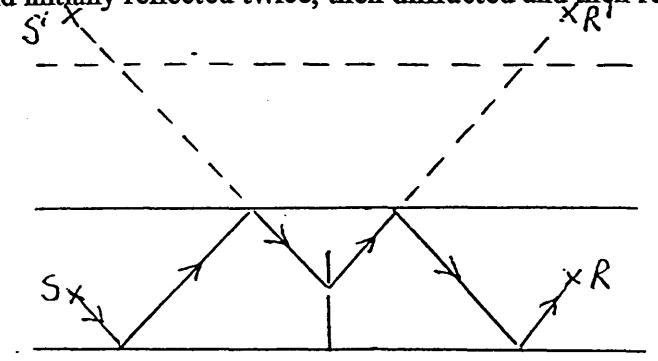

7 Sound initially reflected twice and then diffracted

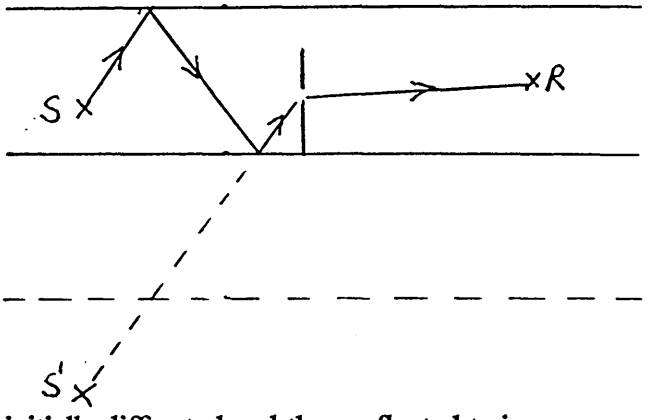

8 Sound initially diffracted and then reflected twice

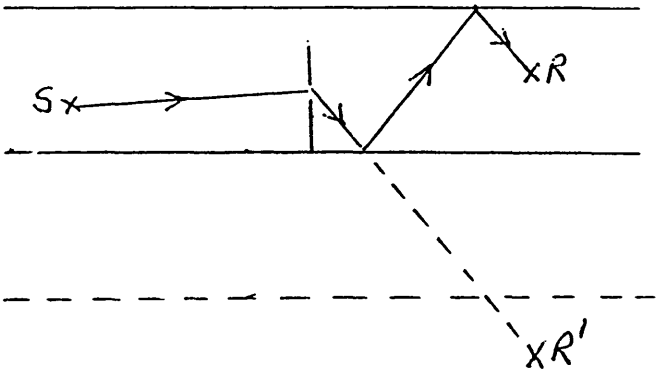

9 Sound initially reflected twice, then diffracted and then reflected twice again

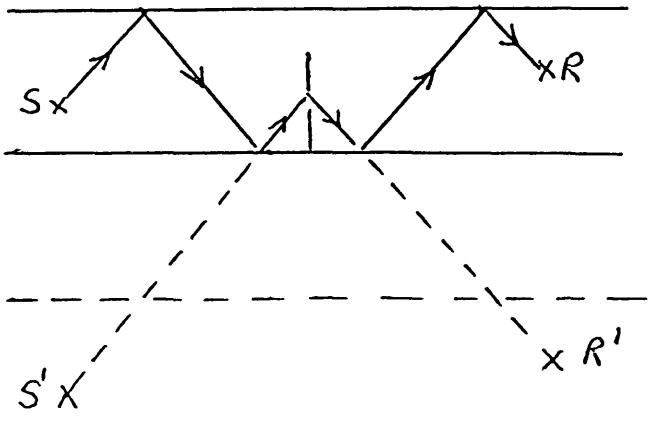

All the sound pressures, illustrated above, plus those of the direct and reflected components from the ground, are combined to produce a total sound pressure for that passing through the hole, ie $\cup_H$

Then the sound pressure around the barrier,

$$\cup_B = \cup_D - \cup_H$$

Sound reflected from the ceiling

(1) Sound initially reflected and then diffracted

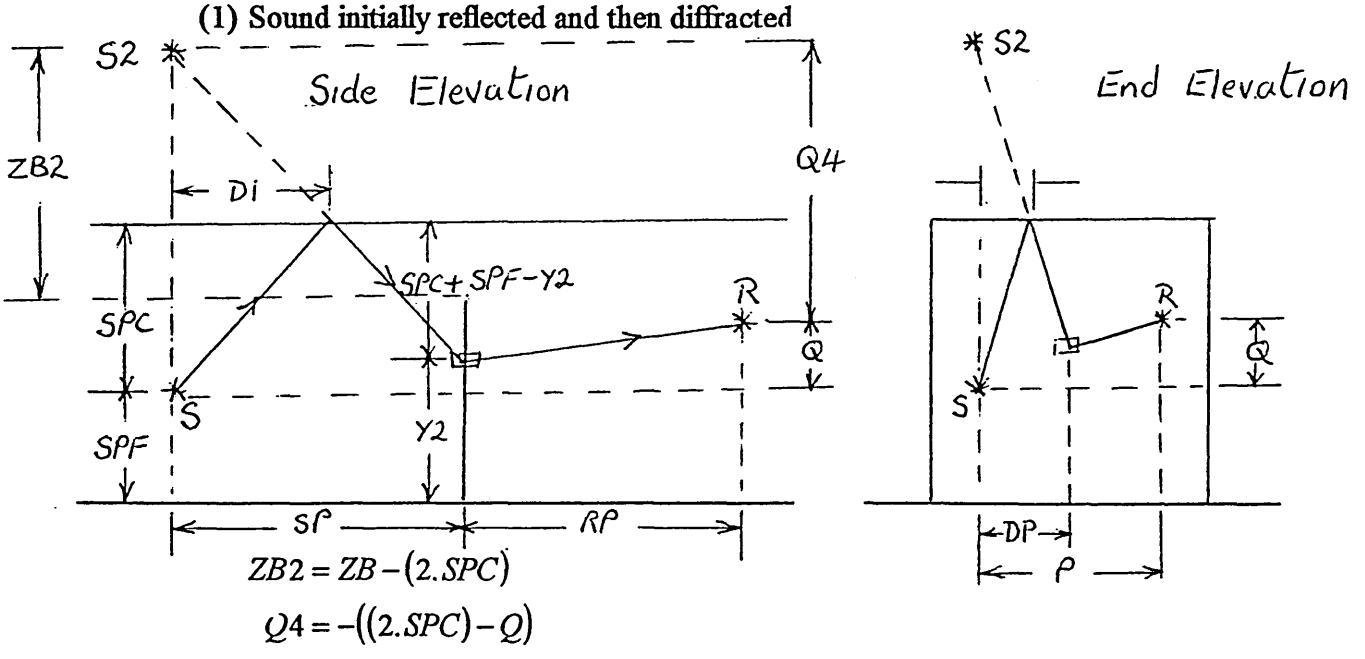

$$ZB2 = ZB - (2.SPC)$$

$$Q4 = -((2.SPC) - Q)$$

For each element we compute the real and imaginary parts of the reflection coefficient ie CORL and COIM, and in order to do this we require the 3-dimensional angle v, between the sound path and the normal.

On the side elevation

$$Y2 = Y - J.DY + DY/2$$

and using similar triangles

$$\frac{SPC}{D1} = \frac{SPC + SPF - Y2}{SP - D1}$$

$$\therefore D1 = \frac{(SP.SPC)}{((2.SPC) + SPF - Y2)}$$

and from the end elevation

$$\frac{SPC}{W1} = \frac{SPC + SPF - Y2}{DP - W1}$$

$$\therefore W1 = \frac{(DP.SPC)}{((2.SPC) + SPF - Y2)}$$

Hence

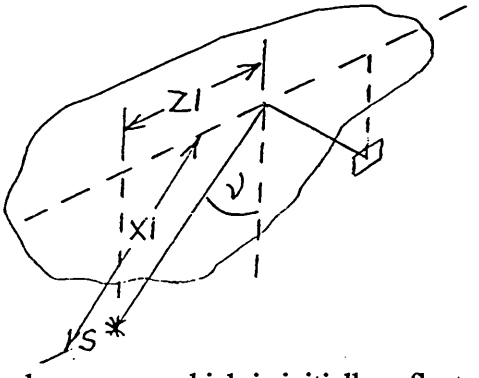

$$Z1 = \left(D1^2 + W1^2\right)^{1/2}$$

$$X1 = \left(SPC^2 + D1^2 + W1^2\right)^{1/2}$$

and $\nu = \arcsin(Z1 / X1)$

The sound pressure, which is initially reflected and then diffracted, can then be computed where

$$SOUND\ PRESSURE = (RL.CORL + UNRL.COIM) + i(UNRL.CORL - RL.COIM)$$

where RL = real part of the sound pressure
UNRL = imaginary part of the sound pressure

(2) Sound initially diffracted then reflected

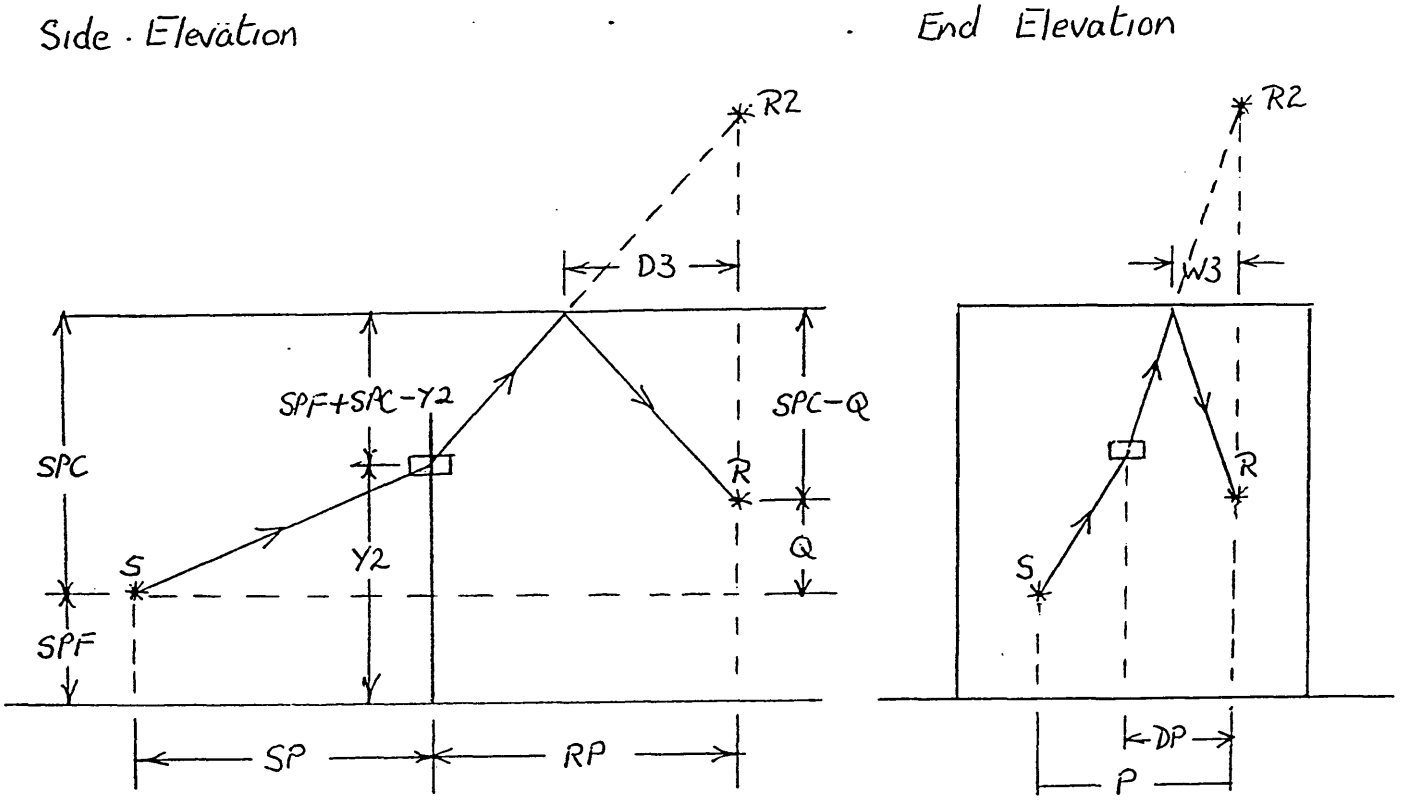

$$Q5 = -\left((2.SPC) - Q\right)$$

For each element we need to compute the real and imaginary parts of the reflection coefficient ie CORL and COIM, and in order to do this we require the 3-dimensional angle ν, between the sound path and the normal.

On the side elevation

$$Y2 = Y - J.DY + DY/2$$

and using similar triangles

$$\frac{SPC - Q}{D3} = \frac{SPF + SPC - Y2}{RP - D3}$$

$$\therefore D3 = \frac{\left(RP(SPC - Q)\right)}{\left((2.SPC) + SPF - Y2 - Q\right)}$$

and from the end elevation

$$DP = \left(\left(ZL - I.DX + DX/2 + P \right)^2 \right)^{1/2}$$

Using similar triangles

$$\frac{SPC - Q}{W3} = \frac{SPF + SPC - Y2}{DP - W3}$$

$$\therefore W3 = \frac{\left(DP(SPC - Q) \right)}{\left((2.SPC) + SPF - Y2 - Q \right)}$$

Hence

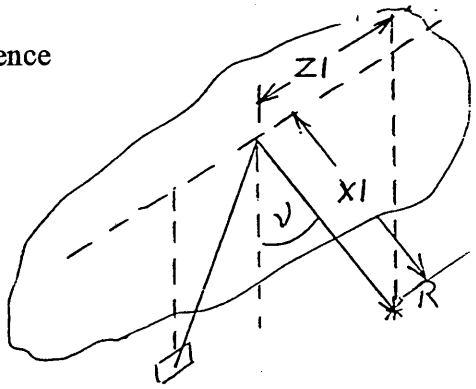

$$Z1 = \left(D3^2 + W3^2 \right)^{1/2}$$

$$X1 = \left((SPC - Q)^2 + D3^2 + W \right.$$

and $\nu = \arcsin(Z1/X1)$

The sound pressure, which is initially diffracted and then reflected, can then be computed where

$$SOUND\ PRESSURE = (RL.CORL + UNRL.COIM) + i(UNRL.CORL - RL.COIM)$$

(3) Sound initially reflected, then diffracted and finally reflected again

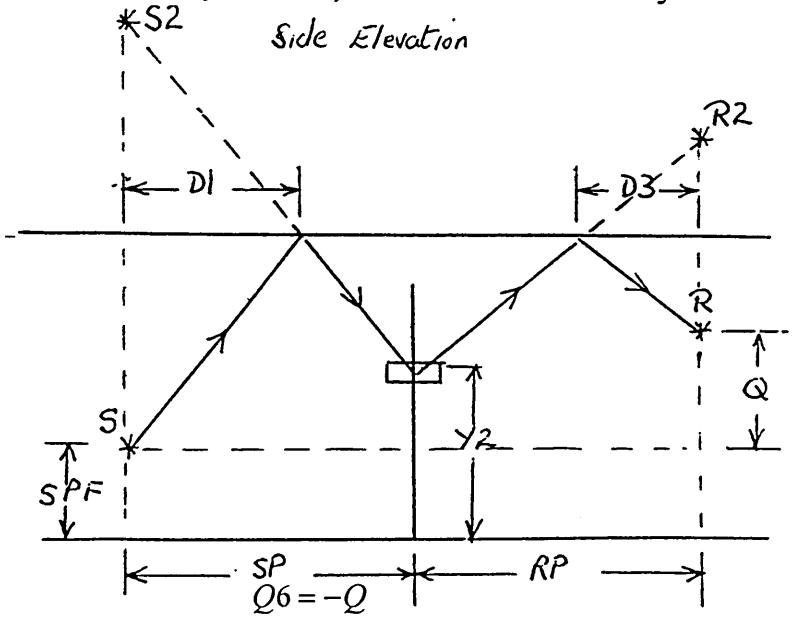

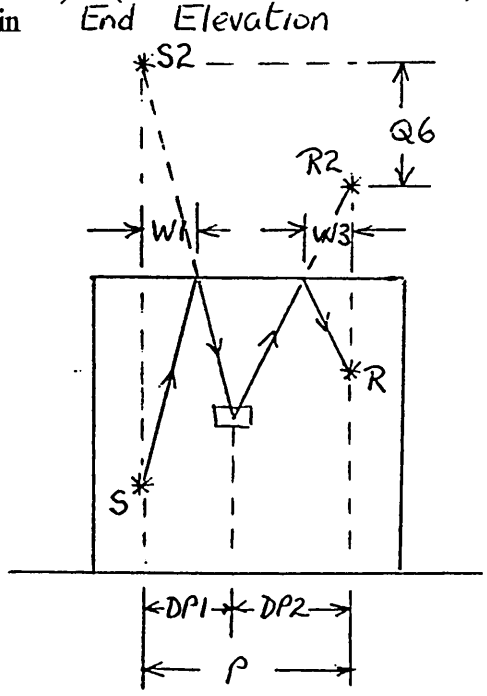

For each element we compute the real and imaginary parts of the reflection coefficient before diffraction takes place, ie CORL1 and COIM1, and also the real and imaginary parts of the reflection coefficient after diffraction, ie CORL2 and COIM2. In order to do this we require the respective 3-dimensional angles ν_1 and ν_2 between the sound path and the normals at the respective points of reflection.

On the side elevation

$$Y2 = Y - J.DY + DY/2$$

and using similar triangles

$$\frac{SPC}{D1} = \frac{SPC + SPF - Y2}{SP - D1}$$

$$\therefore D1 = \frac{(SPC.SP)}{((2.SPC) + SPF - Y2)}$$

and

$$\frac{SPC - Q}{D3} = \frac{SPC + SPF - Y2}{RP - D3}$$

$$\therefore D3 = \frac{(RP(SPC - Q))}{((2.SPC) + SPF - Y2 - Q)}$$

and for the end elevation

$$\frac{SPC}{W1} = \frac{SPC + SPF - Y2}{DP1 - W1}$$

$$\therefore W1 = \frac{(SPC.DP1)}{((2.SPC) + SPF - Y2)}$$

and

$$\frac{SPC - Q}{W3} = \frac{SPC + SPF - Y2}{DP2 - W3}$$

$$\therefore W3 = \frac{(DP^2(SPC - Q))}{((2.SPC) + SPF - Y2 - Q)}$$

Hence

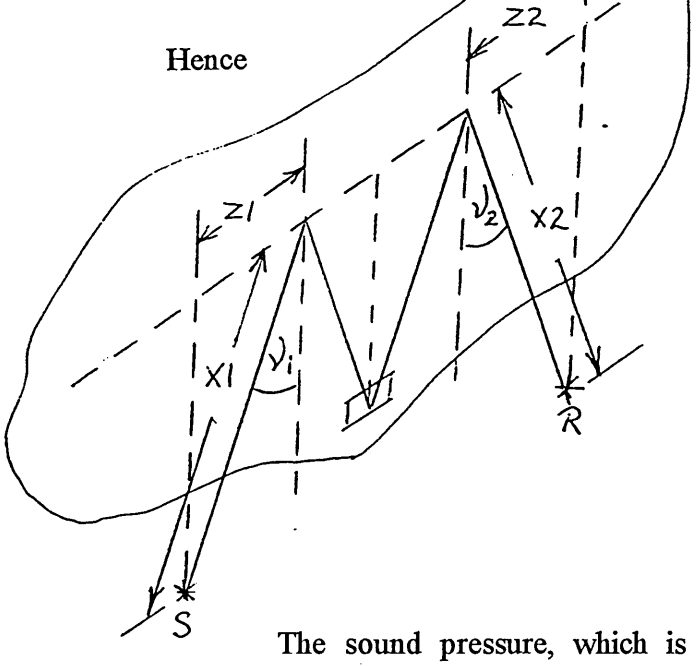

$$Z1 = \left(D1^2 + W1^2\right)^{\frac{1}{2}}$$

$$X1 = \left(SPC^2 + D1^2 + W1^2\right)^{\frac{1}{2}}$$

$$Z2 = \left(D3^2 + W3^2\right)^{\frac{1}{2}}$$

$$X2 = \left(\left(SPC - Q\right)^2 + D3^2 + W3^2\right)^{\frac{1}{2}}$$

and $\nu_1 = \arcsin(Z1 / X1)$

$\nu_2 = \arcsin(Z3 / X3)$

The sound pressure, which is initially reflected, then diffracted and then reflected again, can then be computed where

$$SOUND\ PRESSURE = (RL + iUNRL)(CORL1 - iCOIM1)(CORL2 - iCOIM2)$$
$$= (RL.CORL1.CORL2 + UNRL.COIM1.CORL2 + UNRL.CORL1.COIM2 - RL.COIM1.COIM2)$$
$$+i(UNRL.CORL1.CORL2 - RL.COIM1.CORL2 - RL.CORL1.COIM2 - UNRL.COIM1.COIM2)$$

(4) Sound initially reflected twice and then diffracted.

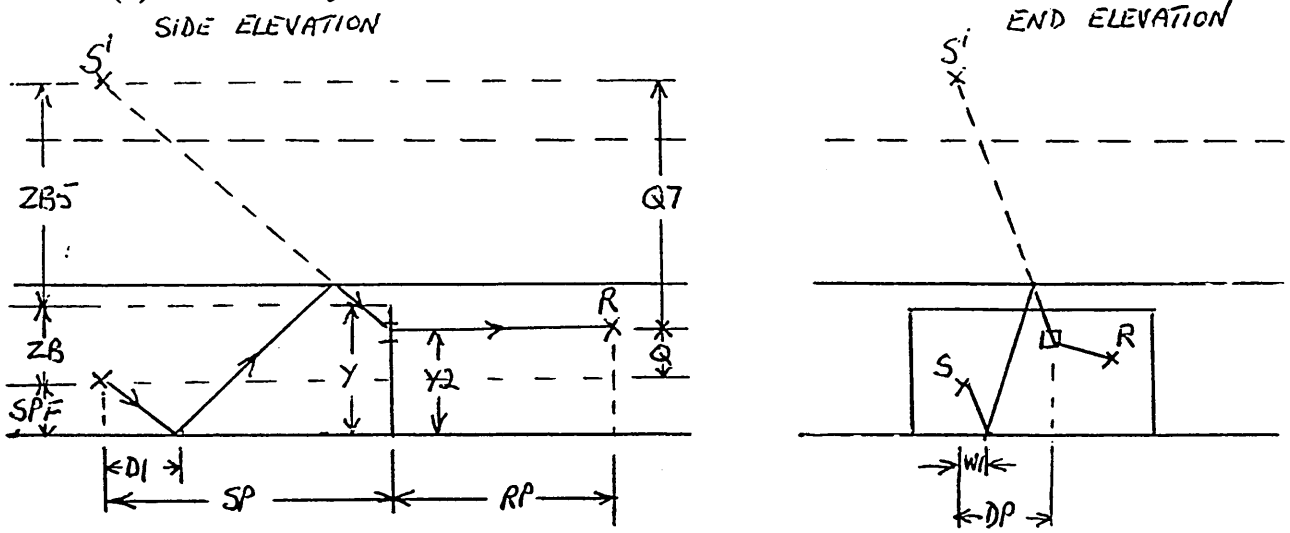

$$ZB5 = -\left(\left(2.\left(SPF + SPC\right)\right) - ZB\right)$$

$$Q7 = -\left(2.\left(SPF = SPC\right)\right) + Q$$

For each element we compute the real and imaginary parts of the reflection coefficient, ie CORL1, CORL2, COIM1 and COIM2, and in order to do this we require the 3-dimensional angle ν, between the sound path and the normal.

On the side elevation

$$Y2 = Y - J.DY + DY/2$$

and using similar triangles

$$\frac{SPF}{D1} = \frac{(3.SPF) + (2.SPC) - 2}{SP}$$

$$\therefore\ D1 = \frac{SP.SPF}{(3.SPF) + (2.SPC) - Y2}$$

and for the end elevation

$$DP = \left((ZL - I.DX + DX/2)^2\right)^{1/2}$$

Using similar triangles

$$\frac{SPF}{W1} = \frac{(3.SPF) + (2.SPC) - Y2}{DP}$$

$$\therefore\ W1 = \frac{DP.SPF}{(3.SPF) + (2.SPC) - Y2}$$

Hence

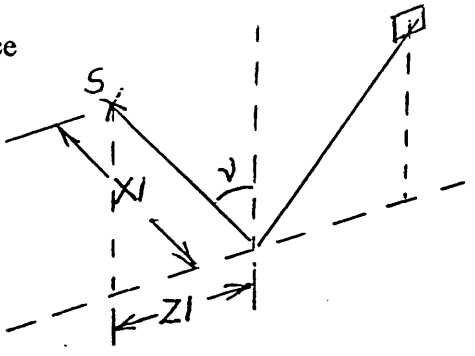

$$Z1 = \left(D1^2 + W1^2\right)^{1/2}$$

$$X1 = \left(SPF^2 + D1^2 + W1^2\right)^{1/2}$$

and $\nu_1 = \arcsin(Z1/X1)$

The sound pressure, which is initially reflected twice and then diffracted, can then be computed where

$$\begin{aligned} SOUND\ PRESSURE = &((RL.CORL1.CORL2) - (UNRL.COIM1.CORL2) - \\ &(RL.COIM1.COIM2) - (UNRL.CORL1.COIM2)) \\ &+ i((RL.CORL1.COIM2) - (UNRL.COIM1.COIM2) + \\ &(RL.COIM1.CORL2) + (UNRL.CORL1.COIM2)) \end{aligned}$$

(5) Sound initially diffracted then reflected twice.

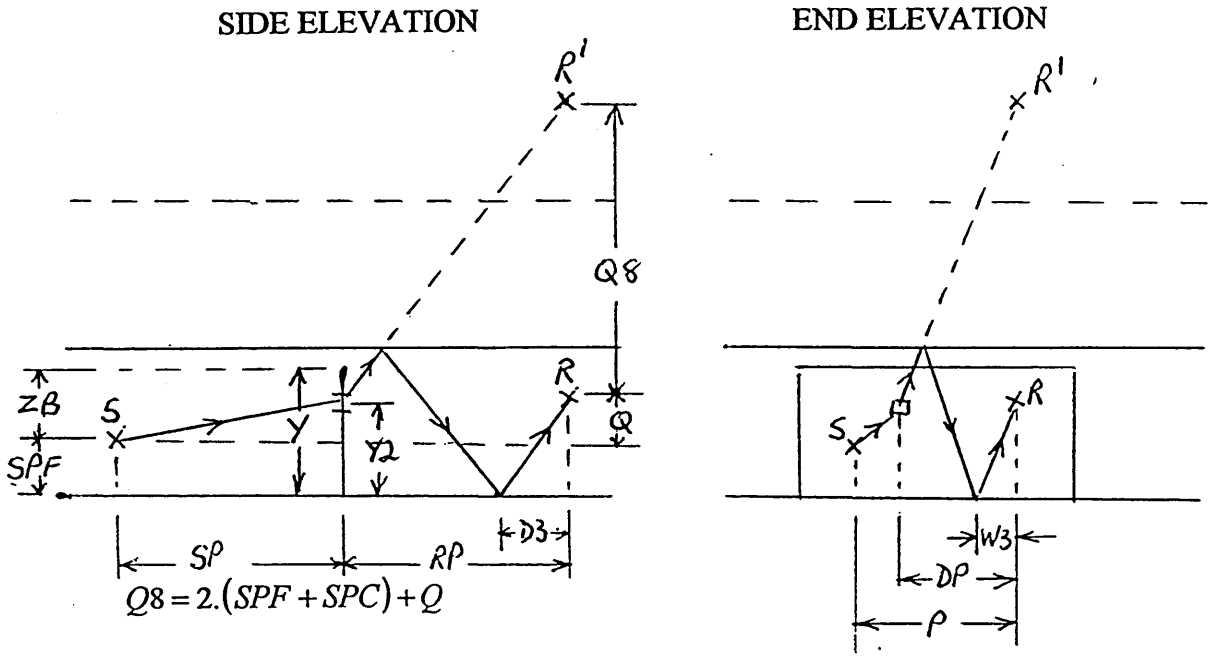

For each element we compute the real and imaginary parts of the reflection coefficientS, ie CORL1, CORL2, COIM1, and COIM2, and in order to do this we require the 3-dimensional angle ν, between the sound path and the normal.

On the side elevation

$$Y2 = Y - J.DY + DY/2$$

and using similar triangles

$$\frac{Y2}{D3} = \frac{SPF + Q}{RP - D3}$$

$$\therefore\ D3 = \frac{(Y2.RP)}{(SPF + Y2 + Q)}$$

and using similar triangles

$$\frac{D3}{SPF + Q} = \frac{RP}{(3.SPF) + (2.SPC) + Q - Y2}$$

$$\therefore D3 = \frac{RP.(SPF + Q)}{(3.SPF) + (2.SPC) + Q - Y2}$$

and for the end elevation

$$DP = \left((ZL - I.DX + DX/2 + P)^2\right)^{1/2}$$

Using similar triangles

$$\frac{W3}{SPF + Q} = \frac{DP}{(3.SPF) + (2.SPC) + Q - Y2}$$

$$\therefore W3 = \frac{DP.(SPF + Q)}{(3.SPF) + (2.SPC) + Q - Y2}$$

Hence

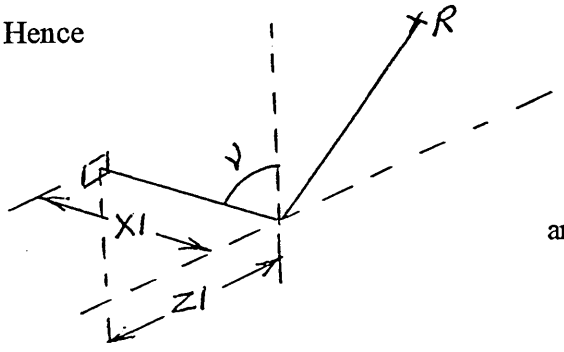

$$Z1 = \left(D3^2 + W3^2\right)^{1/2}$$

$$X1 = \left((SPF + Q)2 + D3^2 + W3^2\right)^{1/2}$$

and $v = \arcsin(Z1/X1)$

The sound pressure, which is initially diffracted and then reflected, can then be computed where

$$SOUND\ PRESSURE = ((RL.CORL1.CORL2) - (UNRL.COIM1.CORL2) - (RL.COIM1.COIM2) - (UNRL.CORL1.COIM2)) + i((RL.CORL1.COIM2) - (UNRL.COIM1.COIM2) + (RL.COIM1.CORL2) + (UNRL.CORL1.COIM2))$$

(6) Sound initially reflected twice, then diffracted and finally reflected twice again.

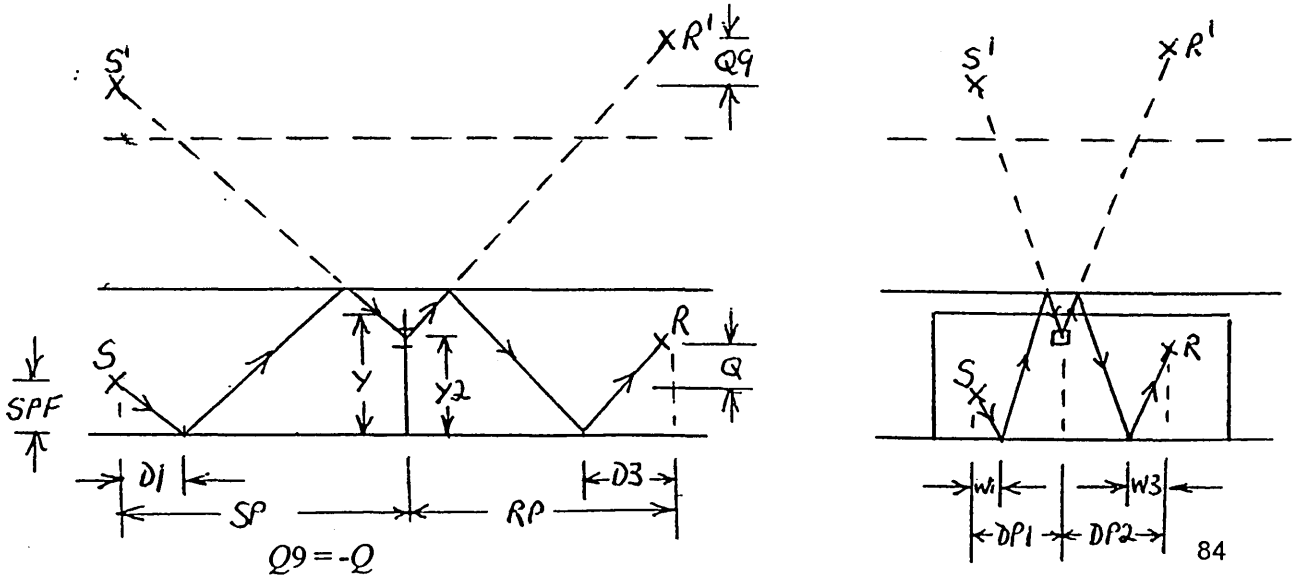

For each element we compute the real and imaginary parts of the reflection coefficients CORL1, CORL2, CORL3, CORL4, COIM1, COIM2, COIM3, COIM4 and in order to do this we require the respective 3-dimensional angles ν_1 and ν_2 between the sound path and the normals.

On the side elevation

$$Y2 = Y - J.DY + DY/2$$

and using similar triangles

$$\frac{SPF}{D1} = \frac{(3.SPF) + (2.SPC) - Y2}{SP}$$

$$\therefore D1 = \frac{SP.SPF}{(3.SPF) + (2.SPC) - Y2}$$

and

$$\frac{D3}{SPF + Q} = \frac{RP}{(3.SPF) + (2.SPC) + Q - Y2}$$

$$\therefore D3 = \frac{RP.(SPF + Q)}{(3.SPF) + (2.SPC) + Q - Y2}$$

and for the end elevation

$$DP1 = \left((ZL - I.DX + DX/2)^2\right)^{1/2}$$

$$DP2 = \left((ZL - I.DX + DX/2 + P)^2\right)^{1/2}$$

Using similar triangles

$$\frac{SPF}{W1} = \frac{(3.SPF) + (2.SPC) - Y2}{DP}$$

$$\therefore W1 = \frac{DP.SPF}{(3.SPF) + (2.SPC) - Y2}$$

and

$$\frac{W3}{SPF+Q} = \frac{DP}{(3.SPF)+(2.SPC)+Q-Y2}$$

$$\therefore W3 = \frac{DP(SPF+Q)}{(3.SPF)+(2.SPC)+Q-Y2}$$

Hence

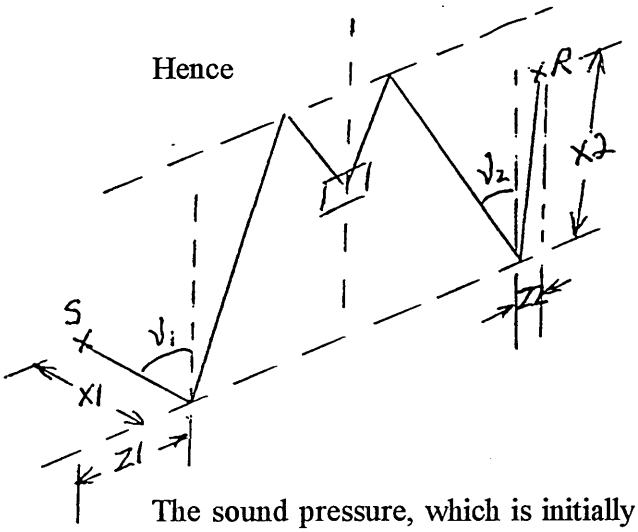

$$X1 = \left(SPF^2 + D1^2 + W1^2\right)^{1/2}$$

$$Z1 = \left(D1^2 + W1^2\right)^{1/2}$$

$$X2 = \left((SPF+Q)^2 + D3^2 + W3^2\right)^{1/2}$$

$$Z2 = \left(D3^2 + W3^2\right)^{1/2}$$

and $\nu_1 = \arcsin(Z1/X1)$

$\nu_2 = \arcsin(Z2/X2)$

The sound pressure, which is initially reflected twice, then diffracted and then reflected twice again, can then be computed where

$$\begin{aligned}
SOUND\ PRESSURE = {} & ((RL.CORL1.CORL2.CORL3.CORL4) - (UNRL.COIM1.CORL2.CORL3.CORL4) \\
& -(UNRL.CORL1.CORL3.CORL4.COIM2) - (RL.COIM1.COIM2.CORL3.CORL4) \\
& -(UNRL.CORL1.CORL2.CORL.4COIM3) - (RL.COIM1.COIM3.CORL2.CORL4) \\
& -(RL.CORL1.CORL4.COIM2.COIM3) + (UNRL.COIM1.COIM2.COIM3.CORL4) \\
& -(RL.CORL1.CORL2.COIM3.COIM4) + (UNRL.COIM1.COIM3.COIM4.CORL2) \\
& +(UNRL.CORL1.COIM2.COIM3.COIM4) + (RL.COIM1.COIM2.COIM3.COIM4) \\
& -(UNRL.CORL1.CORL2.CORL3.COIM4) - (RL.COIM1.COIM4.CORL2.CORL3) \\
& -(RL.CORL1.CORL3.COIM2.COIM4) + (UNRL.COIM1.COIM2.COIM4.CORL3) \\
& +i((RL.CORL1.CORL2.CORL3.COIM4) - (UNRL.COIM1.COIM4.CORL2.CORL3) \\
& -(UNRL.CORL1.CORL3.COIM2.COIM4) - (RL.COIM1.COIM2.COIM4.CORL3) \\
& -(UNRL.CORL1.CORL2.COIM3.COIM4) - (RL.COIM1.COIM3.COIM4.CORL2) \\
& -(RL.CORL1.COIM2.COIM3.COIM4) + (UNRL.COIM1.COIM2.COIM3.COIM4) \\
& +(RL.CORL1.CORL2.CORL4.COIM4) - (UNRL.CORL2.CORL4.COIM1.COIM3) \\
& -(UNRL.CORL1.CORL4.COIM2.COIM3) - (RL.CORL4.COIM1.COIM2.COIM3) \\
& +(UNRL.CORL1.CORL2.CORL3.CORL4) + (RL.CORL2.CORL3.CORL4.COIM1) \\
& +(RL.CORL1.CORL3.CORL4.COIM2) - (UNRL.CORL3.CORL4.COIM1.COIM2)
\end{aligned}$$

(7) Sound initially reflected twice, then diffracted

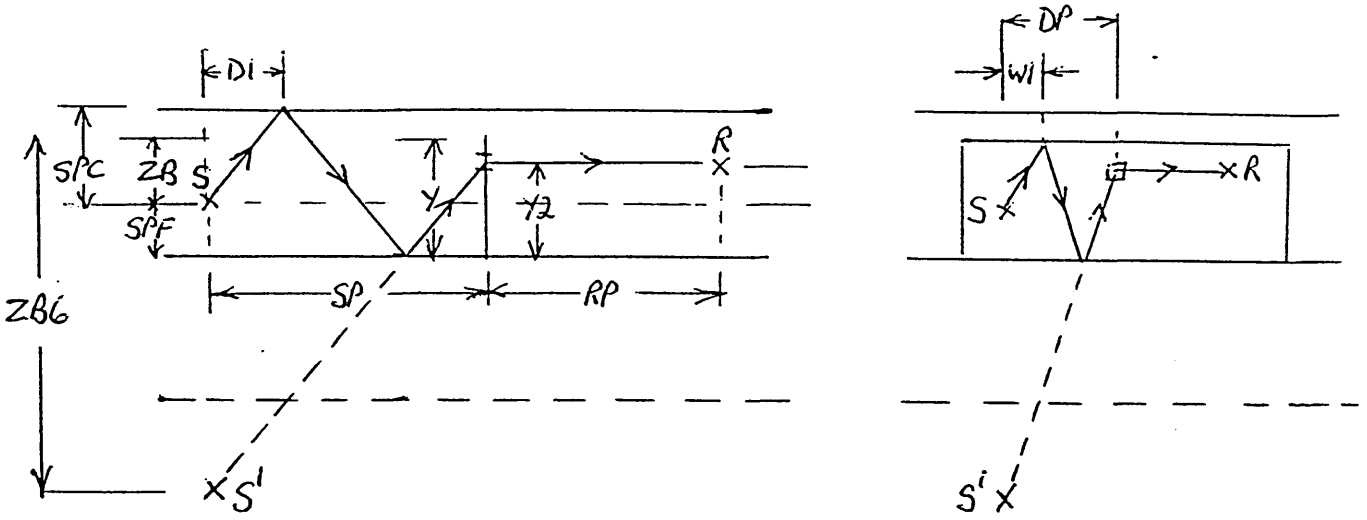

$$ZB6 = \left(2.\left(SPF + SPC\right)\right) + ZB$$
$$Q10 = \left(2.\left(SPF + SPC\right)\right) + Q$$

For each element we compute the real and imaginary parts of the reflection coeffiicents, ie CORL1, CORL2, COIM1, COIM2 and in order to do this we need the 3-dimensional angle, ν, between the sound path and the normal.

On the side elevation

$$Y2 = Y - J.DY + DY/2$$

and using similar triangles

$$\frac{D1}{SPC} = \frac{SP}{(2.SPC) + SPF + Y2}$$
$$\therefore D1 = \frac{SP.SPC}{(2.SPC) + SPF + Y2}$$

and for the end elevation

$$DP = \left(\left(ZL - I.DX + DX/2\right)^2\right)^{1/2}$$

Using similar triangles

$$\frac{W1}{SPC} = \frac{DP}{(2.SPC) + SPF + Y2}$$

$$\therefore W1 = \frac{DP.SPC}{(2.SPC) + SPF + Y2}$$

Hence

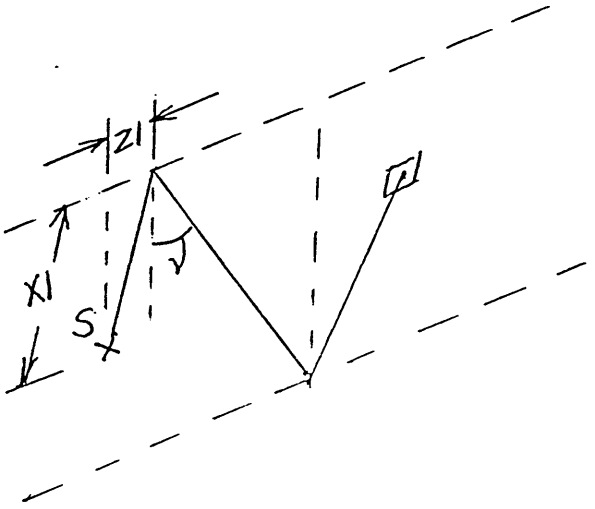

$$Z1 = \left(D1^2 + W1^2\right)^{1/2}$$

$$X1 = \left(SPC^2 + D1^2 + W1^2\right)^{1/2}$$

and $\nu = \arcsin(Z1 / X1)$

The sound pressure, which is initially reflected twice and then diffracted, can then be computed, where

$$\begin{aligned} SOUND\ PRESSURE = &((RL.CORL1.CORL2) - (UNRL.COIM1.CORL2) - \\ &(RL.COIM1.COIM2) - (UNRL.CORL1.COIM2)) \\ &+ i((RL.CORL1.COIM2.) - (UNRL.COIM1.COIM2) \\ &+ (RL.COIM1.CORL2) + (UNRL.CORL1.COIM2)) \end{aligned}$$

(8) Sound initially diffracted, then reflected twice

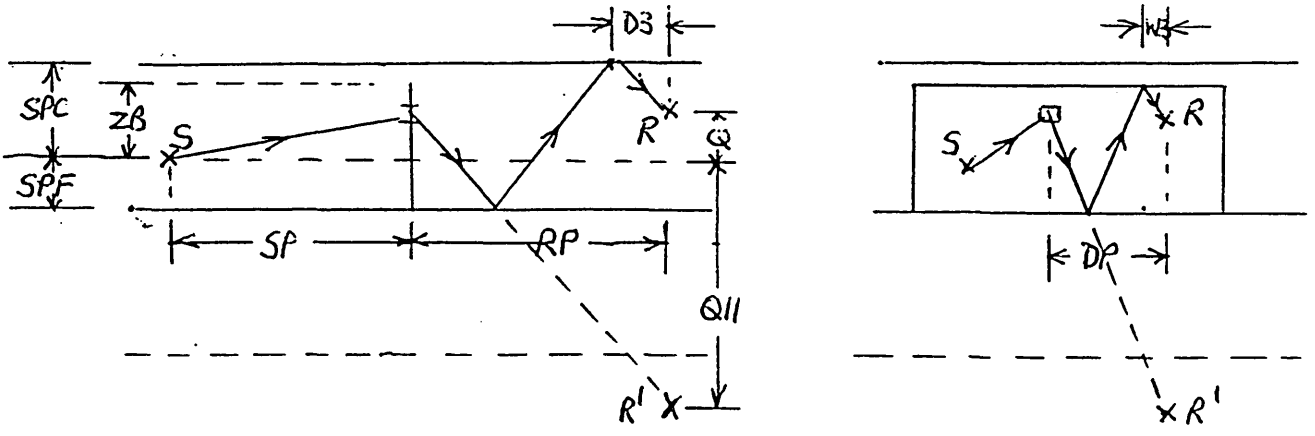

For each element we compute the real and imaginary parts of the reflection coefficients, ie CORL1, CORL2, COIM1, COIM2, and in order to do this we need the 3-dimensional angle, ν, between the sound path and the normal.

On the side elevation

$$Y2 = Y - J.DY + DY/2$$

and using similar triangles

$$\frac{D3}{SPC - Q} = \frac{RP}{(2.SPC) + SPF + Y2 - Q}$$

$$\therefore D3 = \frac{RP.(SPC - Q)}{(2.SPC) + SPF + Y2 - Q}$$

and for the end elevation

$$DP = \left((XL - I.DX + DX/2 + P)^2\right)^{1/2}$$

Using similar triangles

$$\frac{W3}{SPC - Q} = \frac{DP}{(2.SPC) + SPF + Y2 - Q}$$

$$\therefore W3 = \frac{DP.(SPC - Q)}{(2.SPC) + SPF + Y2 - Q}$$

Hence

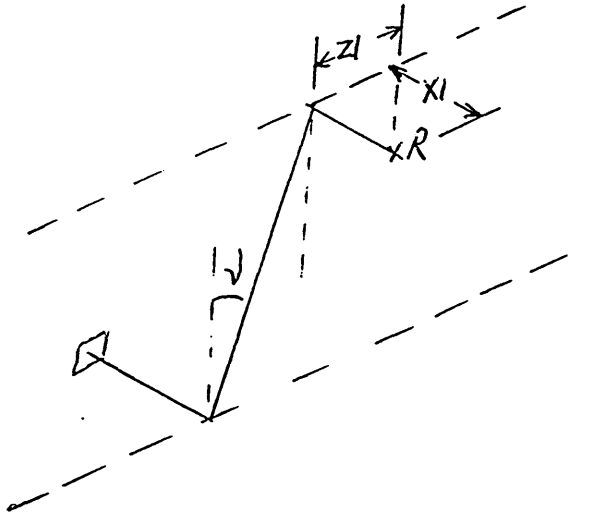

$$Z1 = \left(D3^2 + W3^2\right)^{1/2}$$

$$X1 = \left((SPC - Q)^2 + D3^2 + W3^2\right)$$

and $\nu = \arcsin(Z1/X1)$

The sound pressure, which is initially diffracted and then reflected twice, can then be computed, where

$$SOUND\ PRESSURE = ((RL.CORL1.CORL2) - (UNRL.COIM1.CORL2) - (RL.COIM1.COIM2) - (UNRL.CORL1.COIM2)) + i((RL.CORL1.COIM2) - (UNRL.COIM1.COIM2) + (RL.COIM1.CORL2) + (UNRL.CORL1.COIM2))$$

(9) Sound initially reflected twice, then diffracted and finally reflected twice again.

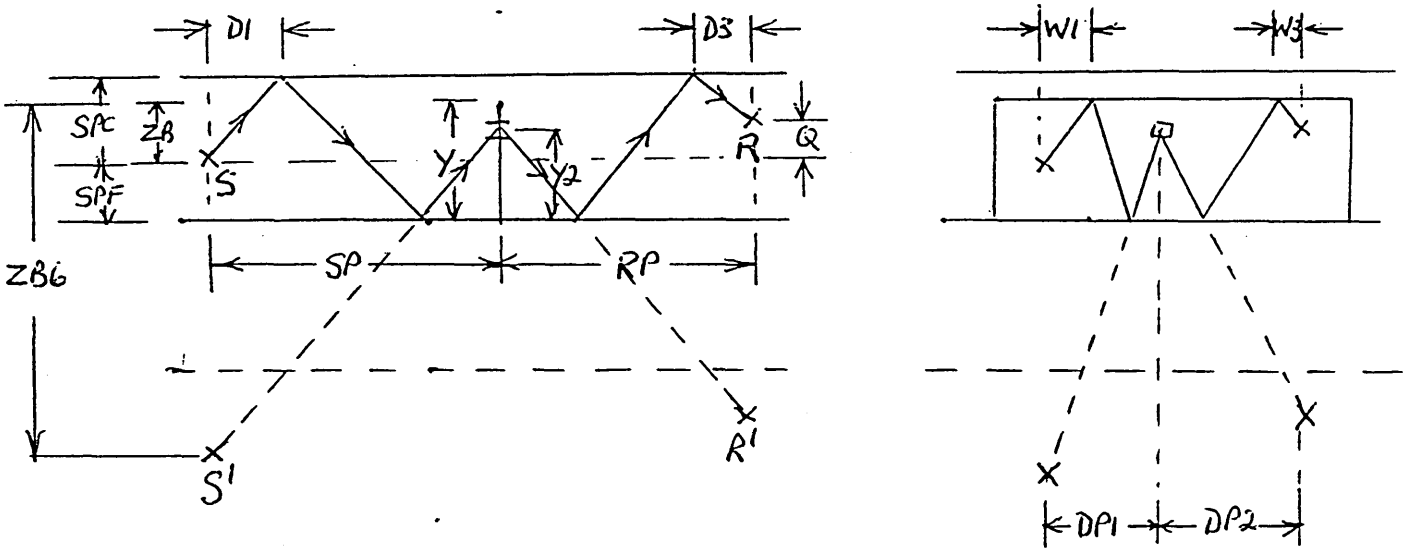

$Q12 = Q$

For each element we compute the real and imaginary parts of the reflection coefficients CORL1, CORL2, CORL3, CORL4, COIM1, COIM2, COIM3, COIM4, and in order to do this we need the 3-dimensional angles, ν_1 and ν_2, between the sound path and the normals.

On the side elevation

$$Y2 = Y - J.DY + DY/2$$

and using similar triangles

$$\frac{D1}{SPC} = \frac{SP}{(2.SPC) + SPF + Y2}$$

$$\therefore D1 = \frac{SP.SPC}{(2.SPC) + SPF + Y2}$$

and for the end elevation

$$DP1 = \left((ZL - I.DX + DX/2)^2\right)^{1/2}$$

$$DP2 = \left((ZL - I.DX + DX/2 + P)^2\right)^{1/2}$$

Using similar triangles

$$\frac{D3}{SPC - Q} = \frac{RP}{(2.SPC) + SPF + Y2 - Q}$$

$$\therefore D3 = \frac{RP.(SPC - Q)}{(2.SPC) + SPF + Y2 - Q}$$

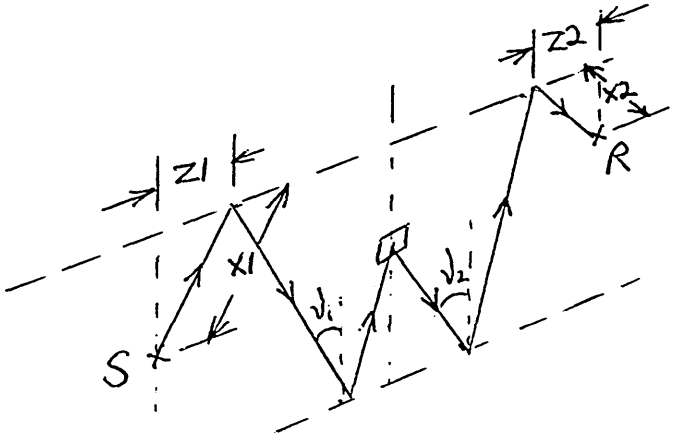

$$Z1 = \left(D1^2 + W1^2\right)^{1/2}$$

$$X1 = \left(SPC^2 + D1^2 + W1^2\right)^{1/2}$$

$$Z2 = \left(D3^2 + W3^2\right)^{1/2}$$

$$X2 = \left((SPC - Q)^2 + D3^2 + W3^2\right)^{1/2}$$

and $\nu_1 = \arcsin(Z1/X1)$

$\nu_2 = \arcsin(Z2/X2)$

The sound pressure, which is initially reflected twice, then diffracted, and then reflected twice again, can then be computed, where

$$
\begin{aligned}
SOUND\ PRESSURE = {} & ((RL.CORL1.CORL2.CORL3.CORL4) - (UNRL.COIM\ 1.CORL2.CORL3.CORL4) \\
& - (UNRL.CORL1.CORL.3CORL4.COIM\ 2) - (RL.COIM\ 1.COIM\ 2.CORL3.CORL4) \\
& - (UNRL.CORL1.CORL2.CORL4.COIM\ 3) - (RL.COIM\ 1.COIM\ 3.CORL2.CORL4) \\
& - (RL.CORL1.CORL4.COIM\ 2.COIM\ 3) + (UNRL.COIM\ 1.COIM\ 2.COIM\ 3.CORL4) \\
& - (RL.CORL1.CORL2.COIM\ 3.COIM\ 4) + (UNRL.COIM\ 1.COIM\ 3.COIM\ 4.CORL2) \\
& + (UNRL.CORL1.COIM\ 2.COIM\ 3.COIM\ 4) + (RL.COIM\ 1.COIM\ 2.COIM\ 3.COIM\ 4) \\
& - (UNRL.CORL1.CORL2.CORL3.COIM\ 4) - (RL.COIM\ 1.COIM\ 4.CORL2.CORL3) \\
& - (UNRL.CORL1.CORL3.COIM\ 2.COIM\ 4) + (UNRL.COIM\ 1.COIM\ 2.COIM\ 4.CORL3)) \\
& + i((RL.CORL1.CORL2.CORL3.COIM\ 4) - (UNRL.COIM\ 1.COIM\ 4.CORL2.CORL3) \\
& - (UNRL.CORL1.CORL3.COIM\ 2.COIM\ 4) - (RL.COIM\ 1.COIM\ 2.COIM\ 4.CORL3) \\
& - (UNRL.CORL1.CORL2.COIM\ 3.COIM\ 4) - (UNRL.COIM\ 1.COIM\ 3.COIM\ 4.CORL2) \\
& - (RL.CORL1.COIM\ 2.COIM\ 3.COIM\ 4) + (UNRL.COIM\ 1.COIM\ 2.COIM\ 3.COIM\ 4) \\
& + (RL.CORL1.CORL2.CORL4.COIM\ 3) - (UNRL.CORL2.CORL4.COIM\ 1.COIM\ 3) \\
& - (UNRL.CORL1.CORL4.COIM\ 2.COIM\ 3) - (RL.CORL4.COIM\ 1.COIM\ 2.COIM\ 3) \\
& + (UNRL.CORL1.CORL2.CORL3.CORL4) + (RL.CORL2.CORL3.CORL4.COIM\ 1) \\
& + (RL.CORL1.CORL3.CORL4.COIM\ 2) - (UNRL.CORL3.CORL4.COIM\ 1.COIM\ 2))
\end{aligned}
$$

The sound pressure in the absence of a barrier, where reflected components from the ground and roof exist, becomes even more complicated than that for ground conditions alone. Again, we treat the sound pressure, in the absence of a barrier, in exactly the same way for the ground model. This sound pressure, at the receiver, is calculated using the elemental theory to compute the sound level through a hole, the same size and geometry as an 'infinitely wide' barrier which is the same height as the room.

The rest of the calculation uses Babinet's Principle in the same way as that for a barrier under ground conditions. The calculation is obviously more complicated because we have to include sound pressures from more reflected components. Again, to perform the calculation correctly, we need to incorporate the complex reflection coefficient, Cr, for all surfaces.

7.2 Results for a barrier in a flat room

After the introduction of a roof results for single and multi-reflections were obtained for this 'flat room' configuration.

Figures 29 and 30 use the model, where the finite barrier extends from the ground to the roof. Both sets of results record the behaviour in insertion loss with increasing frequency. Figure 31 repeats the geometry of the room for Figure 30, but introduces a gap between the top of the barrier and the roof. Figure 32 uses a 2 m x 4 m barrier in a 'flat room' of height 3 m, and shows the variation in insertion loss as the receiver is moved vertically from its central position.

Figure 33 used the 'flat room' model to investigate the variations in insertion loss as the aspect ratio of width/height of the barrier is increased, the barrier extending from the ground to the roof.

7.3 Discussion of results for a barrier in a 'flat room'

The author's model enables both single and multi-reflections from the ground and roof to be included, and using a 2 m x 4 m barrier which extends from the ground to the roof, Figure 29 shows a steady increase in insertion loss with increasing frequency. Figure 30 extends the barrier height to 2.4 m but the rest of the geometry remains the same. The curves are smoother than those for the ground model, the reason being that no diffraction or interference takes place above or below the barrier. Due to increased interference around the sides of the barrier, multi-reflections cause greater deviations from the general trend of the curve than is the case for single reflections.

Figure 31 introduces a gap of 0.1 m between the top of the barrier and the roof, and although the general trend is a steady increase in insertion loss with respective increases in frequency, the curve deviates from this trend, particularly at the high end of the frequency spectrum. A line of best fit is superimposed over the true

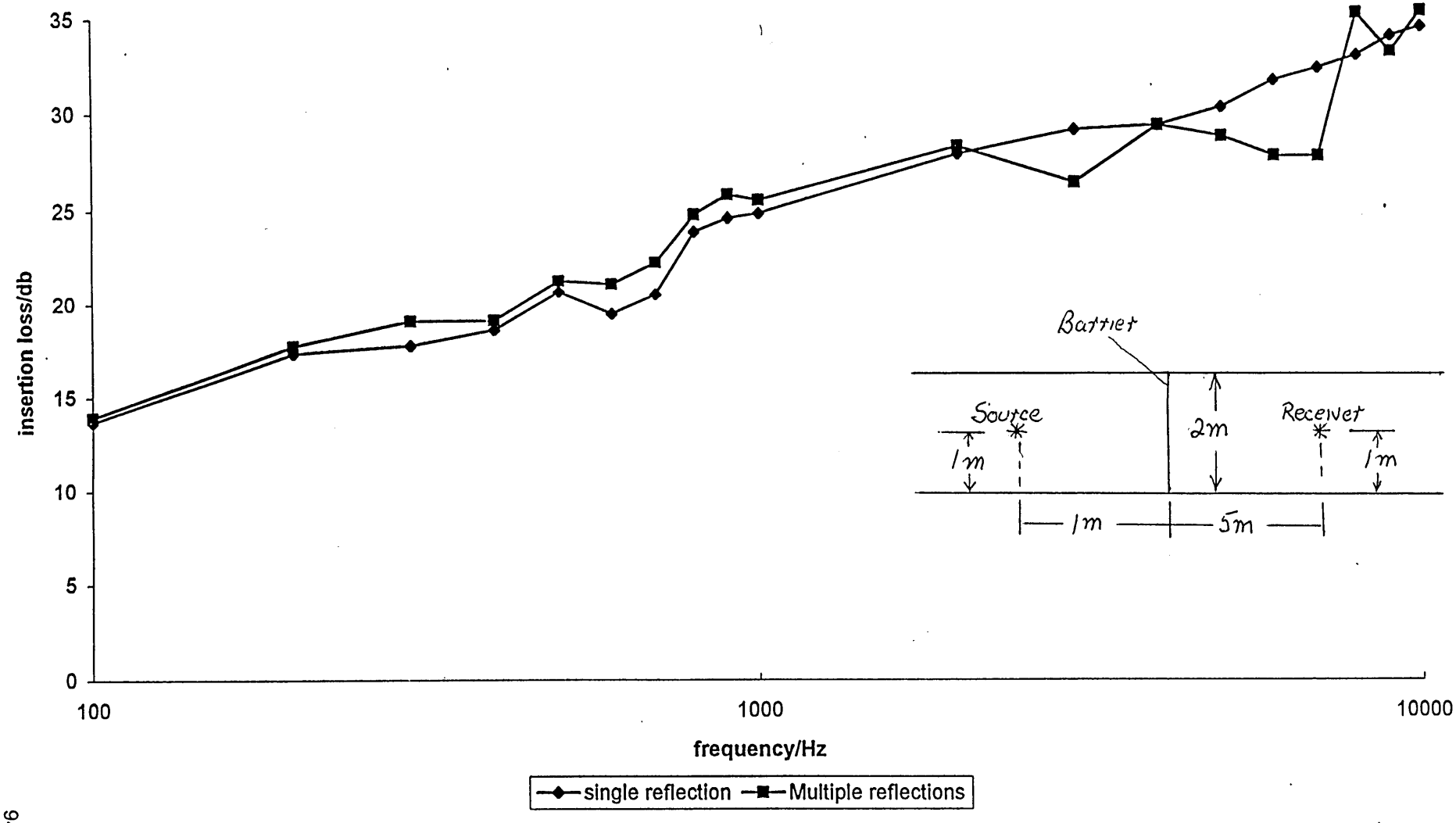

Figure 29 Insertion loss for a 4 m wide barrier in a flat room, using concrete surfaces. Barrier of height 2m, extends from floor to ceiling.

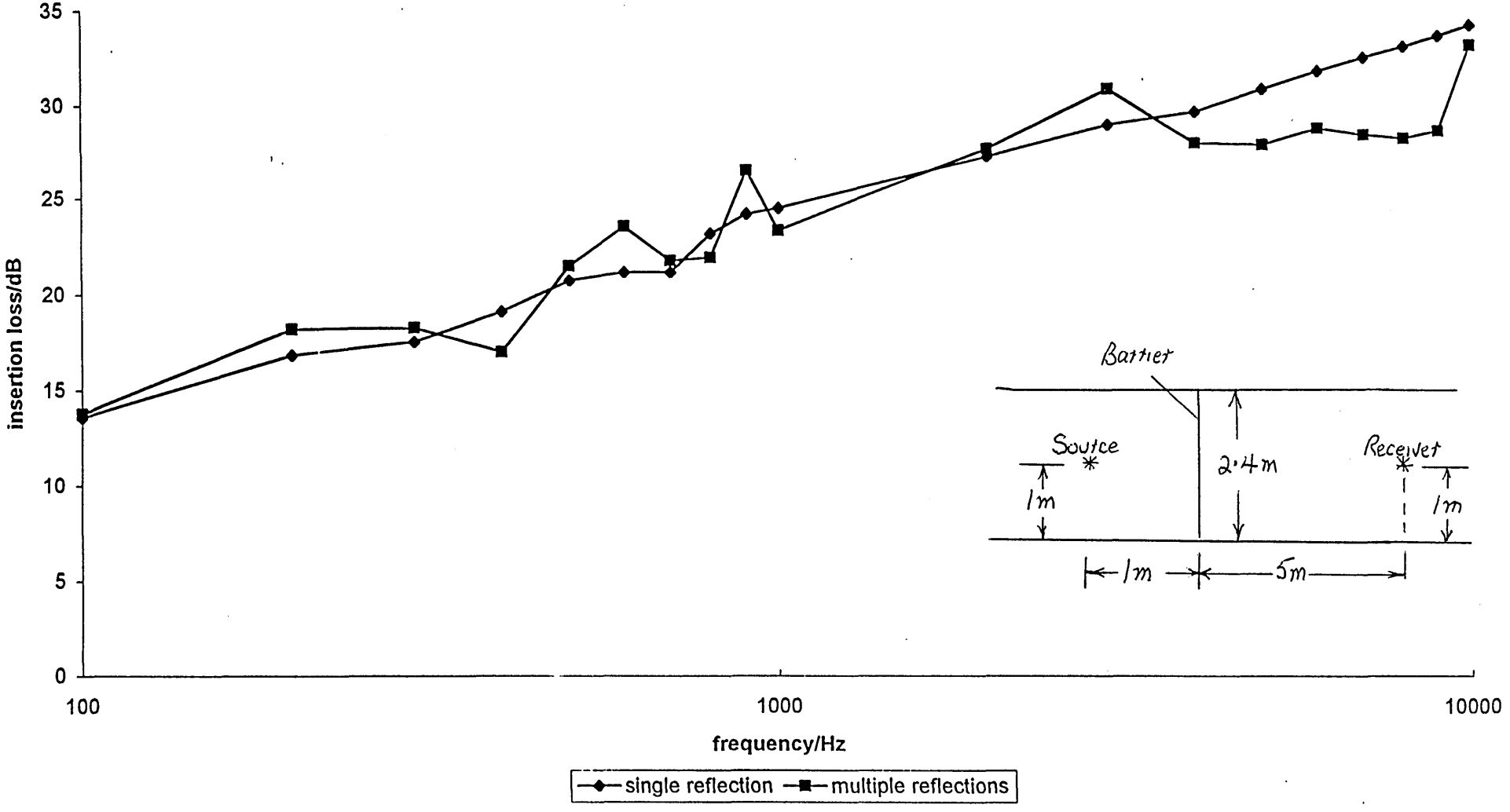

Figure 30 Insertion loss for a 4 m wide barrier in a flat room, using concrete surfaces. Barrier, of height 2.4 m, extends from floor to ceiling

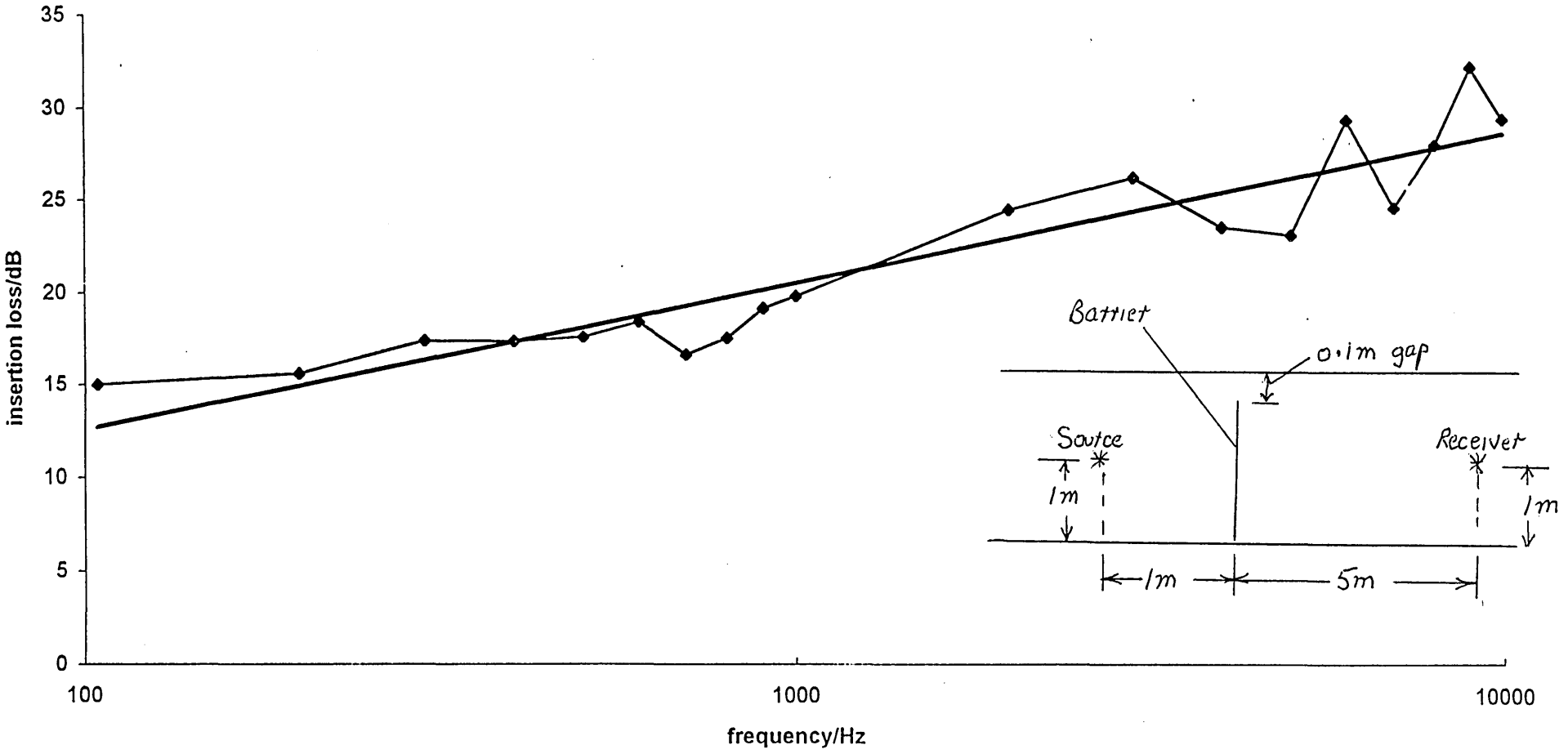

Figure 31 Insertion loss for a 4 m wide barrier in a flat room, using concrete surfaces. The height of the room is 2.4 m with a gap of 0.1 m between the top of the barrier and the ceiling.

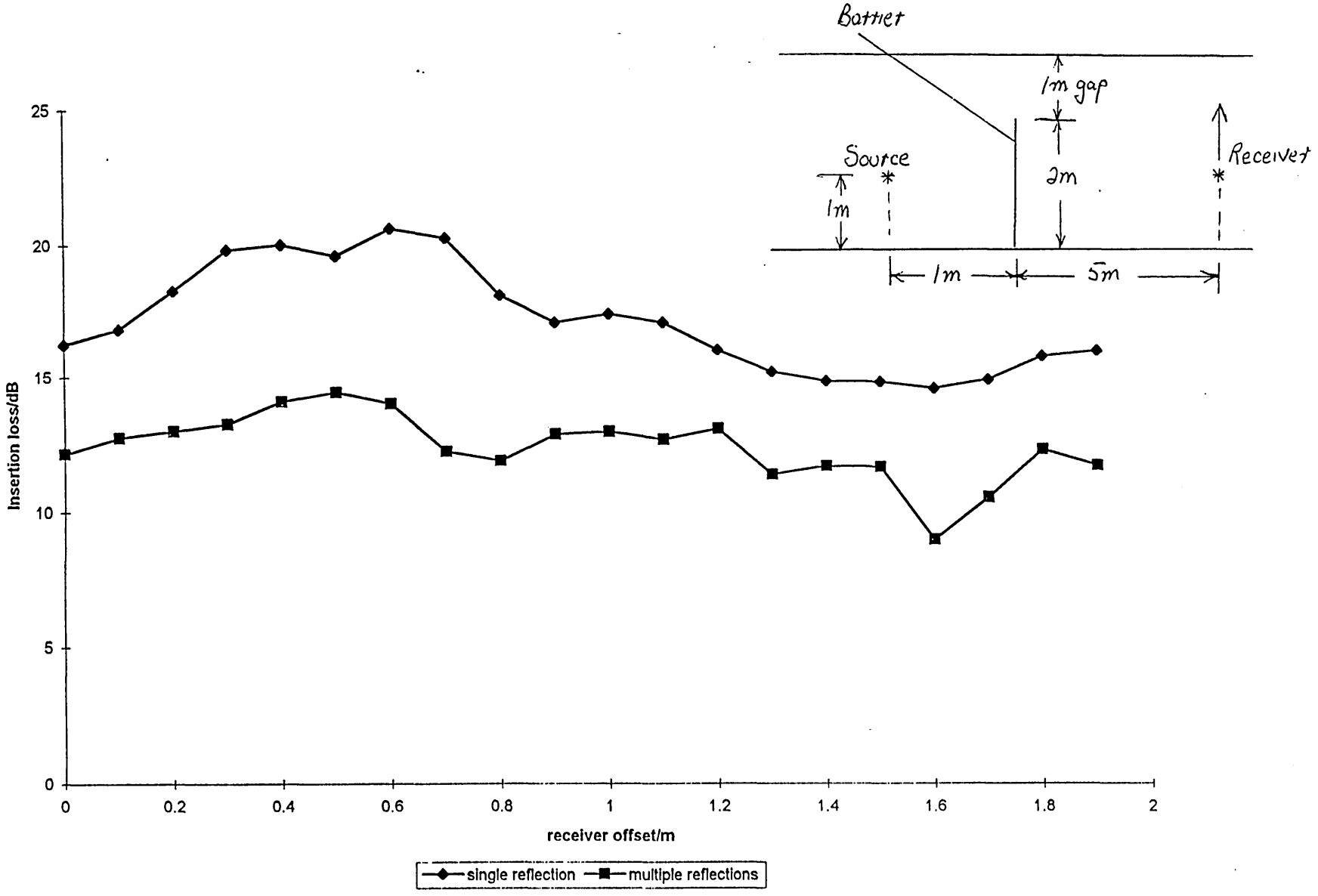

Figure 32 Barrier in a flat room. Effect on insertion loss by changing the receiver position.

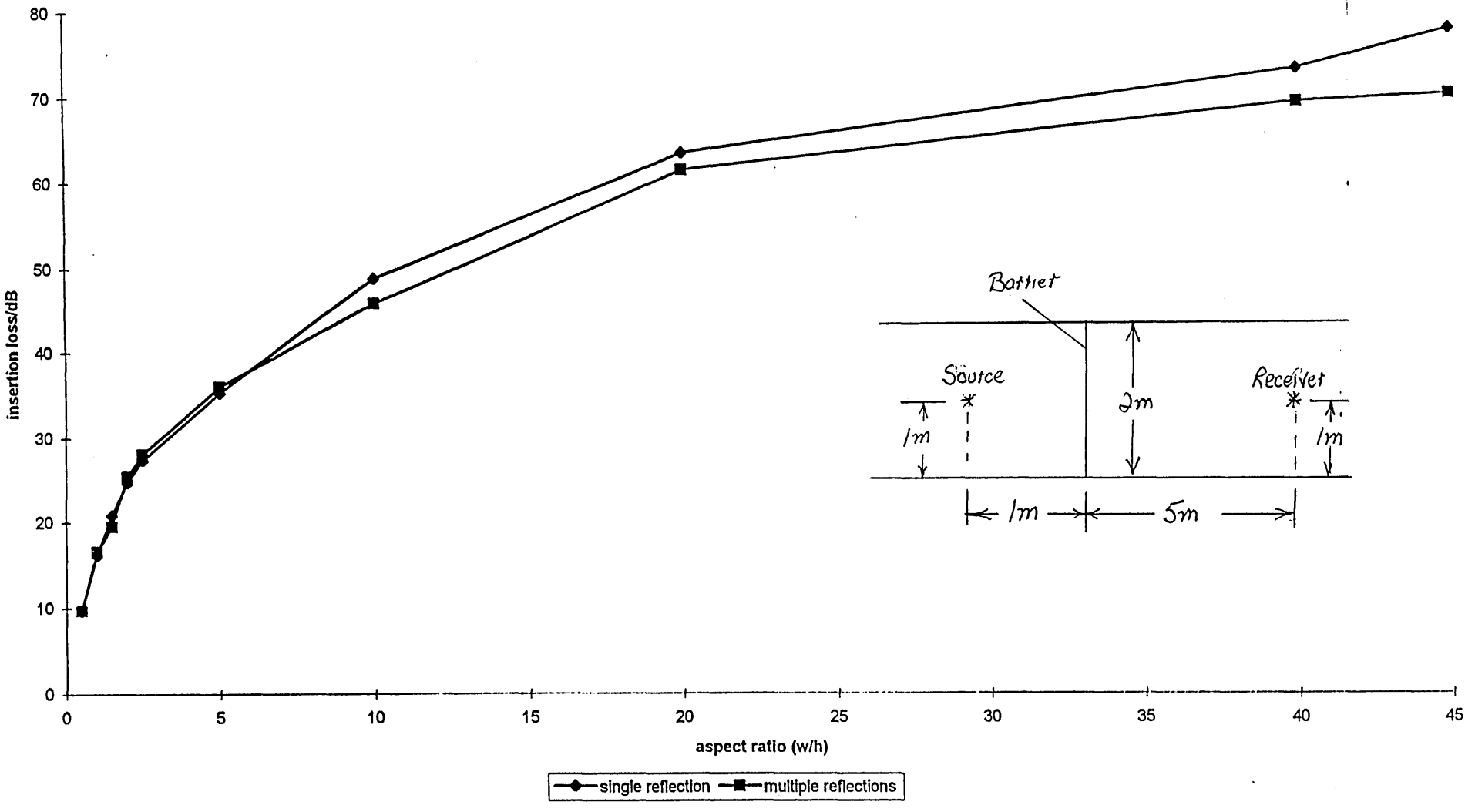

Figure 33 Variation of insertion loss with the aspect ratio (width/height)

curve to demonstrate the magnitude of these deviations. The barrier is finite and therefore diffraction and interference around the sides, as well as over the top, is extremely significant.

Using the geometry shown in Figure 34, the results produced by E Katarbinska, Figure 35, show a similar trend of increasing insertion loss with respective increases in frequency, to the curves produced by the author. The experimental data tends to deviate around the general trend and this data was produced using a model of scale 1:5.

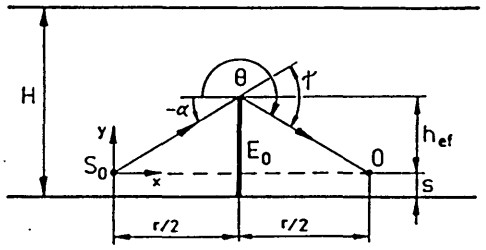

Figure 34 Symbols used in the equations.

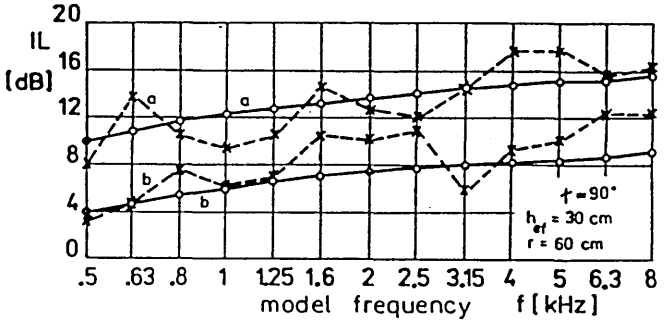

Figure 35 Calculated (O ···O) and experimental (× - - - - ×) data of Insertion Loss of the barrier in a model of a room of two heights: (a) $H = 240$ cm; (b) $H = 120$ cm.

Comparing Figure 32, which uses a 2 m x 4 m barrier in a flat room of height 3 m, with Figure 25 (ground conditions only), it can be seen that there is less reduction in insertion loss as the receiver position is moved vertically, and the deviations from the general trend of the curve are less dramatic. This is especially true for the initial peak value. The curve for multi-reflections gives a lower value in sound reduction than that for single-reflections, but in the case of multi-reflections, the general trend of the curve is to remain static. This suggests that sloping the barrier will have little effect in a 'flat room'.

The 'flat room' model is used to investigate the change in insertion loss as the aspect ratio of width/height of the barrier is increased, the barrier extending from the ground to the roof. Figure 33 shows an initial rapid increase in the curve, which can be interpreted as 'finite' conditions; the increase then becomes less

rapid, giving 'semi-infinite' conditions and finally the curve flattens, where the barrier becomes 'infinite'.

8 BARRIER IN AN ENCLOSURE

Authors of previous research, using barriers in enclosures, have ignored the contribution of boundary walls in their calculations. The author thought it necessary to introduce side walls into his model and compare the results with those, for identical geometries, in his 'flat room' model.

Adding side walls brings added complictions to the 'flat room' model. The reflection coefficient, Cr, is incorporated once again for the specular angle of reflection for all surfaces.

8.1 Computational details

Calculation of the sound passing through the barrier shaped hole is the same for that in the 'flat room' model, but now includes the following cases:

1 Sound initially reflected and then diffracted

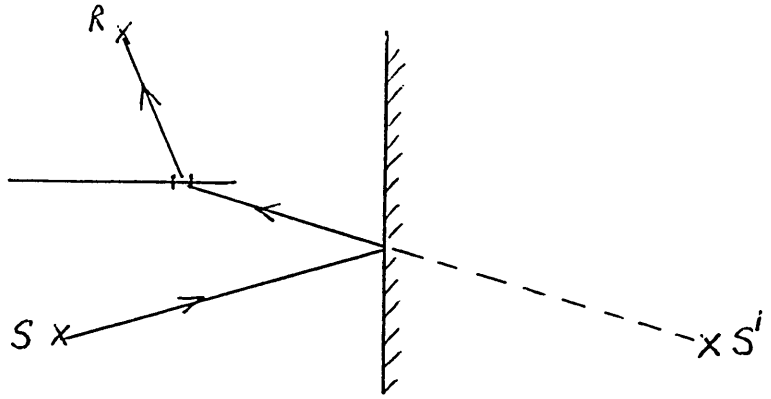

2 Sound initially diffracted and then reflected

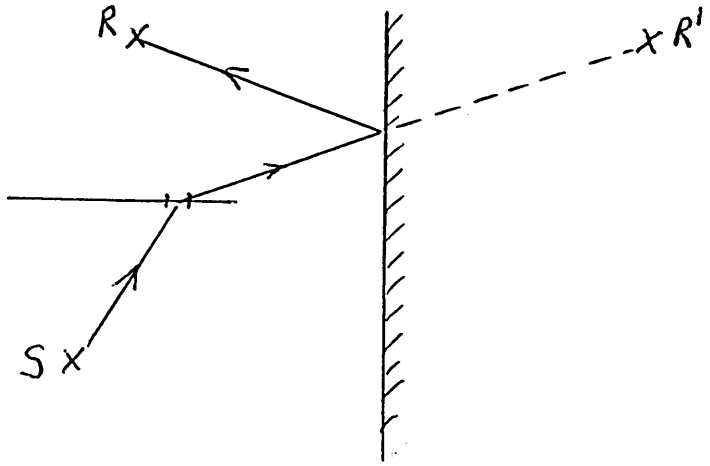

3 Sound initially reflected, then diffracted, and finally reflected again.

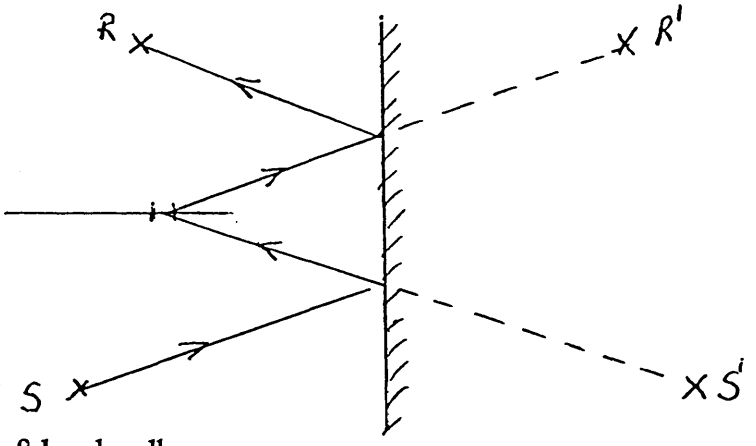

For the left hand wall

4 Sound initially reflected and then diffracted

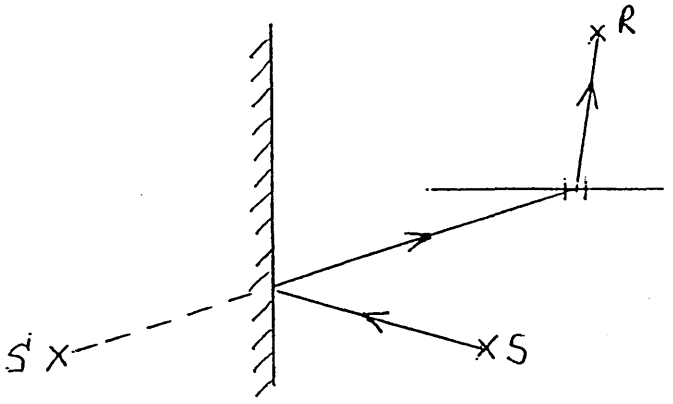

5 Sound initially diffracted and then reflected

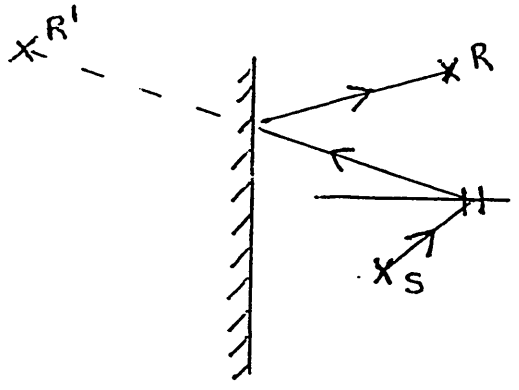

6 Sound initially reflected, then diffracted and finally reflected again.

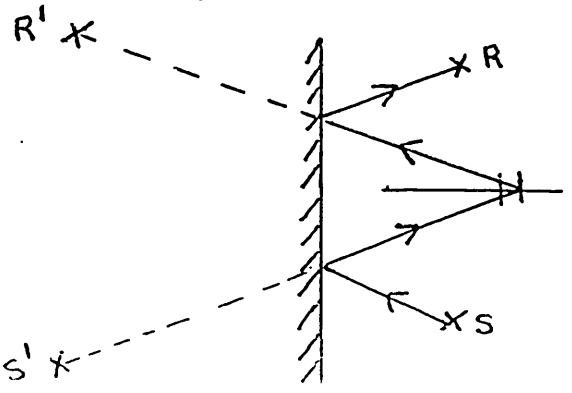

All the sound pressures illustrated above, plus those of the direct and reflected components in the 'flat room' model, are combined to produce a total complex sound pressure for sound passing through the hole, ie $\cup_H$.

Then, again, the sound pressure around the barrier,

$$\cup_B = \cup_D - \cup_H$$

Computation of the above stages:

Sound reflected from the right hand wall

(1) Sound initially reflected an then diffracted

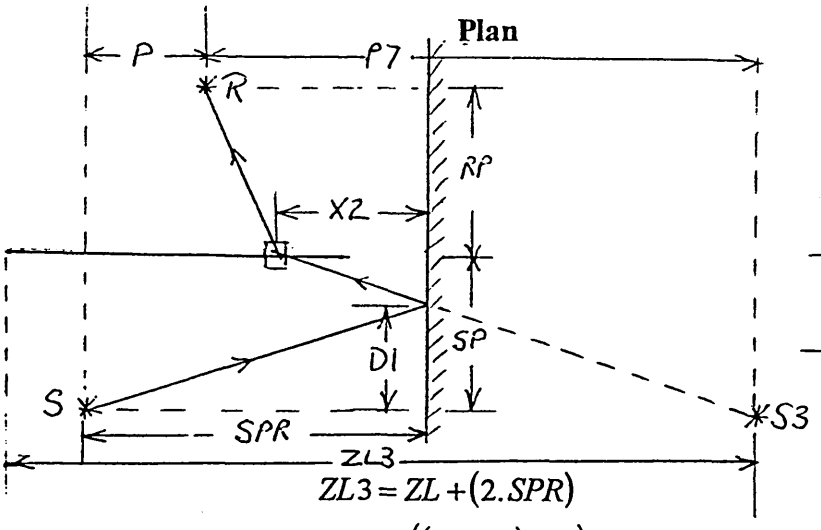

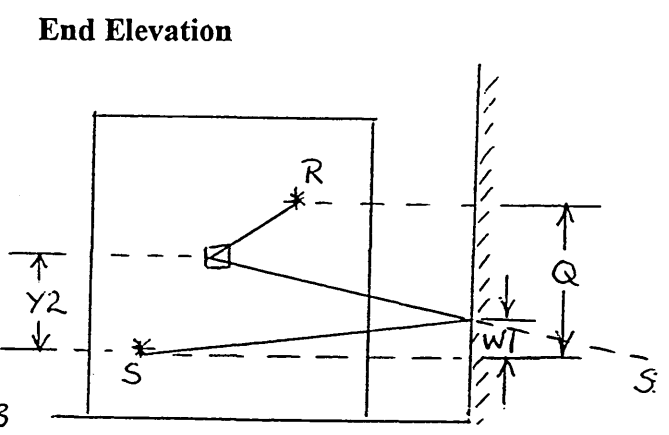

$$ZL3 = ZL + (2.SPR)$$

$$P7 = -((2.SPR) - P)$$

For each element we compute the real and imaginary parts of the reflection coefficient, ie CORL and COIM, and in order to do this we require the 3-dimensional angle ν, between the sound path and the normal.

On the plan

$$Y2 = ZL3 - SPR - I.DX + DX/2$$

and using similar triangles

$$\frac{SPR}{D1} = \frac{X2}{SP - D1}$$

$$\therefore D1 = \frac{(SPR.SP)}{(X2 + SPR)}$$

and from the end elevation

$$Y2 = \left((ZB - J.DY + DY/2)^2\right)^{1/2}$$

Using similar triangles

$$\frac{SPR}{W1} = \frac{X2}{Y2 - W1}$$

$$\therefore W1 = \frac{(SPR.Y2)}{(X2 + SPR)}$$

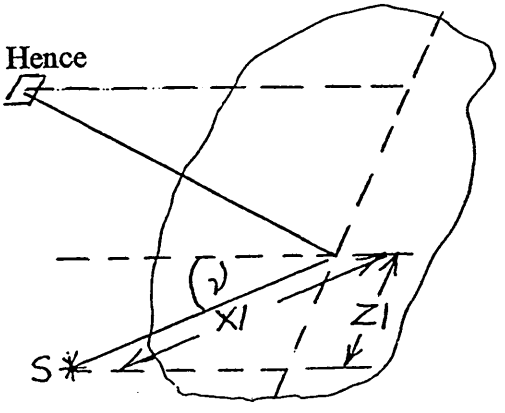

$$Z1 = \left(D1^2 + W1^2\right)^{1/2}$$

$$X1 = \left(SPR^2 + D1^2 + W1^2\right)^{1/2}$$

and $\nu = \arcsin(Z1/X1)$

The sound pressure, which is initially reflected and then diffracted, can then be computed where

$$SOUND\ PRESSURE = (RL.CORL + UNRL.COIM) + i(UNRL.CORL - RL.COIM)$$

(2) Sound initially diffracted and then reflected.

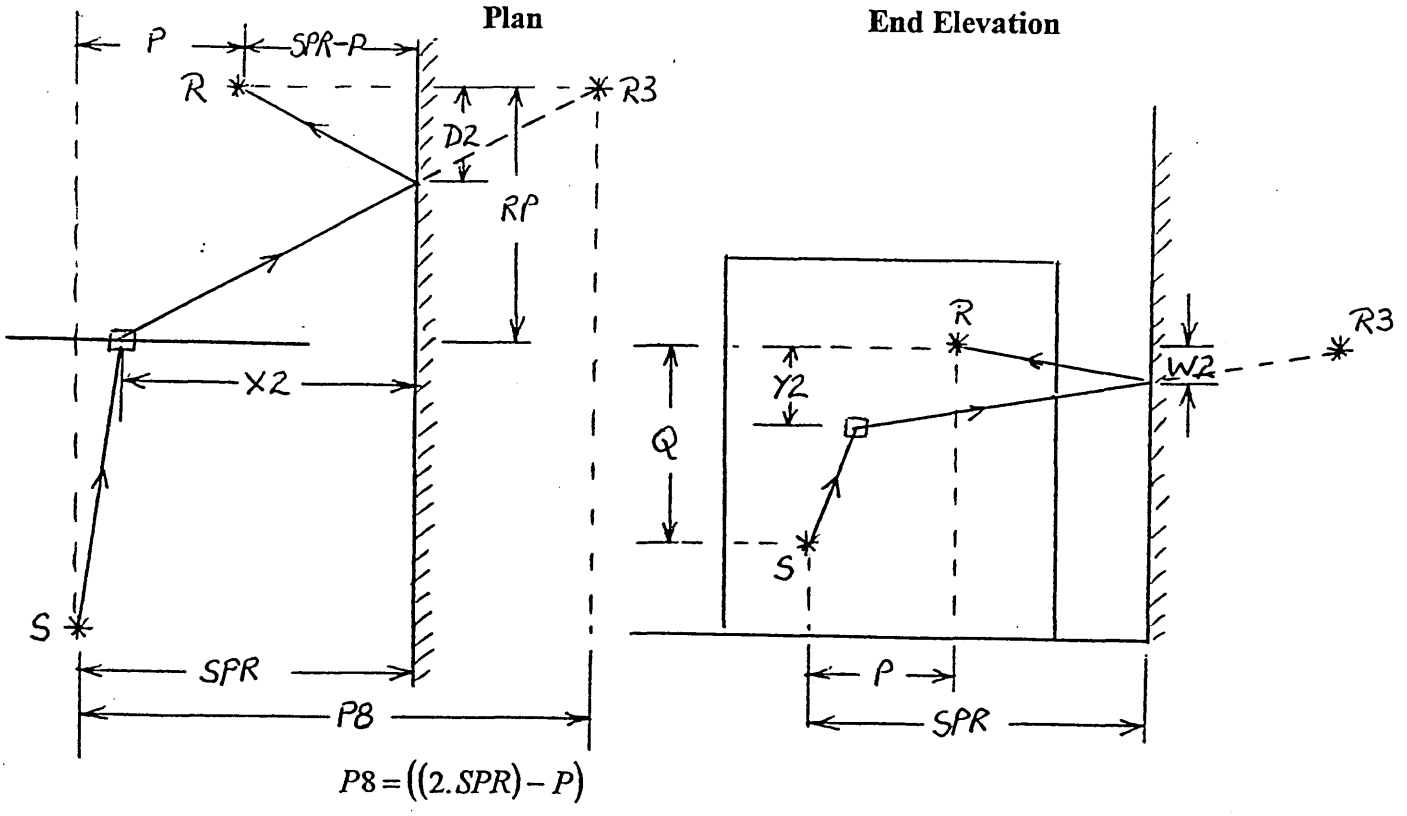

$$P8 = \left((2.SPR) - P\right)$$

For each element we compute the real and imaginary parts of the reflection coefficient, ie CORL and COIM , and in order to do this we require the 3-dimensional angle ν, between the sound path and the normal.

On the plan

$$X2 = ZL + SPR - I.DX + DX/2$$

and using similar triangles

$$\frac{SPR - P}{D2} = \frac{X2}{RP - D2}$$

$$\therefore D2 = \frac{\left(RP(SPR - P)\right)}{\left(X2 + SPR - P\right)}$$

. and from the end elevation

$$Y2 = \left((ZB - Q - J.DY + DY/2)^2\right)^{1/2}$$

Using similar triangles

$$\frac{SPR - P}{W2} = \frac{X2}{Y2 - W2}$$

$$\therefore W2 = \frac{\left(Y2(SPR - P)\right)}{\left(X2 + SPR - P\right)}$$

Hence

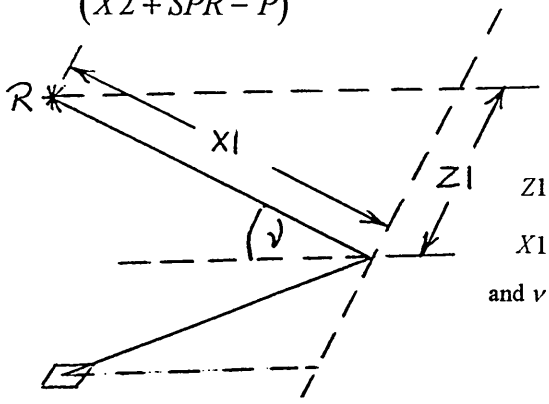

$$Z1 = \left(D2^2 + W2^2\right)^{1/2}$$

$$X1 = \left((SPR - P)^2 + D2^2 + W2^2\right)^{1/2}$$

and $\nu = \arcsin(Z1/X1)$

The sound pressure, which is initially diffracted and then reflected, can then be computed where

$$SOUND\ PRESSURE = \left(RL.CORL + UNRL.COIM\right) + i\left(UNRL.CORL - RL.COIM\right)$$

(3) Sound initially reflected, then diffracted and finally reflected again.

Plan **End Elevation**

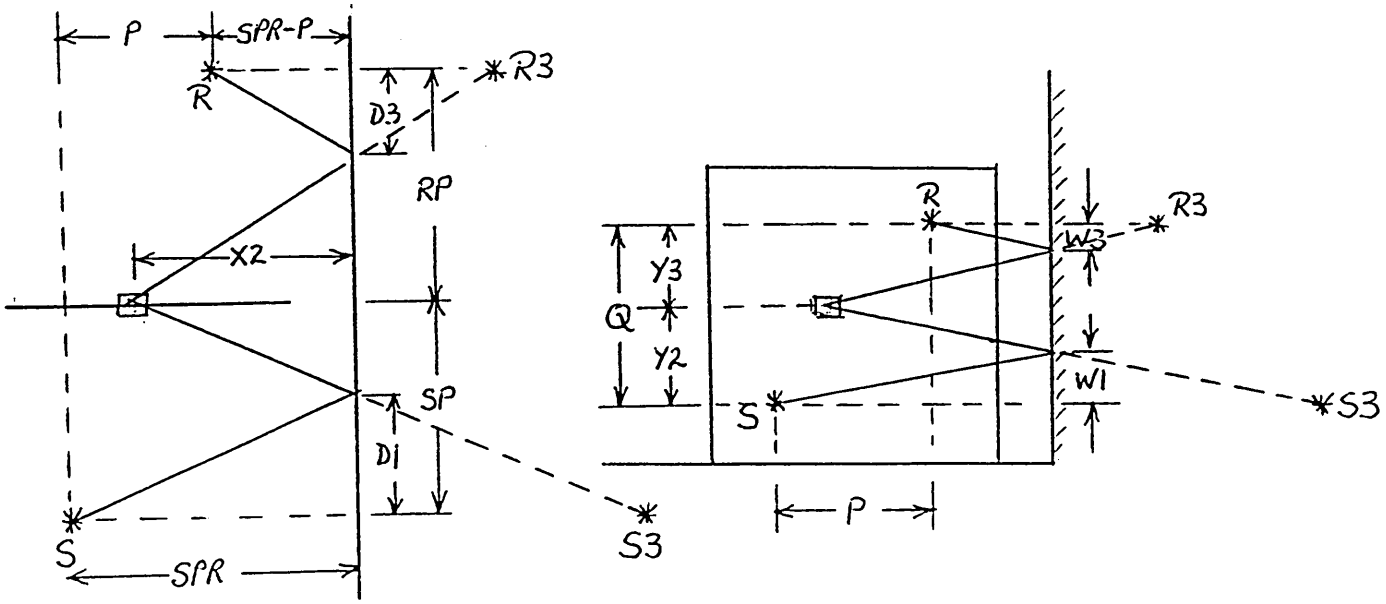

P9 = – P

For each element we compute the real and imaginary parts of the reflection coefficient before diffraction takes place, ie CORL1 and CORL2 and also the real and imaginary parts of the reflection coefficient after diffraction, ie CORL2 and COIM2. In order to do this we require the respective 3-dimensional angles ν_1 and ν_2, between the sound path and the normals at the respective points of reflection.

On the plan

$$X2 = ZL + SPR - I.DX + DX/2$$

and using similar triangles

$$D1 = \frac{(RP(SPR.P))}{(X2 + SPR)}$$

$$\therefore D3 = \frac{(RP(SPR.P))}{(X2 + SPR - P)}$$

and for the end elevation

$$Y2 = \left((ZB - J.DY + DY/2)^2\right)^{1/2}$$

$$Y3 = \left((ZB - Q - J.DY + DY/2)^2\right)^{1/2}$$

Using similar triangles

$$W1 = \frac{(SPR.Y2)}{(X2 + SPR)}$$

$$\therefore W3 = \frac{(Y3(SPR - P))}{(X2 + SPR - P)}$$

Hence

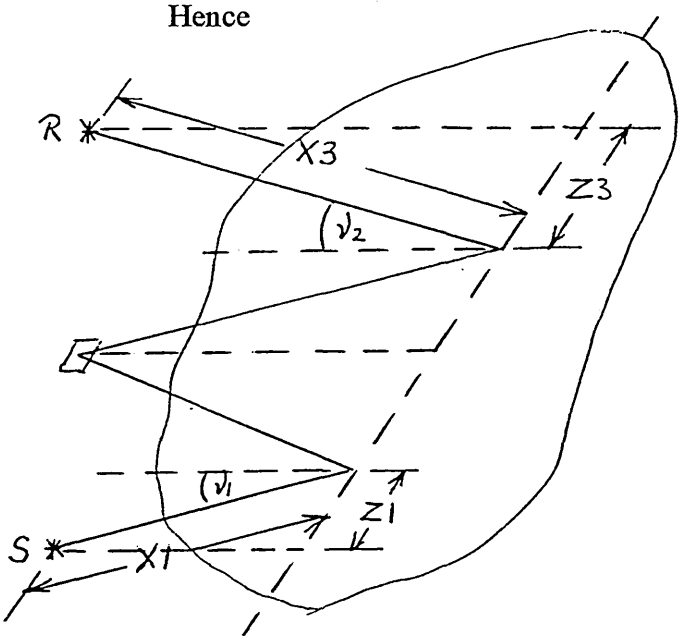

$$Z1 = \left(D1^2 + W1^2\right)^{1/2}$$

$$X1 = \left(SPR^2 + D1^2 + W1^2\right)^{1/2}$$

$$Z3 = \left(D3^2 + W3^2\right)^{1/2}$$

$$X3 = \left(\left(SPR - P\right)^2 + D3^2 + W3^2\right)^{1/2}$$

and $\nu_1 = \arcsin(Z1 / X1)$

$\nu_2 = \arcsin(Z3 / X3)$

The sound pressure which is initially reflected, then diffracted and then reflected again, can then be computed where

$$SOUND\ PRESSURE = (RL + iUNRL)(CORL1 - iCOIM1)(CORL2 - iCOIM2)$$

$$= (RL.CORL1.CORL2 + UNRL.COIM1.CORL2 + UNRL.COIM1.COIM2 - RL.COIM1.COIM2)$$

$$+ i(UNRL.CORL1.CORL2 - RL.COIM1.CORL2 - RL.CORL1.COIM2 - UNRL.COIM1.COIM2)$$

Sound reflected from the left hand wall

(4) Sound initially reflected and then diffracted

Plan **End Elevation**

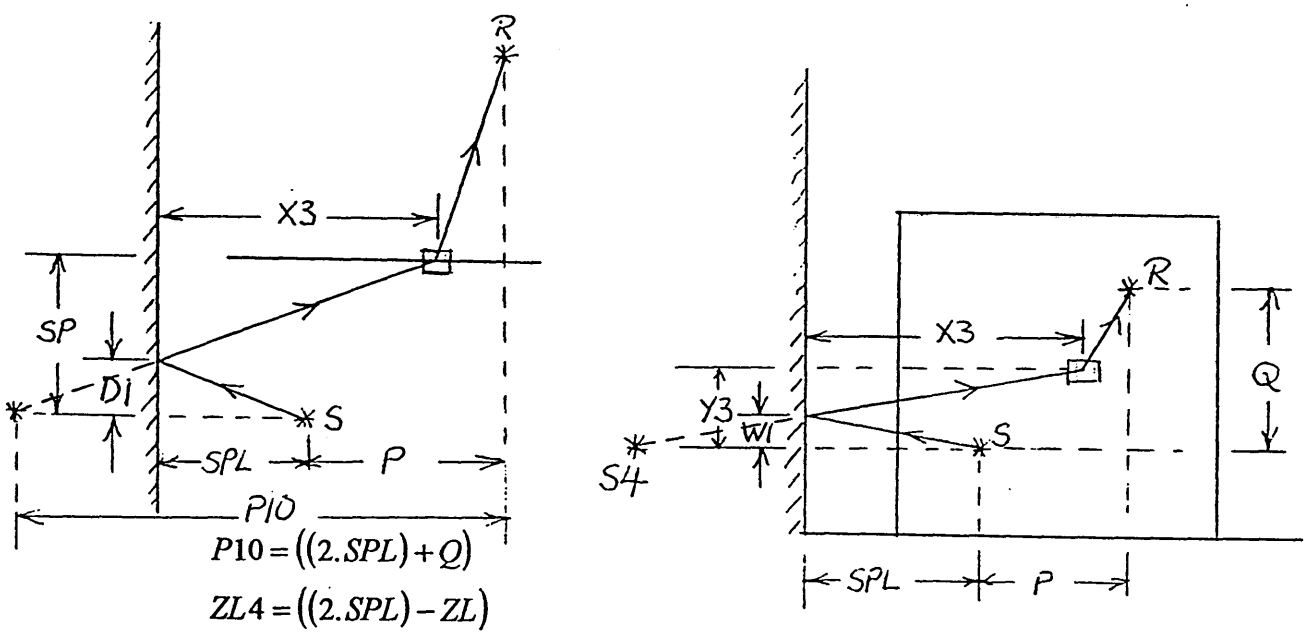

For each element we compute the real and imaginary parts of the reflection coefficient ie CORL and COIM, and in order to do this we require the 3-dimensional angle v, between the sound path and the normal.

On the plan

$$X3 = SPL - ZL + I.DY - DX/2$$

and using similar triangles

$$\frac{SPL}{D1} = \frac{X3}{SP - D1}$$

$$\therefore D1 = \frac{(SPL.SP)}{(X3 + SPL)}$$

and from the end elevation

$$Y3 = \left((ZB - J.DY + DY/2)^2\right)^{1/2}$$

Using similar triangles

$$\frac{SPL}{W1} = \frac{X3}{Y3 - W1}$$

$$\therefore W1 = \frac{(SPL.Y3)}{(X3 + SPL)}$$

Hence

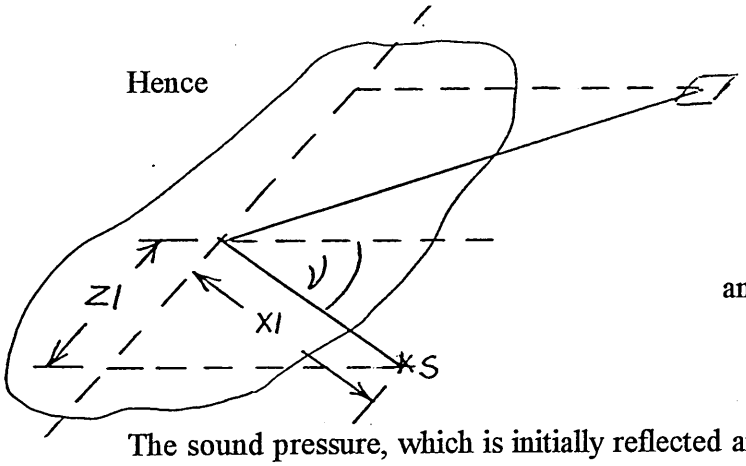

$$Z1 = \left(D1^2 + W1^2\right)^{1/2}$$

$$X1 = \left(SPL^2 + D1^2 + W1^2\right)^{1/2}$$

and $\nu = \arcsin(Z1 / X1)$

The sound pressure, which is initially reflected and then diffracted, can then be computed where

$$SOUND\ PRESSURE = (RL.CORL + UNRL.COIM) + i(UNRL.CORL - RL.COIM)$$

(5) Sound initially diffracted and then reflected

Plan **End Elevation**

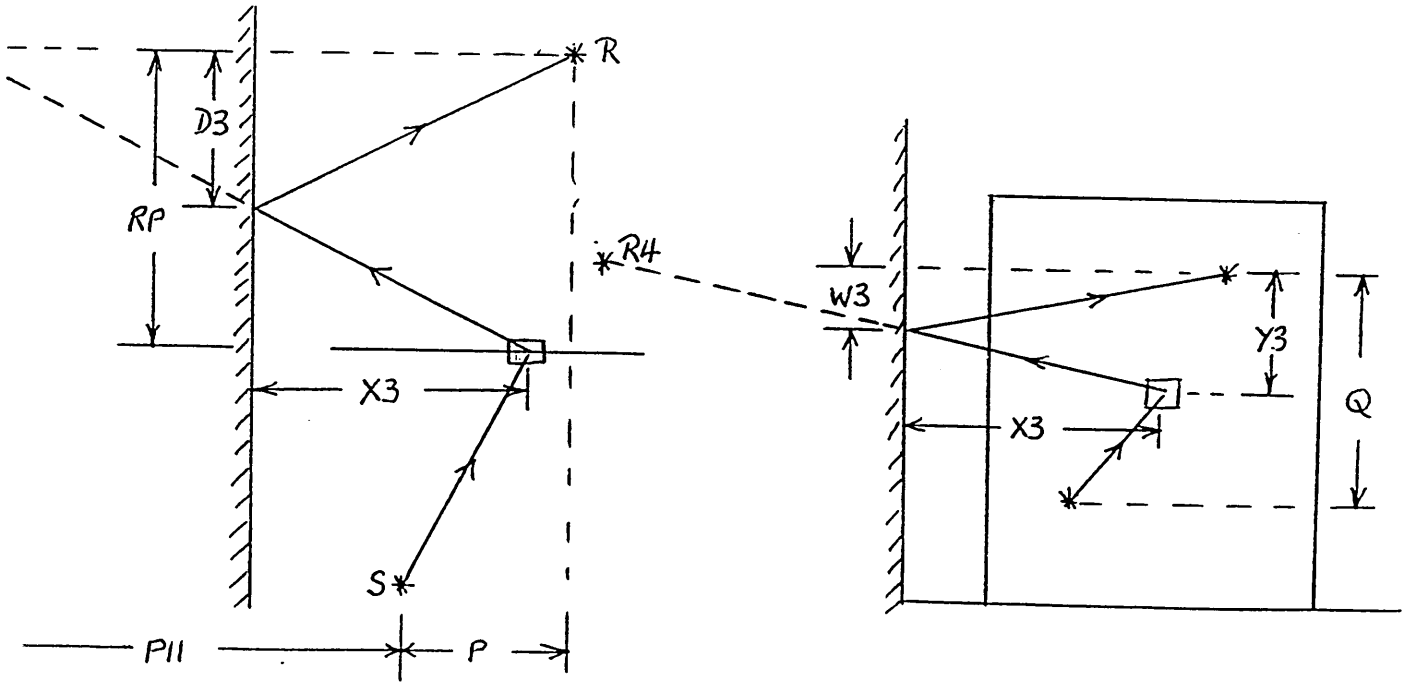

$$P11 = \left((2.SPL) + P\right)$$

For each element we compute the real and imaginary parts of the reflection coefficient, ie CORL and COIM, and in order to do this we require the 3-dimensional angle ν, between the sound path and the normal.

On the plan

$$X3 = SPL - ZL + I.DY - DX/2$$

and using similar triangles

$$\frac{SPL+P}{D3} = \frac{X3}{SP-D3}$$

$$\therefore D3 = \frac{(RP(SPL+P))}{(X3+SPL+P)}$$

and from the end elevation

$$Y3 = \left((ZB - J.DY + DY/2 - Q)^2\right)^{½}$$

Using similar triangles

$$\frac{SPL+P}{W3} = \frac{X3}{Y3-W3}$$

$$\therefore W3 = \frac{(Y3(SPL+P))}{(X3+SPL+P)}$$

Hence

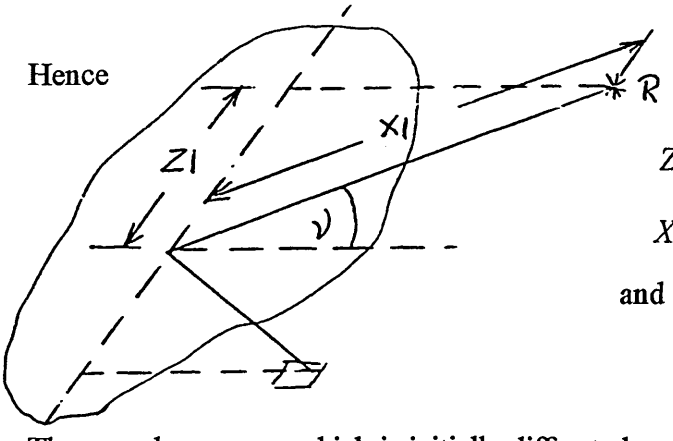

$$Z1 = \left(D3^2 + W3^2\right)^{½}$$

$$X1 = \left((SPL+P)^2 + D3^2 + W3^2\right)^{½}$$

and $\nu = \arcsin(Z1/X1)$

The sound pressure, which is initially diffracted and then reflected, can then be computed where

$$SOUND\ PRESSURE = (RL.CORL + UNRL.COIM) + i(UNRL.CORL - RL.COIM)$$

(6) Sound initially reflected, then diffracted and finally reflected again.

Plan **End Elevation**

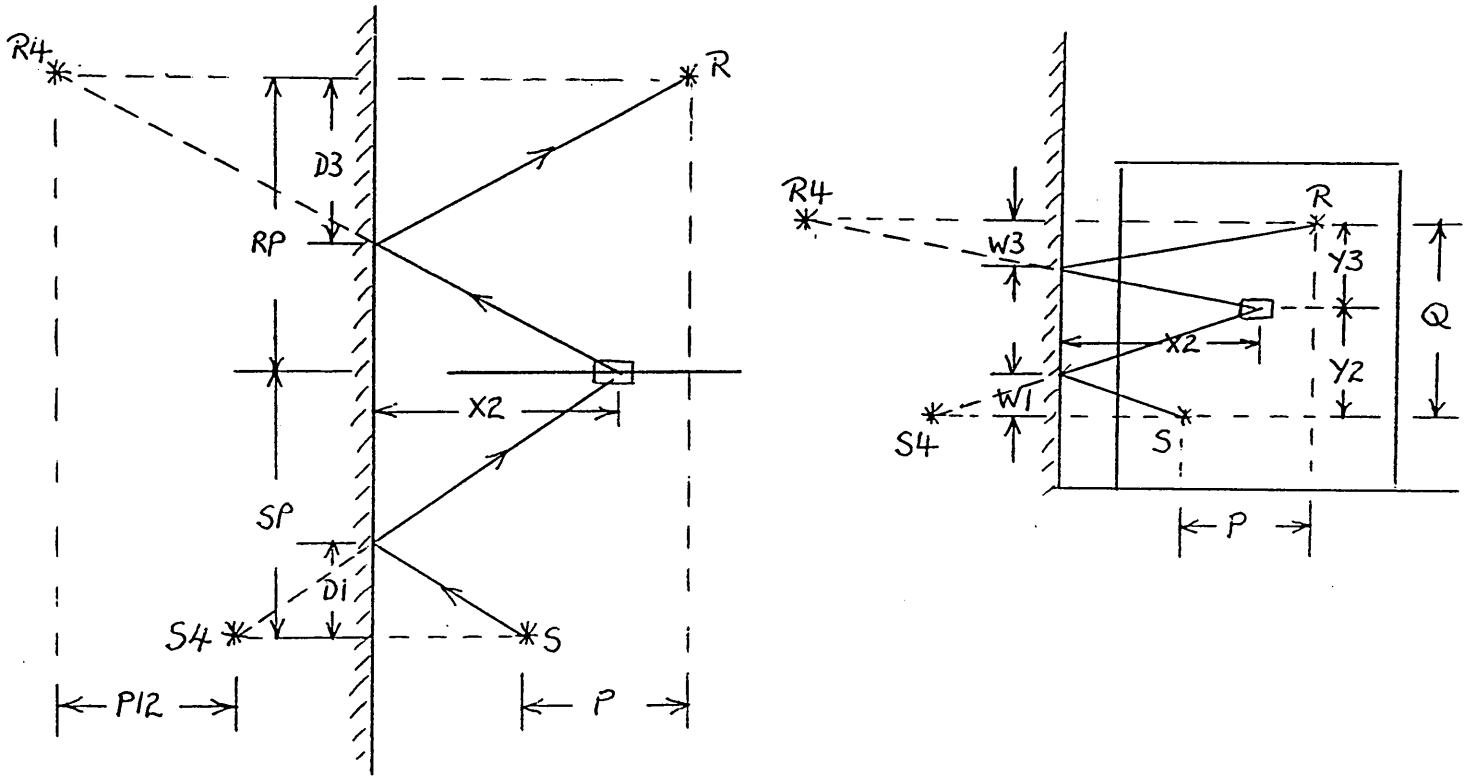

$$P12 = -P$$

For each element we compute the real and imaginary parts of the reflection coefficient before diffraction takes place, ie CORL1 and COIM1, and also the real and imaginary parts of the reflection coefficient after diffraction, ie CORL2 and COIM2. In order to do this we require the respective 3-dimensional angles ν_1 and ν_2 between the sound path and the normals at the respective points of reflection.

On the plan

$$X2 = SPL - ZL + I.DY - DX/2$$

and using similar triangles

$$D1 = \frac{(SPL.SP)}{(X2 + SPL)}$$

$$\therefore D3 = \frac{(RP(SPL + P))}{(X2 + SPL + P)}$$

and from the end elevation

$$Y2 = \left((ZB - J.DY + DY/2)^2\right)^{1/2}$$

$$Y3 = \left((ZB - J.DY + DY/2 - Q)^2\right)^{1/2}$$

Using similar triangles

$$W1 = \frac{(SPL.Y2)}{(X2 + SPL)}$$

$$\therefore W3 = \frac{(Y3(SPL + P))}{(X2 + SPL + P)}$$

Hence

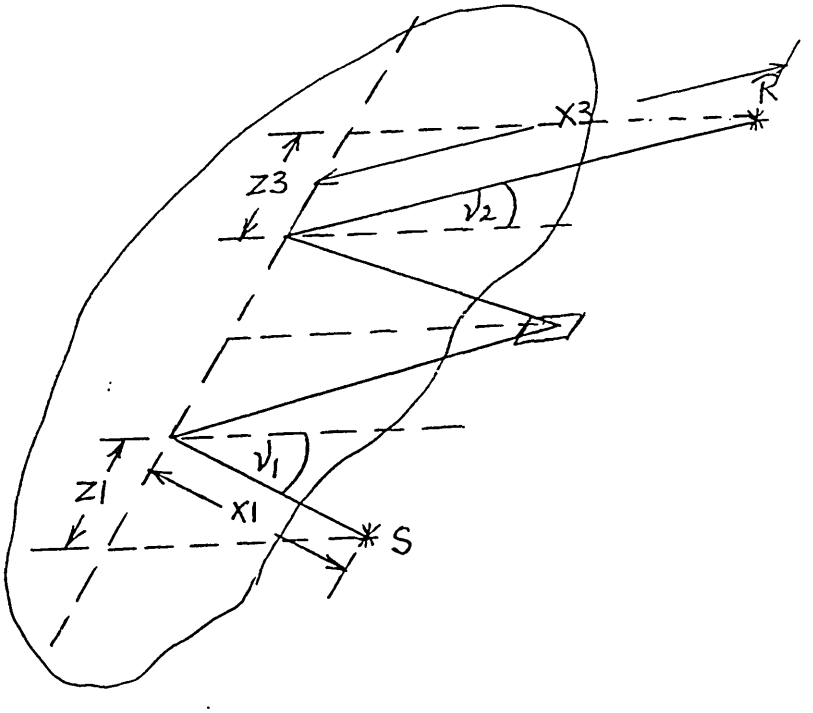

$$Z1 = \left(D1^2 + W1^2\right)^{1/2}$$

$$X1 = \left(SPL^2 + D1^2 + W1^2\right)^{1/2}$$

$$Z3 = \left(D3^2 + W3^2\right)^{1/2}$$

$$X3 = \left((SPL - P)^2 + D3^2 + W3^2\right)^{1/2}$$

and $\nu_1 = \arcsin(Z1/X1)$

$\nu_2 = \arcsin(Z3/X3)$

The sound pressure which is initially reflected, then diffracted and then reflected again, can then be computed where

$$SOUND\,PRESSURE=(RL+iUNRL)(CORL1-iCOIM1)(CORL2-iCOIM2)$$
$$=(RL.CORL1.CORL2+UNRL.COIM1.CORL2+UNRL.CORL1.COIM2-RL.COIM1.COIM2)$$
$$+i(UNRL.CORL1.CORL2-RL.COIM1.CORL2-RL.CORL1.COIM2-UNRL.COIM1.COIM2)$$

The sound pressure, in the absence of a barrier, in an enclosure becomes more complicated than that for the 'flat room' model, due to the added reflective surfaces, introduced by the side walls. Again, we treat the sound pressure, in the absence of a barrier, in the same way as that for a barrier in a 'flat room'. The sound pressure at the receiver, is again calculated by using the elemental theory to compute the sound level through a hole, the same size and geometry as the cross-section of the enclosure.

Once again, the rest of the calculation uses Babinet's Principle, and is even more complicated due to added reflected components from the walls. The complex reflection coefficient, Cr, is once more incorporated for all reflective surfaces.

Results for a barrier in an enclosure

As far as the author is aware, there is no literature which includes the reflective contributions from boundary walls. The author considers it a logical progression to add side walls to his model. Figure 36 uses the same barrier geometries as the 'flat room' model but places the barrier centrally between two walls. Figure 37 superimposes a line of best fit to Figure 36.

Figure 38 uses a 2 m x 4 m barrier in an enclosure of height 3 m and shows the variation in insertion loss as the receiver is moved vertically from its central position. Figure 39 allows comparison with Figure 33, where the aspect ratio changes the value of insertion loss in a 'flat room'.

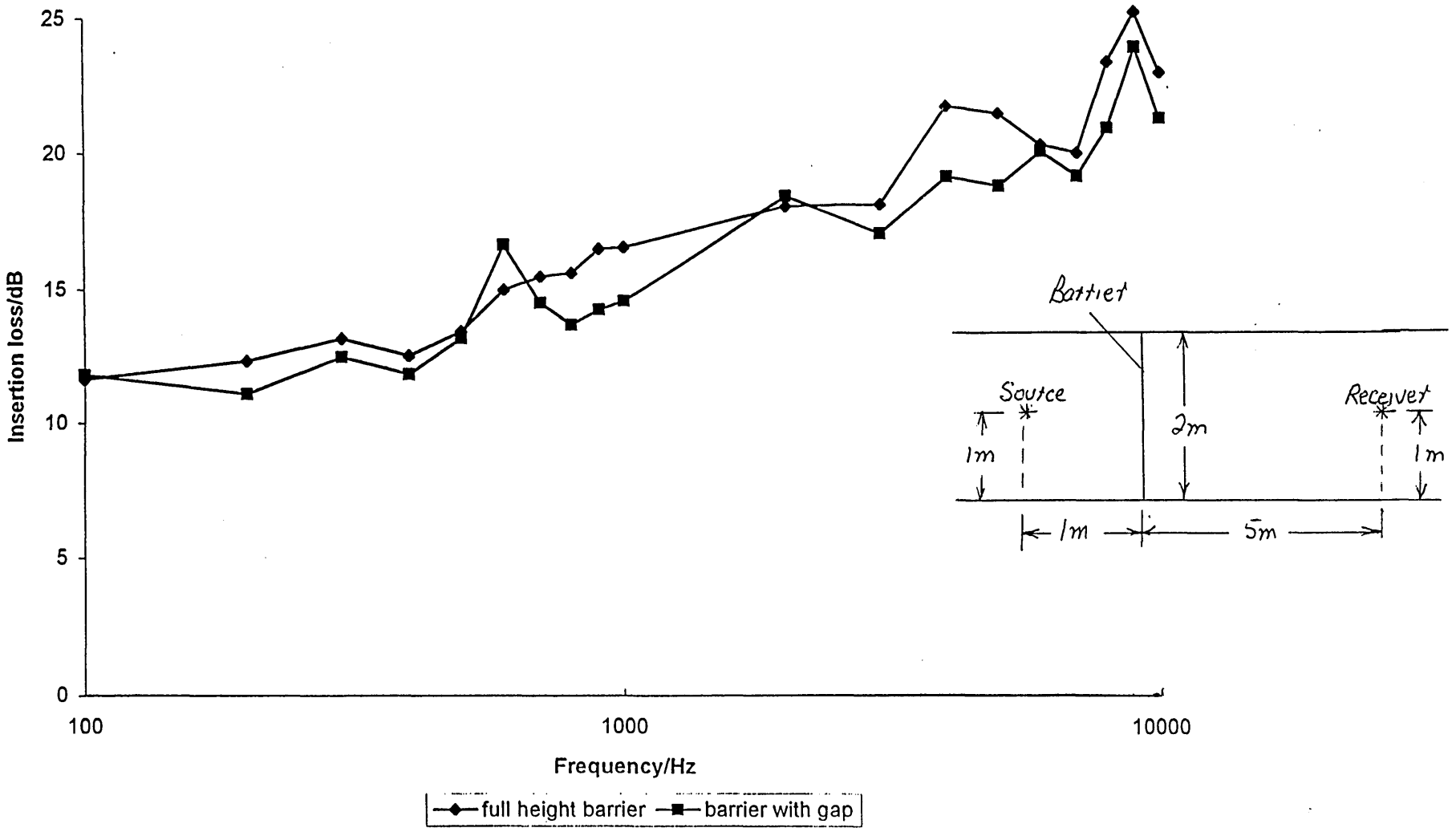

Figure 36 Insertion loss for a 4 m wide barrier, symmetrically placed, in an enclosure, using concrete surfaces, where the side walls are 10 m apart.

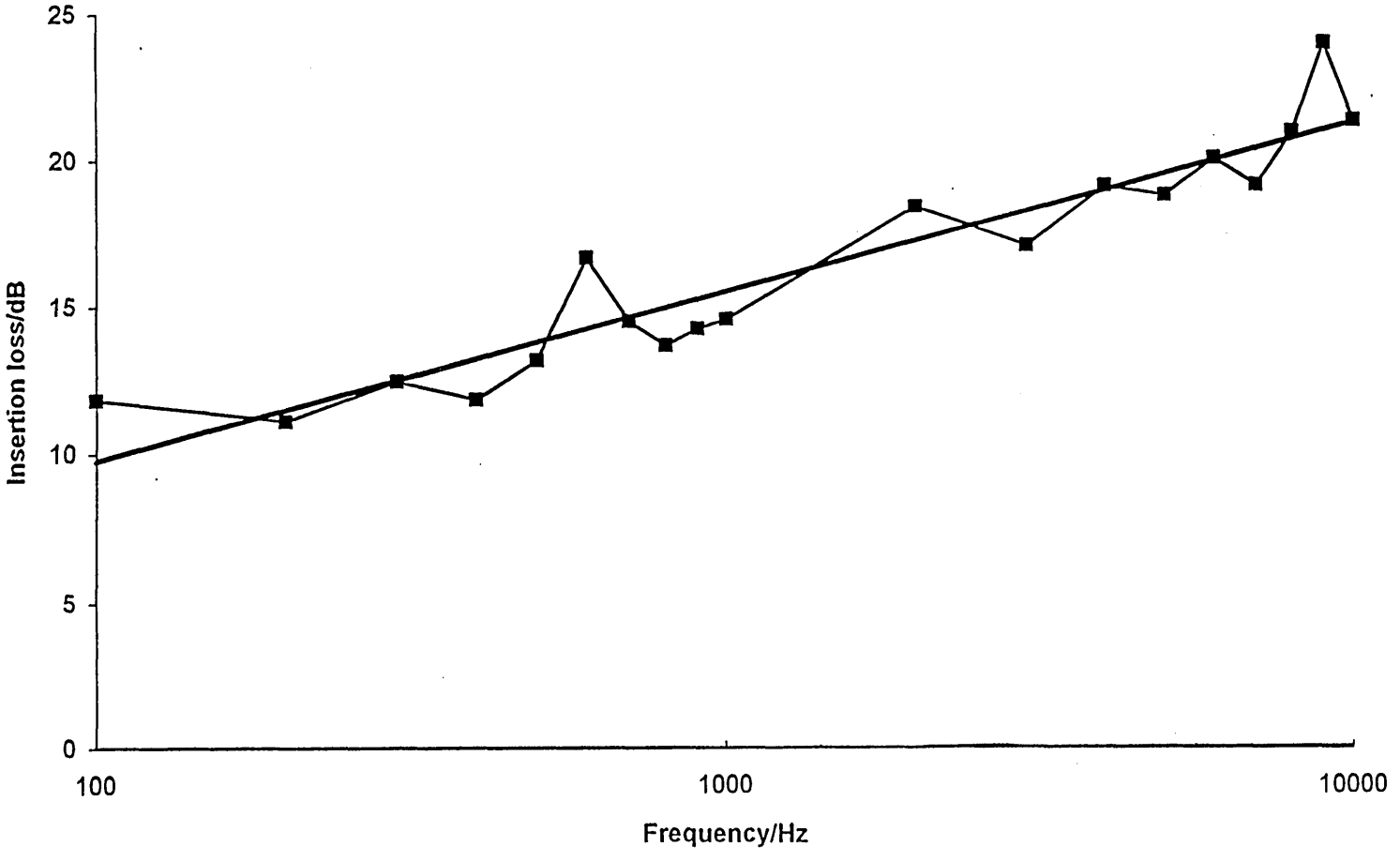

Figure 37 Line of best fit superimposed on Figure 36

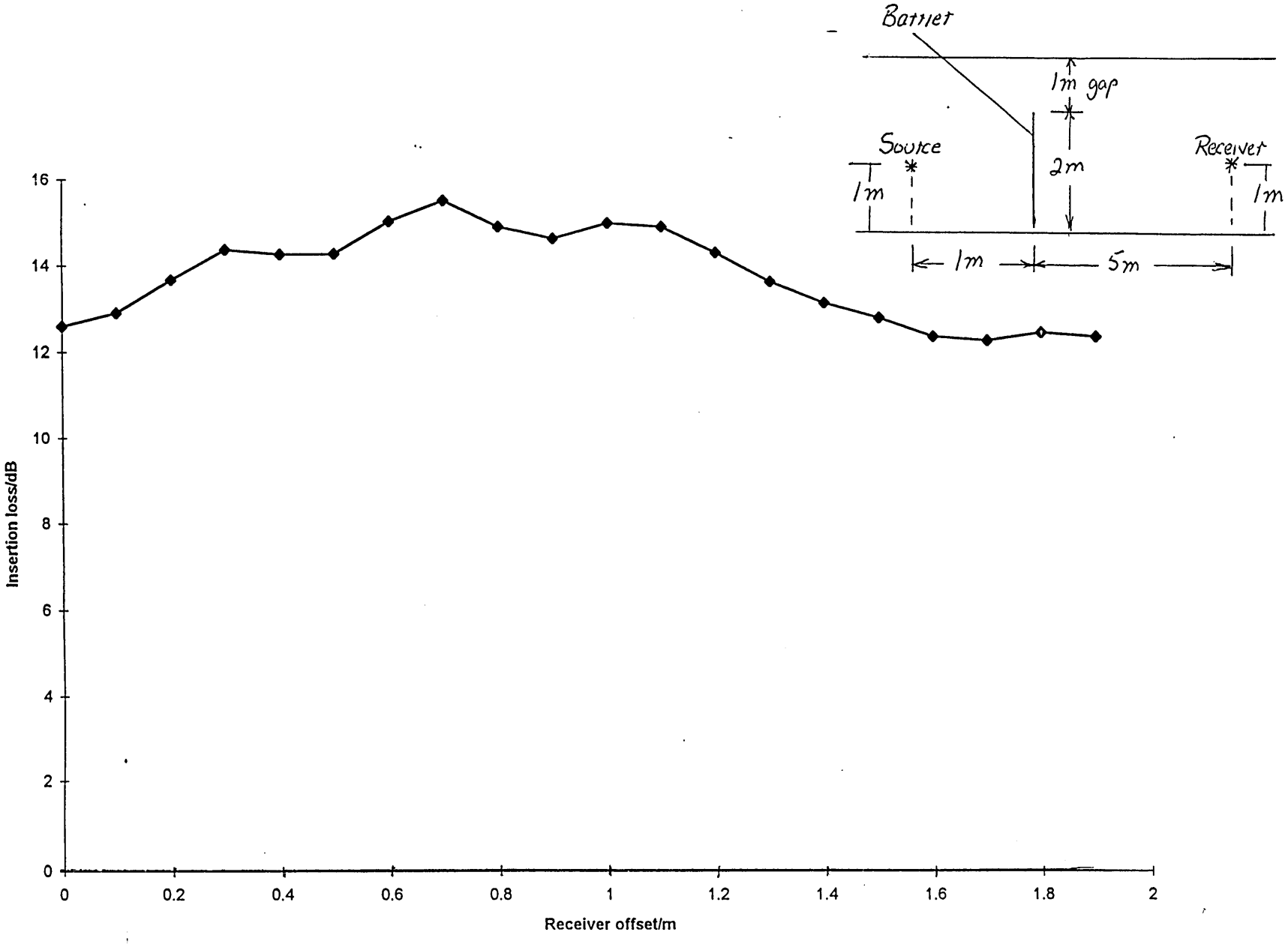

Figure 38 Change in insertion loss for a 4 m wide barrier in an enclosure, by changing the receiver position

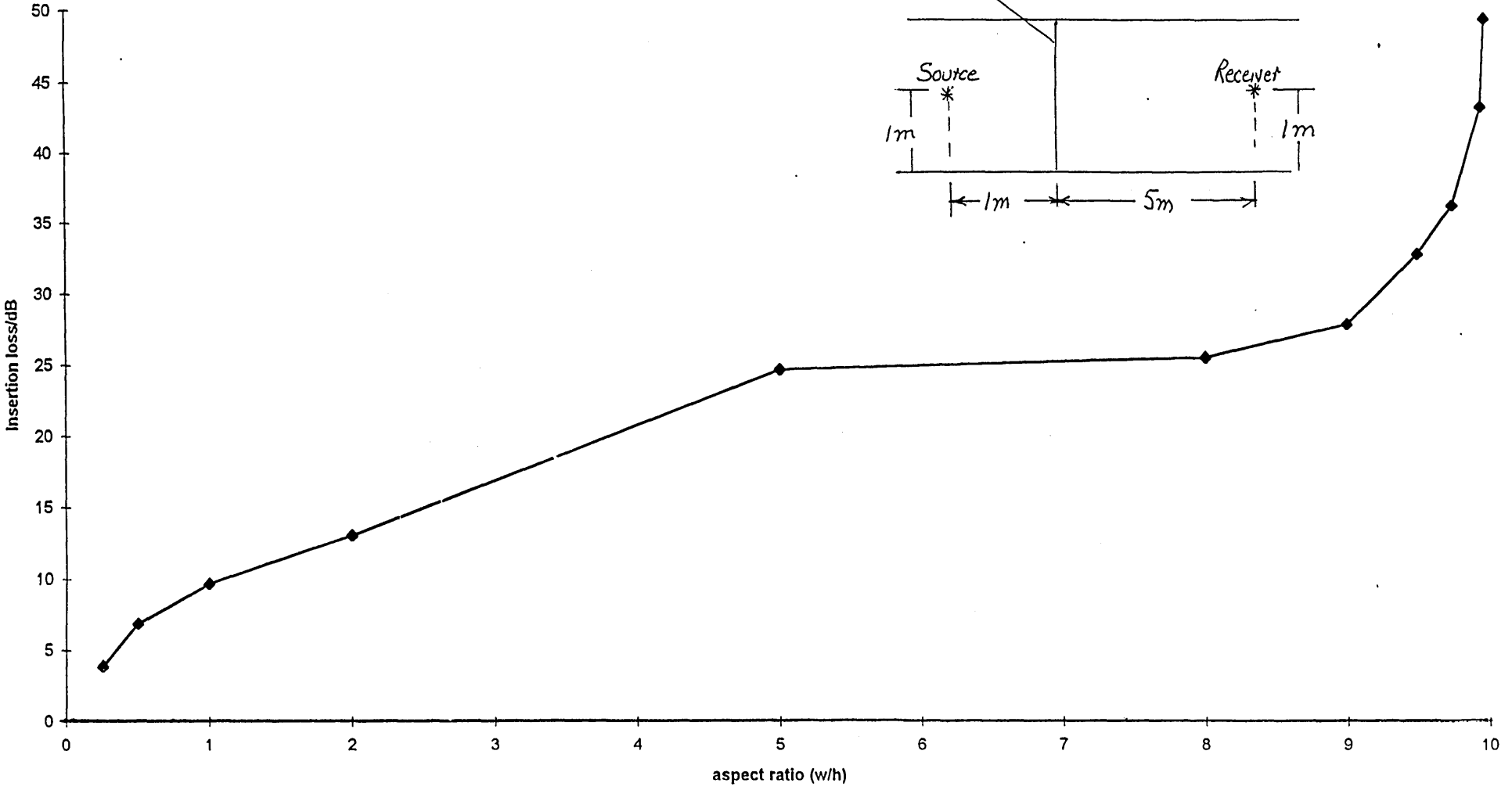

Figure 39 Effect of varying the aspect ratio (width/height) for a barrier in an enclosure.

8.3 **Discussion of results for a barrier in an enclosure**

Although Katarbinska ignored the contributions from the boundary walls, see Figure Page 96, the author introduced side walls to the model. Figure 36 uses the same barrier geometries as the flat room model but places the barrier symmetrically between two side walls 10 m apart. Note that one curve leaves a 0.1 m gap between the top of the barrier and the roof while the other fills the gap between the ground and the roof. The curves behave with the same trend as that for the 'flat room' model, but the introduction of side walls generally lowers the insertion loss by about 4dB. Figure 37 superimposes a line of best fit on Figure 36, for the curve which represents a gap over the top of the barrier, showing reduced values in the magnitude of deviations from the 'flat room' model.

Figure 38 shows the insertion loss as the receiver is moved vertically, using the same barrier geometry except there is a 1 m gap between the top of the barrier and the roof. Comparing with Figure 32, which has identical geometries in a 'flat room', we see that the insertion loss is generally about 4dB lower. Figure 39, the graph of insertion loss against aspect ratio, gives reduced values compared with the model without boundary walls, but the value of insertion loss rises steeply as the barrier width approaches the width of the enclosure.

The research has demonstrated clearly that for finite barriers within an enclosure, the effects of the boundary walls are important in that they are responsible for a significant reduction in the insertion loss.

9 CONCLUSIONS AND SUGGESTIONS FOR FUTURE RESEARCH

Conclusions

The aim of this research was to build a computer model which would predict sound loss due to finite barriers within enclosures thus simulating conditions within factory type buildings. The report uses the classical Kirchhoff-Fresnel diffraction theory throughout and all models divide the barrier's surface into elements. Initially, by incorporating Babinet's Principle into the model, sound attenuation was calculated for a barrier in free space.

Experimentation allowed the optimum element size of 0.0125 m to be found within the precision grade of measurement.

Validation of the model was achieved by comparing it's trends with Fresnel and Fraunhofer diffraction theory. Further validation was effected by using the elemental theory to produce a 6dB reduction in sound level for each respective doubling of source-receiver distance in a free field..

Using a barrier size of 2 m x 4 m, it was shown that sound attenuation steadily increases with respective increases in frequency. However, as the receiver-barrier distance is increased, the curve becomes more unstable, with more rapid deviations from the general trend. Increasing the receiver offset position produces a general decrease in sound attenuation but the curve oscillates about its general trend. A large peak value occurs when the receiver position is close to its central position.

The model was extended to place the barrier in contact with the ground, where direct and reflected sound contributions tend to introduce interference effects. There is much contemporary literature dealing with barriers on the ground, some of which is validated by experimental detail. The author, therefore, compares his results with those of other workers.

As in the case of free space, a 2 m x 4 m barrier in contact with the ground gives a steady rise in insertion loss as the frequency increases. This curve is smoothed by increasing the width of the barrier from 4 m to 10 m, thereby making the effects of diffraction and interference around the sides of the barrier less significant. Increasing the source-barrier distance amplifies the sensitivity of the trigonometric terms, which results in large deviations from the general trend of the curve at the high end of the frequency spectrum.

A steady reduction in insertion loss is observed as the receiver is moved vertically from its central position, but the curve oscillates around this trend with a large initial peak value. It may be possible to reproduce this peak value by sloping the barrier instead of moving the receiver position.

Introduction of a roof enables both single and multi-reflections to be included and from this model we observed steady increases in insertion loss for respective increases in frequency. This trend was also observed by E Katarbinska. Smoother curves are produced than those in the ground model if the barrier extends from the ground to the roof. Due to increased interference, multi-reflections cause greater deviations from the general trend than do single reflections. Moving the receiver position has less effect on the value of insertion loss as compared with ground conditions alone. The 'flat room' model allowed investigation into the effect on insertion loss as the aspect ratio of width/height of the barrier was increased. The resulting curve allowed us to differentiate between terms like 'finite', 'semi-infinite' and 'infinite' barriers.

Finally, side walls were added to the model and placing these walls 10 m apart gave a general reduction of about 4dB in insertion loss. 4dB can be significant in sound calculations and so the introduction of walls to the model is justified.

The models are flexible, and comparison with other literature and experimental evidence show reasonable agreement. Many deviations in results would undoubtedly have been produced if the author could have used the optimum element size of

0.0125 m. Unfortunately, the computing facilities did not allow sufficient time to run some of the models to the required accuracy.

Suggestions for Future Research

Future research may extend to using a point source which emits more than one frequency. Where the author uses hard concrete for all reflecting surfaces, a material which is usually found in most factory conditions, data can be fed into the models to give different reflective properties.

After using multi-reflections in the 'flat room' model, this facility can easily be added to the model within an enclosure. It will also be a relatively simple modification to use the elemental theory to predict sound loss using angled barriers. Modification within the program would be:

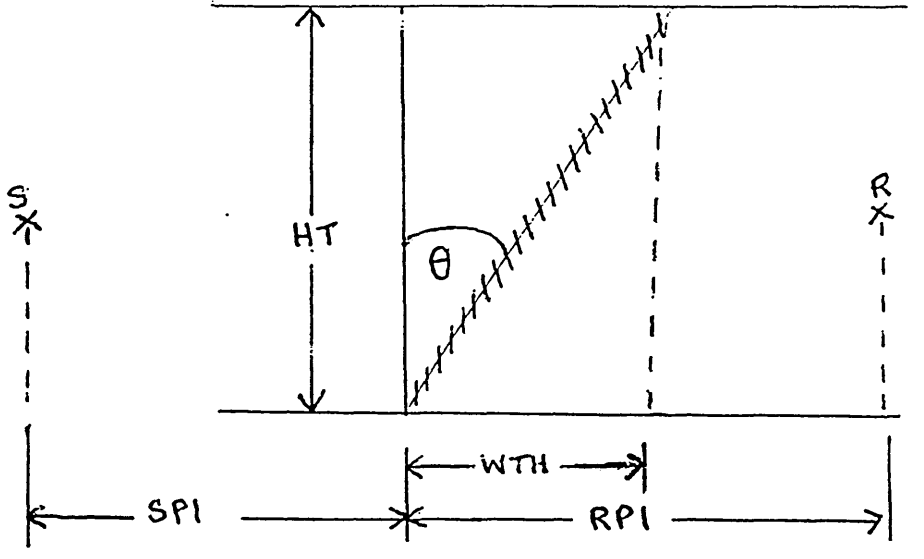

The barrier is moved through an angle θ

The vertical element size

$$DY = HT/N$$

where N is the number of vertical elements

$$WTH = HT \tan \theta$$

Now each vertical element has a new distance from the source and receiver. If the original source and receiver distances are SP1 and RP1 respectively, then for each subroutine of the new program, the new source and receiver positions will be SP and RP where:

$$SP = SP1 + WTH - N.DL + DL/2$$
$$RP = RP1 - WTH + N.DL - DL/2$$

where $DL = WTH/N$

Similar modifications can be made for other barrier geometries, hemispherical, cross-section barriers for example.

The flexibility of the theory will allow excess sound loss to be computed by the use of double and maybe triple barriers.

Double Barrier

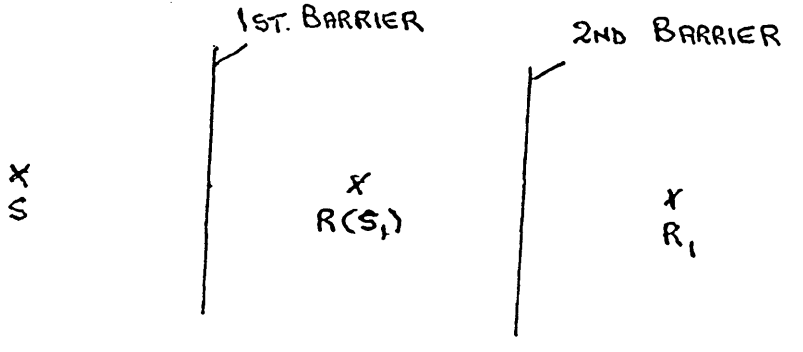

As with all previous models the sound loss at the first receiver position, R, can be calculated. This receiver position then becomes the new source position, S_1, for the second barrier. The sound loss due to the second barrier can then be computed at the second receiver position, R_1. It is then possible to slope both barriers and so form a wedge shaped barrier.

Using the same technique, a third barrier may be added.

Triple Barrier

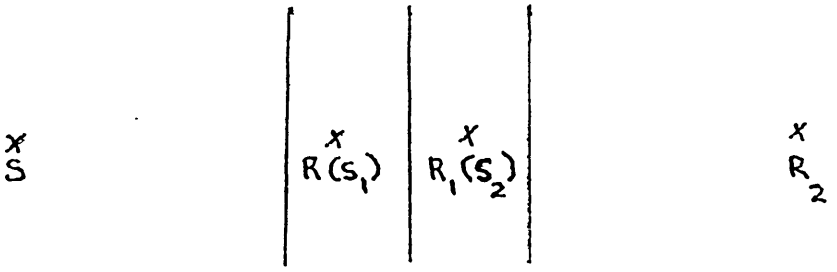

The triple barrier should be very effective because the distance between S_1 and R_1, for the central barrier, can be made quite small compared with the distance SR and S_2R_2.

REFERENCES

1 M Born and E Wolf, '*Principles of Optics*'; Pergamon, New York, 1987, Sixth (Corrected) Edition, 375-380.

2 T Isei, T F W Embleton and J E Piercy, '*Noise reduction by barriers on finite impedance ground*'; 1980, J. Acoustic Society of America, 67(1), 46-58.

3 S W Redfearn, '*Some Acoustical source-observer problems*'; 1940, Philos. Mag. J. 7 (30), 223-236

4 Z Maekawa, '*Experimental study on acoustical designing of a screen for noise reduction*', 1962, J. Acoust. Soc. Japan, 18, 187-196

5 Z Maekawa, '*Noise reduction by screens*', 1968, Appl. Acoust. 1, 157-173.

6 U J Kurze and G S Anderson, '*Sound attenuation by barriers*', 1971, Appl. Acoust. 4, 35-53 .

7 T Kawai, K Fujimoto and T Itow, '*Noise propagation around a thin half plane*', 1978, Acustica, 38, 313-323.

8 J J Bowman, T B A Senior and P L E Uslenghi, '*Electromagnetic and acoustic scattering by simple shapes*', 1969, North Holland, Amsterdam, 308-345.

9 H M Macdonald, '*A class of diffraction problems*', 1915, Proc. London Math. Soc 14, 410-427.

10 K Fujiwara, Y Ando and Z Maekawa, '*Noise reduction by an absorptive barrier*', 1976, J Acoust. Soc. Japan, 32, 430-435.

11 M Yuzawa, '*Sound attenuation by absorptive barriers*', 1977, J Acoust. Soc. Japan, 33, 664-666.

12 A D Pierce, '*Diffraction of sound around corners and over wide barriers*', 1974, J Acoust. Soc. America, 55, 941-955.

13 J B Keller, '*Geometrical theory of diffraction*', 1962, J Opt Soc. America, 52, 116-130.

14 K Fujiwara, Y Ando and Z Maekawa, '*Noise control by barrier*', 1977, Appl. Acoust. 10, 147-159.

15 W E Scholes, A C Salvidge and J W Sargent, '*Field performance of a noise barrier*', 1971, J. Sound Vib. 16, 627-642.

16 T Isei and K Matsuguma, '*Experimental study on noise reduction of line sound source by barrier*', 1976, Proc. Meeting of Acoust. Soc, Japan, 3-1-9, 297-298.

17 H G Jonasson, '*Sound reduction by barriers on the ground*', 1972, J Sound Vib. 22, 113-126.

18 U Ingard, '*On the reflections of a spherical sound wave from an infinite plane*', 1951, J Acoust. Soc. America, 23, 329-335.

19 S I Thomasson, '*Reflections of waves from a point source by an impedance boundary*', 1976, J Acoust. Soc America, 59, 780-785.

20 S I Thomasson, '*Sound propagation above a layer with a large reflection index*', 1977, J Acoust. Soc. America, 61, 659-674.

21 S I Thomasson, '*Diffraction by a screen above an impedance boundary*', 1977, Rep TVBA-1001, Department of Building Acoustics, Lund Institute of Technology, Lund, Sweden.

22 S I Thomasson, '*Theory and experiments on sound propagation above an impedance boundary*', Rep. 75, Division of Buliding Technology, Lund Institute of Technology, Lund, Sweden.

23 T Isei, T F W Embleton and J E Piercy, '*Influence of reflections at the ground on insertion loss of barriers*', 1978, 95th ASA Meeting J. Acoust. Soc. Am. Suppl. I63, S59.

24 T Isei, T F W Embleton and J E Piercy, '*Comparison of theoretical and measured sound levels behind barriers*', 1978, J Acoust. Soc. Am. Suppl. I64, S172.

25 T Isei, T F W Embleton and N Olson, '*Outdoor sound propagation over ground of finite impedence*', 1976, J Acoust. Soc. Am. 59, 267-277.

26 W C Elmore and M A Heald, '*Physics of waves*', 1969, McGraw Hill-Kogakusha, Tokyo, Japan.

27 T F W Embleton, '*Line integral theory of barrier attenuation*', 1980, J Acoust. Soc. America, 67, 42-45.

28 T Isei, '*Absorptive noise barrier on finite impedance ground*', 1980, J Acoust. Soc., Japan 1.

29 F A Jenkins and H E White, '*Fundamentals of Optics*', 378-401.

30 F A Jenkins and H E White, '*Fundamentals of Optics*', 317-324.

31 H Medwin, '*Shadowing by finite noise barriers*', 1980, J Acoust. Soc. Am., Vol 69, No 4, 1060-1064

32 M A Biot and L Tolstoy, *'Formulation of wave propagation in infinite media by normal coordinates with an application to diffraction'*, J. Acoust.Soc. Am. 29, 381-391 (1957)

33 J H Stratton, *'Electromagnetic Theory'*, [McGraw-Hill, New York, 1941]

34 J Rudnick, *'The propagation of an acoustic wave along a plane boundary'*, J Acoust. Soc. Am 19, 348-356 [1947]

35 C J Chessell, *'Propagation of noise along a finite impedance boundary'*, J Acoust. Soc. Am 62, 825-834 [1977]

36 M E Delany and E N Bazley, *'Acoustical properties of fibrous absorber materials'*, Appl. Acoust. 3, 105-116 [1970]

37 P Ambaud and A Bergassoli, *'Le problèm du dièdre en acoustique'*, Acustica 27, 291-298 (1972)

38 W J Hadden and A D Pierce, *'Sound diffraction around screens and wedges for arbitrary point source locations'*, J Acoust. Soc. Am. 69, 1266-1276 (1981)

39 E Katarbinska, *'How to calculate the efficiency of an acoustic barrier in a flat room'*, Applied Acoustics, 23, 99-108 (1987)

40 U Bolleter, *'On the sound propagation in large flat weaving sheds'*, Proc. Inter-Noise, 77, Zurich 1977

41 U J Kurze, *'Scattering of sound in industrial spaces'*, J Sound Vibration, 98(3) 349-364 (1985)

42 André L'Espérance, *'The insertion loss of finite length barriers on the ground'*, J Acoust. Soc. Am. 86(1), (1989)

43 D C Hothersall, S N Chandler-Wilde and M N Hajimirzae, *'Efficiency of single noise barriers'*, Journal of Sound Vibration, 146, 303-322 (1991)

44 Yasuhito Kawai and Toshio Terai, *'The application of integral equation methods to the calculation of sound attenuation by barriers'*, Applied Acoustics 31, 101-117 (1990)

45 Trevor J Cox and Y W Lam, *'Evaluation of methods for predicting the scattering from simple rigid panels'*, Applied Acoustics 40, 123-140 (1992)

46 Y W Lam and S C Roberts, *'A simple method for accurate prediction of finite barrier insertion loss'*, J Acoust. Soc. Am. 93, 1445-1452 (1993)

47 Y W Lam, *'Using Mackawa's chart to calculate finite length barrier insertion loss'*, Applied Acoustics 42, 29-40 (1994)

48 Y W Lam, *'On the modelling of the effect of ground terrain profile in environmental noise calculations'*, Applied Acoustics, 42, 99-123 (1994)

49 Koichi Takagi, Ryota Hotta and Kohei Yamamoto, '*A simple method for the calculation of noise attenuation by a finite length barrier*', Applied Acoustics, 43, 353-365 (1994)

50 ISO, Acoustics - Attenuation of Sound During Propagation Outdoors - Part 2: *A General Method of Calculation* (DIS9613-2). Draft International Standard, ISO, Switzerland, 1992.

51 Conware, *The Propagation of Noise from Petroleum and Petrochemical Complexes to Neighbouring Communities* (CONCAWE Report No 4/81), Madouplein 1, B-1030, Brussels, Belgium, 1981.

52 K J Marsh, *The CONCAWE model for calculating the propagation of noise from open-air industrial plants.* Appl. Acoustics, 15, (1982) 411-28.

53 R Tonin, *Estimating noise levels from petrochemical plants, mines and industrial complexes.* Accoustics, Australia 13(2), (1984), 59-67.

54 J Nicolas, T F W Embleton and J E Piercy, *Precise model measurements versus theoretical prediction of barrier insertion loss in presence of the ground.* J. Acoust. Soc. Am. Vol 73, No 1 (1983) 44-54

55 Leang, L K Yamashita, Y & Matsui M, *Simplified calculation method for oise reduction by barriers on the ground.* J. Acoust. Soc. Japan (E), 11(4), (1990) 199-205

```
      WRITE(6,*)'BARRIER IN FREE SPACE-FIRST ORDER MODEL'
      WRITE(6,*)'THE DATA IS'
      WRITE(6,*)'SOURCE- BARRIER DISTANCE'
      READ(5,*)SP
      WRITE(6,*)'RECEIVER-BARRIER DISTANCE'
      READ(5,*)RP
      WRITE(6,*)'HORIZONTAL RECEIVER OFFSET'
      READ(5,*)P
      WRITE(6,*)'VERTICAL RECEIVER OFFSET'
      READ(5,*)Q
      WRITE(6,*)'X COORDINATE FROM LHS OF BARRIER'
      READ(5,*)XL
      WRITE(6,*)'Y COORDINATE FROM TOP OF BARRIER'
      READ(5,*)YB
      WRITE(6,*)'HORIZONTAL ELEMENT SIZE'
      READ(5,*)DX
      WRITE(6,*)'VERTICAL ELEMENT SIZE'
      READ(5,*)DY
      WRITE(6,*)'NUMBER OF HORIZONTAL ELEMENTS'
      READ(5,*)M
      WRITE(6,*)'NUMBER OF VERTICAL ELEMENTS'
      READ(5,*)N
      WRITE(6,*)'WAVELENGTH'
      READ(5,*)WL
      PI=3.1415926
      WN=(2.0*PI)/WL
      SUMR=0
      SUMI=0
      DO 2 J=1,N
        DO 1 I=1,N
          XO=XL-I*DX+DX/2.0
          YO=YB-J*DY+DY/2.0
          SO=SQRT((SP**2)+(XO**2)+(YO**2))
          RO=SQRT((RP**2)+(XO-P)**2+(YO-Q)**2)
          CUST=SP/SO
          CUSF=RP/RO
          A=(XO/SO)+(XO-P)/RO
          B=(YO/SO)+(YO-Q)/RO
          CUSK=COS(WN*(RO+SO))
          SENK=SIN(WN*(RO+SO))
          AK=1.0/(RO*SO)
          RL=AK**2*CUSK*(RO*CUST+SO*CUSF)+WN*AK*SENK*(CUST+CUSF)
          UNRL=AK**2*SENK*(RO*CUST+SO*CUSF)-WN*AK*CUSK*(CUST+
     +     CUSF)
          FIR=SIN(WN*B*(DY/2.0))*SIN(WN*A*(DX/2.0))/(PI*WN**2*
     +     A*B)
          SUMR=SUMR+RL*FIR
          SUMI=SUMI+UNRL*FIR
    1   CONTINUE
    2 CONTINUE
      DIB=SQRT((P**2)+(Q**2)+(RP+SP)**2)
      UBR=((COS(WN*DIB))/DIB)-SUMR
      UBI=((SIN(WN*DIB))/DIB)-SUMI
      EB=UBR**2+UBI**2
      DB=-10.0*(ALOG10(EB*DIB**2))
      WRITE(6,3)DB
    3 FORMAT('ATTENUATION=',G14.6)
      STOP
```

```
      WRITE(6,*)'BARRIER IN FREE SPACE-ZERO ORDER MODEL'
      WRITE(6,*)'THE DATA IS'
      WRITE(6,*)'SOURCE-BARRIER DISTANCE'
      READ(5,*)SP
      WRITE(6,*)'RECEIVER-BARRIER DISTANCE'
      READ(5,*)RP
      WRITE(6,*)'HORIZONTAL RECEIVER OFFSET'
      READ(5,*)P
      WRITE(6,*)'VERTICAL RECEIVER OFFSET'
      READ(5,*)Q
      WRITE(6,*)'X COORDINATE FROM LHS OF BARRIER'
      READ(5,*)XL
      WRITE(6,*)'Y COORDINATE FROM TOP OF BARRIER'
      READ(5,*)YB
      WRITE(6,*)'HORIZONTAL ELEMENT SIZE'
      READ(5,*)DX
      WRITE(6,*)'VERTICAL ELEMENT SIZE'
      READ(5,*)DY
      WRITE(6,*)'NUMBER OF HORIZONTAL ELEMENTS'
      READ(5,*)M
      WRITE(6,*)'NUMBER OF VERTICAL ELEMENTS'
      READ(5,*)N
      WRITE(6,*)'WAVELENGTH'
      READ(5,*)WL
      PI=3.1415926
      WN=(2.0*PI)/WL
      SUMR=0
      SUMI=0
      DO 2 J=1,N
        DO 1 I=1,M
          XO=XL-I*DX+DX/2.0
          YO=YB-J*DY+DY/2.0
          SO=SQRT((SP**2)+(XO**2)+(YO**2))
          RO=SQRT((RP**2)+(XO-P)**2+(YO-Q)**2)
          CUST=SP/SO
          CUSF=RP/RO
          CUSK=COS(WN*(RO+SO))
          SENK=SIN(WN*(RO+SO))
          AK=1.0/(RO*SO)
          RL=AK**2*CUSK*(RO*CUST+SO*CUSF)+WN*AK*SENK*(CUST+CUSF)
          UNRL=AK**2*SENK*(RO*CUST+SO*CUSF)-WN*AK*CUSK*(CUST+
     +     CUSF)
          FIR=((DX/2.0)*(DY/2.0))/PI
          SUMR=SUMR+RL*FIR
          SUMI=SUMI+UNRL*FIR
    1   CONTINUE
    2 CONTINUE
      DIB=SQRT((P**2)+(Q**2)+(RP+SP)**2)
      UBR=((COS(WN*DIB))/DIB)-SUMR
      UBI=((SIN(WN*DIB))/DIB)-SUMI
      EB=UBR**2+UBI**2
      DB=-10.0*(ALOG10(EB*DIB**2))
      WRITE(6,3)DB
    3 FORMAT('ATTENUATION=',G14.6)
      STOP
      END
```

```
      WRITE(6,*)'BARRIER IN FREE SPACE-FIRST ORDER MODEL-CHANGING
     +ELEMENT SIZE'
      WRITE(6,*)'THE DATA IS'
      WRITE(6,*)'SOURCE-BARRIER DISTANCE'
      READ(5,*)SP
      WRITE(6,*)'RECEIVER-BARRIER DISTANCE'
      READ(5,*)RP
      WRITE(6,*)'HORIZONTAL RECEIVER OFFSET'
      READ(5,*)P
      WRITE(6,*)'VERTICAL RECEIVER OFFSET'
      READ(5,*)Q
      WRITE(6,*)'X COORDINATE FROM LHS OF BARRIER'
      READ(5,*)XL
      WRITE(6,*)'Y COORDINATE FROM TOP OF BARRIER'
      READ(5,*)YB
      WRITE(6,*)'WAVELENGTH'
      READ(5,*)WL
      PI=3.1415926
      WN=(2.0*PI)/WL
      WRITE(6,*)'WIDTH OF BARRIER'
      READ(5,*)WTH
      WRITE(6,*)'HEIGHT OF BARRIER'
      READ(5,*)HT
      DO 5 M=10,100,1
        N=M
        SUMR=0
        SUMI=0
        DX=WTH/M
        DY=HT/N
        DO 2 J=1,N
          DO 1 I=1,M
            XO=XL-I*DX+DX/2.0
            YO=YB-J*DY+DY/2.0
            SO=SQRT((SP**2)+(XO**2)+(YO**2))
            RO=SQRT((RP**2)+(XO-P)**2+(YO-Q)**2)
            CUST=SP/SO
            CUSF=RP/RO
            A=(XO/SO)+(XO-P)/RO
            B=(YO/RO)+(YO-Q)/SO
            CUSK=COS(WN*(RO+SO))
            SENK=SIN(WN*(RO+SO))
            AK=1.0/(RO*SO)
            RL=AK**2*CUSK*(RO*CUST+SO*CUSF)+WN*AK*SENK*
     +       (CUST+CUSF)
            UNRL=AK**2*SENK*(RO*CUST+SO*CUSF)-WN*AK*CUSK*
     +       (CUST+CUSF)
            FIR=SIN(WN*B*(DY/2.0))*SIN(WN*A*(DX/2.0))/
     +       (PI*WN**2*A*B)
            SUMR=SUMR+RL*FIR
            SUMI=SUMI+UNRL*FIR
    1     CONTINUE
    2   CONTINUE
        DIB=SQRT((P**2)+(Q**2)+(RP+SP)**2)
        UBR=((COS(WN*DIB))/DIB)-SUMR
        UBI=((SIN(WN*DIB))/DIB)-SUMI
        EB=UBR**2+UBI**2
        DB=-10.0*(ALOG10(EB*DIB**2))
        WRITE(6,3)M
```

```
3    FORMAT('NUMBER OF ELEMENTS=',I3)
     WRITE(6,4)DB
4    FORMAT('ATTENUATION=',G14.6)
5 CONTINUE
  STOP
  END
```

```
      WRITE(6,*)'BARRIER IN FREE SPACE-ZERO ORDER MODEL-CHANGING
     +ELEMENT SIZE'
      WRITE(6,*)'THE DATA IS'
      WRITE(6,*)'SOURCE-BARRIER DISTANCE'
      READ(5,*)SP
      WRITE(6,*)'RECEIVER-BARRIER DISTANCE'
      READ(5,*)RP
      WRITE(6,*)'HORIZONTAL RECEIVER OFFSET'
      READ(5,*)P
      WRITE(6,*)'VERTICAL RECEIVER OFFSET'
      READ(5,*)Q
      WRITE(6,*)'X COORDINATE FROM LHS OF BARRIER'
      READ(5,*)XL
      WRITE(6,*)'Y COORDINATE FROM TOP OF BARRIER'
      READ(5,*)YB
      WRITE(6,*)'WAVELENGTH'
      READ(5,*)WL
      PI=3.1415926
      WN=(2.0*PI)/WL
      WRITE(6,*)'WIDTH OF BARRIER'
      READ(5,*)WTH
      WRITE(6,*)'HEIGHT OF BARRIER'
      READ(5,*)HT
      DO 6 M=10,100,1
        N=M
        SUMR=0
        SUMI=0
        DX=WTH/M
        DY=HT/N
        DO 2 J=1,N
          DO 1 I=1,M
            XO=XL-I*DX+DX/2.0
            YO=YB-J*DY+DY/2.0
            SO=SQRT((SP**2)+(XO**2)+(YO**2))
            RO=SQRT((RP**2)+(XO-P)**2+(YO-Q)**2)
            CUST=SP/SO
            CUSF=RP/RO
            CUSK=COS(WN*(RO+SO))
            SENK=SIN(WN*(RO+SO))
            AK=1.0/(RO*SO)
            RL=AK**2*CUSK*(RO*CUST+SO*CUSF)+WN*AK*SENK*(CUST+
     +       CUSF)
            UNRL=AK**2*SENK*(RO*CUST+SO*CUSF)-WN*AK*CUSK*
     +       (CUST+CUSF)
            FIR=((DX/2.0)*(DY/2.0))/PI
            SUMR=SUMR+RL*FIR
            SUMI=SUMI+UNRL*FIR
    1     CONTINUE
    2   CONTINUE
        DIB=SQRT((P**2)+(Q**2)+(RP+SP)**2)
        UBR=((COS(WN*DIB))/DIB)-SUMR
        UBI=((SIN(WN*DIB))/DIB)-SUMI
        EB=UBR**2+UBI**2
        DB=-10.0*(ALOG10(EB*DIB**2))
        WRITE(6,4)M
    4   FORMAT('NUMBER OF ELEMENTS=',I3)
        WRITE(6,5)DB
    5   FORMAT('ATTENUATION=',G14.6)
```

```
      DIMENSION AMP(500),REL(500)
      WRITE(6,*)'SIMILATION OF FRESNEL DIFFRACTION'
      WRITE(6,*)'THE DATA IS'
      WRITE(6,*)'SOURCE BARRIER DISTANCE'
      READ(5,*)SP
      WRITE(6.*)'RECEIVER BARRIER DISTANCE'
      READ(5,*)RP
      WRITE(6,*)'X-COORDINATE FROM LHS OF BARRIER'
      READ(5,*)XL
      WRITE(6,*)'ELEMENT SIZE'
      READ(5,*)DX
      WRITE(6.*)'NUMBER OF ELEMENTS'
      READ(5,*)M
      WRITE(6,*)'WAVELENGTH'
      READ(5,*)WL
      PI=3.1415927
      WN=(2.0*PI)/WL
      PUG=PI*DX**2
      SUMR=0
      SUMI=0
      DO 1 I=1,M
        XO=XL-I*DX+DX/2.0
        SO=SQRT((SP**2)+(XO**2))
        RO=SQRT((RP**2)+(XO**2))
        C=(WN*((RO*SP)+(SO*RP)))/((RO**2)*(SO**2))
        B=(((RO**2)*SP)+((SO**2)*RP))/((RO**3)*(SO**3))
        R=WN*(RO+SO)
        RL=(B*COS(R))+(C*SIN(R))
        UNRL=(B*SIN(R))-(C*COS(R))
        SUMR=SUMR+(RL*(2.0*I-1)*PUG)
        SUMI=SUMI+(UNRL*(2.0*I-1)*PUG)
        AMP(I)=SQRT((SUMR**2)+(SUMI**2))
        REL(I)=APM(I)/AMP(1)
        WRITE(6,4)I
    4   FORMAT('ELEMENT NUMBER=',I3)
        WRITE(6,3)AMP(I)
    3   FORMAT('AMPLITUDE=',G14.6)
        WRITE(6,2)REL(I)
    2   FORMAT('RELATIVE AMPLITUDE=',G14.6)
    1 CONTINUE
      STOP
      END
```

```
      DIMENSION EA(500),REL(500)
      WRITE(6,*)'SIMILATION OF FRAUNHOFER DIFFRACTION'
      WRITE(6,*)'THE DATA IS'
      WRITE(6,*)'EXTREME VALUE'
      READ(5,*)X
      WRITE(6,*)'STEP VALUE'
      READ(5,*)Y
      WRITE(6,*)'SOURCE-BARRIER DISTANCE'
      READ(5,*)SP
      WRITE(6,*)'RECEIVER-BARRIER DISTANCE'
      READ(5,*)RP
      WRITE(6,*)'VERTICAL RECEIVER OFFSET'
      READ(5,*)Q
      WRITE(6,*)'X-COORDINATE FROM LHS OF BARRIER'
      READ(5,*)XL
      WRITE(6,*)'Y-COORDINATE FROM TOP OF BARRIER'
      READ(5,*)YB
      WRITE(6,*)'HORIZONTAL ELEMENT SIZE'
      READ(5,*)DX
      WRITE(6,*)'VERTICAL ELEMENT SIZE'
      READ(5,*)DY
      WRITE(6,*)'NUMBER OF HORIZONTAL ELEMENTS'
      READ(5,*)M
      WRITE(6,*)'NUMBER OF VERTICAL ELEMENTS'
      READ(5,*)N
      WRITE(6,*)'WAVELENGTH'
      READ(5,*)WL
      PI=3.1415926
      WN=(2.0*PI)/WL
      DO 5 K=1,X,Y
        SUMR=0
        SUMI=0
        DO 2 J=1,N
          DO 1 I=1,M
            XO=XL-I*DX+DX/2.0
            YO=YP-J*DY+DY/2.0
            SO=SQRT((SP**2)+(XO**2)+(YO**2))
            RO=SQRT((RP**2)+(XO-K)**2+(YO-Q)**2)
            CUST=SP/SO
            CUSF=RP/RO
            A=(XO/SO)+(XO-K)/RO
            B=(YO/SO)+(YO-Q)/RO
            CUSK=COS(WN*(RO+SO))
            SENK=SIN(WN*(RO+SO))
            AK=1.0/(RO*SO)
            RL=AK**2*CUSK*(RO*CUST+SO*CUSF)+WN*AK*SENK*
     +       (CUST+CUSF)
            UNRL=AK**2*SENK*(RO*CUST+SO*CUSF)-WN*AK*CUSK*
     +       (CUST+CUSF)
            FIR=SIN(WN*B*(DY/2.0))*SIN(WN*A*(DX/2.0))/
     +       (PI*WN**2*A*B)
            SUMR=SUMR+RL*FIR
            SUMI=SUMI+UNRL*FIR
    1     CONTINUE
    2   CONTINUE
        EA(K)=SUMR**2+SUMI**2
        REL(K)=EA(K)/EA(1)
        WRITE(6,3)K
```

```
3    FORMAT('RECEIVER OFFSET=',I4.1)
     WRITE(6,4)REL(K)
4    FORMAT('RELATIVE INTENSITY=',G14.6)
5 CONTINUE
  STOP
  END
```

```
      WRITE(6,*)'BARRIER IN FREE SPACE-RECEIVER OFFSET'
      WRITE(6,*)'THE DATA IS'
      WRITE(6,*)'SOURCE-BARRIER DISTANCE'
      READ(5,*)SP
      WRITE(6,*)'RECEIVER-BARRIER DISTANCE'
      READ(5,*)RP
      WRITE(6,*)'HORIZONTAL RECEIVER OFFSET'
      READ(5,*)P
      WRITE(6,*)'X-COORDINATE FROM LHS OF BARRIER'
      READ(5,*)XL
      WRITE(6,*)'Y-COORDINATE FROM TOP OF BARRIER'
      READ(5,*)YB
      WRITE(6,*)'HORIZONTAL ELEMENT SIZE'
      READ(5,*)DX
      WRITE(6,*)'VERTICAL ELEMENT SIZE'
      READ(5,*)DY
      WRITE(6,*)'NUMBER OF HORIZONTAL ELEMENTS'
      READ(5,*)M
      WRITE(6,*)'NUMBER OF VERTICAL ELEMENTS'
      READ(5,*)N
      WRITE(6,*)'WAVELENGTH'
      READ(5,*)WL
      WRITE(6,*)'INITIAL VALUE'
      READ(5,*)R
      WRITE(6,*)'FINAL VALUE'
      READ(5,*)S
      WRITE(6,*)'STEP VALUE'
      READ(5,*)T
      PI=3.1415926
      WN=(2.0*PI)/WL
      DO 5 Q=R,S,T
        SUMR=0
        SUMI=0
        DO 2 J=1,N
          DO 1 I=1,M
            XO=XL-I*DX+DX/2.0
            YO=YB-J*DY+DY/2.0
            SO=SQRT((SP**2)+(XO**2)+(YO**2))
            RO=SQRT((RP**2)+(XO-P)**2+(YO-Q)**2)
            CUST=SP/SO
            CUSF=RP/RO
            A=(XO/SO)+(XO-P)/RO
            B=(YO/SO)+(YO-Q)/RO
            CUSK=COS(WN*(RO+SO))
            SENK=SIN(WN*(RO+SO))
            AK=1.0/(RO*SO)
            RL=AK**2*CUSK*(RO*CUST+SO*CUSF)+WN*AK*SENK*
     +       (CUST+CUSF)
            UNRL=AK**2*SENK*(RO*CUST+SO*CUSF)-WN*AK*CUSK*
     +       (CUST+CUSF)
            FIR=SIN(WN*B*(DY/2.0))*SIN(WN*A*(DX/2.0))/
     +       (PI*WN**2*A*B)
            SUMR=SUMR+RL*FIR
            SUMI=SUMI+UNRL*FIR
    1     CONTINUE
    2   CONTINUE
        DIB=SQRT((P**2)+(Q**2)+(RP+SP)**2)
        UBR=((COS(WN*DIB))/DIB)-SUMR
```

```
      UBI=((SIN(WN*DIB))/DIB)-SUMI
      EB=UBR**2+UBI**2
      DB=-10.0*(ALOG10(EB*DIB**2))
      WRITE(6,3)Q
-----3   FORMAT('RECEIVER OFFSET=',G14.6)
      WRITE(6,4)DB
    4   FORMAT('ATTENUATION=',G14.6)
    5 CONTINUE
      STOP
      END
```

```
      WRITE(6,*)'THE DATA IS'
      WRITE(6,*)'ENTER SOURCE-BARRIER DISTANCE'
      READ(5,*)SP
      WRITE(6,*)'ENTER RECEIVER-BARRIER DISTANCE'
      READ(5,*)RP
      WRITE(6,*)'ENTER HORIZONTAL RECEIVER OFFSET'
      READ(5,*)P
      WRITE(6,*)'ENTER X-COORDINATE OF L.H.S. OF BARRIER'
      READ(5,*)ZL
      WRITE(6,*)'ENTER Y-COORDINATE OF TOP OF BARRIER'
      READ(5,*)ZB
      WRITE(6,*)'ENTER HORIZONTAL ELEMENT SIZE'
      READ(5,*)DX
      WRITE(6,*)'ENTER VERTICAL ELEMENT SIZE'
      READ(5,*)DY
      WRITE(6,*)'ENTER NUMBER OF HORIZONTAL ELEMENTS'
      READ(5,*)M
      WRITE(6,*)'ENTER NUMBER OF VERTICAL ELEMENTS'
      READ(5,*)N
      WRITE(6,*)'ENTER WAVELENGTH'
      READ(5,*)WL
      WRITE(6,*)'ENTER POSITION OF SOURCE FROM FLOOR'
      READ(5,*)Y1
      WRITE(6,*)'ENTER RESONANT FREQUENCY'
      READ(5,*)W0
      WRITE(6,*)'ENTER CHARACTERISTIC ACOUSTIC IMPEDANCE OF MEDIUM'
      READ(5,*)ROEC
      WRITE(6,*)'ENTER MECHANICAL RESISTANCE FACTOR'
      READ(5,*)R
      WRITE(6,*)'ENTER EFFECTIVE MASS PER UNIT AREA'
      READ(5,*)MASS
      WRITE(6,*)'INITIAL VALUE'
      READ(5,*)S
      WRITE(6,*)'EXTREME VALUE'
      READ(5,*)G
      WRITE(6,*)'STEP VALUE'
      READ(5,*)T
      PI=3.1415926
      WN=(2.0*PI)/WL
      W=340.0/WL
      X=M*DX
      WRITE(6,1)X
    1 FORMAT(5X,'WIDTH OF BARRIER=',G14.6)
      Y=N*DY
      WRITE(6,2)Y
    2 FORMAT(5X,'HEIGHT OF BARRIER=',G14.6)
      DO 8 E=S,G,T
        WRITE(6,15)E
   15   FORMAT(5X,'VERTICAL OFFSET=',G14.6)
        CALL BARR1(RP,SP,P,E,ZL,ZB,DX,DY,M,N,PI,WN,SUMC,SUMD)
        D3=(Y1*(RP+SP))/((2.0*Y1)+E)
        Q1=E+(2.0*Y1)
        ZB1=ZB+(2.0*Y1)
        CALL BARR2(RP,SP,Y,P,Q1,ZL,ZB1,DX,DY,M,N,PI,WN,Y1,W,W0,R,
     +   MASS,ROEC,SUME,SUMF)
        Q2=-(E+(2.0*Y1))
        CALL BARR3(RP,SP,Y,P,Q2,E,ZL,ZB,DX,DY,M,N,PI,WN,Y1,W,WO,R,
     +   MASS,ROEC,SUMG,SUMH)
```

```
      Q3=-E
      CALL BARR4(RP,SP,Y,P,Q3,E,ZL,ZB1,DX,DY,M,N,PI,WN,Y1,
     +  W,WO,R,MASS,ROEC,SUMJ,SUMK)
      W3=(Y1*P)/((2.0*Y1)+E)
      XO1=SQRT((Y1**2)+(D3**2)+(W3**2))
      ZO1=SQRT((D3**2)+(W3**2))
      V=ASIN(ZO1/XO1)
      CUSSV=COS(V)
      CALL REFCO(W,W0,R,MASS,CUSSV,ROEC,CORL,COIM)
      DIB1=SQRT((P**2)+(E**2)+(RP+SP)**2)
      DIB2=SQRT(((2.0*Y1)+E)**2+(P**2)+(RP+SP)**2)
      UBR=(COS(WN*DIB1))/DIB1
      UBI=(SIN(WN*DIB1))/DIB1
      UBR1=(((COS(WN*DIB2))*CORL)+((SIN(WN*DIB2))*COIM))/DIB2
      UBI1=(((SIN(WN*DIB2))*CORL)-((COS(WN*DIB2))*COIM))/DIB2
      EBR=UBR+UBR1
      EBI=UBI+UBI1
      UBR2=EBR-(SUMC+SUME+SUMG+SUMJ)
      UBI2=EBI-(SUMD+SUMF+SUMH+SUMK)
      dB=10.0*(ALOG10((EBR**2+EBI**2)/(UBR2**2+UBI2**2)))
      WRITE(6,7)dB
    7  FORMAT(5X,'ATTENUATION=',G14.6)
    8 CONTINUE
      STOP
      END

      SUBROUTINE BARR1(RP,SP,P,Q,XL,YB,DV,DZ,L,N,PI,WN,SUMR,SUMI)
      SUMR=0
      SUMI=0
      DO 4 J=1,N
        DO 3 I=1,L
          XO=XL-I*DV+DV/2.0
          YO=YB-J*DZ+DZ/2.0
          SO=SQRT((SP**2)+(XO**2)+(YO**2))
          RO=SQRT((RP**2)+(XO-P)**2+(YO-Q)**2)
          CUST=SP/SO
          CUSF=RP/RO
          A=(XO/SO)+(XO-P)/RO
          B=(YO/SO)+(YO-Q)/RO
          CUSK=COS(WN*(RO+SO))
          SENK=SIN(WN*(RO+SO))
          AK=1.0/(RO*SO)
          RL=AK**2*CUSK*(RO*CUST+SO*CUSF)+WN*AK*SENK*
     +     (CUST+CUSF)
          UNRL=AK**2*SENK*(RO*CUST+SO*CUSF)-WN*AK*CUSK*
     +     (CUST+CUSF)
          FIR=SIN(WN*B*(DZ/2.0))*SIN(WN*A*(DV/2.0))/
     +     (PI*WN**2*A*B)
          SUMR=SUMR+RL*FIR
          SUMI=SUMI+UNRL*FIR
    3   CONTINUE
    4 CONTINUE
      RETURN
      END

      SUBROUTINE BARR2(RP,SP,Y,P,Q,XL,YB,DV,DZ,L,N,PI,WN,Y1,W,W0,
     +R,MASS,ROEC,SUMR,SUMI)
      SUMR=0
```

```
      SUMI=0
      DO 6 J=1,N
        DO 5 I=1,L
          XO=XL-I*DV+DV/2.0
          YO=YB-J*DZ+DZ/2.0
          SO=SQRT((SP**2)+(XO**2)+(YO**2))
          RO=SQRT((RP**2)+(XO-P)**2+(YO-Q)**2)
          CUST=SP/SO
          CUSF=RP/RO
          A=(XO/SO)+(XO-P)/RO
          B=(YO/SO)+(YO-Q)/RO
          CUSK=COS(WN*(RO+SO))
          SENK=SIN(WN*(RO+SO))
          AK=1.0/(RO*SO)
          RL=AK**2*CUSK*(RO*CUST+SO*CUSF)+WN*AK*SENK*
     +     (CUST+CUSF)
          UNRL=AK**2*SENK*(RO*CUST+SO*CUSF)-WN*AK*CUSK*
     +     (CUST+CUSF)
          FIR=SIN(WN*B*(DZ/2.0))*SIN(WN*A*(DV/2.0))/
     +     (PI*WN**2*A*B)
          Y2=Y-J*DZ+DZ/2.0
          D1=(Y1*SP)/(Y1+Y2)
          DP=SQRT((XL-(I*DV)+(DV/2.0))**2)
          W1=(DP*Y1)/(Y1+Y2)
          X1=SQRT((Y1**2)+(D1**2)+(W1**2))
          Z1=SQRT((D1**2)+(W1**2))
          V=ASIN(Z1/X1)
          CUSV=COS(V)
          CORL=(((W**2)-(W0**2))**2+W**2*((R/MASS)**2-(ROEC/
     +     (MASS*CUSV))**2))/(((W**2)-(W0**2))**2+W**2*
     +     ((R/MASS)+(ROEC/(MASS*CUSV)))**2)
          COIM=(2.0*W*((W**2)-(W0**2))*(ROEC/
     +     (MASS*CUSV)))/(((W**2)-(W0**2))**2+W**2*
     +     ((R/MASS)+(ROEC/(MASS*CUSV)))**2)
          SUMR=SUMR+((RL*CORL)+(UNRL*COIM))*FIR
          SUMI=SUMI+((UNRL*CORL)-(RL*COIM))*FIR
      5   CONTINUE
      6 CONTINUE
        RETURN
        END

        SUBROUTINE BARR3(RP,SP,Y,P,QZ,Q,XL,YB,DV,DZ,L,N,PI,WN,Y1,W,W0,
       +R,MASS,ROEC,SUMR,SUMI)
        SUMR=0
        SUMI=0
        DO 10 J=1,N
          DO 9 I=1,L
            XO=XL-I*DV+DV/2.0
            YO=YB-J*DZ+DZ/2.0
            SO=SQRT((SP**2)+(XO**2)+(YO**2))
            RO=SQRT((RP**2)+(XO-P)**2+(YO-QZ)**2)
            CUST=SP/SO
            CUSF=RP/RO
            A=(XO/SO)+(XO-P)/RO
            B=(YO/SO)+(YO-QZ)/RO
            CUSK=COS(WN*(RO+SO))
            SENK=SIN(WN*(RO+SO))
            AK=1.0/(RO*SO)
```

```
      RL=AK**2*CUSK*(RO*CUST+SO*CUSF)+WN*AK*SENK*
     +  (CUST+CUSF)
      UNRL=AK**2*SENK*(RO*CUST+SO*CUSF)-WN*AK*CUSK*
     +  (CUST+CUSF)
      FIR=SIN(WN*B*(DZ/2.0))*SIN(WN*A*(DV/2.0))/
     +  (PI*WN**2*A*B)
      Y2=Y-J*DZ+DZ/2.0
      D3=(Y2*RP)/(Y1+Y2+Q)
      DP=SQRT((XL-(I*DV)+(DV/2.0)+P)**2)
      W3=(Y2*DP)/(Y1+Y2+Q)
      X1=SQRT((Y2**2)+(D3**2)+(W3**2))
      Z1=SQRT((D3**2)+(W3**2))
      V=ASIN(Z1/X1)
      CUSV=COS(V)
      CORL=(((W**2)-(W0**2))**2+W**2*((R/MASS)**2-(ROEC/
     +  (MASS*CUSV))**2))/(((W**2)-(W0**2))**2+W**2*
     +  ((R/MASS)+(ROEC/(MASS*CUSV)))**2)
      COIM=(2.0*W*((W**2)-(W0**2))*(ROEC/
     +  (MASS*CUSV)))/(((W**2)-(W0**2))**2+W**2*
     +  ((R/MASS)+(ROEC/(MASS*CUSV)))**2)
      SUMR=SUMR+((RL*CORL)+(UNRL*COIM))*FIR
      SUMI=SUMI+((UNRL*CORL)-(RL*COIM))*FIR
    9 CONTINUE
   10 CONTINUE
      RETURN
      END

      SUBROUTINE BARR4(RP,SP,Y,P,QZ,Q,XL,YB,DV,DZ,L,N,PI,WN,Y1,
     +W,W0,R,MASS,ROEC,SUMR,SUMI)
      SUMR=0
      SUMI=0
      DO 12 J=1,N
        DO 11 I=1,L
          XO=XL-I*DV+DV/2.0
          YO=YB-J*DZ+DZ/2.0
          SO=SQRT((SP**2)+(XO**2)+(YO**2))
          RO=SQRT((RP**2)+(XO-P)**2+(YO-QZ)**2)
          CUST=SP/SO
          CUSF=RP/RO
          A=(XO/SO)+(XO-P)/RO
          B=(YO/SO)+(YO-QZ)/RO
          CUSK=COS(WN*(RO+SO))
          SENK=SIN(WN*(RO+SO))
          AK=1.0/(RO*SO)
          RL=AK**2*CUSK*(RO*CUST+SO*CUSF)+WN*AK*SENK*
     +  (CUST+CUSF)
          UNRL=AK**2*SENK*(RO*CUST+SO*CUSF)-WN*AK*CUSK*
     +  (CUST+CUSF)
          FIR=SIN(WN*B*(DZ/2.0))*SIN(WN*A*(DV/2.0))/
     +  (PI*WN**2*A*B)
          Y2=Y-J*DZ+DZ/2.0
          D1=(Y1*SP)/(Y1+Y2)
          DP1=SQRT((XL-(I*DV)+(DV/2.0))**2)
          W1=(DP1*Y1)/(Y1+Y2)
          X1=SQRT((Y1**2)+(D1**2)+(W1**2))
          Z1=SQRT((D1**2)+(W1**2))
          V1=ASIN(Z1/X1)
          CUSV1=COS(V1)
```

```
      CORL1=(((W**2)-(W0**2))**2+W**2*((R/MASS)**2-(ROEC/
     +  (MASS*CUSV1))**2))/(((W**2)-(W0**2))**2+W**2*
     +  ((R/MASS)+(ROEC/(MASS*CUSV1)))**2)
      COIM1=(2.0*W*((W**2)-(W0**2))*(ROEC/
     +  (MASS*CUSV1)))/(((W**2)-(W0**2))**2+W**2*
     +  ((R/MASS)+(ROEC/(MASS*CUSV1)))**2)
      D3=(Y2*RP)/(Y1+Y2+Q)
      DP2=SQRT((XL-I*DV+DV/2.0+P)**2)
      W3=(Y2*DP2)/(Y1+Y2+Q)
      X2=SQRT((Y2**2)+(D3**2)+(W3**2))
      Z2=SQRT((D3**2)+(W3**2))
      V2=ASIN(Z2/X2)
      CUSV2=COS(V2)
      CORL2=(((W**2)-(W0**2))**2+W**2*((R/MASS)**2-(ROEC/
     +  (MASS*CUSV2))**2))/(((W**2)-(W0**2))**2+W**2*
     +  ((R/MASS)+(ROEC/(MASS*CUSV2)))**2)
      COIM2=(2.0*W*((W**2)-(W0**2))*(ROEC/
     +  (MASS*CUSV2)))/(((W**2)-(W0**2))**2+W**2*
     +  ((R/MASS)+(ROEC/(MASS*CUSV2)))**2)
      SUMR=SUMR+(((RL*CORL1*CORL2)+(UNRL*COIM1*CORL2)-
     +  (RL*COIM1*COIM2)+(UNRL*CORL1*COIM2))*FIR)
      SUMI=SUMI+(((UNRL*CORL1*CORL2)-(RL*COIM1*CORL2)-
     +  (RL*CORL1*COIM2)-(UNRL*COIM1*COIM2))*FIR)
11    CONTINUE
12 CONTINUE
   RETURN
   END

   SUBROUTINE REFCO(W,W0,R,MASS,CUSSV,ROEC,CORL,COIM)
   CORL=(((W**2)-(W0**2))**2+W**2*((R/MASS)**2-(ROEC/
  +(MASS*CUSSV))**2))/(((W**2)-(W0**2))**2+W**2*
  +((R/MASS)+(ROEC/(MASS*CUSSV)))**2)
   COIM=(2.0*W*((W**2)-(W0**2))*(ROEC/
  +(MASS*CUSSV)))/(((W**2)-(W0**2))**2+W**2*
  +((R/MASS)+(ROEC/(MASS*CUSSV)))**2)
   RETURN
   END
```

```
WRITE(6,*)'AMPLITUDE'
READ(5,*)AMP
WRITE(6,*)'SOURCE-BARRIER DISTANCE'
READ(5,*)SP
WRITE(6,*)'RECEIVER-BARRIER DISTANCE'
READ(5,*)RP
WRITE(6,*)'HORIZONTAL RECEIVER OFFSET'
READ(5,*)P
WRITE(6,*)'X-COORDINATE FROM L.H.S. OF BARRIER'
READ(5,*)ZL
WRITE(6,*)'Y-COORDINATE FROM TOP OF BARRIER'
READ(5,*)ZB
WRITE(6,*)'HORIZONTAL ELEMENT SIZE OF BARRIER'
READ(5,*)DX
WRITE(6,*)'VERTICAL ELEMENT SIZE OF BARRIER'
READ(5,*)DY
WRITE(6,*)'NUMBER OF HORIZONTAL BARRIER ELEMENTS'
READ(5,*)M
WRITE(6,*)'NUMBER OF VERTICAL BARRIER ELEMENTS'
READ(5,*)N
WRITE(6,*)'WAVELENGTH'
READ(5,*)WL
WRITE(6,*)'X-COORDINATE FROM L.H.S. OF SPACE'
READ(5,*)ZLS
WRITE(6,*)'Y-COORDINATE FROM TOP OF SPACE'
READ(5,*)ZBS
WRITE(6,*)'HORIZONTAL ELEMENT SIZE OF SPACE'
READ(5,*)DXS
WRITE(6,*)'VERTICAL ELEMENT SIZE OF SPACE'
READ(5,*)DYS
WRITE(6,*)'NUMBER OF HORIZONTAL SPACE ELEMENTS'
READ(5,*)MS
WRITE(6,*)'NUMBER OF VERTICAL SPACE ELEMENTS'
READ(5,*)NS
WRITE(6,*)'RESONANT FREQUENCY OF FLOOR'
READ(5,*)W0
WRITE(6,*)'CHARACTERISTIC ACOUSTIC IMPEDANCE OF FLOOR'
READ(5,*)ROEC
WRITE(6,*)'MECHANICAL RESISTANCE FACTOR OF FLOOR'
READ(5,*)R
WRITE(6,*)'EFFECTIVE MASS PER UNIT AREA OF FLOOR'
READ(5,*)MASS
WRITE(6,*)'RESONANT FREQUENCY OF CEILING'
READ(5,*)W05
WRITE(6,*)'CHARACTERISTIC ACOUSTIC IMPEDANCE OF CEILING'
READ(5,*)ROEC5
WRITE(6,*)'MECHANICAL RESISTANCE FACTOR OF CEILING'
READ(5,*)R5
WRITE(6,*)'EFFECTIVE MASS PER UNIT AREA OF CEILING'
READ(5,*)MASS5
WRITE(6,*)'RESONANT FREQUENCY OF RIGHT-HAND WALL'
READ(5,*)W01
WRITE(6,*)'CHARACTERISTIC ACOUSTIC IMPEDANCE OF RIGHT-HAND WALL'
READ(5,*)ROEC1
WRITE(6,*)'MECHANICAL RESISTANCE FACTOR OF RIGHT-HAND WALL'
READ(5,*)R1
WRITE(6,*)'EFFECTIVE MASS PER UNIT AREA OF RIGHT-HAND WALL'
READ(5,*)MASS1
WRITE(6,*)'RESONANT FREQUENCY OF LEFT-HAND WALL'
READ(5,*)W02
WRITE(6,*)'CHARACTERISTIC ACOUSTIC IMPEDANCE OF LEFT-HAND WALL'
READ(5,*)ROEC2
WRITE(6,*)'MECHANICAL RESISTANCE FACTOR OF LEFT-HAND WALL'
READ(5,*)R2
WRITE(6,*)'EFFECTIVE MASS PER UNIT AREA OF LEFT-HAND WALL'
READ(5,*)MASS2
WRITE(6,*)'POSITION OF SOURCE FROM FLOOR'
READ(5,*)SPF
WRITE(6,*)'POSITION OF SOURCE FROM CEILING'
READ(5,*)SPC
WRITE(6,*)'POSITION OF SOURCE FROM RIGHT-HAND WALL'
READ(5,*)SPR
WRITE(6,*)'POSITION OF SOURCE FROM LEFT-HAND WALL'
READ(5,*)SPL
WRITE(6,*)'GROUND OR ENCLOSURE CONDITIONS'
READ(5,*)GE
```

```
      WRITE(6,*)'INITIAL VERTICAL OFFSET'
      READ(5,*)S
      WRITE(6,*)'EXTREME VERTICAL OFFSET'
      READ(5,*)G
      WRITE(6,*)'STEP VALUE OF OFFSET'
      READ(5,*)T
      PI=3.1415926
      WN=(2.0*PI)/WL
      W=340.0/WL
      X=M*DX
      WRITE(6,1)X
    1 FORMAT(5X,'WIDTH OF BARRIER=',G14.6)
      Y=N*DY
      WRITE(6,2)Y
    2 FORMAT(5X,'HEIGHT OF BARRIER=',G14.6)
      Y1=NS*DYS
      DO 8 E=S,G,T
           WRITE(6,19)E
   19      FORMAT(5X,'VERTICAL OFFSET=',G14.6)
           CALL BARR1(RP,SP,P,E,ZL,ZB,DX,DY,M,N,PI,WN,SUMC,SUMD)
           WRITE(6,20)SUMC
   20      FORMAT(5X,'SUMC=',G14.6)
           Q1=E+(2.0*SPF)
           ZB1=ZB+(2.0*SPF)
           CALL BARR2(RP,SP,Y,P,Q1,ZL,ZB1,DX,DY,M,N,PI,WN,SPF,W,W0,R,
     +     MASS,ROEC,SUME,SUMF)
           WRITE(6,21)SUME
   21      FORMAT(5X,'SUME=',G14.6)
           Q2=-(E+(2.0*SPF))
           CALLBARR3(RP,SP,Y,P,Q2,E,ZL,ZB,DX,DY,M,N,PI,WN,SPF,W,W0,R,
     +     MASS,ROEC,SUMG,SUMH)
           WRITE(6,22)SUMG
   22      FORMAT(5X,'SUMG=',G14.6)
           Q3=-E
           CALL BARR4(RP,SP,Y,P,Q3,E,ZL,ZB1,DX,DY,M,N,PI,WN,SPF,W,W0,
     +     R,MASS,ROEC,SUMJ,SUMK)
           WRITE(6,23)SUMJ
   23      FORMAT(5X,'SUMJ=',G14.6)
           Q4=-((2.0*SPC)-E)
           ZB2=ZB-(2.0*SPC)
           CALL BAR2A(RP,SP,Y,P,Q4,ZL,ZB2,DX,DY,M,N,PI,WN,SPF,SPC,W,
     +     W05,R5,MASS5,ROEC5,SUME1,SUMF1)
           WRITE(6,24)SUME1
   24      FORMAT(5X,'SUME1=',G14.6)
           Q5=((2.0*SPC)-E)
           CALL BAR3A(RP,SP,Y,P,Q5,E,ZL,ZB,DX,DY,M,N,PI,WN,SPF,SPC,W,
     +     W05,R5,MASS5,ROEC5,SUMG1,SUMH1)
           WRITE(6,25)SUMG1
   25      FORMAT(5X,'SUMG1=',G14.6)
           Q6=-E
           CALL BAR4A(RP,SP,Y,P,Q6,E,ZL,ZB2,DX,DY,M,N,PI,WN,SPF,SPC,W,
     +     W05,R5,MASS5,ROEC5,SUMJ1,SUMK1)
           WRITE(6,26)SUMJ1
   26      FORMAT(5X,'SUMJ1=',G14.6)
           CALL BARR1(RP,SP,P,E,ZLS,ZBS,DXS,DYS,MS,NS,PI,WN,SUML,SUMM)
           WRITE(6,27)SUML
   27      FORMAT(5X,'SUML=',G14.6)
           ZB3=ZBS+(2.0*SPF)
           CALL BARR2(RP,SP,Y1,P,Q1,ZLS,ZB3,DXS,DYS,MS,NS,PI,WN,SPF,W,
     +     W0,R,MASS,ROEC,SUMN,SUMP)
           WRITE(6,28)SUMN
   28      FORMAT(5X,'SUMN=',G14.6)
           CALL BARR3(RP,SP,Y1,P,Q2,E,ZLS,ZBS,DXS,DYS,MS,NS,PI,WN,SPF,
     +     W,W0,R,MASS,ROEC,SUMQ,SUMR)
           WRITE(6,29)SUMQ
   29      FORMAT(5X,'SUMQ=',G14.6)
           CALL BARR4(RP,SP,Y1,P,Q3,E,ZLS,ZB3,DXS,DYS,MS,NS,PI,WN,SPF,
     +     W,W0,R,MASS,ROEC,SUMS,SUMT)
           WRITE(6,30)SUMS
   30      FORMAT(5X,'SUMS=',G14.6)
           IF (GE.EQ.1.0) GO TO 70
           ZB4=ZBS-(2.0*SPC)
           CALL BAR2A(RP,SP,Y1,P,Q4,ZLS,ZB4,DXS,DYS,MS,NS,PI,WN,SPF,
     +     SPC,W,W05,R5,MASS5,ROEC5,SUMN1,SUMP1)
           WRITE(6,31)SUMN1
   31      FORMAT(5X,'SUMN1=',G14.6)
```

```
      CALL BAR3A(RP,SP,Y1,P,Q5,E,ZLS,ZBS,DXS,DYS,MS,NS,PI,WN,SPF,
     +  SPC,W,W05,R5,MASS5,ROEC5,SUMQ1,SUMR1)
      WRITE(6,32)SUMQ1
32    FORMAT(5X,'SUMQ1=',G14.6)
      CALL BAR4A(RP,SP,Y1,P,Q6,E,ZLS,ZB4,DXS,DYS,MS,NS,PI,WN,SPF,
     +  SPC,W,W05,R5,MASS5,ROEC5,SUMS1,SUMT1)
      WRITE(6,33)SUMS1
33    FORMAT(5X,'SUMS1=',G14.6)
      EBR=SUML+SUMN+SUMQ+SUMS+SUMN1+SUMQ1+SUMS1
      EBI=SUMM+SUMP+SUMR+SUMT+SUMP1+SUMR1+SUMT1
      UBR=EBR-(SUMC+SUME+SUMG+SUMJ+SUME1+SUMG1+SUMJ1)
      UBI=EBI-(SUMD+SUMF+SUMH+SUMK+SUMF1+SUMH1+SUMK1)
      dB=10.0*(ALOG10((EBR**2+EBI**2)/(UBR**2+UBI**2)))
      WRITE(6,7)dB
 7    FORMAT(5X,'INSERTION LOSS FOR SINGLE REFLECTIONS=',G14.6)
      AI1=SQRT(((SUML-SUMC)**2)+((SUMM-SUMD)**2))
      AI2=SQRT((((SUMN-SUME)+(SUMQ-SUMG)+(SUMS-SUMJ))**2)+
     +  (((SUMP-SUMF)+(SUMR-SUMH)+(SUMT-SUMK))**2))
      AI3=SQRT((((SUMN1-SUME1)+(SUMQ1-SUMG1)+(SUMS1-SUMJ1))**2)+
     +  (((SUMP1-SUMF1)+(SUMR1-SUMH1)+(SUMT1-SUMK1))**2))
      ASI1=SQRT(SUML**2+SUMM**2)
      ASI2=SQRT(((SUMN+SUMQ+SUMS)**2)+((SUMP+SUMR+SUMT)**2))
      ASI3=SQRT(((SUMN1+SUMQ1+SUMS1)**2)+((SUMP1+SUMR1+SUMT1)**2))
      EBH=ASI1+ASI2+ASI3
      UBH=AI1+AI2+AI3
      dBB=10.0*(ALOG10((EBH**2)/(UBH**2)))
      WRITE(6,11)dBB
11    FORMAT(5X,'INSERTION LOSS SINGLE2=',G14.6)
      ZB5=-((2.0*(SPF+SPC))-ZB)
      Q7=-(2.0*(SPF+SPC))+E
      CALL BAR2B(RP,SP,Y,P,Q7,ZL,ZB5,DX,DY,M,N,PI,WN,SPF,SPC,
     +  W,W0,R,MASS,ROEC,W05,R5,MASS5,ROEC5,SUME2,SUMF2)
      WRITE(6,55)SUME2
55    FORMAT(5X,'SUME2=',G14.6)
      Q8=(2.0*(SPF+SPC))+E
      CALL BAR3B(RP,SP,Y,P,Q8,E,ZL,ZB,DX,DY,M,N,PI,WN,SPF,SPC,
     +  W,W0,R,MASS,ROEC,W05,R5,MASS5,ROEC5,SUMG2,SUMH2)
      WRITE(6,56)SUMG2
56    FORMAT(5X,'SUMG2=',G14.6)
      Q9=E
      CALL BAR4B(RP,SP,Y,P,Q9,E,ZL,ZB5,DX,DY,M,N,PI,WN,SPF,SPC,
     +  W,W0,R,MASS,ROEC,W05,R5,MASS5,ROEC5,SUMJ2,SUMK2)
      WRITE(6,57)SUMJ2
57    FORMAT(5X,'SUMJ2=',G14.6)
      ZB6=(2.0*(SPF+SPC))+ZB
      Q10=(2.0*(SPF+SPC))+E
      CALL BAR2C(RP,SP,Y,P,Q10,ZL,ZB6,DX,DY,M,N,PI,WN,SPF,SPC,
     +  W,W0,R,MASS,ROEC,W05,R5,MASS5,ROEC5,SUME3,SUMF3)
      WRITE(6,58)SUME3
58    FORMAT(5X,'SUME3=',G14.6)
      Q11=-((2.0*(SPF+SPC))-E)
      CALL BAR3C(RP,SP,Y,P,Q11,E,ZL,ZB,DX,DY,M,N,PI,WN,SPF,SPC,
     +  W,W0,R,MASS,ROEC,W05,R5,MASS5,ROEC5,SUMG3,SUMH3)
      WRITE(6,59)SUMG3
59    FORMAT(5X,'SUMG3=',G14.6)
      Q12=Q
      CALL BAR4C(RP,SP,Y,P,Q12,E,ZL,ZB6,DX,DY,M,N,PI,WN,SPF,SPC,
     +  W,W0,R,MASS,ROEC,W05,R5,MASS5,ROEC5,SUMJ3,SUMK3)
      WRITE(6,60)SUMJ3
60    FORMAT(5X,'SUMJ3=',G14.6)
      CALL BAR2B(RP,SP,Y1,P,Q7,ZLS,ZB5,DXS,DYS,MS,NS,PI,WN,SPF,
     +  SPC,W,W0,R,MASS,ROEC,W05,R5,MASS5,ROEC5,SUMN2,SUMP2)
      WRITE(6,61)SUMN2
61    FORMAT(5X,'SUMN2=',G14.6)
      CALL BAR3B(RP,SP,Y1,P,Q8,E,ZLS,ZBS,DXS,DYS,MS,NS,PI,WN,
     +  SPF,SPC,W,W0,R,MASS,ROEC,W05,R5,MASS5,ROEC5,SUMQ2,SUMR2)
      WRITE(6,62)SUMQ2
62    FORMAT(5X,'SUMQ2=',G14.6)
      CALL BAR4B(RP,SP,Y1,P,Q9,E,ZLS,ZB5,DXS,DYS,MS,NS,PI,WN,
     +  SPF,SPC,W,W0,R,MASS,ROEC,W05,R5,MASS5,ROEC5,SUMS2,SUMT2)
      WRITE(6,63)SUMS2
63    FORMAT(5X,'SUMS2=',G14.6)
      CALL BAR2C(RP,SP,Y1,P,Q10,ZLS,ZB6,DXS,DYS,MS,NS,PI,WN,SPF,
     +  SPC,W,W0,R,MASS,ROEC,W05,R5,MASS5,ROEC5,SUMN3,SUMP3)
      WRITE(6,64)SUMN3
64    FORMAT(5X,'SUMN3=',G14.6)
```

```
      CALL BAR3C(RP,SP,Y1,P,Q11,E,ZLS,ZBS,DXS,DYS,MS,NS,PI,WN,
     +  SPF,SPC,W,W0,R,MASS,ROEC,W05,R5,MASS5,ROEC5,SUMQ3,SUMR3)
      WRITE(6,65)SUMQ3
65    FORMAT(5X,'SUMQ3=',G14.6)
      CALL BAR4C(RP,SP,Y1,P,Q12,E,ZLS,ZB6,DXS,DYS,MS,NS,PI,WN,
     +  SPF,SPC,W,W0,R,MASS,ROEC,W05,R5,MASS5,ROEC5,SUMS3,SUMT3)
      WRITE(6,66)SUMS3
66    FORMAT(5X,'SUMS3=',G14.6)
      EBR1=EBR+SUMN2+SUMQ2+SUMS2+SUMN3+SUMQ3+SUMS3
      EBI1=EBI+SUMP2+SUMR2+SUMT2+SUMP3+SUMR3+SUMT3
      UBR1=EBR1-(SUMC+SUME+SUMG+SUMJ+SUME1+SUMG1+SUMJ1+
     +  SUME2+SUM2+SUMJ2+SUME3+SUMG3+SUMJ3)
      UBI1=EBI1-(SUMD+SUMF+SUMH+SUMK+SUMF1+SUMH1+SUMK1+
     +  SUMF2+SUMH2+SUMK2+SUMF3+SUMH3+SUMK3)
      dB1=10.0*(ALOG10((EBR1**2+EBI1**2)/(UBR1**2+UBI1**2)))
      WRITE(6,9)dB1
 9    FORMAT(5X,'INSERTION LOSS FOR MULTI-REFLECTIONS=',G14.6)
      AI4=SQRT((((SUMN2-SUME2)+(SUMQ2-SUMG2)+(SUMS2-SUMJ2))**2)+
     +  (((SUMP2-SUMF2)+(SUMR2-SUMH2)+(SUMT2-SUMK2))**2))
      AI5=SQRT((((SUMN3-SUME3)+(SUMQ3-SUMG3)+(SUMS3-SUMJ3))**2)+
     +  (((SUMP3-SUMF3)+(SUMR3-SUMH3)+(SUMT3-SUMK3))**2))
      ASI4=SQRT(((SUMN2+SUMQ2+SUMS2)**2)+((SUMP2+SUMR2+
     +  SUMT2)**2))
      ASI5=SQRT(((SUMN3+SUMQ3+SUMS3)**2)+((SUMP3+SUMR3+
     +  SUMT3)**2))
      EBH1=EBH+ASI4+ASI5
      UBH1=UBH+AI4+AI5
      dBB1=10.0*(ALOG10((EBH1**2)/(UBH1**2)))
      WRITE(6,12)dBB1
12    FORMAT(5X,'INSERTION LOSS MULTI2=',G14.6)
      P7=-((2.0*SPR)-P)
      ZL3=ZL+(2.0*SPR)
      CALL BAR2D(RP,SP,P7,E,ZL3,ZB,DX,DY,M,N,PI,WN,SPR,W,W01,
     +  R1,MASS1,ROEC1,SUME4,SUMF4)
      WRITE(6,72)SUME4
72    FORMAT(5X,'SUME4=',G14.6)
      P8=((2.0*SPR)-P)
      CALL BAR3D(RP,SP,P8,P,E,ZL,ZB,DX,DY,M,N,PI,WN,SPR,W,W01,
     +  R1,MASS1,ROEC1,SUMG4,SUMH4)
      WRITE(6,73)SUMG4
73    FORMAT(5X,'SUMG4=',G14.6)
      P9=-P
      CALL BAR4D(RP,SP,P9,P,E,ZL3,ZB,DX,DY,M,N,PI,WN,SPR,W,W01,
     +  R1,MASS1,ROEC1,SUMJ4,SUMK4)
      WRITE(6,74)SUMJ4
74    FORMAT(5X,'SUMJ4=',G14.6)
      P10=(2.0*SPL)+P
      ZL4=-((2.0*SPL)-ZL)
      CALL BAR2E(RP,SP,P10,E,ZL4,ZB,DX,DY,M,N,PI,WN,SPL,W,W02,
     +  R2,MASS2,ROEC2,SUME5,SUMF5)
      WRITE(6,75)SUME5
75    FORMAT(5X,'SUME5=',G14.6)
      P11=-((2.0*SPL)+P)
      CALL BAR3E(RP,SP,P11,P,E,ZL,ZB,DX,DY,M,N,PI,WN,SPL,W,W02,
     +  R2,MASS2,ROEC2,SUMG5,SUMH5)
      WRITE(6,76)SUMG5
76    FORMAT(5X,'SUMG5=',G14.6)
      P12=-P
      CALL BAR4E(RP,SP,P12,P,E,ZL4,ZB,DX,DY,M,N,PI,WN,SPL,W,W02,
     +  R2,MASS2,ROEC2,SUMJ5,SUMK5)
      WRITE(6,77)SUMJ5
77    FORMAT(5X,'SUMJ5=',G14.6)
      ZL5=ZL6+(2.0*SPR)
      CALL BAR2D(RP,SP,P7,E,ZL5,ZBS,DXS,DYS,MS,NS,PI,WN,SPR,W,W01,
     +  R1,MASS1,ROEC1,SUMN4,SUMP4)
      WRITE(6,78)SUMN4
78    FORMAT(5X,'SUMN4=',G14.6)
      CALL BAR3D(RP,SP,P8,P,E,ZLS,ZBS,DXS,DYS,MS,NS,PI,WN,SPR,W,W01,
     +  R1,MASS1,ROEC1,SUMQ4,SUMR4)
      WRITE(6,79)SUMQ4
79    FORMAT(5X,'SUMQ4=',G14.6)
      CALL BAR4D(RP,SP,P9,P,E,ZL5,ZBS,DXS,DYS,MS,NS,PI,WN,SPR,W,W01,
     +  R1,MASS1,ROEC1,SUMS4,SUMT4)
      WRITE(6,80)SUMS4
80    FORMAT(5X,'SUMS4=',G14.6)
      ZL6=-((2.0*SPL)-ZLS)
```

```
      CALL BAR2E(RP,SP,P10,E,ZL6,ZBS,DXS,DYS,MS,NS,PI,WN,SPL,W,W02,
     +  R2,MASS2,ROEC2,SUMN5,SUMP5)
      WRITE(6,81)SUMN5
81    FORMAT(5X,'SUMN5=',G14.6)
      CALL BAR3E(RP,SP,P11,P,E,ZLS,ZBS,DXS,DYS,MS,NS,PI,WN,SPL,W,
     +  W02,R2,MASS2,ROEC2,SUMQ5,SUMR5)
      WRITE(6,82)SUMQ5
82    FORMAT(5X,'SUMQ5=',G14.6)
      CALL BAR4E(RP,SP,P12,P,E,ZL6,ZBS,DXS,DYS,MS,NS,PI,WN,SPL,W,
     +  W02,R2,MASS2,ROEC2,SUMS5,SUMT5)
      WRITE(6,83)SUMS5
83    FORMAT(5X,'SUMS5=',G14.6)
      AI6=SQRT((((SUMN4-SUME4)+(SUMQ4-SUMG4)+(SUMS4-SUMJ4))**2)+
     +  (((SUMP4-SUMF4)+(SUMR4-SUMH4)+(SUMT4-SUMK4))**2))
      AI7=SQRT((((SUMN5-SUME5)+(SUMQ5-SUMG5)+(SUMS5-SUMJ5))**2)+
     +  (((SUMP5-SUMF5)+(SUMR5-SUMH5)+(SUMT5-SUMK5))**2))
      ASI6=SQRT(((SUMN4+SUMQ4+SUMS4)**2)+((SUMP4+SUMR4+SUMT4)**2))
      ASI7=SQRT(((SUMN5+SUMQ5+SUMS5)**2)+((SUMP5+SUMR5+SUMT5)**2))
      EBH2=EBH+ASI6+ASI7
      UBH2=UBH+AI6+AI7
      dBB2=10.0*(ALOG10((EBH2**2)/(UBH2**2)))
      WRITE(6,95)dBB2
95    FORMAT(5X,'INSERTION LOSS FOR ENCLOSURE',G14.6)
70    AI1=SQRT(((SUML-SUMC)**2)+((SUMM-SUMD)**2))
      AI2=SQRT((((SUMN-SUME)+(SUMQ-SUMG)+(SUMS-SUMJ))**2)+
     +  (((SUMP-SUMF)+(SUMR-SUMH)+(SUMT-SUMK))**2))
      ASI1=SQRT(SUML**2+SUMM**2)
      ASI2=SQRT(((SUMN+SUMQ+SUMS)**2)+((SUMP+SUMR+SUMT)**2))
      EEBH=ASI1+ASI2
      UUBH=AI1+AI2
      ddBH=10.0*(ALOG10((EEBH**2)/(UUBH**2)))
      WRITE(6,71)ddBH
71    FORMAT(5X,'INSERTIUN LOSS FOR GROUND CONDITIONS',G14.6)
 8  CONTINUE
     STOP
     END

     SUBROUTINE BARR1(RP,SP,P,Q,XL,YB,DV,DZ,L,N,PI,WN,SUMR,SUMI)
     SUMR=0
     SUMI=0
     DO 4 J=1,N
          DO 3 I=1,L
               XO=XL-I*DV+DV/2.0
               YO=YB-J*DZ+DZ/2.0
               SO=SQRT((SP**2)+(XO**2)+(YO**2))
               RO=SQRT((RP**2)+(XO-P)**2+(YO-Q)**2)
               CUST=SP/SO
               CUSF=RP/RO
               A=(XO/SO)+(XO-P)/RO
               B=(YO/SO)+(YO-Q)/RO
               CUSK=COS(WN*(RO+SO))
               SENK=SIN(WN*(RO+SO))
               AK=1.0/(RO*SO)
               RL=AK**2*CUSK*(RO*CUST+SO*CUSF)+WN*AK*SENK*(CUST+CUSF)
               UNRL=AK**2*SENK*(RO*CUST+SO*CUSF)-WN*AK*CUSK*
     +         (CUST+CUSF)
               FIR=SIN(WN*B*(DZ/2.0))*SIN(WN*A*(DV/2.0))/
     +         (PI*WN**2*A*B)
               SUMR=SUMR+RL*FIR
               SUMI=SUMI+UNRL*FIR
 3        CONTINUE
 4   CONTINUE
     RETURN
     END

     SUBROUTINE BARR2(RP,SP,Y,P,Q,XL,YB,DV,DZ,L,N,PI,WN,SPF,W,W0,
    +R,MASS,ROEC,SUMR,SUMI)
     SUMR=0
     SUMI=0
     DO 6 J=1,N
          DO 5 I=1,L
               XO=XL-I*DV+DV/2.0
               YO=YB-J*DZ+DZ/2.0
               SO=SQRT((SP**2)+(XO**2)+(YO**2))
               RO=SQRT((RP**2)+(XO-P)**2+(YO-Q)**2)
               CUST=SP/SO
```

```
            CUSF=RP/RO
            A=(XO/SO)+(XO-P)/RO
            B=(YO/SO)+(YO-Q)/RO
            CUSK=COS(WN*(RO+SO))
            SENK=SIN(WN*(RO+SO))
            AK=1.0/(RO*SO)
            RL=AK**2*CUSK*(RO*CUST+SO*CUSF)+WN*AK*SENK*(CUST+CUSF)
            UNRL=AK**2*SENK*(RO*CUST+SO*CUSF)-WN*AK*CUSK*
     +      (CUST+CUSF)
            FIR=SIN(WN*B*(DZ/2.0))*SIN(WN*A*(DV/2.0))/
     +      (PI*WN**2*A*B)
            Y2=Y-J*DZ+DZ/2.0
            D1=(SPF*SP)/(SPF+Y2)
            DP=SQRT((XL-I*DV+DV/2.0)**2)
            W1=(DP*SPF)/(SPF+Y2)
            X1=SQRT((SPF**2)+(D1**2)+(W1**2))
            Z1=SQRT((D1**2)+(W1**2))
            V=ASIN(Z1/X1)
            CUSV=COS(V)
            CORL=(((W**2)-(W0**2))**2+W**2*((R/MASS)**2-(ROEC/
     +      (MASS*CUSV))**2))/(((W**2)-(W0**2))**2+W**2*
     +      ((R/MASS)+(ROEC/(MASS*CUSV)))**2)
            COIM=-(2.0*W*((W**2)-(W0**2))*(ROEC/
     +      (MASS*CUSV)))/(((W**2)-(W0**2))**2+W**2*
     +      ((R/MASS)+(ROEC/(MASS*CUSV)))**2)
            SUMR=SUMR+((RL*CORL)-(UNRL*COIM))*FIR
            SUMI=SUMI+((RL*COIM)+(UNRL*CORL))*FIR
 5      CONTINUE
 6  CONTINUE
    RETURN
    END

    SUBROUTINE BARR3(RP,SP,Y,P,QZ,Q,XL,YB,DV,DZ,L,N,PI,WN,SPF,W,W0,
   +R,MASS,ROEC,SUMR,SUMI)
    SUMR=0
    SUMI=0
    DO 10 J=1,N
        DO 9 I=1,L
            XO=XL-I*DV+DV/2.0
            YO=YB-J*DZ+DZ/2.0
            SO=SQRT((SP**2)+(XO**2)+(YO**2))
            RO=SQRT((RP**2)+(XO-P)**2+(YO-QZ)**2)
            CUST=SP/SO
            CUSF=RP/RO
            A=(XO/SO)+(XO-P)/RO
            B=(YO/SO)+(YO-QZ)/RO
            CUSK=COS(WN*(RO+SO))
            SENK=SIN(WN*(RO+SO))
            AK=1.0/(RO*SO)
            RL=AK**2*CUSK*(RO*CUST+SO*CUSF)+WN*AK*SENK*(CUST+CUSF)
            UNRL=AK**2*SENK*(RO*CUST+SO*CUSF)-WN*AK*CUSK*
     +      (CUST+CUSF)
            FIR=SIN(WN*B*(DZ/2.0))*SIN(WN*A*(DV/2.0))/
     +      (PI*WN**2*A*B)
            Y2=Y-J*DZ+DZ/2.0
            D3=(Y2*RP)/(SPF+Y2+Q)
            DP=SQRT((XL-(I*DV)+(DV/2.0)+P)**2)
            W3=(Y2*DP)/(SPF+Y2+Q)
            X1=SQRT((Y2**2)+(D3**2)+(W3**2))
            Z1=SQRT((W3**2)+(D3**2))
            V=ASIN(Z1/X1)
            CUSV=COS(V)
            CORL=(((W**2)-(W0**2))**2+W**2*((R/MASS)**2-(ROEC/
     +      (MASS*CUSV))**2))/(((W**2)-(W0**2))**2+W**2*
     +      ((R/MASS)+(ROEC/(MASS*CUSV)))**2)
            COIM=-(2.0*W*((W**2)-(W0**2))*(ROEC/
     +      (MASS*CUSV)))/(((W**2)-(W0**2))**2+W**2*
     +      ((R/MASS)+(ROEC/(MASS*CUSV)))**2)
            SUMR=SUMR+((RL*CORL)-(UNRL*COIM))*FIR
            SUMI=SUMI+((RL*COIM)+(UNRL*CORL))*FIR
 9      CONTINUE
10  CONTINUE
    RETURN
    END

    SUBROUTINE BARR4(RP,SP,Y,P,QZ,Q,XL,YB,DV,DZ,L,N,PI,WN,SPF,W,W0,
```

```
     +R,MASS,ROEC,SUMR,SUMI)
      SUMR=0
      SUMI=0
      DO 12 J=1,N
           DO 11 I=1,L
                XO=XL-I*DV+DV/2.0
                YO=YB-J*DZ+DZ/2.0
                SO=SQRT((SP**2)+(XO**2)+(YO**2))
                RO=SQRT((RP**2)+(XO-P)**2+(YO-QZ)**2)
                CUST=SP/SO
                CUSF=RP/RO
                A=(XO/SO)+(XO-P)/RO
                B=(YO/SO)+(YO-QZ)/RO
                CUSK=COS(WN*(RO+SO))
                SENK=SIN(WN*(RO+SO))
                AK=1.0/(RO*SO)
                RL=AK**2*CUSK*(RO*CUST+SO*CUSF)+WN*AK*SENK*(CUST+CUSF)
                UNRL=AK**2*SENK*(RO*CUST+SO*CUSF)-WN*AK*CUSK*
     +          (CUST+CUSF)
                FIR=SIN(WN*B*(DZ/2.0))*SIN(WN*A*(DV/2.0))/
     +          (PI*WN**2*A*B)
                Y2=Y-J*DZ+DZ/2.0
                D1=(SPF*SP)/(SPF+Y2)
                DP1=SQRT((XL-(I*DV)+(DV/2.0))**2)
                W1=(DP1*SPF)/(SPF+Y2)
                X1=SQRT((SPF**2)+(D1**2)+(W1**2))
                Z1=SQRT((D1**2)+(W1**2))
                V1=ASIN(Z1/X1)
                CUSV1=COS(V1)
                CORL1=(((W**2)-(W0**2))**2+W**2*((R/MASS)**2-(ROEC/
     +          (MASS*CUSV1))**2))/(((W**2)-(W0**2))**2+W**2*
     +          ((R/MASS)+(ROEC/(MASS*CUSV1)))**2)
                COIM1=-(2.0*W*((W**2)-(W0**2))*(ROEC/
     +          (MASS*CUSV1)))/(((W**2)-(W0**2))**2+W**2*
     +          ((R/MASS)+(ROEC/(MASS*CUSV1)))**2)
                D3=(Y2*RP)/(SPF+Y2+Q)
                DP2=SQRT((XL-I*DV+DV/2.0+P)**2)
                W3=(Y2*DP2)/(SPF+Y2+Q)
                X2=SQRT((Y2**2)+(D3**2)+(W3**2))
                Z2=SQRT((D3**2)+(W3**2))
                V2=ASIN(Z2/X2)
                CUSV2=COS(V2)
                CORL2=(((W**2)-(W0**2))**2+W**2*((R/MASS)**2-(ROEC/
     +          (MASS*CUSV2))**2))/(((W**2)-(W0**2))**2+W**2*
     +          ((R/MASS)+(ROEC/(MASS*CUSV2)))**2)
                COIM2=-(2.0*W*((W**2)-(W0**2))*(ROEC/
     +          (MASS*CUSV2)))/(((W**2)-(W0**2))**2+W**2*
     +          ((R/MASS)+(ROEC/(MASS*CUSV2)))**2)
                SUMR=SUMR+(((RL*CORL1*CORL2)-(UNRL*COIM1*CORL2)-
     +          (RL*COIM1*COIM2)-(UNRL*CORL1*COIM2))*FIR)
                SUMI=SUMI+(((RL*CORL1*COIM2)-(UNRL*COIM1*COIM2)+
     +          (RL*COIM1*CORL2)+(UNRL*CORL1*COIM2))*FIR)
11         CONTINUE
12    CONTINUE
      RETURN
      END

      SUBROUTINE BAR2A(RP,SP,Y,P,Q,XL,YB,DV,DZ,L,N,PI,WN,SPF,SPC,W,W0,
     +R,MASS,ROEC,SUMR,SUMI)
      SUMR=0
      SUMI=0
      DO 14 J=1,N
           DO 13 I=1,L
                XO=XL-I*DV+DV/2.0
                YO=YB-J*DZ+DZ/2.0
                SO=SQRT((SP**2)+(XO**2)+(YO**2))
                RO=SQRT((RP**2)+(XO-P)**2+(YO-Q)**2)
                CUST=SP/SO
                CUSF=RP/RO
                A=(XO/SO)+(XO-P)/RO
                B=(YO/SO)+(YO-Q)/RO
                CUSK=COS(WN*(RO+SO))
                SENK=SIN(WN*(RO+SO))
                AK=1.0/(RO*SO)
                RL=AK**2*CUSK*(RO*CUST+SO*CUSF)+WN*AK*SENK*(CUST+CUSF)
                UNRL=AK**2*SENK*(RO*CUST+SO*CUSF)-WN*AK*CUSK*
```

```
     +          (CUST+CUSF)
                FIR=SIN(WN*B*(DZ/2.0))*SIN(WN*A*(DV/2.0))/
     +          (PI*WN**2*A*B)
                DP=SQRT((XL-(I*DV)+(DV/2.0))**2)
                Y2=Y-J*DZ+DZ/2.0
                D1=(SP*SPC)/((2.0*SPC)+SPF-Y2)
                W1=(DP*SPC)/((2.0*SPC)+SPF-Y2)
                X1=SQRT((SPC**2)+(D1**2)+(W1**2))
                Z1=SQRT((D1**2)+(W1**2))
                V=ASIN(Z1/X1)
                CUSV=COS(V)
                CORL=(((W**2)-(W0**2))**2+W**2*((R/MASS)**2-(ROEC/
     +          (MASS*CUSV))**2))/(((W**2)-(W0**2))**2+W**2*
     +          ((R/MASS)+(ROEC/(MASS*CUSV)))**2)
                COIM=-(2.0*W*((W**2)-(W0**2))*(ROEC/
     +          (MASS*CUSV)))/(((W**2)-(W0**2))**2+W**2*
     +          ((R/MASS)+(ROEC/(MASS*CUSV)))**2)
                SUMR=SUMR+((RL*CORL)-(UNRL*COIM))*FIR
                SUMI=SUMI+((UNRL*CORL)+(RL*COIM))*FIR
   13       CONTINUE
   14   CONTINUE
        RETURN
        END

        SUBROUTINE BAR3A(RP,SP,Y,P,QZ,Q,XL,YB,DV,DZ,L,N,PI,WN,SPF,SPC,
       +W,W0,R,MASS,ROEC,SUMR,SUMI)
        SUMR=0
        SUMI=0
        DO 16 J=1,N
             DO 15 I=1,L
                XO=XL-I*DV+DV/2.0
                YO=YB-J*DZ+DZ/2.0
                SO=SQRT((SP**2)+(XO**2)+(YO**2))
                RO=SQRT((RP**2)+(XO-P)**2+(YO-QZ)**2)
                CUST=SP/SO
                CUSF=RP/RO
                A=(XO/SO)+(XO-P)/RO
                B=(YO/SO)+(YO-QZ)/RO
                CUSK=COS(WN*(RO+SO))
                SENK=SIN(WN*(RO+SO))
                AK=1.0/(RO*SO)
                RL=AK**2*CUSK*(RO*CUST+SO*CUSF)+WN*AK*SENK*(CUST+CUSF)
                UNRL=AK**2*SENK*(RO*CUST+SO*CUSF)-WN*AK*CUSK*
     +          (CUST+CUSF)
                FIR=SIN(WN*B*(DZ/2.0))*SIN(WN*A*(DV/2.0))/
     +          (PI*WN**2*A*B)
                Y2=Y-J*DZ+DZ/2.0
                DP=SQRT((XL-(I*DV)+(DV/2.0)+P)**2)
                D3=(RP*(SPC-Q))/((2.0*SPC)+SPF-Q-Y2)
                W3=(DP*(SPC-Q))/((2.0*SPC)+SPF-Q-Y2)
                X1=SQRT((SPC-Q)**2+(D3**2)+(W3**2))
                Z1=SQRT((D3**2)+(W3**2))
                V=ASIN(Z1/X1)
                CUSV=COS(V)
                CORL=(((W**2)-(W0**2))**2+W**2*((R/MASS)**2-(ROEC/
     +          (MASS*CUSV))**2))/(((W**2)-(W0**2))**2+W**2*
     +          ((R/MASS)+(ROEC/(MASS*CUSV)))**2)
                COIM=-(2.0*W*((W**2)-(W0**2))+(ROEC/
     +          (MASS*CUSV)))/(((W**2)-(W0**2))**2+W**2*
     +          ((R/MASS)+(ROEC/(MASS*CUSV)))**2)
                SUMR=SUMR+((RL*CORL)-(UNRL*COIM))*FIR
                SUMI=SUMI+((UNRL*CORL)+(RL*COIM))*FIR
   15       CONTINUE
   16   CONTINUE
        RETURN
        END

        SUBROUTINE BAR4A(RP,SP,Y,P,QZ,Q,XL,YB,DV,DZ,L,N,PI,WN,SPF,SPC,
       +W,W0,R,MASS,ROEC,SUMR,SUMI)
        SUMR=0
        SUMI=0
        DO 18 J=1,N
             DO 17 I=1,L
                XO=XL-I*DV+DV/2.0
                YO=YB-J*DZ+DZ/2.0
                SO=SQRT((SP**2)+(XO**2)+(YO**2))
```

```
            RO=SQRT((RP**2)+(XO-P)**2+(YO-QZ)**2)
            CUST=SP/SO
            CUSF=RP/RO
            A=(XO/SO)+(XO-P)/RO
            B=(YO/SO)+(YO-QZ)/RO
            CUSK=COS(WN*(RO+SO))
            SENK=SIN(WN*(RO+SO))
            AK=1.0/(RO*SO)
            RL=AK**2*CUSK*(RO*CUST+SO*CUSF)+WN*AK*SENK*(CUST+CUSF)
            UNRL=AK**2*SENK*(RO*CUST+SO*CUSF)-WN*AK*CUSK*
     +      (CUST+CUSF)
            FIR=SIN(WN*B*(DZ/2.0))*SIN(WN*A*(DV/2.0))/
     +      (PI*WN**2*A*B)
            Y2=Y-J*DZ+DZ/2.0
            DP1=SQRT((XL-(I*DV)+(DV/2.0))**2)
            D1=(SP*SPC)/((2.0*SPC)+SPF-Y2)
            W1=(DP1*SPC)/((2.0*SPC)+SPF-Y2)
            X1=SQRT((SPC**2)+(D1**2)+(W1**2))
            Z1=SQRT((D1**2)+(W1**2))
            V1=ASIN(Z1/X1)
            CUSV1=COS(V1)
            CORL1=(((W**2)-(W0**2))**2+W**2*((R/MASS)**2-(ROEC/
     +      (MASS*CUSV1))**2))/(((W**2)-(W0**2))**2+W**2*
     +      ((R/MASS)+(ROEC/(MASS*CUSV1)))**2)
            COIM1=-(2.0*W*((W**2)-(W0**2))*(ROEC/
     +      (MASS*CUSV1)))/(((W**2)-(W0**2))**2+W**2*
     +      ((R/MASS)+(ROEC/(MASS*CUSV1)))**2)
            DP2=SQRT((XL-I*DV+DV/2.0+P)**2)
            D3=(RP*(SPC-Q))/((2.0*SPC)+SPF-Q-Y2)
            W3=(DP2*(SPC-Q))/((2.0*SPC)+SPF-Q-Y2)
            X2=SQRT((SPC-Q)**2+(D3**2)+(W3**2))
            Z2=SQRT((D3**2)+(W3**2))
            V2=ASIN(Z2/X2)
            CUSV2=COS(V2)
            CORL2=(((W**2)-(W0**2))**2+W**2*((R/MASS)**2-(ROEC/
     +      (MASS*CUSV2))**2))/(((W**2)-(W0**2))**2+W**2*
     +      ((R/MASS)+(ROEC/(MASS*CUSV2)))**2)
            COIM2=-(2.0*W*((W**2)-(W0**2))*(ROEC/
     +      (MASS*CUSV2)))/(((W**2)-(W0**2))**2+W**2*
     +      ((R/MASS)+(ROEC/(MASS*CUSV2)))**2)
            SUMR=SUMR+(((RL*CORL1*CORL2)-(UNRL*COIM1*CORL2)-
     +      (RL*COIM1*COIM2)-(UNRL*CORL1*COIM2))*FIR)
            SUMI=SUMI+(((RL*CORL1*COIM2)-(UNRL*COIM1*COIM2)+
     +      (RL*COIM1*CORL2)+(UNRL*CORL1*COIM2))*FIR)
17      CONTINUE
18  CONTINUE
    RETURN
    END

    SUBROUTINE BAR2B(RP,SP,Y,P,Q,XL,YB,DV,DZ,L,N,PI,WN,SPF,SPC,
   +W,W0,R,MASS,ROEC,W05,R5,MASS5,ROEC5,SUMR,SUMI)
    SUMR=0
    SUMI=0
    DO 41 J=1,N
        DO 40 I=1,L
            XO=XL-I*DV+DV/2.0
            YO=YB-J*DZ+DZ/2.0
            SO=SQRT((SP**2)+(XO**2)+(YO**2))
            RO=SQRT((RP**2)+(XO-P)**2+(YO-Q)**2)
            CUST=SP/SO
            CUSF=RP/RO
            A=(XO/SO)+(XO-P)/RO
            B=(YO/SO)+(YO-Q)/RO
            CUSK=COS(WN*(RO+SO))
            SENK=SIN(WN*(RO+SO))
            AK=1.0/(RO*SO)
            RL=AK**2*CUSK*(RO*CUST+SO*CUSF)+WN*AK*SENK*(CUST+CUSF)
            UNRL=AK**2*SENK*(RO*CUST+SO*CUSF)-WN*AK*CUSK*
     +      (CUST+CUSF)
            FIR=SIN(WN*B*(DZ/2.0))*SIN(WN*A*(DV/2.0))/
     +      (PI*WN*A*B)
            Y2=Y-J*DZ+DZ/2.0
            D1=(SP*SPF)/((3.0*SPF)+(2.0*SPC)-Y2)
            DP=SQRT((XL-I*DV+DV/2.0)**2)
            W1=(DP*SPF)/((3.0*SPF)+(2.0*SPC)-Y2)
            X1=SQRT((SPF**2)+(D1**2)+(W1**2))
```

```
            Z1=SQRT((D1**2)+(W1**2))
            V=ASIN(Z1/X1)
            CUSV=COS(V)
            CORL1=(((W**2)-(W0**2))**2+W**2*((R/MASS)**2-(ROEC/
     +      (MASS*CUSV))**2))/(((W**2)-(W0**2))**2+W**2*
     +      ((R/MASS)+(ROEC/(MASS*CUSV)))**2)
            COIM1=-(2.0*W*((W**2)-(W0**2))*(ROEC/
     +      (MASS*CUSV)))/(((W**2)-(W0**2))**2+W**2*
     +      ((R/MASS)+(ROEC/(MASS*CUSV)))**2)
            CORL2=(((W**2)-(W05**2))**2+W**2*((R5/MASS5)**2-(ROEC5/
     +      (MASS5*CUSV))**2))/(((W**2)-(W05**2))**2+W**2*
     +      ((R5/MASS5)+(ROEC5/(MASS5*CUSV)))**2)
            COIM2=-(2.0*W*((W**2)-(W05**2))*(ROEC5/
     +      (MASS5*CUSV)))/(((W**2)-(W05**2))**2+W**2*
     +      ((R5/MASS5)+(ROEC5/(MASS5*CUSV)))**2)
            SUMR=SUMR+(((RL*CORL1*CORL2)-(UNRL*COIM1*CORL2)-
     +      (RL*COIM1*COIM2)-(UNRL*CORL1*COIM2))*FIR)
            SUMI=SUMI+(((RL*CORL1*COIM2)-(UNRL*COIM1*COIM2)+
     +      (RL*COIM1*CORL2)+(UNRL*CORL1*COIM2))*FIR)
40      CONTINUE
41  CONTINUE
    RETURN
    END

    SUBROUTINE BAR3B(RP,SP,Y,P,QZ,Q,XL,YB,DV,DZ,L,N,PI,WN,SPF,SPC,
   +W,W0,R,MASS,ROEC,W05,R5,MASS5,REC5,SUMR,SUMI)
    SUMR=0
    SUMI=0
    DO 43 J=1,N
        DO 42 I=1,L
            XO=XL-I*DV+DV/2.0
            YO=YB-J*DZ+DZ/2.0
            SO=SQRT((SP**2)+(XO**2)+(YO**2))
            RO=SQRT((RP**2)+(XO-P)**2+(YO-QZ)**2)
            CUST=SP/SO
            CUSF=RP/RO
            A=(XO/SO)+(XO-P)/RO
            B=(YO/SO)+(YO-QZ)/RO
            CUSK=COS(WN*(RO+SO))
            SENK=SIN(WN*(RO+SO))
            AK=1.0/(RO*SO)
            RL=AK**2*CUSK*(RO*CUST+SO*CUSF)+WN*AK*SENK*(CUST+CUSF)
            UNRL=AK**2*SENK*(RO*CUST+SO*CUSF)-WN*AK*CUSK*
     +      (CUST+CUSF)
            FIR=SIN(WN*B*(DZ/2.0))*SIN(WN*A*(DV/2.0))/
     +      (PI*WN**2*A*B)
            Y2=Y-J*DZ+DZ/2.0
            D3=(RP*(SPF+Q))/((3.0*SPF)+(2.0*SPC)+Q-Y2)
            DP=SQRT((XL-I*DV+DV/2.0+P)**2)
            W3=(DP*(SPF+Q))/((3.0*SPF)+(2.0*SPC)+Q-Y2)
            X3=SQRT((SPF+Q)**2+(D3**2)+(W3**2))
            Z3=SQRT((D3**2)+(W3**2))
            V=ASIN(Z3/X3)
            CUSV=COS(V)
            CORL1=(((W**2)-(W0**2))**2+W**2*((R/MASS)**2-(ROEC/
     +      (MASS*CUSV))**2))/(((W**2)-(W0**2))**2+W**2*
     +      ((R/MASS)+(ROEC/(MASS*CUSV)))**2)
            COIM1=-(2.0*W*((W**2)-(W0**2))*(ROEC/
     +      (MASS*CUSV)))/(((W**2)-(W0**2))**2+W**2*
     +      ((R/MASS)+(ROEC/(MASS*CUSV)))**2)
            CORL2=(((W**2)-(W05**2))**2+W**2*((R5/MASS5)**2-(ROEC/
     +      (MASS5*CUSV))**2))/(((W**2)-(W05**2))**2+W**2*
     +      ((R5/MASS5)+(ROEC5/(MASS5*CUSV)))**2)
            COIM2=-(2.0*W*((W**2)-(W05**2))*(ROEC5/
     +      (MASS5*CUSV)))/(((W**2)-(W05**2))**2+W**2*
     +      ((R5/MASS5)+(ROEC5/(MASS5*CUSV)))**2)
            SUMR=SUMR+(((RL*CORL1*CORL2)-(UNRL*COIM1*CORL2)-
     +      (UNRL*CORL1*COIM2)-(RL*COIM1*COIM2))*FIR)
            SUMI=SUMI+(((UNRL*CORL1*CORL2)+(RL*COIM1*CORL2)+
     +      (RL*CORL1*COIM2)-(UNRL*COIM1*COIM2))*FIR)
42      CONTINUE
43  CONTINUE
    RETURN
    END
```

```
      SUBROUTINE BAR4B(RP,SP,Y,P,QZ,Q,XL,YB,DV,DZ,L,N,PI,WN,SPF,SPC,
     +W,W0,R,MASS,ROEC,W05,R5,MASS5,ROEC5,SUMR,SUMI)
      SUMR=0
      SUMI=0
      DO 45 J=1,N
          DO 44 I=1,L
              XO=XL-I*DV+DV/2.0
              YO=YB-J*DZ+DZ/2.0
              SO=SQRT((SP**2)+(XO**2)+(YO**2))
              RO=SQRT((RP**2)+(XO-P)**2+(YO-QZ)**2)
              CUST=SP/SO
              CUSF=RP/RO
              A=(XO/SO)+(XO-P)/RO
              B=(YO/SO)+(YO-QZ)/RO
              CUSK=COS(WN*(RO+SO))
              SENK=SIN(WN*(RO+SO))
              AK=1.0/(RO*SO)
              RL=AK**2*CUSK*(RO*CUST+SO*CUSF)+WN*AK*SENK*(CUST+CUSF)
              UNRL=AK**2*SENK*(RO*CUST+SO*CUSF)-WN*AK*CUSK*
     +        (CUST+CUSF)
              FIR=SIN(WN*B*(DZ/2.0))*SIN(WN*A*(DV/2.0))/
     +        (PI*WN**2*A*B)
              Y2=Y-J*DZ+DZ/2.0
              D1=(SP*SPF)/((3.0*SPF)+(2.0*SPC)-Y2)
              DP1=SQRT((XL-I*DV+DV/2.0)**2)
              W1=(DP1*SPF)/((3.0*SPF)+(2.0*SPC)-Y2)
              X1=SQRT((SPF**2)+(D1**2)+(W1**2))
              Z1=SQRT((D1**2)+(W1**2))
              V1=ASIN(Z1/X1)
              CUSV1=COS(V1)
              CORL1=(((W**2)-(W0**2))**2+W**2*((R/MASS)**2-(ROEC/
     +        (MASS*CUSV1))**2))/(((W**2)-(W0**2))**2+W**2*
     +        ((R/MASS)+(ROEC/(MASS*CUSV1)))**2)
              COIM1=-(2.0*W*((W**2)-(W0**2))*(ROEC/
     +        (MASS*CUSV1)))/(((W**2)-(W0**2))**2+W**2*
     +        ((R/MASS)+(ROEC/(MASS*CUSV1)))**2)
              CORL2=(((W**2)-(W05**2))**2+W**2*((R5/MASS5)**2-(ROEC5/
     +        (MASS5*CUSV1))**2))/(((W**2)-(W05**2))**2+W**2*
     +        ((R5/MASS5)+(ROEC5/(MASS5*CUSV1)))**2)
              COIM2=-(2.0*W*((W**2)-(W05**2))*(ROEC5/
     +        (MASS5*CUSV1)))/(((W**2)-(W05**2))**2+W**2*
     +        ((R5/MASS5)+(ROEC5/(MASS5*CUSV1)))**2)
              D3=(RP*(SPF+Q))/((3.0*SPF)+(2.0*SPC)+Q-Y2)
              DP2=SQRT((XL-I*DV+DV/2.0+P)**2)
              W3=(DP2*(SPF+Q))/((3.0*SPF)+(2.0*SPC)+Q-Y2)
              X3=SQRT((SPF+Q)**2+(D3**2)+(W3**2))
              Z3=SQRT((D3**2)+(W3**2))
              V2=ASIN(Z3/X3)
              CUSV2=COS(V2)
              CORL3=(((W**2)-(W0**2))**2+W**2*((R/MASS)**2-(ROEC/
     +        (MASS*CUSV2))**2))/(((W**2)-(W0**2))**2+W**2*
     +        ((R/MASS)+(ROEC/(MASS*CUSV2)))**2)
              COIM3=-(2.0*W*((W**2)-(W0**2))*(ROEC/
     +        (MASS*CUSV2)))/(((W**2)-(W0**2))**2+W**2*
     +        ((R/MASS)+(ROEC/(MASS*CUSV2)))**2)
              CORL4=(((W**2)-(W05**2))**2+W**2*((R5/MASS5)**2-(ROEC5/
     +        (MASS5*CUSV2))**2))/(((W**2)-(W05**2))**2+W**2*
     +        ((R5/MASS5)+(ROEC5/(MASS5*CUSV2)))**2)
              COIM4=-(2.0*W*((W**2)-(W05**2))*(ROEC5/
     +        (MASS5*CUSV2)))/(((W**2)-(W05**2))**2+W**2*
     +        ((R5/MASS5)+(ROEC5/(MASS5*CUSV2)))**2)
              SUMR=SUMR+(((RL*CORL1*CORL2*CORL3*CORL4)-(UNRL*COIM1*
     +        CORL2*CORL3*CORL4)-(UNRL*CORL1*CORL3*CORL4*COIM2)-
     +        (RL*COIM1*COIM2*CORL3*CORL4)-(UNRL*CORL1*CORL2*CORL4*
     +        COIM3)-(RL*COIM1*COIM3*CORL2*CORL4)-(RL*CORL1*CORL4*
     +        COIM2*COIM3)+(UNRL*COIM1*COIM2*COIM3*CORL4)-(RL*CORL1*
     +        CORL2*COIM3*COIM4)+(UNRL*COIM1*COIM3*COIM4*CORL2)+
     +        (UNRL*CORL1*COIM2*COIM3*COIM4)+(RL*COIM1*COIM2*COIM3*
     +        COIM4)-(UNRL*CORL1*CORL2*CORL3*COIM4)-(RL*COIM1*COIM4*
     +        CORL2*CORL3)-(RL*CORL1*CORL3*COIM2*COIM4)+(UNRL*COIM1*
     +        COIM2*COIM4*CORL3))*FIR)
              SUMI=SUMI+(((RL*CORL1*CORL2*CORL3*COIM4)-(UNRL*COIM1*
     +        COIM4*CORL2*CORL3)-(UNRL*CORL1*CORL3*COIM2*COIM4)-
     +        (RL*COIM1*COIM2*COIM4*CORL3)-(UNRL*CORL1*CORL2*COIM3*
     +        COIM4)-(RL*COIM1*COIM3*COIM4*CORL2)-(RL*CORL1*COIM2*
     +        COIM3*COIM4)+(UNRL*COIM1*COIM2*COIM3*COIM4)+(RL*CORL1*
```

```
     +         CORL2*CORL4*COIM3)-(UNRL*CORL2*CORL4*COIM1*COIM3)-
     +         (UNRL*CORL1*CORL4*COIM2*COIM4)-(RL*CORL4*COIM1*COIM2*
     +         COIM3)+(UNRL*CORL1*CORL2*CORL3*CORL4)+(RL*CORL2*
     +         CORL3*CORL4*COIM1)+(RL*CORL1*CORL3*CORL4*COIM2)-
     +         (UNRL*CORL3*CORL4*COIM1*COIM2))*FIR)
  44     CONTINUE
  45 CONTINUE
     RETURN
     END


     SUBROUTINE BAR2C(RP,SP,Y,P,Q,XL,YB,DV,DZ,L,N,PI,WN,SPF,SPC,
    +W,W0,R,MASS,ROEC,W05,R5,MASS5,ROEC5,SUMR,SUMI)
     SUMR=0
     SUMI=0
     DO 47 J=1,N
         DO 46 I=1,L
            XO=XL-I*DV+DV/2.0
            YO=YB-J*DZ+DZ/2.0
            SO=SQRT((SP**2)+(XO**2)+(YO**2))
            RO=SQRT((RP**2)+(XO-P)**2+(YO-Q)**2)
            CUST=SP/SO
            CUSF=RP/RO
            A=(XO/SO)+(XO-P)/RO
            B=(YO/SO)+(YO-Q)/RO
            CUSK=COS(WN*(RO+SO))
            SENK=SIN(WN*(RO+SO))
            AK=1.0/(RO*SO)
            RL=AK**2*CUSK*(RO*CUST+SO*CUSF)+WN*AK*SENK*(CUST+CUSF)
            UNRL=AK**2*SENK*(RO*CUST+SO*CUSF)-WN*AK*CUSK*
     +      (CUST+CUSF)
            FIR=SIN(WN*B*(DZ/2.0))*SIN(WN*A*(DV/2.0))/
     +      (PI*WN**2*A*B)
            Y2=Y-J*DZ+DZ/2.0
            D1=(SP*SPC)/((2.0*SPC)+SPF+Y2)
            DP=SQRT((XL-I*DV+DV/2.0)**2)
            W1=(DP*SPC)/((2.0*SPC)+SPF+Y2)
            X1=SQRT((SPC**2)+(D1**2)+(W1**2))
            Z1=SQRT((D1**2)+(W1**2))
            V=ASIN(Z1/X1)
            CUSV=COS(V)
            CORL1=(((W**2)-(W0**2))**2+W**2*((R/MASS)**2-(ROEC/
     +      (MASS*CUSV))**2))/(((W**2)-(W0**2))**2+W**2*
     +      ((R/MASS)+(ROEC/(MASS*CUSV)))**2)
            COIM1=-(2.0*W*((W**2)-(W0**2))*(ROEC/
     +      (MASS*CUSV)))/(((W**2)-(W0**2))**2+W**2*
     +      ((R/MASS)+(ROEC/(MASS*CUSV)))**2)
            CORL2=(((W**2)-(W05**2))**2+W**2*((R5/MASS5)**2-(ROEC5/
     +      (MASS5*CUSV))**2))/(((W**2)-(W05**2))**2+W**2*
     +      ((R5/MASS5)+(ROEC5/(MASS5*CUSV)))**2)
            COIM2=-(2.0*W*((W**2)-(W05**2))*(ROEC5/
     +      (MASS5*CUSV)))/(((W**2)-(W05**2))**2+W**2*
     +      ((R5/MASS5)+(ROEC5/(MASS5*CUSV)))**2)
            SUMR=SUMR+(((RL*CORL1*CORL2)-(UNRL*COIM1*CORL2)-
     +      (UNRL*CORL1*COIM2)-(RL*COIM1*COIM2))*FIR)
            SUMI=SUMI+(((UNRL*CORL1*CORL2)+(RL*COIM1*CORL2)+
     +      (RL*CORL1*COIM2)-(UNRL*COIM1*COIM2))*FIR)
  46     CONTINUE
  47 CONTINUE
     RETURN
     END


     SUBROUTINE BAR3C(RP,SP,Y,P,QZ,Q,XL,YB,DV,DZ,L,N,PI,WN,SPF,SPC,
    +W,W0,R,MASS,ROEC,W05,R5,MASS5,ROEC5,SUMR,SUMI)
     SUMR=0
     SUMI=0
     DO 49 J=1,N
         DO 48 I=1,L
            XO=XL-I*DV+DV/2.0
            YO=YB-J*DZ+DZ/2.0
            SO=SQRT((SP**2)+(XO**2)+(YO**2))
            RO=SQRT((RP**2)+(XO-P)**2+(YO-QZ)**2)
            CUST=SP/SO
            CUSF=RP/RO
            A=(XO/SO)+(XO-P)/RO
```

```
            B=(YO/SO)+(YO-QZ)/RO
            CUSK=COS(WN*(RO+SO))
            SENK=SIN(WN*(RO+SO))
            AK=1.0/(RO*SO)
            RL=AK**2*CUSK*(RO*CUST+SO*CUSF)+WN*AK*SENK*(CUST+CUSF)
            UNRL=AK**2*SENK*(RO*CUST+SO*CUSF)-WN*AK*CUSK*
     +      (CUST+CUSF)
            FIR=SIN(WN*B*(DZ/2.0))*SIN(WN*A*(DV/2.0))/
     +      (PI*WN**2*A*B)
            Y2=Y-J*DZ+DZ/2.0
            D3=(RP*(SPC-Q))/((2.0*SPC)+SPF+Y2-Q)
            DP=SQRT((XL-I*DV+DV/2.0+P)**2)
            W3=(DP*(SPC-Q))/((2.0*SPC)+SPF+Y2-Q)
            X3=SQRT((SPC-Q)**2+(D3**2)+(W3**2))
            Z3=SQRT((D3**2)+(W3**2))
            V=ASIN(Z3/X3)
            CUSV=COS(V)
            CORL1=(((W**2)-(W0**2))**2+W**2*((R/MASS)**2-(ROEC/
     +      (MASS*CUSV))**2))/(((W**2)-(W0**2))**2+W**2*
     +      ((R/MASS)+(ROEC/(MASS*CUSV)))**2)
            COIM1=-(2.0*W*((W**2)-(W0**2))+(ROEC/
     +      (MASS*CUSV)))/(((W**2)-(W0**2))**2+W**2*
     +      ((R/MASS)+(ROEC/(MASS*CUSV)))**2)
            CORL2=(((W**2)-(W05**2))**2+W**2*((R5/MASS5)**2-(ROEC5/
     +      (MASS5*CUSV))**2))/(((W**2)-(W05**2))**2+W**2*
     +      ((R5/MASS5)+(ROEC5/(MASS5*CUSV)))**2)
            COIM2=-(2.0*W*((W**2)-(W05**2))+(ROEC5/
     +      (MASS5*CUSV)))/(((W**2)-(W05**2))**2+W**2*
     +      ((R5/MASS5)+(ROEC5/(MASS5*CUSV)))**2)
            SUMR=SUMR+(((RL*CORL1*CORL2)-(UNRL*COIM1*CORL2)-
     +      (UNRL*CORL1*COIM2)-(RL*COIM1*COIM2))*FIR)
            SUMI=SUMI+(((UNRL*CORL1*CORL2)+(RL*COIM1*CORL2)+
     +      (RL*CORL1*COIM2)-(UNRL*COIM1*COIM2))*FIR)
48      CONTINUE
49  CONTINUE
    RETURN
    END


    SUBROUTINE BAR4C(RP,SP,Y,P,QZ,Q,XL,YB,DV,DZ,L,N,PI,WN,SPF,SPC,
   +W,W0,R,MASS,ROEC,W05,R5,MASS5,ROEC5,SUMR,SUMI)
    SUMR=0
    SUMI=0
    DO 51 J=1,N
        DO 50 I=1,L
            XO=XL-I*DV+DV/2.0
            YO=YB-J*DZ+DZ/2.0
            SO=SQRT((SP**2)+(XO**2)+(YO**2))
            RO=SQRT((RP**2)+(XO-P)**2+(YO-QZ)**2)
            CUST=SP/SO
            CUSF=RP/RO
            A=(XO/SO)+(XO-P)/RO
            B=(YO/SO)+(YO-QZ)/RO
            CUSK=COS(WN*(RO+SO))
            SENK=SIN(WN*(RO+SO))
            AK=1.0/(RO*SO)
            RL=AK**2*CUSK*(RO*CUST+SO*CUSF)+WN*AK*SENK*(CUST+CUSF)
            UNRL=AK**2*SENK*(RO*CUST+SO*CUSF)-WN*AK*CUSK*
     +      (CUST+CUSF)
            FIR=SIN(WN*B*(DZ/2.0))*SIN(WN*A*(DV/2.0))/
     +      (PI*WN**2*A*B)
            Y2=Y-J*DZ+DZ/2.0
            D1=(SP*SPC)/((2.0*SPC)+SPF+Y2)
            DP1=SQRT((XL-I*DV+DV/2.0)**2)
            W1=(DP1*SPC)/((2.0*SPC)+SPF+Y2)
            X1=SQRT((SPC**2)+(D1**2)+(W1**2))
            Z1=SQRT((D1**2)+(W1**2))
            V1=ASIN(Z1/X1)
            CUSV1=COS(V1)
            CORL1=(((W**2)-(W0**2))**2+W**2*((R/MASS)**2-(ROEC/
     +      (MASS*CUSV1))**2))/(((W**2)-(W0**2))**2+W**2*
     +      ((R/MASS)+(ROEC/(MASS*CUSV1)))**2)
            COIM1=-(2.0*W*((W**2)-(W0**2))*(ROEC/
     +      (MASS*CUSV1)))/(((W**2)-(W0**2))**2+W**2*
     +      ((R/MASS)+(ROEC/(MASS*CUSV1)))**2)
            CORL2=(((W**2)-(W05**2))**2+W**2*((R5/MASS5)**2-(ROEC5/
```

```
     +          (MASS5*CUSV1))**2))/(((W**2)-(W05**2))**2+W**2*
     +          ((R5/MASS5)+(ROEC5/(MASS5*CUSV1)))**2)
                COIM2=-(2.0*W*((W**2)-(W05**2))*(ROEC5/
     +          (MASS5*CUSV1)))/(((W**2)-(W05**2))**2+W**2*
     +          ((R5/MASS5)+(ROEC5/(MASS5*CUSV1)))**2)
                D3=(RP*(SPC-Q))/((2.0*SPC)+SPF+Y2-Q)
                DP2=SQRT((XL-I*DV+DV/2.0+P)**2)
                W3=(DP2*(SPC-Q))/((2.0*SPC)+SPF+Y2-Q)
                X3=SQRT((SPC-Q)**2+(D3**2)+(W3**2))
                Z3=SQRT((D3**2)+(W3**2))
                V2=ASIN(Z3/X3)
                CUSV2=COS(V2)
                CORL3=(((W**2)-(W0**2))**2+W**2*((R/MASS)**2-(ROEC/
     +          (MASS*CUSV2))**2))/(((W**2)-(W0**2))**2+W**2*
     +          ((R/MASS)+(ROEC/(MASS*CUSV2)))**2)
                COIM3=-(2.0*W*((W**2)-(W0**2))*(ROEC/
     +          (MASS*CUSV2)))/(((W**2)-(W0**2))**2+W**2*
     +          ((R/MASS)+(ROEC/(MASS*CUSV2)))**2)
                CORL4=(((W**2)-(W05**2))**2+W**2*((R5/MASS5)**2-(ROEC5/
     +          (MASS5*CUSV2))**2))/(((W**2)-(W05**2))**2+W**2*
     +          ((R5/MASS5)+(ROEC5/(MASS5*CUSV2)))**2)
                COIM4=-(2.0*W*((W**2)-(W05**2))*(ROEC5/
     +          (MASS5*CUSV2)))/(((W**2)-(W05**2))**2+W**2*
     +          ((R5/MASS5)+(ROEC5/(MASS5*CUSV2)))**2)
                SUMR=SUMR+(((RL*CORL1*CORL2*CORL3*CORL4)-(UNRL*COIM1*
     +          CORL2*CORL3*CORL4)-(UNRL*CORL1*CORL3*CORL4*COIM2)-
     +          (RL*COIM1*COIM2*CORL3*CORL4)-(UNRL*CORL1*CORL2*CORL4*
     +          COIM3)-(RL*COIM1*COIM3*CORL2*CORL4)-(RL*CORL1*CORL4*
     +          COIM2*COIM3)+(UNRL*COIM1*COIM2*COIM3*CORL4)-(RL*CORL1*
     +          CORL2*COIM3*COIM4)+(UNRL*COIM1*COIM3*COIM4*CORL2)+
     +          (UNRL*CORL1*COIM2*COIM3*COIM4)+(RL*COIM1*COIM2*COIM3*
     +          COIM4)-(UNRL*CORL1*CORL2*CORL3*COIM4)-(RL*COIM1*COIM4*
     +          CORL2*CORL3)-(RL*CORL1*CORL3*COIM2*COIM4)+(UNRL*COIM1*
     +          COIM2*COIM4*CORL3))*FIR)
                SUMI=SUMI+(((RL*CORL1*CORL2*CORL3*COI4)-(UNRL*COIM1*
     +          COIM4*CORL2*CORL3)-(UNRL*CORL1*CORL3*COIM2*COIM4)-
     +          (RL*COIM1*COIM2*COIM4*CORL3)-(UNRL*CORL1*CORL2*COIM3*
     +          COIM4)-(RL*COIM1*COIM3*COIM4*CORL2)-(RL*CORL1*COIM2*
     +          COIM3*COIM4)+(UNRL*COIM1*COIM2*COIM3*COIM4)+(RL*CORL1*
     +          CORL2*CORL4*COIM3)-(UNRL*CORL2*CORL4*COIM1*COIM3)-
     +          (UNRL*CORL1*CORL4*COIM2*COIM3)-(RL*CORL4*COIM1*COIM2*
     +          COIM3)+(UNRL*CORL1*CORL2*CORL3*CORL4)+(RL*CORL2*CORL3*
     +          CORL4*COIM1)+(RL*CORL1*CORL3*CORL4*COIM2)-(UNRL*CORL3*
     +          CORL4*COIM1*COIM2))*FIR)
50         CONTINUE
51    CONTINUE
      RETURN
      END

      SUBROUTINE BAR2D(RP,SP,P,Q,XL,YB,DV,DZ,L,N,PI,WN,SPR,W,W0,R,MASS,
     +ROEC,SUMR,SUMI)
      SUMR=0
      SUMI=0
      DO 80 J=1,N
           DO 79 I=1,L
                XO=XL-I*DV+DV/2.0
                YO=YB-J*DZ+DZ/2.0
                SO=SQRT((SP**2)+(XO**2)+(YO**2))
                RO=SQRT((RP**2)+(XO-P)**2+(YO-Q)**2)
                CUST=SP/SO
                CUSF=RP/RO
                A=(XO/SO)+(XO-P)/RO
                B=(YO/SO)+(YO-Q)/RO
                CUSK=COS(WN*(RO+SO))
                SENK=SIN(WN*(RO+SO))
                AK=1.0/(RO*SO)
                RL=AK**2*CUSK*(RO*CUST+SO*CUSF)+WN*AK*SENK*(CUST+CUSF)
                UNRL=AK**2*SENK*(RO*CUST+SO*CUSF)-WN*AK*CUSK*
     +          (CUST+CUSF)
                FIR=SIN(WN*B*(DZ/2.0))*SIN(WN*A*(DV/2.0))/
     +          (PI*WN**2*A*B)
                X2=XL-SPR-I*DV+DV/2.0
                Y2=SQRT((YB-J*DZ+DZ/2.0)**2)
                D1=(SPR*SP)/(X2+SPR)
                W1=(SPR*Y2)/(X2+SPR)
                X1=SQRT((SPR**2)+(D1**2)+(W1**2))
```

```
            Z1=SQRT((D1**2)+(W1**2))
            V=ASIN(Z1/X1)
            CUSV=COS(V)
            CORL=(((W**2)-(W0**2))**2+W**2*((R/MASS)**2-(ROEC/
     +      (MASS*CUSV))**2))/(((W**2)-(W0**2))**2+W**2*
     +      ((R/MASS)+(ROEC/(MASS*CUSV)))**2)
            COIM=-(2.0*W*((W**2)-(W0**2))*(ROEC/
     +      (MASS*CUSV)))/(((W**2)-(W0**2))**2+W**2*
     +      ((R/MASS)+(ROEC/(MASS*CUSV)))**2)
            SUMR=SUMR+((RL*CORL)+(UNRL*COIM))*FIR
            SUMI=SUMI+((UNRL*CORL)-(RL*COIM))*FIR
79      CONTINUE
80  CONTINUE
    RETURN
    END

    SUBROUTINE BAR3D(RP,SP,PZ,P,Q,XL,YB,DV,DZ,L,N,PI,WN,SPR,W,W0,
   +R,MASS,ROEC,SUMR,SUMI)
    SUMR=0
    SUMI=0
    DO 82 J=1,N
        DO 81 I=1,L
            XO=XL-I*DV+DV/2.0
            YO=YB-J*DZ+DZ/2.0
            SO=SQRT((SP**2)+(XO**2)+(YO**2))
            RO=SQRT((RP**2)+(XO-PZ)**2+(YO-Q)**2)
            CUST=SP/SO
            CUSF=RP/RO
            A=(XO/SO)+(XO-PZ)/RO
            B=(YO/SO)+(YO-Q)/RO
            CUSK=COS(WN*(RO+SO))
            SENK=SIN(WN*(RO+SO))
            AK=1.0/(RO*SO)
            RL=AK**2*CUSK*(RO*CUST+SO*CUSF)+WN*AK*SENK*(CUST+CUSF)
            UNRL=AK**2*SENK*(RO*CUST+SO*CUSF)-WN*AK*CUSK*
     +      (CUST+CUSF)
            FIR=SIN(WN*B*(DZ/2.0))*SIN(WN*A*(DV/2.0))/
     +      (PI*WN**2*A*B)
            X2=XL+SPR-I*DV+DV/2.0
            Y2=SQRT((YB-Q-J*DZ+DZ/2.0)**2)
            D2=(RP*(SPR-P))/(X2+SPR-P)
            W2=(Y2*(SPR-P))/(X2+SPR-P)
            X1=SQRT((SPR-P)**2+(D2**2)+(W2**2))
            Z1=SQRT((D2**2)+(W2**2))
            V=ASIN(Z1/X1)
            CUSV=COS(V)
            CORL=(((W**2)-(W0**2))**2+W**2*((R/MASS)**2-(ROEC/
     +      (MASS*CUSV))**2))/(((W**2)-(W0**2))**2+W**2*
     +      ((R/MASS)+(ROEC/(MASS*CUSV)))**2)
            COIM=-(2.0*W*((W**2)-(W0**2))*(ROEC/
     +      (MASS*CUSV)))/(((W**2)-(W0**2))**2+W**2*
     +      ((R/MASS)+(ROEC/(MASS*CUSV)))**2)
            SUMR=SUMR+((RL*CORL)+(UNRL*COIM))*FIR
            SUMI=SUMI+((UNRL*CORL)-(RL*COIM))*FIR
81      CONTINUE
82  CONTINUE
    RETURN
    END

    SUBROUTINE BAR4D(RP,SP,PZ,P,Q,XL,YB,DV,DZ,L,N,PI,WN,SPR,W,W0,
   +R,MASS,ROEC,SUMR,SUMI)
    SUMR=0
    SUMI=0
    DO 84 J=1,N
        DO 83 I=1,L
            XO=XL-I*DV+DV/2.0
            YO=YB-J*DZ+DZ/2.0
            SO=SQRT((SP**2)+(XO**2)+(YO**2))
            RO=SQRT((RP**2)+(XO-PZ)**2+(YO-Q)**2)
            CUST=SP/SO
            CUSF=RP/RO
            A=(XO/SO)+(XO-PZ)/RO
            B=(YO/SO)+(YO-Q)/RO
            CUSK=COS(WN*(RO+SO))
            SENK=SIN(WN*(RO+SO))
            AK=1.0/(RO*SO)
```

```
            RL=AK**2*CUSK*(RO*CUST+SO*CUSF)+WN*AK*SENK*(CUST+CUSF)
            UNRL=AK**2*SENK*(RO*CUST+SO*CUSF)-WN*AK*CUSK*
     +      (CUST+CUSF)
            FIR=SIN(WN*B*(DZ/2.0))*SIN(WN*A*(DV/2.0))/
     +      (PI*WN**2*A*B)
            X2=XL-SPR-I*DV+DV/2.0
            Y2=SQRT((YB-J*DZ+DZ/2.0)**2)
            D1=(SPR*SP)/(X2+SPR)
            W1=(SPR*Y2)/(X2+SPR)
            X1=SQRT((SPR**2)+(D1**2)+(W1**2))
            Z1=SQRT((D1**2)+(W1**2))
            V1=ASIN(Z1/X1)
            CUSV1=COS(V1)
            CORL1=(((W**2)-(W0**2))**2+W**2*((R/MASS)**2-(ROEC/
     +      (MASS*CUSV1))**2))/(((W**2)-(W0**2))**2+W**2*
     +      ((R/MASS)+(ROEC/(MASS*CUSV1)))**2)
            COIM1=-(2.0*W*((W**2)-(W0**2))*(ROEC/
     +      (MASS*CUSV1)))/(((W**2)-(W0**2))**2+W**2*
     +      ((R/MASS)+(ROEC/(MASS*CUSV1)))**2)
            Y3=SQRT((YB-Q-J*DZ+DZ/2.0)**2)
            D3=(RP*(SPR-P))/(X2+SPR-P)
            W3=(Y3*(SPR-P))/(X2+SPR-P)
            X3=SQRT((SPR-P)**2+(D3**2)+(W3**2))
            Z3=SQRT((D3**2)+(W3**2))
            V2=ASIN(Z3/X3)
            CUSV2=COS(V2)
            CORL2=(((W**2)-(W0**2))**2+W**2*((R/MASS)**2-(ROEC/
     +      (MASS*CUSV2))**2))/(((W**2)-(W0**2))**2+W**2*
     +      ((R/MASS)+(ROEC/(MASS*CUSV2)))**2)
            COIM2=-(2.0*W*((W**2)-(W0**2))*(ROEC/
     +      (MASS*CUSV2)))/(((W**2)-(W0**2))**2+W**2*
     +      ((R/MASS)+(ROEC/(MASS*CUSV2)))**2)
            SUMR=SUMR+(((RL*CORL1*CORL2)-(UNRL*COIM1*CORL2)-
     +      (RL*COIM1*COIM2)-(UNRL*CORL1*COIM2))*FIR)
            SUMI=SUMI+(((RL*CORL1*COIM2)-(UNRL*COIM1*COIM2)+
     +      (RL*COIM1*CORL2)+(UNRL*CORL1*COIM2))*FIR)
83      CONTINUE
84  CONTINUE
    RETURN
    END

    SUBROUTINE BAR2E(RP,SP,P,Q,XL,YB,DV,DZ,L,N,PI,WN,SPL,W,W0,
   +R,MASS,ROEC,SUMR,SUMI)
    SUMR=0
    SUMI=0
    DO 86 J=1,N
        DO 85 I=1,L
            XO=XL-I*DV+DV/2.0
            YO=YB-J*DZ+DZ/2.0
            SO=SQRT((SP**2)+(XO**2)+(YO**2))
            RO=SQRT((RP**2)+(XO-P)**2+(YO-Q)**2)
            CUST=SP/SO
            CUSF=RP/RO
            A=(XO/SO)+(XO-P)/RO
            B=(YO/SO)+(YO-Q)/RO
            CUSK=COS(WN*(RO+SO))
            SENK=SIN(WN*(RO+SO))
            AK=1.0/(RO*SO)
            RL=AK**2*CUSK*(RO*CUST+SO*CUSF)+WN*AK*SENK*(CUST+CUSF)
            UNRL=AK**2*SENK*(RO*CUST+SO*CUSF)-WN*AK*CUSK*
     +      (CUST+CUSF)
            FIR=SIN(WN*B*(DZ/2.0))*SIN(WN*A*(DV/2.0))/
     +      (PI*WN**2*A*B)
            X3=SPL-XL+I*DV-DV/2.0
            Y3=SQRT((YB-J*DZ+DZ/2.0)**2)
            D1=(SPL*SP)/(X3+SPL)
            W1=(SPL*Y3)/(X3+SSPL)
            X1=SQRT((SPL**2)+(D1**2)+(W1**2))
            Z1=SQRT((D1**2)+(W1**2))
            V=ASIN(Z1/X1)
            CUSV=COS(V)
            CORL=(((W**2)-(W0**2))**2+W**2*((R/MASS)**2-(ROEC/
     +      (MASS*CUSV))**2))/(((W**2)-(W0**2))**2+W**2*
     +      ((R/MASS)+(ROEC/(MASS*CUSV)))**2)
            COIM=-(2.0*W*((W**2)-(W0**2))*(ROEC/
     +      (MASS*CUSV)))/(((W**2)-(W0**2))**2+W**2*
```

```
     +          ((R/MASS)+(ROEC/(MASS*CUSV)))**2)
                SUMR=SUMR+((RL*CORL)+(UNRL*COIM))*FIR
                SUMI=SUMI+((UNRL*CORL)-(RL*COIM))*FIR
   85       CONTINUE
   86    CONTINUE
         RETURN
         END

         SUBROUTINE BAR3E(RP,SP,PZ,P,Q,XL,YB,DV,DZ,L,N,PI,WN,SPL,W,W0,
        +R,MASS,ROEC,SUMR,SUMI)
         SUMR=0
         SUMI=0
         DO 88 J=1,N
             DO 87 I=1,L
                XO=XL-I*DV+DV/2.0
                YO=YB-J*DZ+DZ/2.0
                SO=SQRT((SP**2)+(XO**2)+(YO**2))
                RO=SQRT((RP**2)+(XO-PZ)**2+(YO-Q)**2)
                CUST=SP/SO
                CUSF=RP/RO
                A=(XO/SO)+(XO-PZ)/RO
                B=(YO/SO)+(YO-Q)/RO
                CUSK=COS(WN*(RO+SO))
                SENK=SIN(WN*(RO+SO))
                AK=1.0/(RO*SO)
                RL=AK**2*CUSK*(RO*CUST+SO*CUSF)+WN*AK*SENK*(CUST+CUSF)
                UNRL=AK**2*SENK*(RO*CUST+SO*CUF)-WN*AK*CUSK*
     +          (CUST+CUSF)
                FIR=SIN(WN*B*(DZ/2.0))*SIN(WN*A*(DV/2.0))/
     +          (PI*WN**2*A*B)
                X3=SPL-XL+I*DV-DV/2.0
                Y3=SQRT((YB-J*DZ+DZ/2.0-Q)**2)
                D3=(RP*(SPL+P))/(X3+SPL+P)
                W3=(Y3*(SPL+P))/(X3+SPL+P)
                X1=SQRT((SPL+P)**2+(D3**2)+(W3**2))
                Z1=SQRT((D3**2)+(W3**2))
                V=ASIN(Z1/X1)
                CUSV=COS(V)
                CORL=((W**2)-(W0**2))**2+W**2*((R/MASS)**2-(ROEC/
     +          (MASS*CUSV))**2))/(((W**2)-(W0**2))**2+W**2*
     +          ((R/MASS)+(ROEC/(MASS*CUSV)))**2)
                COIM=-(2.0*W*((W**2)-(W0**2))*(ROEC/
     +          (MASS*CUSV)))/(((W**2)-(W0**2))**2+W**2*
     +          ((R/MASS)+(ROEC/(MASS*CUSV)))**2)
                SUMR=SUMR+((RL*CORL)+(UNRL*COIM))*FIR
                SUMI=SUMI+((UNRL*CORL)-(RL*COIM))*FIR
   87       CONTINUE
   88    CONTINUE
         RETURN
         END

         SUBROUTINE BAR4E(RP,SP,PZ,P,Q,XL,YB,DV,DZ,L,N,PI,WN,SPL,W,W0,
        +R,MASS,ROEC,SUMR,SUMI)
         SUMR=0
         SUMI=0
         DO 90 J=1,N
             DO 89 I=1,L
                XO=XL-I*DV+DV/2.0
                YO=YB-J*DZ+DZ/2.0
                SO=SQRT((SP**2)+(XO**2)+(YO**2))
                RO=SQRT((RP**2)+(XO-PZ)**2+(YO-Q)**2)
                CUST=SP/SO
                CUSF=RP/RO
                A=(XO/SO)+(XO-PZ)/RO
                B=(YO/SO)+(YO-Q)/RO
                CUSK=COS(WN*(RO+SO))
                SENK=SIN(WN*(RO+SO))
                AK=1.0/(RO*SO)
                RL=AK**2*CUSK*(RO*CUST+SO*CUSF)+WN*AK*SENK*(CUST+CUSF)
                UNRL=AK**2*SENK*(RO*CUST+SO*CUSF)-WN*AK*CUSK*
     +          (CUST+CUSF)
                FIR=SIN(WN*B*(DZ/2.0))*SIN(WN*A*(DV/2.0))/
     +          (PI*WN**2*A*B)
                X2=SPL-XL+I*DV+DV/2.0
                Y2=SQRT((YB-J*DZ+DZ/2.0)**2)
                D1=(SPL*SP)/(X2+SPL)
```